INSTITUT
PASCAL
sciences de l'ingénierie et des systèmes

INSTITUT PASCAL

Highlights (2010 – 2015)

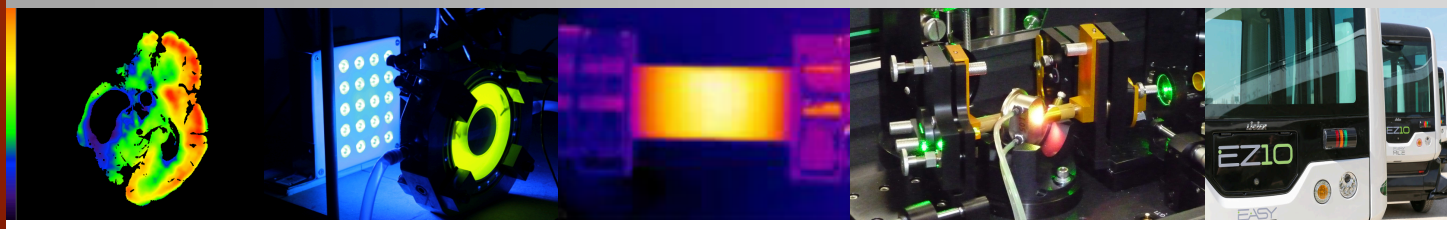

CLERMONT UNIVERSITÉ
UNIVERSITÉ BLAISE PASCAL CLERMONT-FERRAND
Université d'Auvergne
cnrs
IFMA INSTITUT FRANÇAIS DE MÉCANIQUE AVANCÉE

Table of contents

#57	Room temperature polariton condensation based on ZnO and GaN microcavities
#58	Accurate determination of excitonic parameters of GaN and ZnO by linear and non-linear spectroscopies
#59	Optical properties of AlGaN/AlGaN heterostructures for the realization of a solid-state vertical surface emitting laser operating at 280 nm
#60	Ultralong defect-free single crystal phase GaAs and GaN nanowires
#61	HVPE growth of (In,Ga)N structures with controlled morphologies
#62	Elaboration of nitrided III-V thin films, under ultra high vacuum conditions. Nanostructured surfaces and their passivation
#63	Multi-mode elastic peak electron spectroscopy (MM-EPES): experimental measurements combined with Monte Carlo simulations
#64	Organic/mineral hybrid nanomaterials for gas sensing applications
#65	Highly selective NO_2 sensor system for air quality control: towards a technology transfer
#66	Uncertainty quantification and propagation for computational and experimental electromagnetic compatibility (EMC) reliability
#67	Matrix pencil method applied to smart monitoring, electromagnetic compatibility and ultra wide band RADAR
#68	Novel modulation of dual-vsi fed open-end motor to enhance efficiency for electrical and hybrid vehicles applications
#69	Evaluations of screening performance for new generation braided cable shields
#70	BIOEM research laboratory corresponding partnership
#71	Redudancy-based optimization approach to optimize robotic cell behaviour
#72	The C^3Bots project: collaborative cross and carry modile robots
#73	Detection of acetic acid using electrochemically modified electrodes based on metallophtalocyanines and porphyrins derivatives
#74	Bioprocesses intensification with high frequency electromagnetic fields
#75	The aperiodic Fourier modal method for computing micro-organisms cross sections
#76	Mechanical-probabilistic modeling of a compression test on food
#77	Electromagnetic compatibility integrity of cables in complex stochastic environments
#78	Reliability-based optimization of energy performance buildings
#79	A coupled model for a hydrogel diffraction grating used in pH-sensing
#80	Modeling of active piezoelectric composite structures with cracks
#81	Shape-from-Template (SfT)
#82	Seeing in 3D in Monocular Laparoscopy
#83	Computer-Aided Uterine Laparosurgery with Augmented Reality
#84	Laparoscopy-like operative vaginoscopy
#85	Analysis of Intracoronary Prosthesis by Optical Coherence Tomography (sous-thème 1)
#86	Interventional Planning and Assistance for Ascending Aorta Dissections (sous-thème 2)
#87	Standardization of transcatheter arterial chemo-embolization of the liver (sous-thème 3)
#88	Joint Estimation of Myocardial Strain and Contraction Phase from Data Assimilation (sous-thème 4)
#89	4.7-Tesla Magnetic Resonance Imaging Atlas of Human Deep Brain
#90	3D MRI reconstruction based on transfinite approximation
#91	Variation Maps of 18F-fluorodesoxyglucose Pet-Scans of Severe Brain Injured Patients: Individual Comparison of Deep Brain Stimulation in On and Off Conditions
#92	Set-up of combined accelerometry, electrophysiology and clinical assessments during DBS
#93	Contribution of the recording of local field potential during deep brain stimulation
#94	Mapping the structural connectivity of language with DTI tractography
#95	Processing of speech with graduated emotional charge: an fMRI study to detect residual capacity in patients with disorders of conciousness
#96	DBS Targeting in Brain Injured Patients with Severe Anatomical Lesions
#97	Time-course of myelination and atrophy on MRI in PLP1-related disorders
#98	Databases monitoring and evaluation
#99	Immediate post partum Blood loss evaluation
#100	Severe Secondary Postpartum Hemorrhage: incidence, causes and risk factors
#101	Partnership in mother and child health in Ukraine
#102	Health risk assessment for babies linked to disinfection by-products detected in the chlorinated water of swimming pool
#103	Risk assessment after in utero phtalated exposure and obstretical outcomes
#104	Contractualizations with Supersonic Imagine Corp.

Scientific achievement #1
High efficiency photobioreactor with solar light-flux dilution

Photobioreactors with high thermodynamic efficiency and volumetric biomass growth-rates are required in order to tackle the challenge of developing industrial processes producing solar fuels from only water and CO_2. The conception, sizing, optimization and control of such complex reactors can only be achieved if predictive knowledge models are built and validated. This work is led in the lab since the 90's and has recently produced important results and original concepts like photobioreactors with dilution of the incident solar flux. A patented prototype of 25 L working volume is currently under theoretical and experimental investigation.

Microalgae cultivation in solar photobioreactors is identified as a promising way to produce a wide range of interesting renewable molecules for chemistry and energy. Nevertheless the industrial-scale implementation of photobioreactors first requires the development of new technologies, or the optimisation of existing concepts, in order to reach thermodynamic efficiencies of at least 10%. This goal, imposed by the competitiveness with other solar processes, can only be achieved if predictive and robust models of the process are available for their design, sizing, optimization, control and operation. Combining these models with recent thermodynamic-based optimization techniques (Constructal theory, domain sensitivity Monte Carlo analysis, etc.) leads to the DiCoFluV concept of high-efficiency photobioreactor (see Cornet, 2010 and list of patents hereafter). On this basis, a cylindrical reactor prototype in which the incident light flux density is diluted in the culture volume thanks to a thousand of light-diffusing optical fibres has been developed in the lab (see Figure 1). Before testing the thermodynamic efficiencies in actual solar conditions, the photobioreactor is currently studied with perfectly controlled artificial light (discharge white lamps) and its experimental performances are compared with the results of our model.

This multi-scale and reified model is based, at the smallest scale, on the calculation of optical and radiative properties of microalgae with complex shapes, using a state-of-the-art predictive theoretical chain that is unique in the world (see Figure 2 and Dauchet et al., 2015). Then the radiative transfer problem (Boltzmann photon-transport equation) is solved in any complex geometry of photobioreactors using the most recent advances in the field of radiative transfer Monte Carlo (Dauchet et al., 2013), including integral formulation, sensitivity analyses and zero-variance approaches.

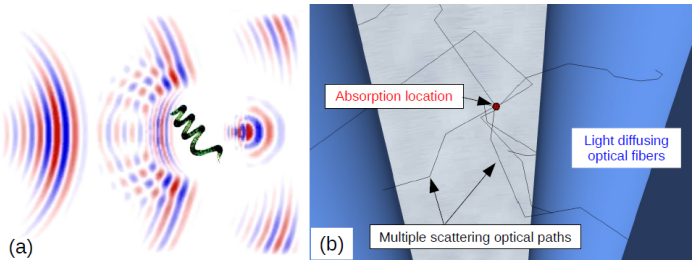

Fig. 2: Photobioreactor modelling at two different scales. (a): Resolution of Maxwell's equations for micro-algae particles with complex shape in order to retrieve the absorption and scattering properties of photosynthetic suspensions (Dauchet et al., 2015). (b): Resolution of radiative transfer equation within the complex geometry of the DiCoFluV reactor in order to retrieve the rate of photon absorption by micro-algae at any location within the anisotropically scattering and non- gray absorbing photosynthetic media characterized in (b) (Dauchet et al., 2013).

It rigorously estimates the amount of photons absorbed locally per unit time per microalgae at any location **x** within the culture volume. The algorithm consists in the backward sampling of multiple-scattering and reflection optical-paths from **x** (the absorption location) to the emitting surfaces (see Figure 2). This algorithm is implemented in the EDStar development environment, that makes available to radiation physicists a set of computation tools issued from the computer graphics research community during the last 20 years, in particular in the framework of the Physically Based Rendering Techniques (PBRT) project. The thermo-kinetic coupling with photosynthesis rates and efficiencies is then formulated using the thermodynamics of irreversible processes to determine the energetic and quantum yields. This led also to recent and new developments in the field of nonlinear Monte Carlo integral formulation.

As a perspective, the prototype must be used and operated in actual solar conditions in order to confirm that it can deliver efficiencies of roughly 15% in the visible light domain with a full-sunlight incident flux. Linked to a wavelength splitting system and converting infrared radiation into work, a future demonstrator could reach 15-20% on the entire solar spectrum, which is highly competitive with the photovoltaic technology, including additional possibility of chemical fuel storage.

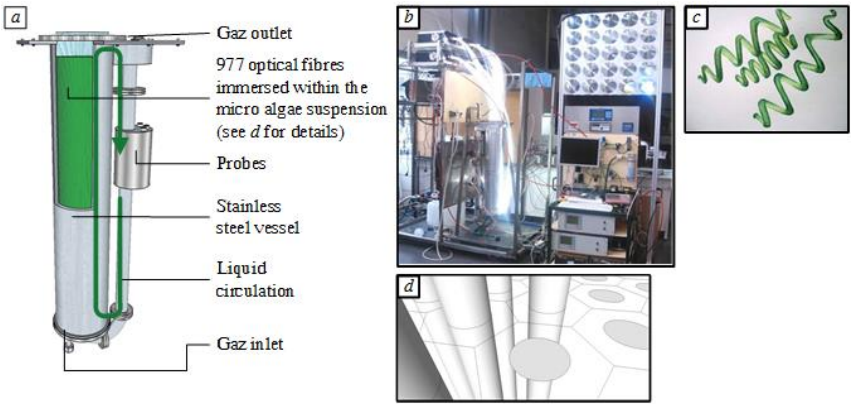

Fig. 1: DiCoFluV photobioreactor in which incident light provided by discharge lamps (as a preliminary stage before actual solar functioning) is diluted within a 22 L Arthrospira platensis culture (see micrograph c) via 977 lateral diffusing optical fibres. (a) Computer Aided Design. (b) The complete pilot plant. (d) Close up on the hexagonal fibres lattice.

CONTACTS

Jean-François CORNET
j-françois.cornet@univ-bpclermont.fr

FURTHER READING

Calculation of the radiative properties of photosynthetic microorganisms
J. Dauchet et al., Journal of Quantitative Spectroscopy and Radiative Transfer 161, 60 (2015)

The practice of recent radiative transfer Monte Carlo advances and its contribution to the field of micro-organisms cultivation in photobioreactors
J. Dauchet et al., Journal of Quantitative Spectroscopy and Radiative Transfer 128, 52 (2013)

Calculation of optimal design and ideal productivities of volumetrically-lightened photobioreactors using the constructal approach
J.F. Cornet, Chemical Engineering Journal 65, 985 (2010)

CONTRACTS

ANR Biosolis (2008-2011)
ANR PRIAM (2013-15)
PIE CNRS Photorad (2010-2011)
PEPS CNRS ITRPHPV (2012-13)
European ESA project NGPC (2015-2017)
Industrial contract : Study and simulation for a R&D microalgae platform development, with GEPEA St-Nazaire, TOTAL and AIRBUS (2010)
LabEx IMobS3 : action μ-APHIPE (2012-2017)
Idex Toulouse/Albi : action ALGUE (2015-2017)
1 French (2010) and US (2014) patents; 1 international patent (2012), 1 Soleau enveloppe (2014) and 1 patent currently under examination (CNRS)

PhD

J. Charon, J. Dauchet, V. Rochatte

Scientific achievement #2
Bioactive Polysaccharides from microalgae

Marine organisms are one of the most underutilized biological resources. The extreme diversity of microalgae, unicellular photosynthetic organisms that are known to produce large quantities of polysaccharides, makes them very attractive for bioprospecting and potential exploitation as commercial sources of exopolysaccharides. Applying a biorefinery strategy, the aim of this work was to increase the level of knowledge about the processes of production and the structures of exopolysaccharides from red marine microalgae. Their potential as antimicrosporidian agent both *in vitro* and *in vivo* on *Apis mellifera* (honeybee) model has been successfully evaluated.

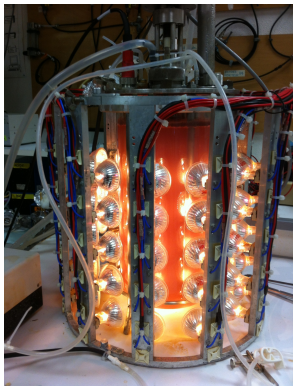

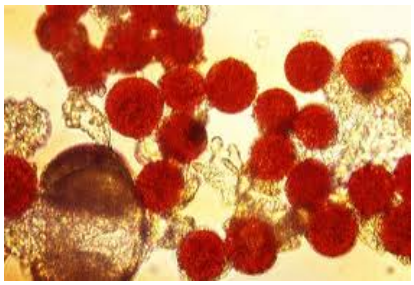

Fig. 2: Red marine microalgae belonging to Porphyridium sp. and its culture in a cylindrical photobioreactor.

Microalgae are photosynthetic microorganisms from fresh water and marine environments. Autotrophic microalgae require a light energy source to convert inorganic compounds such as CO_2, N, S, P into biomass via photosynthesis with high efficiencies generally exceeding those of terrestrial plants. The growing interest of the scientific community for these microorganisms is linked to their ability to produce a range of high-value compounds such as biofuels, additives for human food and animal feed and bioactive molecules. Among them, red marine microalgae are an interesting source of hydrocolloids.

Strategy of our work is to identify new exopolysaccharide producers, to improve their culture conditions, to partially characterize polymers on a structural and rheological basis, and in some case, to develop some collaborations in order to valorize them as hydrocolloids or biological agents. For this, culture medium is first modified on the basis of its stoichiometric analysis and comparisons with the elemental analysis of biomass. Moreover, influence of physicochemical parameters such as irradiance, temperature and pH on the photosynthesis activity of cells is studied, allowing determination of optimal growth parameters (Figure 1).

The autotrophic growth of microalgae strains (such as *Rhodella* and *Porphyridium* sp.) is then studied in photobioreactors with the objective to analyse the incidence of modifications on the exopolysaccharide production (Figure 2).

Results showed that the use of optimal conditions led to significant increases of biomass and exopolysaccharide productions. Structural characterization of these polysaccharides showed they had a good potential as mimicry of glycosaminoglycans (GAGs) as they showed uronic acids and sulphates in their composition. GAGs are linear and negatively charged polysaccharides ubiquitous in animal bodies and possessing multiple biological functions essential for life. As an example of valorisation, these sulphated polysaccharides were used to control the development of microsporidia in *Nosema ceranae*-infected adult honeybees (Nosemosis) in collaboration with another laboratory of the Blaise Pascal University (Laboratoire Microorganismes Génome Environnement).

The nosemosis is one of the most common diseases of adults honey bees. *Nosema,* the causal agent, is a microsporidia which is an obligatory intracellular eukaryotic parasite and the only one treatment available, fumagillin, is no more licensed in several European countries. Two polysaccharides extracted from *Porphyridium* sp. allowed a decrease of both the parasite load and the mortality due to *N. ceranae* infection. The results obtained suggest that microalgal sulphated polysaccharides could be used to control nosemosis in apiaries.

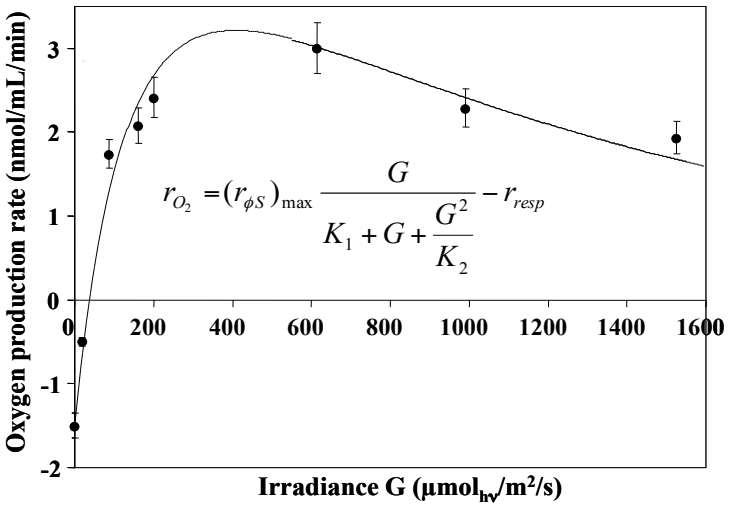

Fig. 1: Photosynthetic activity of a Rhodella strain measured with an oxygraph system as function of irradiance. -♦- experimental data; --- model plot (Eilers and Peeters 1988. Ecol. Model. *42, 199-215). rO2: O2 production (nmol.mL-1.min-1); rresp: O2 consumption (nmol.mL-1.min-1); G: irradiance (µmol photons.m-2.s-1); K1 and K2: constants.*

CONTACTS

Céline LAROCHE
Celine.LAROCHE@univ-bpclermont.fr
Philippe MICHAUD
Philippe.MICHAUD@univ-bpclermont.fr

FURTHER READING

Sulphated polysaccharide composition
P. Michaud et al., WO2014076261

Optimization of culture parameters for exopolysaccharides production by the microalga Rhodella violacea
A. Villay et al., Bioresource Technology 146, 732 (2013)

Separation and fractionation of exopolysaccharide from Porphyridium cruentum
A. Villay et al., Bioresource Technology 145, 345 (2012)

CONTRACTS

ANR Blanc Algoraffinerie (2010-2013)
ANR Emergence Bio (2012-2015)

PhD

A. Villay

Scientific achievement #3
Biorefinery of microalgae

Microalgae are photosynthetic microorganisms from fresh water and marine environments. Most of published papers state the use of microalgae as non-food feedstock for the production of biofuels. However depending on the microalgae species, various high-value compounds such as pigments, antioxidants, polysaccharides and proteins can be extracted. Biorefinery concept is a sequence of non-destructive processes that must be implemented to achieve the fractionation of intracellular components. Nevertheless, there is a lack of information concerning microalgae to achieve such target. Here we apply for the first time the previous knowledge of terrestrial biorefineries to the microalgal biomass.

Microalgae are photosynthetic microorganisms used for third generation biofuel production and carbon dioxide sequestration. Nevertheless, processing costs are still too high to be profitable, leading to a need to find high value byproducts in addition to biofuel. In this context, we develop biorefinery concept i.e. sequence of unit operations to achieve the whole fractionation and/or transformation of biomass to produce multiple products. However the diversity of microalgae strains implies to verify to which extend processes applied on one strain can be applicable to other. As an example we discuss the effect of process condition on the extraction and functionality of protein, pigments, high value lipids and polysaccharides of four strains used as models: *Chlorella vulgaris*, *Haematococcus pluvialis*, *Porphyridium cruentum* and *Arthrospira platensis* (Figure 1).

As a first step, it is necessary to identify, quantify and characterize main constituting fractions i.e. lipids, proteins, sugars and pigments after cells lysis by physical or chemical treatments.

For *Chlorella vulgaris,* solubilisation of proteins from cell has been studied under different operation conditions including high pressure cell disrupter with or without pH shifting. The higher solubilisation yield was obtained when using combination of alkaline solutions and mechanical treatments. Proteins collected by precipitation or ultrafiltration showed emulsifying properties higher than those of commercial ingredients such as soya bean. For *Haematococcus pluvialis,* if pH shifting increases the yield of protein recovery it reduces emulsion capacity of extracted proteins. In the case of *Arthrospira platensis,* high pressure disruption didn't improve protein solubilisation. Freezing followed by thawing permitted the protein recovery from microalgae. In both cases, extracted proteins present excellent emulsion functionality. High pressure disruption was not adapted for protein extraction from *Porphyridium cruentum* as the mucilage of this strain led to development of pseudogels.

Concerning pigments, the extraction and purification of two classes of them has been explored. That of hydrosoluble pigments such as phycocyanin from *Arthrospira platensis* or B-phycoerythrin from *P. cruentum* and this of liposoluble astaxanthin from *H. pluvialis.*

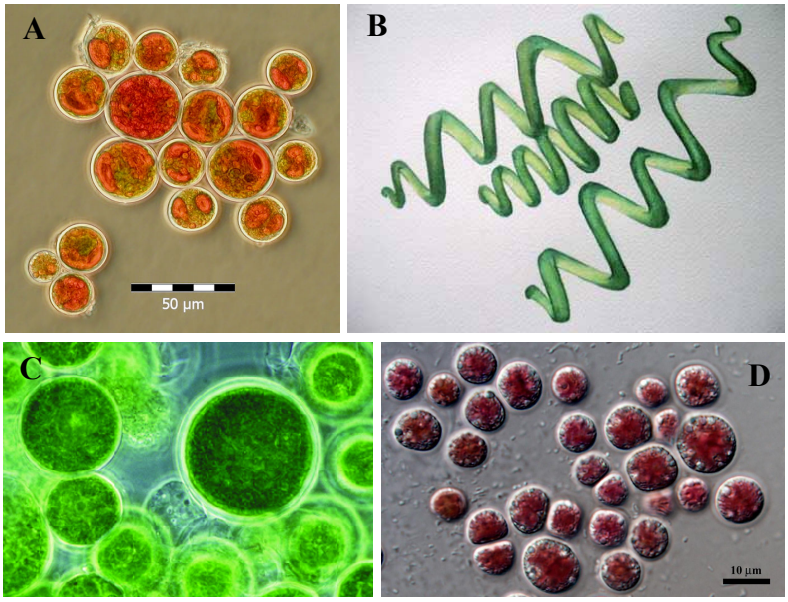

Fig. 1: A: Haematococcus pluvialis; B: Arthrospira platensis; C: Chlorella vulgaris; D: Porphyridium cruentum.

The first class was successfully extracted using tangential ultrafiltration and/or selective precipitation (acids or $CaCl_2$) whereas for the second one centrifugal partition chromatography has been successfully tested in collaboration with GEPEA laboratory from University of St-Nazaire. The polysaccharidic fraction was only identified in the *Porphyridium* strain excluding cell wall polysaccharides or starch from other strains. It was extracted and partially separated from the pigment and proteic compounds after filtration strategy.

CONTACTS

Gholamreza DJELVEH
gholamreza.djelveh@ensccf.fr
Céline LAROCHE
Céline.LAROCHE@univ-bpclermont.fr
Philippe MICHAUD
Philippe.MICHAUD@ univ-bpclermont.fr

FURTHER READING

Understanding the effect of cell disruption methods on the diffusion of Chlorella vulgaris proteins and pigments in the aqueous phase
C. Safi et al., Algal Research (2015)

Extraction, fractionation and functional properties of proteins from the microalgae Chlorella vulgaris
A. Ursu et al., Bioresource Technology 157, 134 (2014)

Extraction and fractionation of polysaccharides and B-phycoerythrin from the microalga Porphyridium cruentum by membrane technology
A. Marcati et al., Algal Research 5, 258 (2014)

CONTRACTS

ANR Blanc Algoraffinerie (2010-2013)
Labex IMobS3, Biorefinery Action
ADEME Project Alg-I-Gaz (Biorefinery part) (2014-2016)

PhD/Post Doc

F. Ba/A. Patel, A.V. Ursu

Scientific achievement #4
Bioenergy from agricultural and food waste

Anaerobic fermentation with mixed cultures was applied to meat and lignocellulosic byproducts for the coproduction of biohydrogen and Volatile Fatty Acids (VFAs). VFAs were subsequently used as the substrate for the production of microbial lipids using inexpensive oleaginous yeasts in a second stage. An anaerobic submerged membrane reactor was designed for circumventing the inhibitory effects of VFAs and soluble H_2: H_2 content in the gas phase achieved 60%, with a yield of 1.2 mol/mol of substrate. In the second stage, the crude lipid content reached 60% of the dry biomass, which achieved 90 g/L for optimum operating conditions, *i.e.* at high C/N ratio.

With the increasing demand of energy, there is a growing interest in the development alternative sources of energy, especially renewable resources. Unlike other renewable energy sources, biomass can be converted directly into liquid or gaseous fuels, to help meet transportation fuel needs because transportation depends on fossil fuels for 95%. Among biofuel technologies, those linked to 2nd generation biofuels present the advantage to bypass many limitations of the 1st generation in terms of sustainability and life cycle assessment because they use lignocellulosic biomass, agricultural residues or food waste as raw materials. They also do not compete with possible food and feed uses of 1st generation raw materials.

In addition to bioethanol and biodiesel that can derive from both generation technologies, 2nd generation biohydrogen ($BioH_2$) can also be produced through acidogenic fermentation. $BioH_2$ is a clean and sustainable alternative fuel. Acidogenic fermentation is an anaerobic digestion process similar to methanation, but in which the methanogenic step has been removed. $BioH_2$ is obtained through the butyrate and the acetate H_2-producting pathways, which implies the simultaneous coproduction of $BioH_2$ and VFAs. For sustainability, VFAs can be used as platform molecules for bioproducts or biofuels. The optimization of dark fermentation is, therefore, a difficult task, as $BioH_2$ productivity can be impaired by several inhibitory effects, such as pH and hydrogen partial pressure: it requires the analysis of the complex interaction between biotic and abiotic factors.

Highlighting an additional inhibition due to total VFAs content, the objective of the GePEB group of Institut Pascal was to design a bioreactor that could enhance the production of $BioH_2$ from agrowaste (Fig. 1a), while the liquid phase enriched in VFAs could be used as the substrate for the production of microbial lipids in a second stage [1].

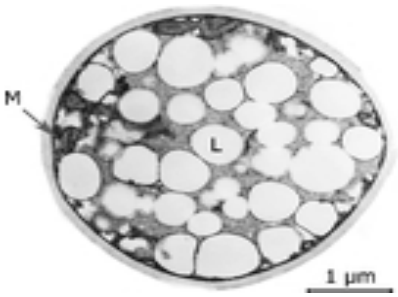

Fig. 2: Microbial lipids in oleaginous yeast.

The technology of anaerobic membrane bioreactors was selected for the first stage (R.R. Singhania's Post Doc). An innovative submerged membrane bioreactor [2] equipped with an external hollow fiber module was designed, so that it could be operated under controlled pH and atmospheric pressure, while benefiting from the advantages of external membrane devices. The abiotic factors of this bioreactor including the flow rate in the loop and the membrane cleaning procedures were optimized (Z. Trad's PhD). Computational Fluid Dynamics (CFD) was also applied to better understand the effect of mixing (Fig. 1b) [3]. The influence of ferrous iron in the culture medium was evidenced; H_2 content in the gas phase achieved 60%, with a yield of 2 mol/mol of substrate (A. Noblecourt's PhD). In parallel, the production of microbial lipids with the oleaginous yeast *Crypotoccocus curvatus* using VFAs as the substrate was optimized, so that the crude lipid content reached 60% of the dry biomass which achieved 90 g/L for optimum operating conditions, *i.e.* at high C/N ratio (Fig. 2).

A metabolic model able to predict lipid productivity was established (V. Beligon's PhD). These results highlight the feasibility of coupling the two stages for the simultaneous production of $BioH_2$ and lipids as biodiesel precursors.

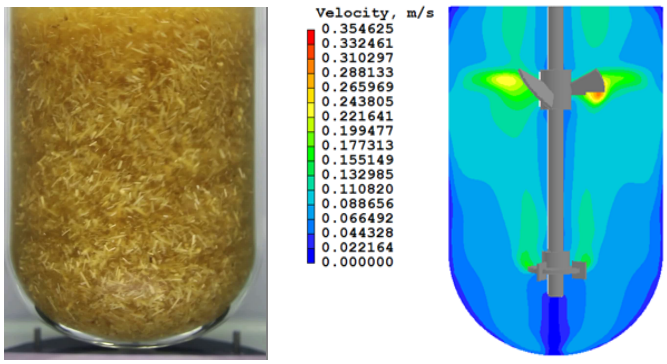

Fig. 1: Anaerobic bioreactor: (left) with straw as substrate; modelled by CFD (right).

CONTACTS

Christophe.VIAL
Christophe.VIAL@univ-bpclermont.fr
Christian LARROCHE
Christian LARROCHE@univ-bpclermont.fr
Pierre FONTANILLE
Pierre FONTANILLE@univ-bpclermont.fr
Gwendoline CHRISTOPHE
Gwendoline CHRISTOPHE@univ-bpclermont.fr

FURTHER READING

[1] *Bioconversion of volatile fatty acids into microbial lipids by the oleaginous yeast Yarrowia lipolytica*
P. Fontanille et al., Bioresource Technology, 114, 443 (2012)

[2] *Immersed membrane bioreactors: An overview with special emphasis on anaerobic bioprocesses*
R.R. Singhania et al., Bioresource Technology 122, 171 (2012)

[3] *Modeling of hydrodynamics and mixing in a submerged membrane bioreactor*
Z. Trad et al., Chemical Engineering Journal, *In press: doi:10.1016/j.cej.2015.04.119* (2015)

CONTRACTS

ANR Bioénergies AnaBioH_2 (2008-2012)
FUI BAMI (2008-2013)
LABEX IMobS_3, Challenge 3, AGVFuel project (since 2012)
PEPS thématique Cellule Énergie ScaleH_2 (2014)

PhD / Post Doc

V. Beligon, V. Kumar, A. Noblecourt, A. Patel, R.R. Singhania, Z. Trad

Scientific achievement #5
MELiSSA: the European Bioregenerative Life Support System project

MELiSSA (Micro Ecological Life Support System Alternative) has been conceived as an ecosystem based on microorganisms and higher plants, intended as a tool to gain understanding of the behaviour of artificial ecosystems. This concerns the development of technologies for a future biological life support system (BLSS) for long term manned space missions, e.g. a lunar/Mars bases or missions. Initiated in 1989, this European Space Agency (ESA) program is the leading Closed Ecological Life Support Systems (CELSS) European project. It involves ten teams in Europe and Canada. Since the beginning, GePEB group has a significant contribution for supporting the chemical engineering approach of the project, especially for bioreactor engineering: *(i)* cultivation, analysis, balances analysis in bioreactor; *(ii)* modelling by mechanistic approach at multi-scale level; *(iii)* High performance photobioreactors engineering.

MELiSSA project is one of the few CELSS developed in the world as a part of Environmental Control and Life Support Systems (ECLSS). The ECLSS consists of an air revitalization system, water coolant loop systems, atmosphere revitalization pressure control system, active thermal control system, supply water and waste water system, waste collection system and airlock support system. These systems interact to provide a habitable environment for the (space) flight crew in the crew compartment in addition to cooling or heating various orbiter systems or components. The driving element of MELISSA is the recovering of food, water and oxygen from waste (feces, urea), carbon dioxide and minerals. Based on the principle of an "aquatic" ecosystem, MELISSA is comprised of 5 main compartments (figure 1) colonised respectively by thermophilic anoxygenic bacteria, photohererotrophic bacteria, nitrifying bacteria, photosynthetic bacteria, higher plants, and the crew. MELiSSA is a collaborative project managed by ESA and involving several independent organisations: University of Ghent, University of Mons (B), University Blaise Pascal (GePEB) (F), SHERPA (F), SCK (B), VITO (B), University Autonoma de Barcelona (E) and University of Guelph (CDN). It is co-funded by ESA, the MELISSA partners, and several European delegations.

Since the beginning of MELiSSA, GePEB has been is involved in the 3 main phases of the project.

Phase 1 - basic research and development: the contribution of GePEB covers all the compartments of the MELiSSA loop. This concerns the analysis and the modelling of the compartments (bioreactors) and of the complete loop (feasibly, degree of freedom and ECLSS scenario) from a metabolic level scale up to the bioprocess scale.

Both microbiological and physical processes and bottlenecks were considered allowing the development of mechanistic models suitable for predictive control. This is used for design and for scale-up of the bioreactors. Obviously the tuning and validation of the models have required to performed lab-scale experiments (1 to 5-Litre bioreactors). The most relevant results obtained are illustrated by: (i) photobioreactor model (associated to a light diffusion model) used as well for control and for designing pilot scale photobioreactor (figure 1); (ii) nitrifying packed-bed model predicting non measurable variables such as fixed biomass distribution (figure 2). Current studies at GePEB deals also with higher plant growth chambers and interaction between plant growth and environmental conditions (gravity, humidity, etc.)

Phase 2 - preliminary Flight experiments: GePEB was involved in flight experiments projects such as: *(i)* design of a microgravity membrane photobioreactor for the study of the growth of *A. platensis*; *(ii)* design of an experiment for the validation of the atmosphere control (O_2 production / CO_2 removal) in a coupled animal compartment /photobioreator (BioRat project).

Phase 3 - ground and space demonstration: as photobioreactor and model experts in the MELiSSA group, GePEB is associated to the development of the MELiSSA Pilot Plant (MPP) assembled in Universitat Autotnoma de Barcelona. Basically, MPP is sized for fulfilling 100% of atmosphere, 100% of water and 20% of food for 1 man.

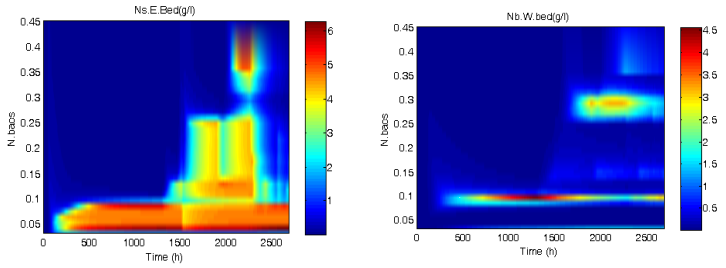

Fig. 2: Compartment 3 (nitrifying Packed Bed Reactor) modeling. Result of the distribution of the fixed biomasses of N. Europeae and Nb. Winogradskyi on the fixed bed during a 120 days continuous culture.

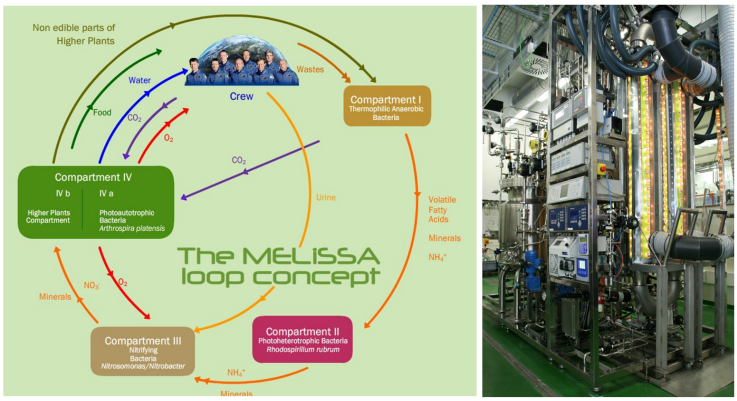

Fig. 1: MELiSSA loop concept: 4 micro-biological compartments (bioreactors) + Higher Plant chamber + crew habitat and MELiSSA 100L compartment 4a (A. Platensis photobioreactor) in operation in the MELiSSA Pilot Plant (Univertat Autonoma de Barcelona), designed from GePEB expertise in photobioreactors.

CONTACTS

Claude-Gilles DUSSAP
C-Gilles.DUSSAP@univ-bpclermont.fr
Catherine CREULY
Catherine.CREULY@univ-bpclermont.fr
Jean-Pierre FONTAINE
J-pierre.fontaine@univ-bpclermont.fr
Jean-François CORNET
j-françois.cornet@univ-bpclermont.fr
Laurent POUGHON
Laurent.POUGHON@univ-bpclermont.fr

FURTHER READING

Axenic Cultures of Nitrosomonas europaea and Nitrobacter winogradskyi in Autotrophic Conditions: a New Protocol for Kinetic Studies
B. Farges et al., Applied Biochemistry and Biotechnology 167, 1076 (2012)

Study of mass transfer by condensation in humid air for life support systems
A. Tiwari et al., Proceeding of ICES-2012, AIAA, 3562 (2012)

Knowledge models for the engineering and optimization of photobioreactors
J. Pruvost et al., in : *Microalgal Biotechnology vol.1 "Potential and Production"*, Editeurs: C.Posten and C.Walter, De Gruyter GmbH & Co. KG, Chap. 10, pp. 181-224, ISBN 978-3-11-022501-3

CONTRACTS

ITT ESTEC Contract (2010-2015)
TEC-MMG ESTEC Contract (2014-2016)
MPP-CNT ESA Contract (2013-2016)

PhD

N. Cruvellier, P. Hezard, L. Poulet, S. Sasidharan

Scientific achievement #6

Process for extraction and characterization of polysaccharides from endemic plants and macroalgae

Chemical compounds extracted from plants and algae are of primary interest as sources of novel texturing agents and biological active compounds. Polysaccharides have been largely identified as one of the major constituent responsible of these activities. Considering the wide structural heterogeneity of this class of polymers, this work aims at increasing the level of knowledge about the potential of natural polysaccharides from diverse ecosystems.

Since decades, polysaccharides are used in industry due to their abundance, renewability, non-toxicity, and biodegradability. These macromolecules have exceptional texturing properties that make them major players as additives and processing aids for numerous fields, from food to oil industries. Furthermore, their biological and physico-chemical properties are easily adjustable through chemical and/or biochemical modifications. Confined for a long time to energetic (starch, glycogen, glucomannan) or structural (cellulose, pectin, glycosaminoglycan) functions, the recent changes in the field of glycomic have updated multiple and complex biological functions. Today, polysaccharides are still underexploited for their biological activities except some glycosaminoglycans in medicine. Polysaccharides exhibit a large variety of chemical structures based on glycosidically-linked combinations of up to 40 different monosaccharides. Various substituents such as acyl groups, amino acids and sulfates may be attached, increasing the structural complexity. Thus, inventory of polysaccharide structures is still incomplete and steadily evolves thanks to commercial successes in various fields from niche markets (cosmetic, nutraceutic) to broader applications (food, adhesive, biosourced materials, …). Polysaccharides can be extracted from microorganisms (xanthan, scleroglucan,…), algae (alginate, carrageenan,…), shellfish (chitin,…), mammal (heparin, sulfate chondroitin,…) and plants (pectin, galactomannan,…). Endemic plants and macroalgae are good candidates to produce original green polysaccharides but this goal requires both controlling bioprocess for their extraction and purification. Respecting Nagoya protocol, this work is jointly conducted by GePEB and local (African, Asian) academic partners, notably through co-supervised PhD theses (Ouargla, Algeria; Antsiranana, Madagascar). Plants and/or algae are botanically defined, collected and dried; green extraction and purification processes are developed to obtain polysaccharides; analytical methods (NMR (^{1}H and ^{13}C), FTIR, HPAEC, GC/MS-EI and colorimetric assays) are then carried out to elucidate the structures of polysaccharides. They are then tested for their biological activities (anticoagulant, antimicrobial, antiparasitic, anti-inflammatory, prebiotic, etc.) and physicochemical properties (rheology).

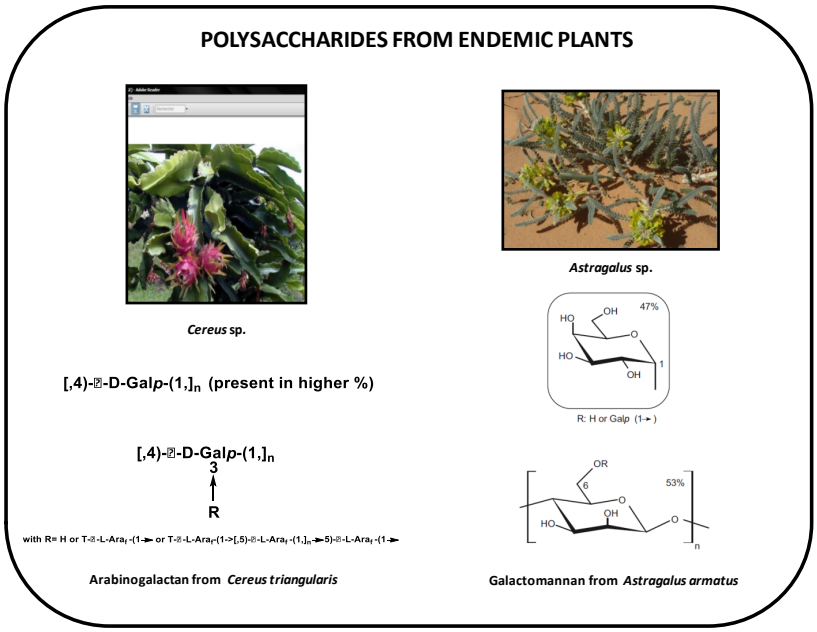

Fig. 1: Examples of two polysaccharides extracted from endemic plant from Africa.

In this context, two polysaccharides have been extracted from two endemic plants traditionally use in pharmacopeia in Africa. The first one was a galactomannan from *Astragalus armatus* Lam (Fabaceae), a semi-arid flowering plant mainly found in Septentrional Sahara of Algeria. The second one was an arabinogalactan-rich mucilage from *Cereus triangularis*, an epiphytic cactus of tropical dry zones of the North region of Madagascar.

CONTACTS

Cédric DELATTRE
Cedric.DELATTRE@univ-bpclermont.fr
Guillaume PIERRE
Guillaume.PIERRE@univ-bpclermont.fr
Philippe MICHAUD
Philippe.MICHAUD@univ-bpclermont.fr

FURTHER READING

Characterization of arabinogalactan-rich mucilage from Cereus triangularis cladodes
B. Petera et al., Carbohydrate Polymers 127, 372 (2015)

Mediterranean semi-arid plant Astragalus armatus as source of bioactive galactomannan
Z. Boual et al., Bioactive Carbohydrates and Dietary Fibre 5, 10 (2015)

Galactans and its applications
G. Pierre et al., *In:* Polysaccharides, K. Gopal Ramawat, J.-M. Mérillon (Eds.), SpringerLink (2014)

CONTRACTS

Partenariat Hubert Curien TASSILI 2015

PhD

F. Benaoun, T. Chouana, B. Petera

Scientific achievement #7
Interface phenomena and FUI Valeco^2

In France, over 190000 t/year of cooked ham are produced inducing the generation of 13000 m^3 of effluents containing mainly proteins and salt. Poorly valorised and classified as wastes, these effluents must be treated to avoid environmental impact. An efficient utilization of these effluents could also increase the profitability of cooked ham industry. The key ingredient for valorization of liquid effluent remains the protein not only because of its amphiphilic character but also by its effect on the rheological behavior and the stability of the final product. That is why extraction and characterization of this ingredient from different raw materials (including bioresources and meat co-products) is included in the research activity. These competences lead us to be involved as a main partner in a research program (Valeco^{2}*) including three industrial partners for the valorization of portions from ham liquid effluents.

Investigation on the phenomena at the interfaces between liquid/liquid (emulsion) and gas/liquid (foaming) in multi-component systems is one of the main activities in our lab. This is a multi-scale *"formulation/process/product"* original approach whose main objective is (i) to understand how and with what kinetics an ingredient (protein, polysaccharides, fat) integrates a global matrix and observe the consequences on the rheological and interfacial properties of the matrix; (ii) to study the combined effect of matrix properties and operating conditions (residence time, mixing condition, gas and liquid flow rates) on the properties of the final product (texture, stability, rheological properties). Based on 20 years of experience on academic and industrial scientific programs the main results are:

- Design of an original device for the production of aerated material (figure 1a).
- Development of an on-line image analysis system (figure 1b and 1c).
- Expertise on the relation between rheological properties of the continuous phase (viscosity, pseudo-plasticity...) and the mechanism of gas dispersion in given devices.
- Expertise on the relation between proteins properties (surface and interfacial tension) and the mechanism of gas dispersion in given devices.
- Generalization of the Weber number in laminar flow for scale-up purposes in foaming processes.
- Applications on model food close to commercial products: ice cream, whipped cream, meat foam.

The know-how on the interface phenomena allowed us to obtain the following data for the valorisation of proteins from ham liquid effluent during the past two years:

- Determination of the effluents compositions and rheological properties.
- Concentration by ultrafiltration and spray-drying.
- Determination of functional properties of proteins matrix (salt and protein mixture) as emulsifying or foaming agents.
- Elaboration of model food using ingredient from native and concentrated effluents (figure 2).

Based on these results, an industrial recipe is being developed by one of the industrial partners.

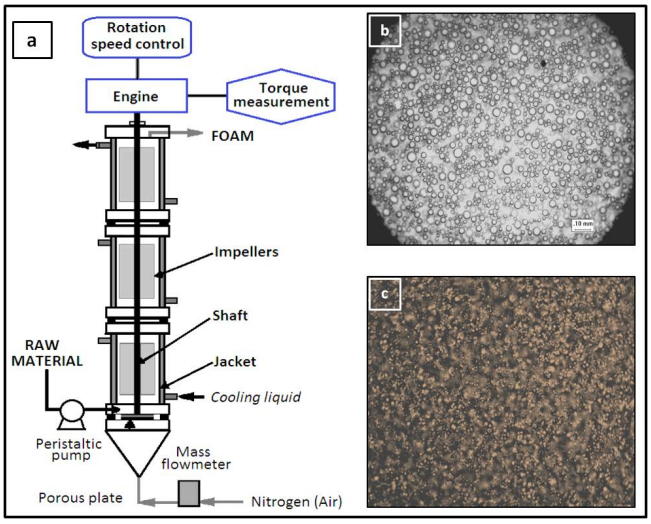

Fig. 1: Original devices developed in the lab for the study of interfacial phenomena: a) Stirred column with narrow annular gap for the steady-state generation of foams; b) on-line measurement of foams bubbles diameter; c) visualization of an emulsion.

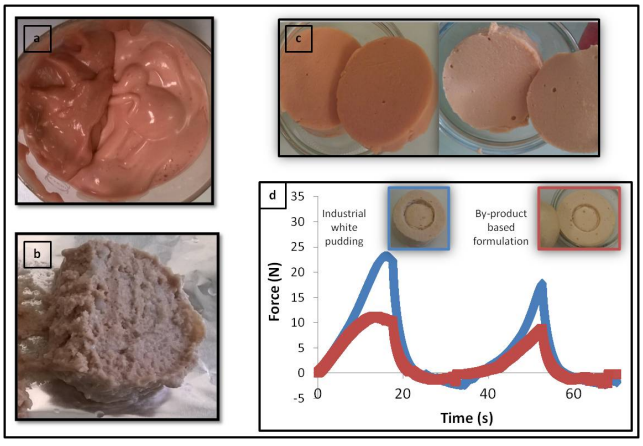

Fig. 2: Formulations developed using ham industrial effluents: a) liver mousse before (dark reddish) and after air incorporation (pink), b) example of liver mousse after cooking; c) examples of sausage-type formulation using various ratio of effluents; d) comparison of texture profile analyses of industrial product and a formulation developed in the project.

CONTACTS

Gholamreza DJELVEH
gholamreza.djelveh@ensccf.fr
Alain MARCATI
alain.marcati@ensccf.fr

CONTRACTS

FUI Valeco2 (Valorisation économique et écologique des coproduits)

Scientific achievement #8
Na-Project: how to reduce salt content in dry and cooked hams

Sodium chloride is the main ingredient in pork meat processing. Food business operators of the meat industry initiated the lowering of sodium chloride content of their products. Nut, they have reached a level, which is further hard to lower with actual practices. The aims of the project were:

- To have a better understanding of the links existing between quantity of sodium added during the manufacturing and the qualities of the products.
- To identify parameters that can be used as indicator for the qualities of the products.
- To design a modelling tool which can help food business operators to have a global and rational approach to propose products with lower sodium content and appropriate qualities.

For several years, the health authorities try to decrease the consumption of sodium responsible for the high blood pressure and for the cardiovascular diseases. The producers of hams have accept to participate to the challenge of the Na- project that was to reduce by 60% the amount of NaCl used during the manufacturing of cooked or dry ham while keeping the nutritional and sanitary qualities of these products.

A classical approach of process improvement by trials and errors is always very long and expensive especially in the case of the dry ham, because nine months are needed on average to obtain a dry quality ham. It is thus necessary to develop process simulators, which can predict the evolution of the sensory, nutritional and sanitary qualities of hams according to the parameters controlling the process (temperature and relative humidity of the air or the salting conditions for example). To do this, it is necessary to establish the laws of the temperature evolution in ham, of the salt penetration, of the texture variation and so on. The developed simulators will allow the companies to strongly decrease the quantities of salt used during production and to satisfy the expectations of the public authorities and of the consumers.

Describing the transformation of meat in dry or cooked ham is equivalent to describe a set of physical, chemical, biochemical and microbiological processes: heat and mass transfers cause the advent of differences of temperature and concentration (water, salt, etc.) in the product. These differences in temperature and in local composition involve differences in physicochemical properties (pH, etc.), which determine the microbial growth rate or the evolution sensorial properties. Experimental techniques have appealed to the thermodynamics of solutions, to process engineering, to biochemistry and to microbiology. They allowed for example to better understand the evolution of dry-cured ham texture or the sliceability of cooked ham (adhesion of two muscles in of cooked ham).

The data obtained were then processed by mathematical model. They simulate numerically the current processes or new processes. By varying the inputs (temperature, salt content, etc.), it is possible to determine the evolution of the properties of dry ham 24 to 48 h instead of 9 months.

Describing the transformation of meat in dry or cooked ham is equivalent to describe a set of physical, chemical, biochemical and microbiological processes: heat and mass transfers cause the advent of differences of temperature and concentration (water, salt, etc.) in the product. Experimental techniques have appealed to the thermodynamics of solutions, to process engineering, to biochemistry and to microbiology. They allowed for example to better understand the evolution of dry-cured ham texture or the sliceability of cooked ham (adhesion of two muscles in of cooked ham).

The data obtained were then processed by mathematical models. Process simulators have been developed by combining all of these models. They simulate numerically the current processes or new processes. By varying the inputs (temperature, salt content, etc.), it is possible to determine the evolution of the properties of dry ham 24 to 48 h instead of 9 months .

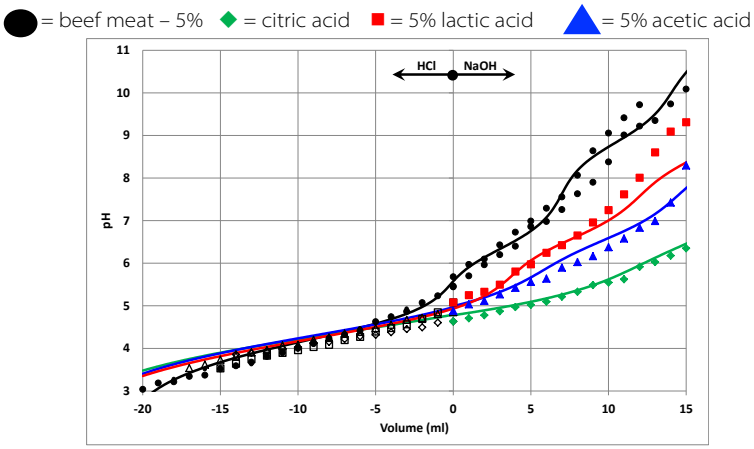

Fig. 1: Comparison between experimental and calculated titration curves of meat and meat with one organic acid at 25°C (symbols = measurement – lines = prediction).

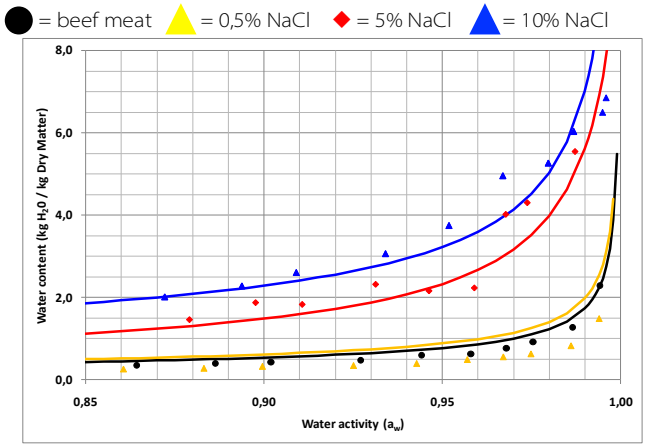

Fig. 2: Incidence of different NaCl content on beef meat sorption isotherms curves measured and predicted at 25°C (symbols = measurement – lines = prediction).

CONTACTS

André LEBERT
Andre.LEBERT@univ-bpclermont.fr
Claude-Gilles DUSSAP
c-gilles.dussap@univ-bpclermont.fr

FURTHER READING

Titre ?
R. Harhouss et al., Food Chemistry 151, 7 (2014)

Titre ?
O. Touré et al., Oil & Gas Science and Technology 68(2), 178 (2013)

Titre ?
O. Touré et al., Chemical Engineering Research and Design 92(11), 2873 (2014)

CONTRACTS

ANR Alia Na-Project (2010-2013)

PhD

L. Bombrun, R. Harhouss, O. Touré

Scientific achievement #9
Prediction of the equilibrium properties in biomedia with COSMO-RS

The prediction of the equilibrium properties of in biomedia requires fully predictive thermodynamic models, knowing their highly complex composition. The chemical potential is a key variable. It depends on two variables: the Gibbs free energy of formation and the prediction of the activity coefficient. The aim of this work in GePEB is to take benefit of the predicting capacity of COSMO-RS, which is extensively used in chemical engineering calculations, adapting the approach to electrolyte, carbohydrate and macromolecules solutions. A tool based on the recent advances of quantum mechanics has been developed in order to predict gas phase formation properties. By combining concepts of thermodynamics, quantum physics, electrostatics and statistical physics, it has been demonstrated that it was possible to use the COSMO-RS to predict physicochemical and formation properties (a_W, pH, E_h) in food and biological systems.

The simulation and optimization of processes require the knowledge of the physicochemical properties of pure components and mixtures that are involved. Indeed, processed foods (like cooked or dry meats, milk, honey, or juices), medicines, and biochemical solutions are all a myriad of interacting dissolved solute molecules. Water is generally the main component in most of these systems and equilibrium properties of water are considered as reference properties (*e.g.* water activity) in food processing. Foods and biological solutions are generally treated as aqueous mixtures that are very complex these media containing a wide variety of components, including for example organic compounds (sugars, organic acids), salts or electrolytes, dissolved gases and macromolecules. Due to the presence of different (liquid, solid and gaseous) phases, the modeling of such systems requires a homogeneous treatment of both physical equilibria (*e.g.* VLE, LLE, SLE) and chemical equilibria (*e.g.* dissociation, hydration, complexation and redox) as mentioned in the previous studies performed in our lab.

In the framework of an ANR project (project 'Na moins') the objective was to update the previous approaches with recent thermodynamic models of solution. The main goal was to develop a predictive thermodynamic model that enables to characterize the equilibrium thermodynamic properties in the aqueous mixtures encountered in food and biological systems and to compensate for the lack of experimental data or more exactly for the huge number of variables that appear in a complex biological solution. By comparing these models, our choice leads to the COSMO-RS (Conductor-like Screening Model for Real Solvents) model for the representation of short-range interactions.

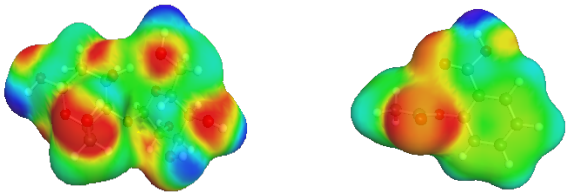

Fig. 1: Examples of COSMO simulations: lactose and aspirin.

In comparison to classical predictive models based on the concept of group contributions, like UNIFAC, the chosen model does not require the knowledge of any pure component data and does not need any binary interaction parameters. The COSMO-RS method is an *a priori* fully predictive method widely used in chemical engineering. Our goal was to apply it to biological systems and to add electrostatic and chemical hydration terms, deriving a new extension of COSMO models: COSMO-RS-PDHS-V (1, 2). The advantage is that COSMO-RS is an excess Gibbs energy model, like UNIFAC, not requiring identification of interactions parameters between chemical groups, offering the capability to predict properties of reaction such as pK_a values for several components of interest in food and biological systems like amino-acids, dipeptides and tripeptides (3,4), redox potentials, etc.

The predictive power of the COSMO-RS-PDHS-V model was investigated for ions (H^+, Li^+, Na^+, K^+, Cl^-, Br^-, I^-) the predicted water activity and mean activity coefficients of salts being in excellent agreement with experimental data (1 to 4). Similarly the model was validated on a large set of systems containing electrolytes and carbohydrates, the COSMO-RS-PDHS-V appearing as the most promising and fully predictive activity coefficient model, *i.e.* an excellent model for excess properties. The model is now extended for the prediction of formation and thermochemical properties of metabolites, opening the applications to the understanding of the energetics of metabolic fluxes regulation (ANR AlgoH2).

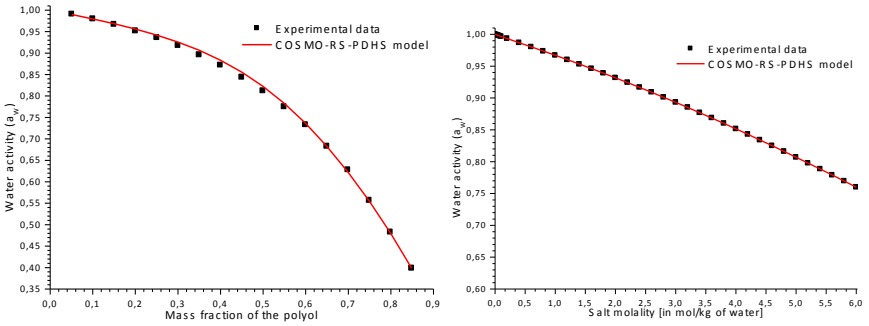

Fig. 2: Water activity in NaCl and glycerol solution by COSMO-RS-PDHS-V.

CONTACTS

Claude-Gilles DUSSAP
C-Gilles.DUSSAP@univ-bpclermont.fr
André LEBERT
Andre.LEBERT@univ-bpclermont.fr
Fabrice AUDONNET
Fabrice.AUDONNET@univ-bpclermont.fr

FURTHER READING

Titres ?
O. Toure et al., The Canadian Jounral of Chemical Engineering 93(2), 443 et 465 (2015)

Titre ?
O. Toure et al., Chemical Engineering Research and Design 92(12), 2873 (2014)

Titre ?
O. Toure et al., Oil & Gas Science and Technology–Revue d'IFP Energies nouvelles 68(2), 281 (2013)

CONTRACTS

ANR Na-Moins (2011-2014)
ANR AlgoH2 (2012-2015)
Contrats de recherche : Société Roquette Frères (2014 et 2015)

PhD

N. Soane, O. Touré

Scientific achievement #10
Use of the oxidoreduction potential in food and bioreactor processes

Oxidoreduction potential (ORP) is the tendency for a compound to acquire electrons. Thus, two compounds are required for an oxidation–reduction reaction to occur, during which the reducing compound donates electrons to the oxidizing compound. Compared to pH value that provides information of protons, ORP represents "activities of electrons". Therefore, ORP is more sensitive to delicate changes of intracellular metabolism and is thus now considered as a new external parameter to control all the processes where electron transfer is implied. Concerning the GePEB group, the study of the influence of the ORP concerns food and bioreactors applications.

Fermentations have a long history since human ancestor started to produce flavor food and beverages. Many of these fermentations are anaerobic or microaerobic for desirable flavors, and in the meantime for contamination control since most unwanted microbes propagate quickly under aerobic conditions. More recently, biofuels such as ethanol and butanol produced under microaerobic and anaerobic fermentation conditions respectively have garnered worldwide attention to address concerns on the sustainable supply of crude oil and the impact of over-consumption of petroleum-based products, particularly transportation fuels, on ecological environment.

Unlike aerobic cultures and fermentations in which dissolved oxygen can be monitored online, a big challenge for microaerobic and anaerobic fermentations is lacking of real-time process monitoring technologies, since pH detection that is commonly employed with these fermentation processes reflects proton activity only, and thus is not sensitive to delicate changes of intracellular metabolism. Redox potential, known as oxidoreduction potential (ORP), reflects overall electron transfer and redox balance involved in intracellular metabolism. Although ORP theory and measurement have been well established with relatively simple chemical reaction systems, investigation on ORP's impact on intracellular metabolism, the core of complex biological systems, and applications of ORP control in bioprocess engineering are still very limited.

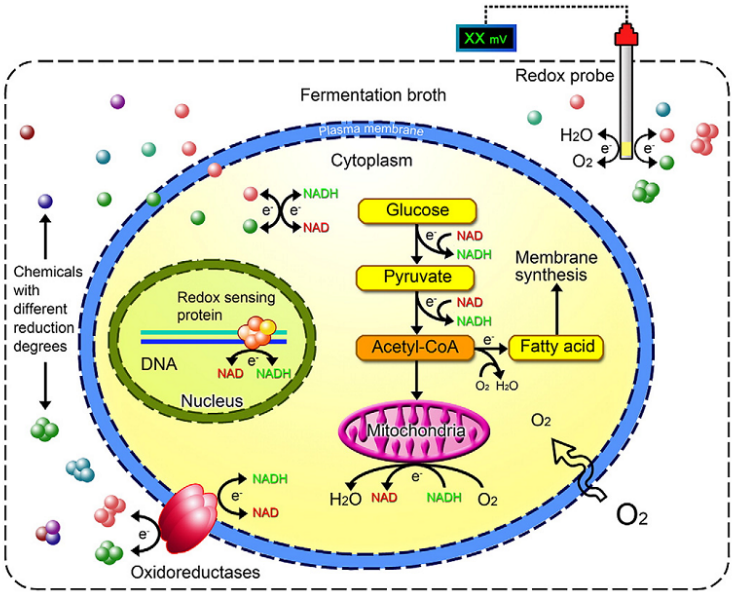

*Fig. 1: Figure from Liu et al., Biotechnology Advances, **31**, 257–265 (2013). Interactions between environmental redox potential (ORP) and intracellular metabolism characterized by electron transfer and redox balance. The ORP of fermentation broth is determined by chemicals with different reduction degrees such as dissolved oxygen. Intracellular ORP, dominated by the ratio of NAD(P)H/NAD(P)$^+$, can be affected by metabolism and extracellular ORP level.*

Some advanced technologies, such as nanosensors that can penetrate into individual cells, have been developed to measure intracellular ORP directly for deep understanding on intracellular redox balance and impact on cell physiology and metabolism. However, extracellular ORP, which can be detected conveniently in fermentation broth, reflects intracellular ORP status. Therefore, as illustrated in Fig. 1, ORP control strategies can be developed and applied for altering intracellular ORP conditions and metabolic profiles.

Another field where the ORP is under development concerns the food industry. Indeed, a recent investigation with one major distribution group has shown that about 3% of meats are taken away due to problems of color or microbiology, without counting the withdrawals of out of date products. Moreover, processed meat products such as dry sausages are also often affected by defects linked to alteration phenomena that reduce the organoleptic quality of products or to the contamination by pathogens that make unsafe consumption. Thus, it becomes necessary to limit such defects by adapting conservation techniques according to the type of product. For example, new constraints are going to be added to cooked and dry meat products as dry sausages by reducing nitrites and nitrates content. These technological ingredients are usually used to inhibit pathogenic bacteria and to develop a typical characteristic colour and taste. The reduction of the nitrites/nitrates content, even their complete disappearance, can be envisaged by acting on the ORP by at least two different ways: modification of process conditions and use of selected starters. The use of the COSMO-RS modeling (see Scientific Achievement #9) seems to be a good starting point to improve the process conditions.

CONTACTS

Fabrice AUDONNET
Fabrice.AUDONNET@univ-bpclermont.fr
Claude-Gilles DUSSAP
C-Gilles.DUSSAP@univ-bpclermont.fr
Pierre FONTANILLE
Pierre.FONTANILLE@univ-bpclermont.fr
André LEBERT
Andre.LEBERT@univ-bpclermont.fr

CONTRACTS

FRI2 Cluster RedPot (2013-2014)
FRI2 Cluster RedPot^2 (2015-2016)

Scientific achievement #11
Electrocoagulation as a pretreatment for seawater desalination

An original application of electrocoagulation (EC) devoted to the pretreatment of reverse osmosis (RO) for seawater desalination has been developed. The objective was to enhance the removal of natural organic matter and of weakly soluble inorganic compounds so as to improve the shelf life of the RO membranes and reduce their maintenance cost. Within the framework of a French-Moroccan PICS program between CNRS/CNRST, an EC cell has been designed by the GePEB group which removes efficiently organic compounds and a pilot plant powered by solar panels will be built in Morocco next year.

Fresh water is vital to life, but it becomes scarce, especially around the Mediterranean Sea, not only in North Africa, but also in Southern Europe, as the resources are adversely affected by climate change and population growth. To tackle the problem of water scarcity, reverse osmosis (RO) is the most reliable and cost-effective technology for producing fresh water from seawater. But a disadvantage of RO is the need for significant preconditioning of the feed water to protect the membranes: chemicals for pretreatment and cleaning constitute one of the major operating and maintenance costs of seawater desalination.

Electrocoagulation (EC) is a non-specific electrochemical water and wastewater treatment that uses the anodic corrosion of a metal for pollution abatement. It consists in the controlled dissolution of metal cations using constant electrical current. These can play the role as a coagulant, a precipitating and an adsorbent. EC is able to remove nearly all the types of polluting substances: natural or anthropic organic matter, suspended solids and colloids, heavy metals, turbidity, colour, but also inorganic anion [1] and organic micropollutants [2] (T. Yehya's PhD). Electrical power requirements are weak in seawater due its high conductivity. EC is, therefore, attractive to address the pretreatment of seawater in which salinity, temperature and the composition of microbial communities that promote membrane biofouling may strongly vary.

Within the framework of a French-Moroccan PICS program between CNRS/CNRST (2014-2016), the objective of the GePEB group of Institut Pascal was to design an EC cell able to remove efficiently organic and inorganic compounds, so as to better prevent colloidal and biological fouling, while avoiding chlorine damage in RO.

The research program is aimed at building a hybrid EC-RO pilot plant in Morocco with the financial support of the Moroccan CNRST (300k€) and the Hasan II University of Casablanca (75 k€). The strategy involved the design of a lab-scale continuous EC cell that includes all the technologies of the pilot plant unit through a modelling approach based on Computational Fluid Dynamics (CFD), so as to predict the hydrodynamics, the potential distribution within the electrodes and the spatial distribution of coagulant species [3]. The objective was to predict the quality of EC effluents for coupling the EC call and the RO unit, while establishing a scale-up methodology that could be used for other applications of EC for water and wastewater treatment.

The EC cell designed in the GePEB group in 2014 (Fig. 1) has been tested using real seawater in Morocco, highlighting the ability of EC to remove efficiently the natural organic matter of seawater and 30% of the initial calcium content. Simulations (Fig. 2) predict within 5% the spatial distribution of coagulant.

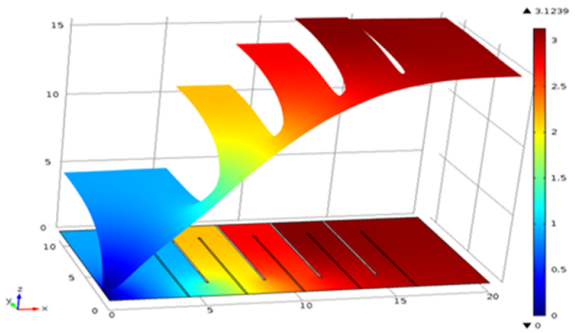

Fig. 2: Simulation of the spatial distribution of the coagulant in the EC cell.

This opens the gate to the treatment of EC effluents in the RO unit for the optimization of the pioneering EC-RO process, and to future applications for the recovery of marine microalgae using EC for bioenergy production (N. Fayad's PhD).

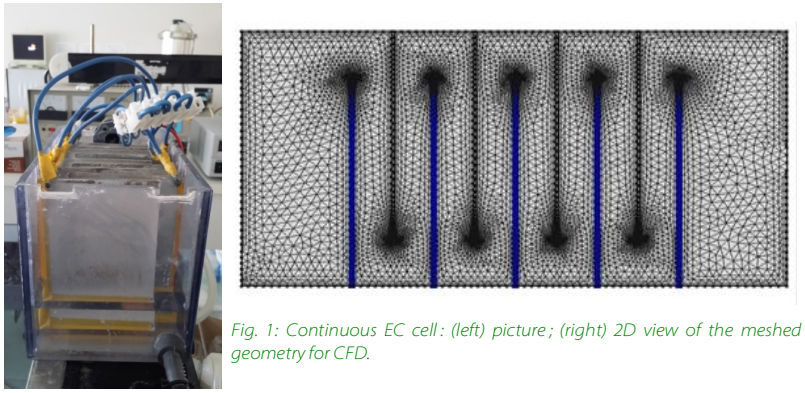

Fig. 1: Continuous EC cell : (left) picture ; (right) 2D view of the meshed geometry for CFD.

CONTACTS

Christophe VIAL
Christophe.VIAL@univ-bpclermont.fr
Fabrice AUDONNET
Fabrice.AUDONNET@univ-bpclermont.fr

FURTHER READING

[1] *Experimental analysis and modeling of denitrification using electrocoagulation process*
T. Yehya et al., Separation and Purification Technology 132, 644 (2015)

[2] *Removal of carbamazepine by electrocoagulation: investigation of some key operational parameters*
T. Yehya et al., Environmental Engineering and Management Journal 14, 639 (2015)

[3] *Modeling and Simulation By CFD of an Electrocoagulation Reactor*
M. Acil et al., Proceedings of the 12th International Conference on Gas-Liquid & Gas-Liquid-Solid Reactor Engineering - GLS12, New York, USA (2015)

CONTRACTS

PICS CNRS-CNRST ECOSEAD (2014-2016)

PhD

N. Fayad, T. Yehya

Scientific achievement #12
Surface reconstruction

Most of methods for the automatic surface reconstruction from an image sequence include both structure-from-motion (SfM) and dense stereo. From the computational standpoint, it would be interesting to avoid dense stereo and to generate a surface directly from the sparse cloud of 3D points and their visibility information provided by SfM. In this context, we introduce methods that maximize the visibility consistency encoded in a 3D Delaunay triangulation of the sparse cloud and enforce the manifold constraint. We experiment with car/hand/helmet-held omnidirectional cameras and generate 3D models from images taken in cities.

The automatic 3d modeling of environments using images is still an active topic research in Computer Vision. Standard methods have three steps : moving a camera in the environment to take an image sequence, reconstructing the geometry, and applying a dense stereo method to obtain a surface model of the environment. In the second step, interest points are detected and matched in images, then camera poses and a sparse cloud of 3d points corresponding to the interest points are simultaneously estimated. In the third step, all pixels of images are used to reconstruct a surface by estimating a dense cloud of 3d points or by optimizing photo-consistency.

Since the third step (dense stereo) is computationally expensive and sometimes impossible in the low textured areas of the input images, we propose to generate a surface directly from the sparse point cloud and its visibility information provided by the second step (geometry estimation). Advantages are low time and space complexities ; this is also useful for obtaining compact models of large and complete environments like a city.

To do so, we propose a surface reconstruction method based on sculpting the 3d Delaunay triangulation of the reconstructed points. This triangulation is a partition of the convex hull of the points into tetrahedra, and the target surface is searched as a subset of the triangle faces of these tetrahedra. Two kinds of constraints are enforced on the surface: it should be a 2-manifold and meet the visibility constraints "as most as possible". The manifold constraint regularizes the surface and is required for a lot of post-processing such as denoising, refinement by photo-consistency optimization, and rendering. The visibility information is used to classify the tetrahedra in free-space and matter: every free-space tetrahedron is intersected by at least one ray (line segment) between a reconstructed point and a camera location. Then a greedy method estimates a subset O of free-space tetrahedra such that the sum of their ray intersections is maximal under the constraint that the boundary B of O is a 2-manifold surface. The final surface is B followed by standard post-processing. This method is also extended to the incremental case: each time a new key-frame is selected in the input image sequence, new 3d points and camera pose are estimated, then the reconstructed surface is locally updated.

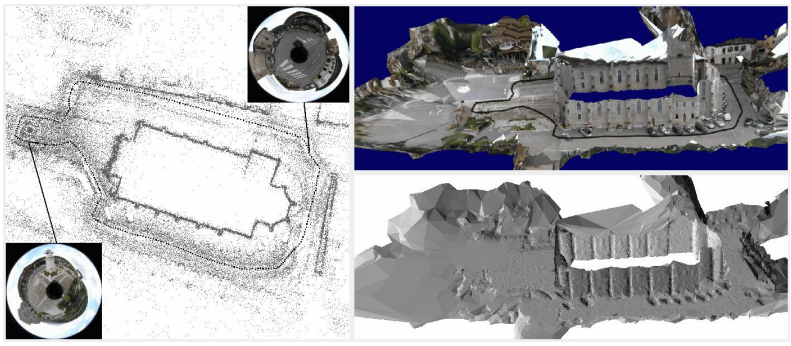

Fig. 1: Overview of the results for a hand-held (catadioptric) camera. Left: top view of 136k points and 343 poses reconstructed by SfM and images of the sequence. Right: oblique views of the resulting surface (152k triangles) including triangle normals (gray) and trajectory (black).

In experiments, textured models of complete environments (including ground, building, vegetation) are reconstructed thanks to the use of omnidirectional cameras. The geometry step is done using structure-from-motion methods previously developed in our team. An example is provided in the joint figure using 343 images taken by a hand-held catadioptric camera during a complete walk around a church. Future work can improve the surface quality while staying in our sparse feature scheme and maintaining a low computational cost: reconstruct and integrate the image contours in the 3D Delaunay, improve both optimized score function and matching, design a dedicated surface denoising method for sparse SfM point clouds.

CONTACTS

Maxime LHUILLIER
Maxime.LHUILLIER@univ-bpclermont.fr

FURTHER READING

Manifold surface reconstruction of an environment from sparse structure-from-motion data
M. Lhuillier et al., Computer Vision and Image Understanding 117, 1628 (2013)

CONTRACTS

ANR Predit City VIP (2010-2013)
Convention allocation recherche "Bourse recherche filière" + FEDER (2011-2014)

PhD

V. Litvinov, S. Yu

Scientific achievement #13
Pose and motion estimation with non-global acquisition cameras

We study the development of spatio-temporal projection models and 3D pose and motion estimation, for use on cameras whose acquisition mode is not global, such as rolling shutter or dynamic region of interest (ROI) reconfiguration. In the case of rolling shutter, we proposed a polynomial and globally convergent monocular pose and velocity computation method which handles distortions due to motion during image acquisition. Unlike previous methods, this formulation does not require an initial guess of the solution. This makes possible its use for automatic feature matching in a RANSAC framework. In the case of dynamic ROI reconfiguration, we proposed a very fast 3D motion tracking basing on a sequential acquisition of small ROIs centered on interest points instead of the entire image to reduce the amount of data to transfer and to process.

In earlier work we have developed a geometrical projection model for rolling shutter cameras which enables to compute simultaneously the pose and the velocity of a known rigid object. This can be seen as the PnP problem augmented with the instantaneous velocity. All the methods were based on the optimization of a non linear cost function using iterative least squares. After that, we proposed two different formulations of the pose and velocity estimation.

The first proposed method is a polynomial projection model for rolling shutter cameras and a constrained global optimization of its parameters. This is done by means of a semi definite programming problem obtained from the generalized problem of moments method. Contrarily to previous work, our optimization does not require an initialization and ensures that the global minimum is achieved. This allows us to build automatically robust 2D-3D correspondences using a template to provide an initial set of correspondences. Experiments show that our method slightly improves previous work on both simulated and real data. This is due to local minima into which previous methods get trapped. We also successfully experimented building 2D-3D correspondences automatically with both simulated and real data [1].

The second approach proposes a generic model for rolling shutter cameras and its application to the estimation of a dynamic, time-varying, pose. The model parameters are initialized from a 'Piecewise Global Shutter' approximation and refined by a non-linear minimization of the reprojection error under 'Derivative Based Smooth Rolling Shutter' constraints. Contrary to previous work, our rolling shutter camera model makes it possible to estimate non uniform dynamic pose [2].

The spatio-temporal projection model was also adapted to the problem of high speed 3D pose tarcking. The main problem in high speed vision is the bottleneck phenomenon which limits the video rate transmission.

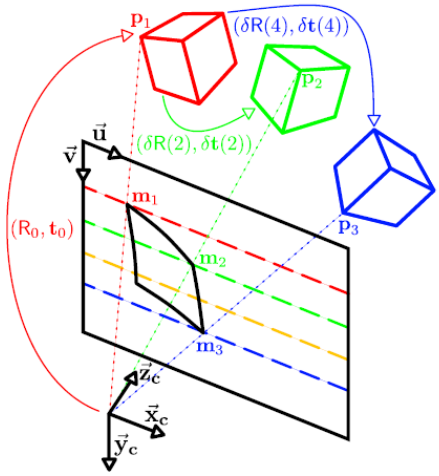

Fig. 1: Spatio-temporal projection model of a moving object viewed by a rolling shutter camera. Each point Pi of the object projects on pixel raw at a different times ti.

The proposed approach circles the problem out by increasing the information density instead of the data rate transmission. This strategy is based on a rotary sequential acquisition of selected regions of interest (ROI) which provides space-time data. This acquisition mode induces an image projection deformation of dynamic objects. We show how to use this artifact for the simultaneous measure of both pose and velocity, at the same very high frequency as the ROI's acquisition one. Thanks to this work two versatile control laws were developed for robot arms control : a position-based dynamic visual servoing and an image based dynamic visual servoing. Both control laws were designed to compute the control torques exclusively from a sequential acquisition of regions of interest (ROI) containing the visual features to achieve an accurate trajectory tracking [3].

Current work focuses on adapting the proposed methods to multiple view geometry in order to achieve fast 3D reconstruction and localization under specific constraint such as non-holonome motion.

Fig. 2: Only data from a rotary sequential acquisition of selected regions of interest are sent to the system memory and used for 3D pose tracking.

CONTACTS

Omar AIT AIDER
Omar.AIT-AIDER@univ-bpclermont.fr

FURTHER READING

[1] *Global Optimization of Object Pose and Motion from a Single Rolling Shutter Image with Automatic 2D-3D Matching*
L. Magerand et al., European Conference on Computer Vision (ECCV), 456 (2012)

[2] *A Generic Rolling Shutter Camera Model and its Application to Dynamic Pose Estimation*
L. Magerand et al., 3D Data Processing, Visualization and Transmission (3DPVT) (2010)

[3] *Dynamic visual servoing from sequential regions of interest acquisition*
R. Dahmouche et al., nternational Journal of Robotic Research (IJRR), 31(4), 520 (2012)

CONTRACTS

ANR Jeunes Chercheurs VIRAGO (2007-2011)

PhD

R. Dahmouche, L. Magerand

Scientific achievement #14
Constrained structure from motion

The real-time localization of a camera in an unknown or partially known environment is a problem addressed by CSLAM algorithms (*Constrained Simultaneous Localization And Map- ping*). We propose several major contributions to improve structure from motion based methods applied to CSLAM: 1) new sensor fusion framework, 2) new parameters families and 3) heterogeneous constraints. We show improvement of localization accuracy and precision related to state of the art methods on both robotic and augmented reality applications. These contributions have been published into state of the art journal and patented.

SLAM technics compute at the same time the 3D pose of the camera and features from the environment using a sequence of temporally ordered images. Two different formalizations are used to solve this problem: probabilistic methods based on a recursive bayesian filter, and optimization methods based on bundle adjustment. We focus on bundle adjustment (BA) methods that offer a good trade-off between accuracy and execution time. Usually, SLAM algorithm minimizes the reprojection error corresponding to the distance in pixel between the 3D point projected in a camera frame and the observed feature. However, these methods suffer from the scale factor drift and the error accumulation. To tackle these limitations, several contributions have been published or patented by Institut Pascal.

We have proposed a perception system with two non-overlapped camera (rear and front) to solve the scale factor drift. The distance between the two sensors has been introduced as a constraint into the 3D reconstruction algorithm and an original calibration method has been developed. This solution is currently exploited within the EZ10 car (international patent). Other sensors information can provide constraints like laser sensors or GPS. New bundle adjustment algorithms have been proposed to fuse GPS and Vision information in the same process while ensuring an upper bound on the final reprojection error [Lhuillier]. These methods are incremental and can process several kilometers video sequences from a camera embedded onto a car.

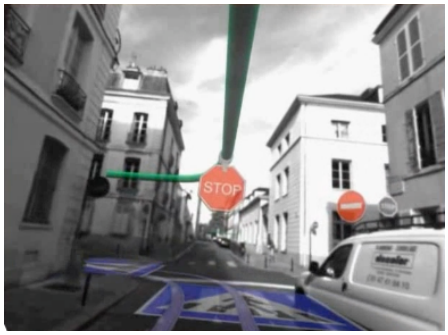

Fig. 1: Augmented reality from a constrained SLAM algorithm. A prior map is used to superimpose information related to the way to follow or traffic signs.

One of the key ideas of constrained SLAM is to use prior models to add constraints within the bundle adjustment. In [Tamaazousti], constraints provided by an accurate model of the observed object are added into the Bundle adjustment. Visual features (interest points and edges) are divided into two categories: 1) those belonging to a known object are constrained to be projected onto the surface of the 3D object model and 2) 3D reconstruction of the other features is achieved without additional constraint. High-level models like semantic maps may also be used to constraint 3D points to belong to building planes [Larnaout].

Constrained SLAM technics have been used for both real time localization and augmented reality applications (Fig.1 and Fig.2).

Future works include new constraints (provided by sensors, maps or known objects) and parameterizations for constrained SLAM applied to various applications such as reality augmented, mobile robot localization or medical imaging.

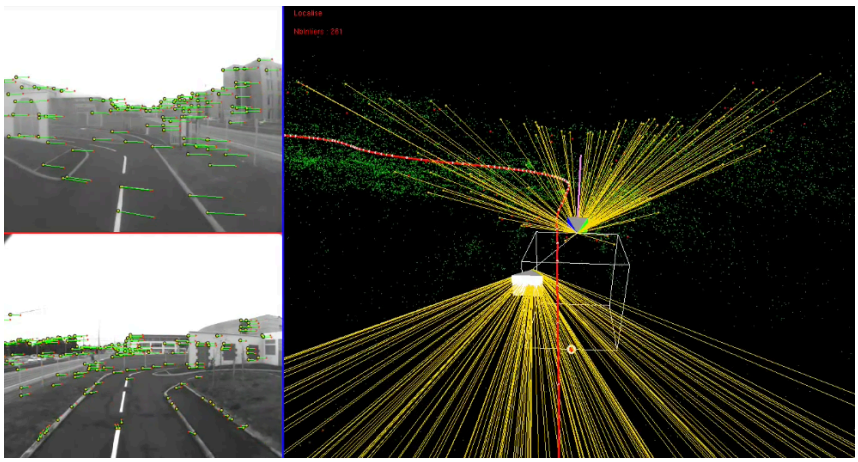

Fig. 2: An illustration of a mobile robot vision based localization process with: 1) top left, the front camera view 2) bottom left, the rear camera view and 3) right the 2D/3D localisation process.

CONTACTS

Michel DHOME
Michel.DHOME@univ-bpclermont.fr
Eric ROYER
Eric.ROYER@univ-bpclermont.fr
Maxime LHUILLIER
Maxime.LHUILLIER@univ-bpclermont.fr
Thierry CHATEAU
Thierry.CHATEAU@univ-bpclermont.fr

FURTHER READING

Non Linear refinement of structure from motion reconstruction by taking advantage of a partial knowledge of the environment
M. Tamaazousti et al., 2011 IEEE Conference on Computer Vision and Pattern Recognition (CVPR), 3073 (2011)

Incremental Fusion of Structure-from-Motion and GPS Using Constrained Bundle Adjustments
M. Lhuillier et al., IEEE Transactions on Pattern Analysis and Machine Intelligence 34(12), 2489 (2012)

Driving in an augmented-city: from fast and automatic large scale environment modeling to on-line 6DOF vehicle localization
D. Larnaout et al., Proc. of the 12th ACM SIGGRAPH Int. Conf. on Virtual-Reality Continuum and Its Applications in Industry, 9-16 (2013)

CONTRACTS

Projet Régional VIPA (2008-2011)
Thèse CEA
Bourse Région

PhD/Post Doc

D. Larnaout, P. Lebraly, D. Ramadasan, M. Slade, M. Tamaazousti

Scientific achievement #15

Technology transfer: from a Visual SLAM algorithm to an autonomous vehicle/shuttle ready for industrialisation

An autonomous vehicle/shuttle has been developed based on a visual SLAM algorithm. This work was started in 2003 and continuously improved. During the 2010-2015 period, the algorithm reached a state which allows its transfer to an industrial partner in order to be embedded in a commercial autonomous shuttle named EZ-10. This highlight details the scientific advances which led to this technology transfer.

The work on visual localization of a mobile robot started in 2003. The first achievement was the ability to drive autonomously on a path with a camera as the single sensor. Since then, the algorithms have been continuously improved in order to show that visual slam is mature enough to develop an autonomous vehicle/shuttle ready for industrialization (figure 1).

In the last 10 years, many experiments were conducted in different places (industrial sites, pedestrian areas in city centers, hospitals …). They involved between one and four vehicles and lasted from a few days to several months. This gives us a very good knowledge of the difficulties a computer vision algorithm has to cope with in the real world: difficult and changing light conditions, parking areas with a lot of changes from one day to the next… These observations drove our new algorithmic developments and at the same time, those public experiments convinced our industrial partners (Ligier Group) that the algorithm was viable.

Compared to our first experiments with a single camera, the major change we made was to add a second camera looking at the rear of the vehicle. This is necessary to have at least one well-exposed image in bad lighting situations (at sunrise or when entering a building for example). Those cameras have a large baseline and non-overlapping fields of view. Instead of instantiating two visual localization algorithms, we consider a rigid multi-camera system in order to make use of all the geometric constraints. With an external auto-calibration, this system allows to build a very accurate 3D reconstruction of the environment with very low drift (see figure 2). This map is then used to localize the vehicle in real-time and to control the steering.

For its security, the vehicle needs to detect obstacles. This is done with LIDAR sensors. So even if it possible to localize the vehicle based only on vision, we have started work to integrate the LIDAR data in the localization process in order to improve the localization robustness and to geo-localize the reference trajectory by using cadastral data.

On the transfer point of view and since 2008, the researchers at Institut Pascal, in collaboration with Ligier Group, have been developing automatic driverless shuttle that can transport up to 10 people along short trajectories (up to 1 or 2 kilometers), rather like a horizontal elevator.

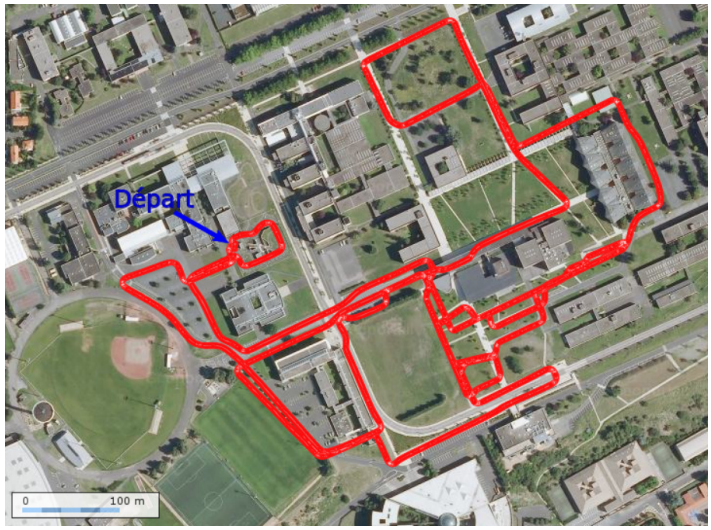

Fig. 2: A 3.5km long trajectory built by the visual SLAM algorithm with non-overlapping cameras. The drift is only 4m without loop closure.

The vehicles, which are designed to be used at specific sites such as industrial sites, airports and amusement parks, are able to deal with obstacles thanks to laser rangefinders fitted on all four sides of the vehicle. The shuttle vehicle can detect the presence of an obstacle at a distance of 50 meters and in this way modify its speed or even stop, depending on the potential danger.

The researchers now intend to turn their attention to running a fleet of five vehicles at the Michelin Europe Technology Center at Ladoux (Clermont-Ferand). The aim is to deal with multiple and potentially simultaneous requests from call points or smartphones, in real time and on a large industrial site, rather like an automatic taxi service. The localization technology, which is reliable and inexpensive, was be unveiled at the Michelin Challenge Bibendum in Chengdu (China) from 11 to 14 November 2014.

Fig. 1: The EZ-10 vehicle-shuttle made by Ligier Group integrating the visual SLAM algorithm from Institut Pascal.

CONTACTS

Michel DHOME
Michel.DHOME@univ-bpclermont.fr
Eric ROYER
Eric.ROYER@univ-bpclermont.fr
Omar AIT-AIDER
Omar.AIT-AIDER@univ-bpclermont.fr
Maxime LHUILLIER
Maxime.LHUILLIER@univ-bpclermont.fr
François MARMOITON
Francois.MARMOITON@univ-bpclermont.fr
Serge ALIZON
Serge.ALIZON@univ-bpclermont.fr

FURTHER READING

Method Of Calibrating a Computer-based Vision System Onboard a Craft
M. Dhome et al., Brevet International, WO Patent 2,013,053,701 (2013)

Fast Calibration of Embedded Non-Overlapping Cameras
P. Lébraly et al., International Conference on Robotics and Automation (2011)

CONTRACTS

Projet Régional VIPA (2008-2011)
Projet Eco-Cité PIA1, Clermont-Communauté, VIPA-CHU Estaing (2012-2014)
FUI VipaFleet (2013-2016)

PhD

P. Lébraly, M. Slade

Scientific achievement #16
Improving learning based detectors

Machine learning based models are very popular in Computer Vision to solve tasks such as categorisation, object detection or visual tracking. A key point for a generic classifier is the construction of a large training dataset containing all the possible appearances of the object in different directions and a significant number of negative images. An alternative is to specialize the detector toward specific situations using priors. We have proposed several contributions to achieve this specialization automatically. The resulting detectors outperform generic ones on several situations like face detection in uncontrolled images or pedestrian detection for automatic CCTV applications.

Recent work in computer vision are increasingly interested in learning methods. More specifically, state of the art object detection models use statistical training on huge datasets to cover the wide variability of appearance of objects such as pedestrians or vehicles. When dealing with a specific scene, the variability of samples used in the training dataset can be reduced to a target domain.

A way to reduce the training set variability is then to specialize the detector toward a specific scene. We have proposed to specialize a classifier by tacking into account the context of the camera. An offline semi-supervised approach has been introduced using an oracle. This latter must automatically label a video, in order to extract contextualized training data. The proposed oracle is composed of several detectors. Each of them is trained on a different signal: appearance, background extraction and optical flow signals. Then, signals are merged to provide more confident detections. A specialized detector is then built on the resulting dataset (Figure 1.). Designed for improving camera network installation procedure, this method is fully automatic and does not need any knowledge about the scene.

In many computer vision detection applications, the algorithm has to handle partial observations, i.e., the object is partially occluded or has to be detected in a pose different than the one learned. To include such situations into a detector, a large set of samples has to be produced within the training dataset.

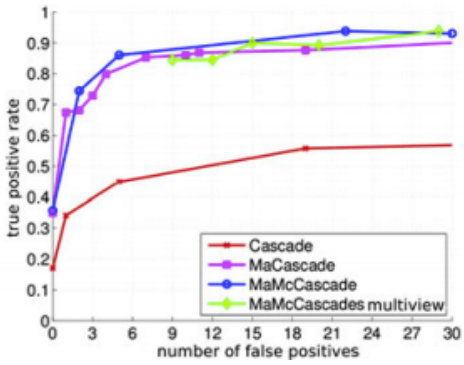

Fig. 2: Performances for faces turned at 45°. The detector Cascade is the upright face detector. The detector MaCascade is built from the upright face detector and aims to detect turned faces. Subwindow positions are modified and unavailable weak classifiers are handled by the naive approach. The detector MaMcCascade is the same detector as MaCascade except that unavailable weak classifiers are handled with a McCascade. The detector MaMcCascade multiview is a multiview system that combines three MaMcCascades: one for the angle 22.5°, one for 45°, and one for 67.5. Figure shows that proposed classifiers outperforms the classical one (in red).

As an alternative, we have proposed a generic framework to handle missing weak classifiers at testing stage in a boosted cascade. The main contribution is a probabilistic formulation of the cascade structure that considers the uncertainty introduced by missing weak classifiers. This new formulation involves two problems: (1) the approximation of posterior probabilities on each level and (2) the computation of thresholds on these probabilities to make a decision. Automatic thresholds have been introduced and are fixed through an iterative procedure that minimizes a cost function. The method has been applied to two popular computer vision applications: detecting occluded faces and detecting faces in a pose different than the one learned. Experimental results are provided using conventional databases to evaluate the proposed strategies related to basic ones. All aspects of the proposed solution have been tested. Moreover, the method has been successfully applied to two specific applications that involve occluded faces (figure 2).

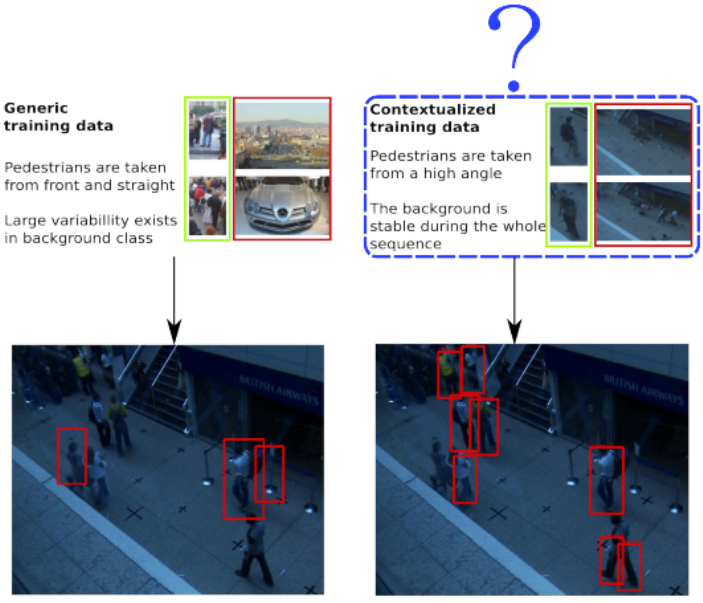

Fig. 1: A detector trained on a generic dataset (left) reaches lower performances than a contextualised classifier (right) when the point of view of the learning and the detection bases are too different.

CONTACTS

Thierry CHATEAU
Thierry.CHATEAU@univ-bpclermont.fr

FURTHER READING

Handling missing weak classifiers in boosted cascade: application to multiview and occluded face detection
P. Bouges et al., EURASIP Journal on Image and Video Processing 1, 1-22 (2013)

A multi-cue spatio-temporal framework for automatic frontal face clustering in video sequences
S. Schwab et al., EURASIP Journal on Image and Video Processing 1, 1-12 (2013)

Automatic Process to Build a Contextualized Detector
T. Chesnais et al., VISAPP Int. Joint Conf. on Computer Vision, Imaging and Computer Graphics Theory and Application (1), 513 (2012)

CONTRACTS

CEA PhD Grant and OSEO BIORAFALE Program

PhD

P. Bouges, T. Chesnais

Scientific achievement #17
How Big is this Neoplasia? Live Colonoscopic Size Measurement

Colonoscopy is the reference medical examination for early diagnosis and treatment of colonic diseases. This minimally invasive technique allows endoscopists to explore the colon cavity and remove neoplasias which may develop into malignant tumors. The size, shape and appearance of a neoplasia are essential clues for diagnosis. However, the size is difficult to estimate because the absolute scale of the observed tissue is not directly conveyed in the 2D colonoscopic images. An erroneous size estimate may lead to inappropriate treatment. There currently exists no solutions to reproduce neoplasia size measurement so we proposed colonoscopic size measurement solutions.

Colorectal cancer is the fourth leading cause of death by cancer according to the World Health Organization in 2008. Regular screening is necessary for early diagnosis and surveillance of abnormal growths of tissue, neoplasias, which may spread and transform into malignant tumors. Colonoscopy is currently the reference medical examination because the main advantage of this minimally invasive technique is that it allows the endoscopist to excise and biopsy neoplasias during the examination. Besides the shape and appearance of these lesions, the size is an essential criterion for diagnostics and the timing of surveillance intervals. However, a small neoplasia imaged close to the colonoscope looks like a larger neoplasia imaged at a further depth: this is the scale ambiguity. While no practical solutions allows the endoscopists to reliably estimate the size of neoplasias, we proposed a passive size measurement system (figure 1), based on the Infocus-Breakpoint (IB) detection method, which can handle regular colonoscopic conditions and an active size measurement system (figure 2), based on a Laser Speckle Pattern Projector (LSPP) with a 3D shape reconstruction.

The IB is the sharp/blur breakpoint which arises while the colonoscope moves toward the colonic tissue. Because most of the current colonoscopes host a prime lens, the IB corresponds to a fixed reference depth which can be calibrated. We have proposed a thin plate spline blur-estimating technique which simultaneously tracks a neoplasia along a video and estimates the optical defocus. Combined with an optical blur model, this method allows one to accurately extract the IB and infer measurements of a neoplasia, assuming the lesion is planar and frontoparallel to the colonoscope's distal end. Experimental results, and more particularly results obtained on phantom videos, validate the applicability of our colonoscopy. The proposed method relies on a simple medical protocol which has proved to be well adapted to real conditions of colonoscopy (both in terms of method efficiency and convenience of the medical protocol).

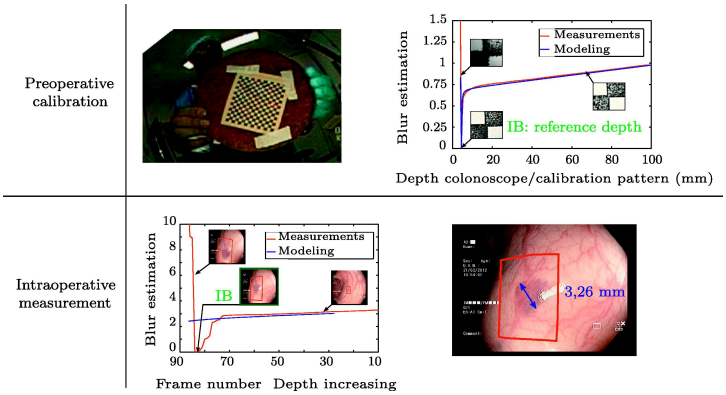

Fig. 1: ***Scale estimation by Infocus-Breakpoint.*** *Top row: preoperative calibration for the GIF type N180 colonoscope. Bottom row: intraoperative measurement of a neoplasia. The Infocus-Breakpoint (IB) is calibrated preoperatively and used to resolve scale intraoperatively.*

The active approach is based on the development of the software and hardware for interactively measuring the size of polyps: the realization of a miniature laser projection unit that emits a speckled pattern of light at the tip of the colonoscope, and the computer vision software that interprets images of this pattern in order to obtain the 3D information to enable 3D measurements. This algorithm is divided in three steps: calibration, 3D reconstruction with the absolute scale and the measure. Calibration is carried out only once, and performed when the LSPP is fitted to the colonoscope. Because it is done once (away from the clinic), the requirements in terms of computation time is not the main concern and the main concern is to achieve an accurate calibration. The dense 3D reconstruction is resolved within a region-of-interest (ROI) and computes a depthmap using a new method based on correlation window matching. After that, a smooth 3D surface is fitted on this initial depthmap. It can then be used to easily measure 3D distances between any two points within the ROI (clicks from the clinician). The depths of these points give their positions in 3D space. Given these positions their mutual distance is computed trivially.

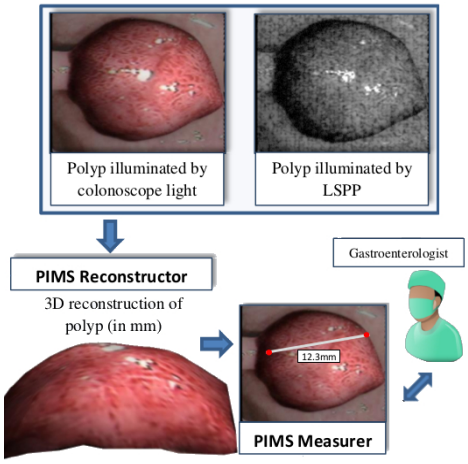

Fig. 2: ***The Polyp Interactive Measurement System (PIMS).*** *The acquisition is done by the projection of a speckle pattern by a laser on the interest surface (polyp). 3D dense reconstruction computes the shape at the absolute scale. The measure is realized by clicking and by estimating the distance on the reconstructed surface.*

CONTACT

Christophe TILMANT
Christophe.TILMANT@univ-bpclermont.fr

FURTHER READING

How big is this neoplasia? Live colonoscopic size measurement using the Infocus-Breakpoint
F. Chadebecq et al., Medical Image Analysis 19, 58 (2015)

Measuring the Size of Object in-vivo in Colonoscopy using Active Vision
T. Collins et al., Patent pending (2015)

CONTRACTS

ANR TecSan SYSEO (2011-2015)
Fonds Régionaux d'Innovation Région Auvergne-OSEO/PIMS (2012-2014)
Bourse Innovation Région Auvergne /Yansys (2010-2011)

PhD/Post Doc

F. Chadebecq/T. Collins

Scientific achievement #18
Mobile ground-based radar sensor for localization and mapping in outdoor environment

The interest of radar technology is its long range and the robustness of radar waves to atmospheric conditions, making it well-suited for outdoor robotic applications. Two Simultaneous Localization And Mapping (SLAM) approaches using data obtained from a 360° field of view microwave radar sensor were developed. A first trajectory-oriented SLAM technique estimates the ego-motion using the Fourier-Mellin transform for registering radar images, without landmark assumptions. The second approach uses the consequence of using a rotating range sensor in high-speed robotics: movement combinations create distortions in the collected data. The vehicle's displacement and then the radar map are achieved by analyzing these measurement distortions.

The increased autonomy of robots is directly linked to their capability to perceive their environment. Simultaneous Localization and Mapping (SLAM) techniques, which associate perception and movement, are particularly interesting because they provide advanced autonomy to vehicles such as robots. In outdoor environments, climatic constraints or operational context (dust, light condition, rain, etc.) show the limits of usual perception systems. Radar is an alternative to existing perception systems for ground mobile robots. Its ability to work in all weather, day and night, makes the radar very attractive for outdoor applications. In the two SLAM techniques developed, data from a 360° field of view radar sensor are used. This microwave radar scanner is based on the Frequency Modulated Continuous Wave (FMCW) technology and was developed by a team from the IRSTEA Institute.

In order to overcome the complexity of radar image analysis, a trajectory-oriented EKF-SLAM (Extended Kalman Filter) technique has been developed. This process makes no landmark assumptions and avoids the data association problem. The method of ego-motion estimation makes use of the Fourier-Mellin transform for registering radar images in a sequence, from which the rotation and translation of the sensor motion can be estimated. In the context of the scan-matching SLAM, the use of the Fourier-Mellin transform is original and provides an accurate and efficient way of computing the rigid transformation between consecutive scans. Our SLAM approach estimates the trajectory defined by the state vector describing the location and orientation of the vehicle at each time. There is no explicit map; rather each pose estimate has an associated scan of raw sensed data that can be next aligned to form a global map.

In a robotics context, it is usually assumed that the scan of a range sensor is a collection of depth measurements taken from a single robot position. This can be done when working with lasers that are much faster than radar sensors and can be considered instantaneous when compared with the dynamics of the vehicle. However, when the robot is moving at high speed, this assumption is unacceptable. Important distortion phenomena appear and cannot be ignored. Our second method computes the velocimetry of the vehicle by explicitly analyzing these measurement distortions. The stated assumption is the local constant velocity of the vehicle during two successive measurements. The pose of each measurement is directly linked to the observation pose and to the angle of observation. This pose can be expressed with the constant velocity model of the vehicle and is only a function of the linear and angular speed of the robot.

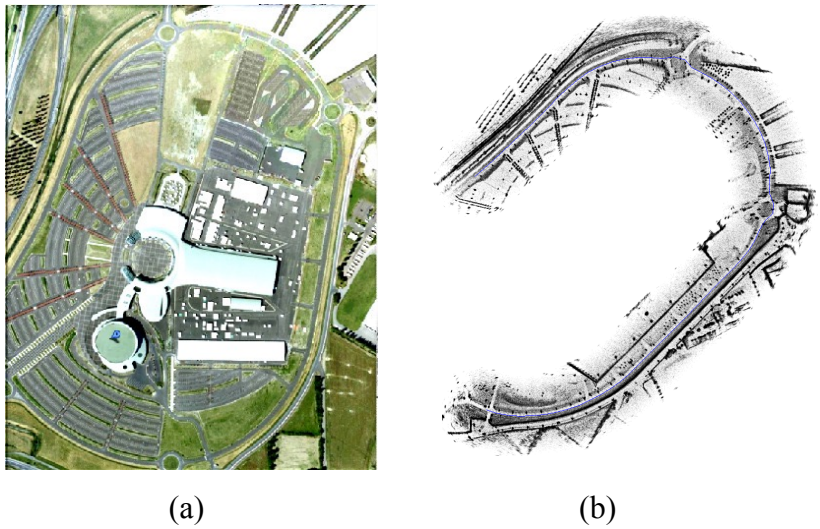

Fig. 1: (a) Aerial Google view. (b) Radar map obtained by the Fourier-Mellin transform SLAM process.

Such radar-based odometry does not use any proprioceptive sensors. This part of our work can be extended to any kind of non-instantaneous rotating sensor.

Our two approaches work without any knowledge of the vehicle's surroundings; not only do they allow estimating the robot's trajectory, they also permit building a map of the environment. An evaluation and a comparative study of the two proposed methods on real-world data over a 2.5 km course have been conducted, which have demonstrated their feasibility and reliability for mobile ground vehicles at high speed (30 km/h). A result is presented in Fig. 1.

CONTACTS

Paul CHECCHIN
Paul.CHECCHIN@univ-bpclermont.fr
Roland CHAPUIS
Roland.CHAPUIS@univ-bpclermont.fr

FURTHER READING

Localization and Mapping Using Only a Rotating FMCW Radar Sensor
D. Vivet et al., Sensors 13(4), 4527 (2013)

Mobile Ground-based Radar Sensor for Localization and Mapping: An Evaluation of Two Approaches
D. Vivet et al., International Journal of Advanced Robotic Systems 10(307), 12 (2013)

Odométrie radar par analyse de la distorsion - Application à un véhicule roulant à vitesse élevée
D. Vivet et al., in Actes du dix-huitième congrès francophone AFRIF-RFIA, Lyon. Prix du meilleur article (2012)

CONTRACTS

ANR PSIRob IMPALA (2007-2011)

PhD

F. Gerossier, D. Vivet

Scientific achievement #19
Sparse EKF visual SLAM for outdoor applications

Robot localization is nowadays a very challenging task that allows several applications like trajectory following or convoy control. Using absolute localisation (like GPS) is very common and widely used. However, sometimes GPS signal is not available (because of urban buildings for instance) and it become mandatory to use other sensor modalities. Moreover an absolute localisation is not always required for some applications (for instance for following another vehicle in a convoy). We therefore developed a visual sparse SLAM dedicated to this kind of applications: a first vehicle with an embedded camera (and proprioceptive sensors) observes feature points (landmarks) in the scene and records its trajectory in this scene. It transmits these points and the trajectory waypoints to a follower vehicle which detects the same points and control its steer angle to follow the transmitted trajectory. The main process has been demonstrated in real time with two vehicles on the PAVIN platform mainly with the ANR project SafePlatoon.

Numerous mobile robots applications require a precise localisation stage. However, keeping a global absolute localisation can be challenging because the classical GPS signal (that is more often used in theses cases) can be hidden or even no be precise enough to allow a precise control.

A solution can be to use a RTK GPS (centimeter accuracy) but the cost is very high and the availability is not guaranteed in urban scenes. So we developed a SLAM (Simultaneous Localization and Mapping) system using a monocular camera embedded in a vehicle. The principle is to extract feature points (*Harris* corners) and track them along the trajectory. Having a set of such points allows to compute not only the 3D coordinates of theses points but also the vehicle displacement.

Several approaches can be used there but we used a Kalman filter based one because it is easier to fuse with the data coming from the other embedded sensors. Moreover, this approach permits real time evolution with very small number of landmarks to obtain a *sparse* map. This constraint is required to allow the communication with a low bandwidth between several mobile robots in a convoy (required for example in the ANR project Rinavec).

Using a sparse map involves however a very accurate feature management. Indeed, an EKF (Extended Kalman Filter) for a SLAM is not easy because of the non linearity of the projection process. The classical linearizations make the filter can diverge or give spurious results. More precisely, we improved the updating stage of the filter to avoid these false results, by proposing improvements on the Kalman filter able to deal with the non linearities in the case of non linear but rational shapes of the observation equation.

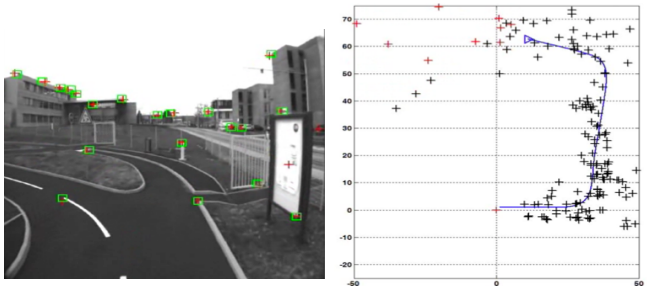

*Fig. 1: **Sparse SLAM illustration.** (Left): detected landmarks and their region of interest to track them for next frames. (Right): Sparse reconstructed map. Red landmarks are not yet stabilized.*

Moreover, in order to maintain a good precision, it is worthwhile to track the features along a large set of frames. But in this case, because of these non linearities, their prediction is not easy. We therefore developed also a geometrical approach to update their region of interest allowing to track them for long distances (figure 1).

Finally it can be useful to fuse this visual SLAM with the classical proprioceptive sensors of the robot, or even with another SLAM launched on data coming from another camera. We also developed such architecture able to fuse the sensors data wherever they come from.

The approach has been demonstrated several times, especially on the PAVIN platform where we shown an original purely visual based convoy control. In this application a VipaLab vehicle follows in real time the trajectory of a leader one wherever it goes (figure 2).

CONTACTS

Romuald AUFRERE
Romuald.AUFRERE@univ-bpclermont.fr
Roland CHAPUIS
Roland.CHAPUIS@univ-bpclermont.fr

FURTHER READING

Real-Time Monocular SLAM With Low Memory Requirements
G. Bresson et al., IEEE Transactions on Intelligent Transportation Systems, 1-13 (2015)

Consistent Multi-robot Decentralized SLAM with Unknown Initial Positions
G. Bresson et al., 16th International Conference on Information FUSION (2013)

CONTRACTS

ANR VTT SafePlatoon(2011-2014)
ANR PSIRob Rinavec (2007-2011)

PhD

G. Bresson, T. Féraud

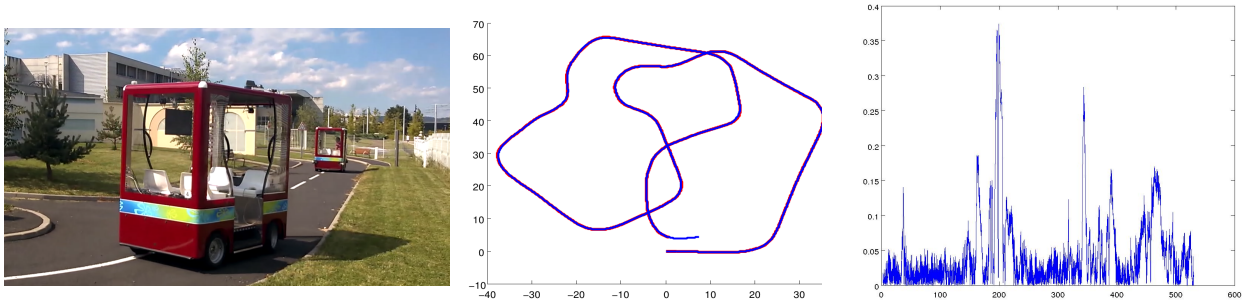

Fig. 2: (left) VipaLab vehicles used for the visual convoy. The first one is driven manually and the second one follows automatically in real time the leader's trajectory. (center) Comparison between the leader (blue) and the follower (red) trajectories (380m long). (right) Error between leader and follower trajectories (in cm). The 37 cm error (time 200) is due to the not flat road.

Scientific achievement #20
Real-Time multi-sensor absolute localization of a mobile robot based on a Bayesian Network

The estimation of the absolute localization of mobile robots is nowadays very important. Generally, the data provided by the embedded sensors are associated with a map by a classical map-matching process. Most popular methods try to optimize a global cost in a bottom-up process: each sensor data is analyzed even if it is not relevant (like a GPS in indoor environment) and all are fused together in order to estimate the localization. Unlike these classical approaches, the proposed method uses a top-down multi-sensorial analysis coupled with a map of the environment. Indeed instead of fusing all the data, a Bayesian network is used to select the best feature to detect with the best sensor at each time. This selection is done by taking into account the actual localization and the objectives of precision and integrity of the robot localization at a given time. This process makes it possible the solve for instance the kidnapped robot problem but can be extended to deal with map errors or imprecision. We demonstrated this method with the real time localization of a mobile robot embedding several laser range-finders and a low-cost GPS.

Nowadays vehicles are smarter from day to day, and the applications are varied like autonomous driving, assistance systems to the human drivers, platooning, agricultural applications, elderly people assistance, etc. To achieve those tasks properly, the robot needs some awareness of its environment, and a reliable and accurate localization is almost mandatory.

There are two kinds of localization methods depending if the map is already known or not. If the map is not known, the robot has to be able to build the map itself in order to compute its localization. This is the well-known SLAM method (Simultaneous Localization And Mapping). Most SLAM approaches are based on range finder or vision sensors. The obtained map contains most of the time a large amount of landmarks. In the localization step, the robot has to deal with this large amount of information which can be ambiguous, noisy, or irrelevant. The main problem affecting every SLAM algorithms is the inherent drift mainly because of the highly nonlinear models used. The second approach is based on the assumption that the robot will perform its tasks in a well or partially known environment. The major advantage of this method is to allow the use of existent absolute maps and consequently the drift problem disappears. The only condition is that the robot has sensors and the associated algorithms (detectors) to detect and localize the landmarks given by the map. Nowadays, the availability of very complete maps (openStreetMap, googleMap, etc) makes this approach very interesting for mobile robots localization and navigation. The main advantage of such methods is that the localization is world referenced and can therefore be fused with absolute localizations sensors like GPS. Moreover, unlike SLAM approach, no drift biases and the localization using data coming from other vehicles (in platooning or convoy applications) is drastically simplified.

The presented method relies on an absolute localization and a *top-down* fusion: the system selects by itself at each time the feature to detect in order to optimize its localisation estimation. Once the detection has been done, there are two possibilities: the detection was successful or not. According this result, a Bayesian network (figure 1) is used to update several events like "*is this landmark the one I expected ?*" or "*is the vehicle at this current estimated position ?*" but can be extended to "*is this sensor still alive*" or "*is this landmark in the map still in the world ?*".

In this case the approach allows not only to localize a robot but can also be used to update the map (landmarks addition or suppression or accuracy improvement).

The approach has been demonstrated with a realtime localisation of a manually driven mobile robot on the PAVIN platform (figure 2). The accuracy is about 8cm standard deviation (mainly due to map imprecision: figure 3). The method will be extended soon for open classical urban scenes where an *OpenStreetMap* Mapping is available.

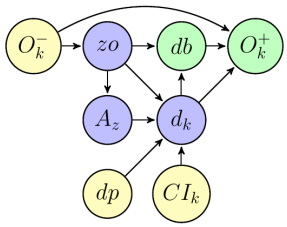

Fig. 1: Bayesian network used. The nodes are the events ;for instance Ok- represents the probability to belong to the current estimated position before detection and Ok+, is the same probability after a landmark detection. dk is the detection event. The network allows to update all the possible probability events in case of detection or false detection of the current selected landmark.

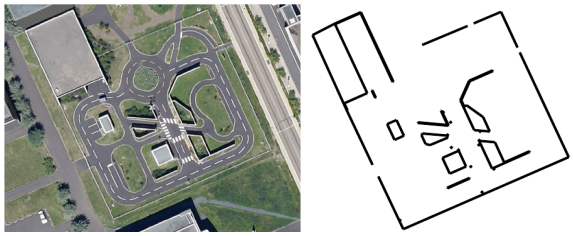

Fig. 2: ***Pavin area.*** *(left) Bird eye view. (right) Extracted map used with the approach.*

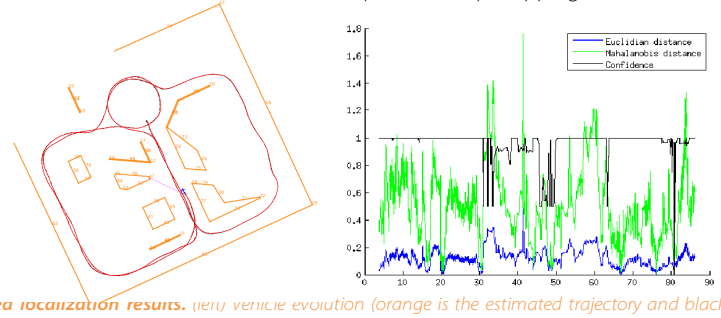

Fig. 3: ***Obtained localization results.*** *(left) Vehicle evolution (orange is the estimated trajectory and black the ground-truth, in magenta is the beam showing the current selected landmark to detect). (right) Localisation errors (in blue), the confidence in the estimation (in black) and the Mahalanobis error (in green: 1 means 1 standard deviation of the current estimation.*

CONTACTS

Romuald AUFRERE
Romuald.AUFRERE@univ-bpclermont.fr
Roland CHAPUIS
Roland.CHAPUIS@univ-bpclermont.fr

FURTHER READING

Real time vehicle localization using a top-down process
C. Aynaud et al., in 17th International Conference on Information Fusion, Salamanca (2014)

Vehicle localization by using a multi-modality top down approach
C. Aynaud et al., in 13 th International Conference on Control, Automation, Robotics and Vision (2014)

A Top-Down Perception Approach for Object Recognition
C. Bernay-Angeletti et al., in International Conference on Artificial Intelligence, Las Vegas Nevada USA (2014)

CONTRACTS

Action LocFus - LabEx IMobS3 Défi1 (2012-2014)
ANR VTT SafePlatoon (2011-2014)

PhD

C. Aynaud, L. Delobel

Scientific achievement #21
Automatic 3D urban cartography

An 3D cartography and modeling in the cluttered urban environment necessitate the extraction of non-permanent objects from the scene to obtain the permanent part of the environment. The occluded features or regions due to these temporarily present objects then needs to be completed. In this context, two approaches are explored for the extraction of these occluding objects i.e. segmentation of 3D points belonging to moving objects during the acquisition of 3D LiDAR data and also segmentation based classification of a registered 3D point cloud. In order to complete the occluded regions, a concept of multiple passages based on incremental updating is exploited. It is also shown that the proposed method of temporal integration also helps in improved semantic analysis of the urban environment, specially building façades.

Lately, applications such as Google Street View, Microsoft Visual Earth or Géoportail, provide effective visualizations of large scale urban models which are accessible to large public who enthusiastically view the real-like 3D visualizations of cities, created by mobile terrestrial image acquisition techniques. However, in urban environments, the quality of data acquired by these hybrid terrestrial vehicles is widely hampered by the presence of temporary stationary and dynamic objects (pedestrians, cars, etc.) in the scene.

In the methods developed, we first classify the urban environment into permanent and temporary classes. Two approaches are explored. In the first approach we classify the 3d points directly at the time of acquisition from a rotating range finding sensor such as Velodyne. The first algorithm developed to perform this classification only use the telemetric sensor by exploiting the notion of probability of occupancy. Multiple observations of the same volume of space by the sensor give an estimate if it was empty or full at a given time. This information allows us to reconsider the input data and make a classification. The second method uses the information of camera data. The main idea lies in the exploitation of a photo-consistency criterion based on the simple fact that a static object has an identical color at all times and regardless of the point of view. Conversely, the place where a mobile object moves sees its texture changed during the sequence. This distinction leads to the construction of a robust criterion to classify rangefinder data in mobile or static objects. Some of the results are presented in Fig. 1. In the second approach the registered 3D point clouds obtained from LiDAR are first segmented into voxels that are then characterized by several attributes transforming them into super-voxels. These are joined together by using a link-chain method rather than the usual region growing algorithm to create objects. These objects are then classified using geometrical models and local descriptors into basic object types. The objects classified as temporary are then removed from the 3D point cloud leaving behind a perforated 3D point cloud of the urban environment. These perforations along with other imperfections are then analyzed and progressively removed by incremental updating exploiting the concept of multiple passages. The changes occurring in the urban landscape over this period of time are detected and analyzed using cognitive functions of similarity and the resulting 3D cartography is progressively modified accordingly. Different specialized functions are also introduced, to help remove the different imperfections due to occlusions, misclassifications and different changes occurring in the environment over time, thus increasing the robustness of the method.

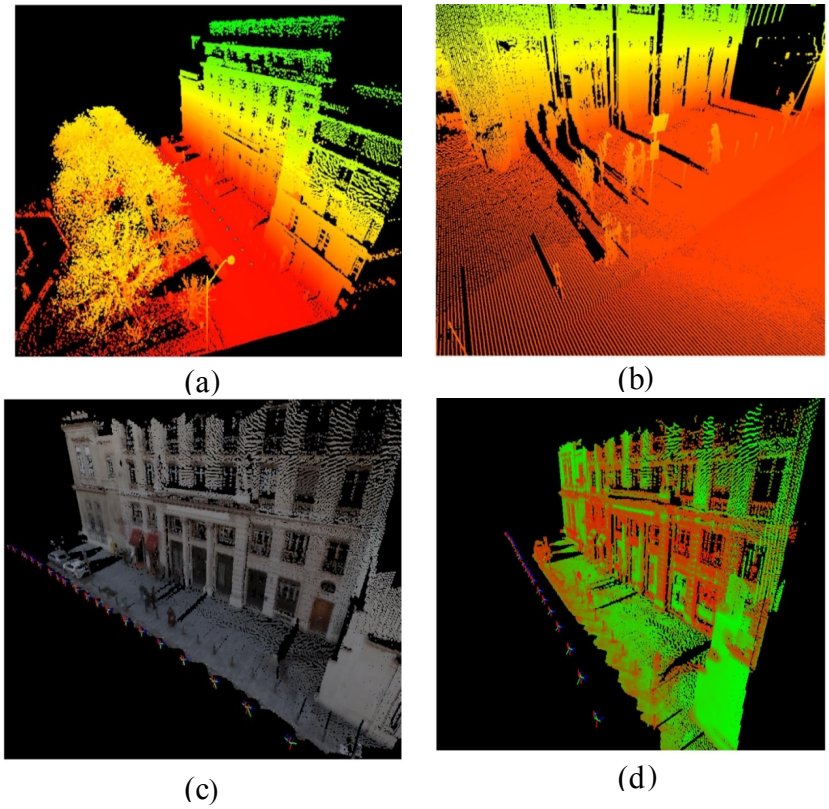

Fig. 1: (a) & (b) show the two different instances of the original point cloud of a street corner in Paris center. (c) & (d) presents the point cloud color coded by photo-consistency and score respectively.

It is also shown that the proposed method of temporal integration also helps in improved semantic analysis of the urban environment, specially building façades.

The results not only demonstrate the efficiency, scalability and technical prowess of the methods but also that they can be easily integrated and are ideally suited for different commercial or non-commercial applications pertaining to urban landscape modeling and cartography requiring frequent database updating.

CONTACTS

Paul CHECCHIN
Paul.CHECCHIN@univ-bpclermont.fr
Laurent TRASSOUDAINE
Laurent.TRASSOUDAINE@univ-bpclermont.fr

FURTHER READING

Automatic Detection and Feature Estimation of Windows in 3D Urban Point Clouds Exploiting Façade Symmetry and Temporal Correspondences
A.K. Aijazi et al., Int. Journal of Remote Sensing 35 (22), 7726 (2014)

Automatic Removal of Imperfections and Change Detection for Accurate 3D Urban Cartography by Classification and Incremental Updating
A.K. Aijazi et al., Remote Sensing 5 (8), 3701 (2013)

Segmentation Based Classification of 3D Urban Point Clouds: A Super-Voxel Based Approach
A.K. Aijazi et al., Remote Sensing 5 (4), 1624 (2013)

CONTRACTS

ANR CONTINT iSpace&Time (2012-2014)

PhD

A.K. Aijazi, C. Deymier

Scientific achievement #22
Control of off-road mobile robots

Generic observer and control algorithms have been designed to enhance both safety and motion control for vehicles or wheeled mobile robots operating off-road. Three aspects have been specifically addressed: first, the prevention of the rollover risk for manually driven vehicles operating on sloping and slippery terrains; next, safe and high accurate path tracking for autonomous wheeled mobile robots acting in such environments; eventually, formation control for a fleet of networked heterogeneous vehicles or mobile robots operating off-road. These developments have been consistently supported by thorough full-scale experiments and a patent has been claimed.

Vehicle or mobile robot motion in off-road context can be accurately described from 3D dynamical models. However, these models are hardly tractable from a control point of view: they are large and intricate and demand for the knowledge of numerous parameters hardly measurable and possibly fast varying (such as the parameters describing the grip conditions). Consequently, we defend an alternative approach where complementary partial dynamical models are first designed, with the aim of reporting the preponderant features of the vehicle/robot behavior in various off-road conditions while remaining as simple as possible. Next, observers are derived in order to estimate on-line the macro-parameters (overall grip conditions, local slope, etc.) introduced into these models. Eventually, taking advantage of these models with a simple structure and all their variables available (either measured or supplied by the observers), efficient control laws are designed in order to either predict imminent risky situations or achieve accurate path tracking.

Quad bikes are vehicles offering high maneuverability, however on the flip side, numerous fatal accidents are reported. Observers requiring a set of sensors consistent with the cost of a quad bike (inertial measurement unit, Doppler radar and steering angular sensor) have therefore been designed to estimate on-line the vehicle dynamical state (local slope, grip conditions, roll and pitch). Next, predictive control techniques have been considered to anticipate the future longitudinal and lateral load transfer and then detect imminent rollover situations. Finally, a mechatronic device acting on the quad throttle handle has been developed to compel the driver to slow down when his safety is at risk.

Grape harvesters are also prone to rollover since they present a special geometry and move on steep terrains. Stability assessment is here more intricate since the height of the center of gravity and the vehicle weight are varying, when the slope correction system is activated and the grape receptacle is filled, respectively. A combined observer has been designed to estimate on-line these two quantities from the intermittent pressure information delivered by the hydraulic cylinders used for slope correction (available only when these latter are in steady state), so that the rollover risk can still be relevantly predicted at each instant. This work has been patented.

For path tracking applications, a reactive observer estimating separately the grip conditions at the front and the rear axles has been designed and allows to identify at each instant whether the robot is under- or over-steering. This has enabled safe and high accurate path tracking up to 10m/s: spin round situations are anticipated and predictive control techniques permit to adjust, if needed, the robot velocity in order to guarantee that it does not leave a safe corridor.

Fig. 1: Rollover prevention - test vehicles: quad bike Massey Fergusson MF400H (left) and grape harvester Gregoire G7-240 (right).

Fig. 2: Vehicles used to investigate formation control: a farm tractor Massey Fergusson 8680 leading RobuFast and Arocco mobile robots.

When in formation, the networked robots track the same reference path, supplied beforehand or created on-line by a manually driven leader, with lateral gaps and desired inter-distances, both possibly varying, defining the current formation shape. Longitudinally, each robot is controlled wrt to several others to prevent oscillations within the formation and actuator capabilities of possibly heterogeneous robots are explicitly taken into account.

CONTACT

Benoit THUILOT
Benoit.THUILOT@univ-bpclermont.fr

FURTHER READING

Adaptable robot formation control: Adaptive and predictive formation control of autonomous vehicles
A. Guillet et al., IEEE Robotics & Automation Magazine 21, 28 (2014)

Mixed kinematic and dynamic sideslip angle observer for accurate control of fast off-road mobile robots
R. Lenain et al., J. of Field Robotics 27, 181 (2010)

Method for reducing the risk of rollover of an automotive vehicle provided with a controllable suspension system
R. Lenain et al., Patent PCT/EP2014/056011 IRSTEA / Institut Pascal (2014)

CONTRACTS

ANR PsiRob FAST (2008-2011)
ANR VTT ActiSurTT (2010-2014)
ANR VTT SafePlatoon (2011-2014)

PhD

J.B. Braconnier, C. Cariou, D. Denis, M. Deremetz, A. Guillet, M. Richier

Scientific achievement #23

Stable and flexible multi-controller architecture based waypoints for autonomous vehicle's navigation in cluttered environment

The research shown in this document emphasizes the fact that it is not absolutely mandatory (as commonly admitted and broadly used in the literature) to have a predetermined trajectory to be followed by a robot to perform reliable and safe navigation in urban and/or cluttered environment. A new definition of navigation task, using only discrete waypoints in the environment will be presented and applied for an urban electric vehicle. This approach permits to reduce the vehicle computations and permits to lead to an even more flexible navigation, mainly if the environment is cluttered and/or dynamic.

A vehicle navigation using only waypoints allows to avoid any path/trajectory planning which could be time-consuming and complex, mainly in cluttered and dynamic environment. Moreover, this kind of navigation does not require to know the pose of the closest point to the followed trajectory (w.r.t. the robot configuration) and/or the value of the curvature at this point. Consequently, the navigation problem is simplified to a waypoint reaching problem, i.e., the vehicle is guided by waypoints instead of following a specific fixed path. Moreover, it is important to notice that if the successive waypoints are closer to each other then the vehicle tends to perform a path following navigation. The proposed approach tends therefore to gather the different navigation technics. In addition, the use of only waypoints to control the vehicle instead of a fixed trajectory, allows the robot to carry out local operations (to avoid such obstacle) while maintaining overall stability of the used hybrid multi-controller architectures (continuous / discrete). The obstacle avoidance is one of the most important building blocks to achieve autonomous navigation of mobile robots in cluttered environments. Obstacle avoidance techniques based on cycles-limits are developed in the laboratory for over 6 years. They avoid as much static and dynamic obstacles with very satisfactory robustness to noise. The obstacle avoidance controller has been integrated easily to the developed multi-controller architecture. Several experiments with VipaLAB (mono-robot configuration as multi-robot) were performed showing the robustness of the developed techniques (navigation in cluttered environment).

CONTACTS

Lounis ADOUANE
Lounis.ADOUANE@univ-bpclermont.fr
Youcef MEZOUAR
Youcef.MEZOUAR@univ-bpclermont.fr

FURTHER READING

A novel safe and flexible control strategy based on target reaching for the navigation of urban vehicles
J.M. Vilca et al., Robotics and Autonomous Systems (RAS) (2015)

Optimal multi-criteria waypoint selection for autonomous vehicle navigation in structured environment
J.M. Vilca et al., Journal of Intelligent and Robotic Systems (2015)

CONTRACTS

ANR VTT SafePlatoon (2011-2014)
Action AVOMNI LabEx IMobS3 (2012-2015)

PhD

J.M. Vilca Ventura

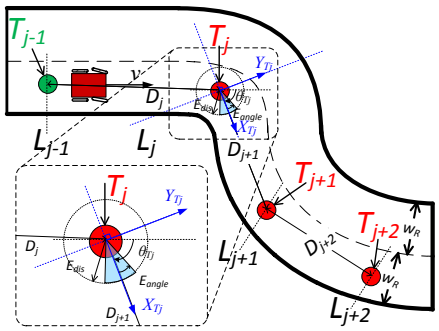

Fig. 1: Waypoints and target assignment strategy.

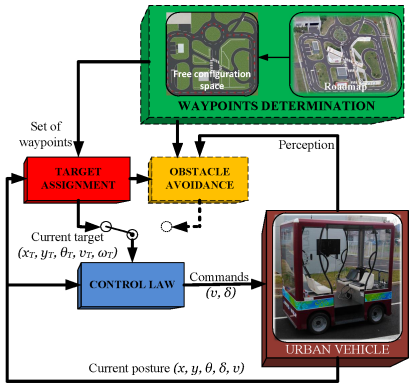

Fig. 2: Overview of the used multi-controller architecture to perform the autonomous navigation.

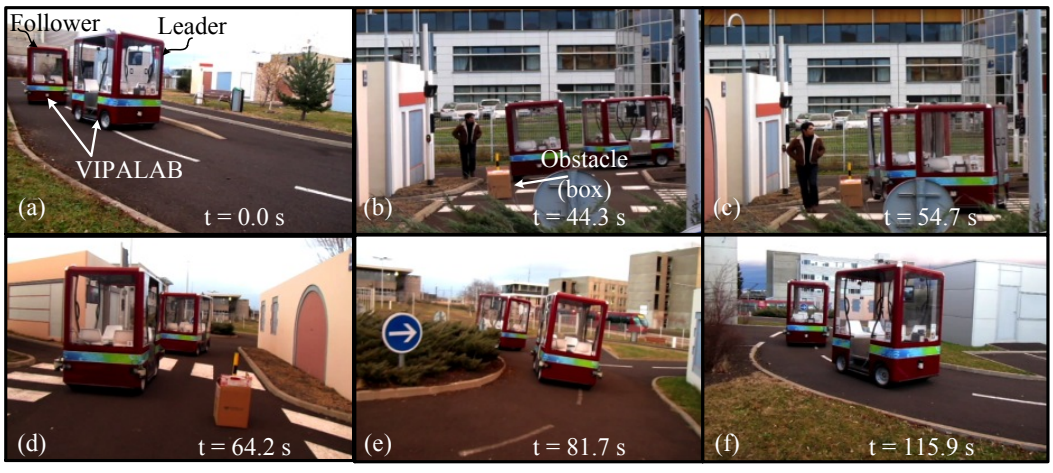

Fig. 3: Experiment of the used strategy of navigation for a group of VipaLab in platooning formation.

Scientific achievement #24
Fast hierarchical topological mapping using omnidirectional images

A topological mapping approach for omnidirectional images capable of answering loop closure queries at multiple resolutions is presented. The environment is mapped hierarchically using two layers of which the first layer consists of individual images and the second layer represents regions of the environment composed of groups of images from the first layer. A hierarchical algorithm is formulated that exploits this map structure for an efficient and accurate loop closure without the need of geometric verification. The vital parameters of loop closure are automatically learned from training data. Performance of our loop closure algorithm is experimentally evaluated on various publicly available datasets and compared to two state of the art techniques.

Topological maps represent environments as topological graphs with connections between places that are adjacent, with no metrical information. As a result, expensive techniques like drift correction or bundle adjustment are not necessary making it scalable to large environments.

Loop closure, the crux of all the topological mapping algorithms, adds new connections in the map between places which are topologically connected. Vision based loop closure has two main problems namely *Scalability* and *Perceptual Aliasing*. While building a map, new images are added at every time step inflating the loop closure search space. A loop closure algorithm has to be scalable to the search space that keeps on growing at every time step. The second problem, perceptual aliasing is a situation where two spatially distant places look visually similar suggesting a false loop closure (false positive). False positives create false connections in a topological map destroying the map consistency. Therefore the most desirable properties of a loop closure algorithm should be scalability and zero false positives.

In order to effectively capture visual similarity across images in a region, Omnidirectional/Panoramic cameras with their 360 degree field of view prove to be the best choice as compared to the tradition cameras with a limited and unidirectional field of view. Apart from that, omnidirectional cameras are also useful in detecting loop closures when the robot is re-traversing the environment in a reverse direction which is impossible with traditional cameras.

To build an accurate topological map very fast and with zero false positives, we employ the following steps:

- *Node Level Loop Closure:* A given newly acquired image is compared with all the existing nodes/places and a small subset of places is retrieved. The new image might have been acquired at one of these places. This process is performed using Vector of Locally Aggregated Descriptors (VLAD) computed over the new image and over the retrieved nodes.
- *Image Level Loop Closure:* We retrieve the image most similar to the new image among the images belonging nodes retrieved during the node level loop closure. The similarity is evaluated using local image descriptors like SIFT, SURF, etc and the omnidirectioal image constraints over the spatial locations of the features in each of the reference images and the new image. This process uses spatial constraints and eliminates false positives bypassing the need for an expensive scene geometry evaluation common among many contemporary approaches.

The approach yielded high recall rates with 100% precision (no false positives) with the geometry evaluation step. The approach was tested on three publicly available datasets and it has been observed that the recall rates obtained on all these datasets have been greater than that of FABMAP 2.0. The approach is fast enough to process 8-10 images per second on average.

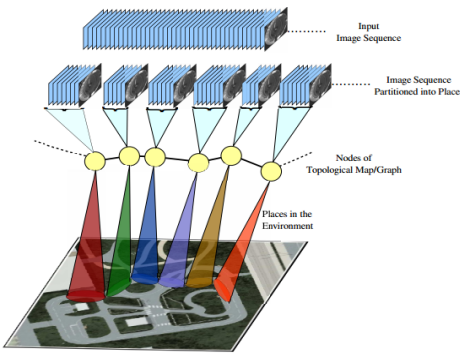

Fig. 1: Hierarchical topological map with the input image sequence partitioned and each partition represented as a node in the topological graph.

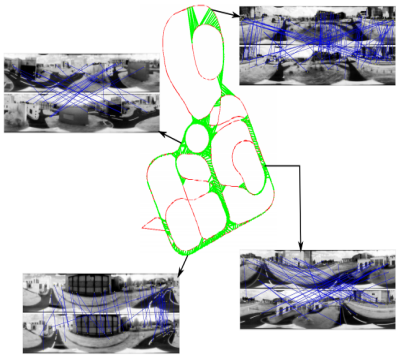

Fig. 2: Loop closures detected on the PAVIN sequence shown in green color and the trajectory of the robot shown in red color. Image matches at four different loop closure locations have been depicted.

CONTACTS

Youcef MEZOUAR
Youcef.MEZOUAR@univ-bpclermont.fr

FURTHER READING

Vision based sparse topological mapping
H. Korrapati et al., Elsevier: Robotics and Autonomous Systems (RAS) (2014)

Hierarchical visual mapping with omnidirectional images
H. Korrapati et al., IEEE/RSJ Int. Conf. on Intelligent Robots and Systems (IROS) (2013)

CONTRACTS

ANR R-Discover (2009-2013)
BRI Corée du Sud

PhD

H. Korrapati, F. Uzer

Scientific achievement #25
Formation Control of Mobile Robots using Multiple Cameras

A new vision-based control method to drive a set of robots moving on the ground plane to a desired formation is presented. As contribution, we propose to use multiple camera-equipped Unmanned Aerial Vehicles (UAVs) as control units. Each camera views, and is used to control, a subset of the ground team. Thus, the method is partially distributed, combining the simplicity of centralized schemes with the scalability and robustness of distributed strategies. Relying on a homography computed for each UAV-mounted camera, our approach is purely image-based and has low computational cost. We formally guarantee the stabilization of the formation, considering unicycle robots. Finally, our control strategy can be combined with feature-based map merging strategies in robot networks.

Multiagent systems are very interesting in robotics due to their ability to perform complex tasks with great efficiency and reliability. In this context, we have addressed the problem of bringing a set of ground mobile robots to a desired geometric configuration, which is also referred to as formation stabilization. Typically, the formation to be stabilized is defined in terms of absolute positions for the robots to reach, or as relative position vectors or distances between the agents. Between the two latter varieties, distance based formation control employs simpler information and does not require a global reference frame for the robots, while relative position-based methods exhibit stronger stability properties. In this and other related multirobot problems, distributed control strategies tend to be preferred, for robustness and scalability. A very relevant characteristic of the method we propose is the use of vision. The use of external cameras for the control task has the advantage of allowing the robots to carry simpler onboard equipment, since they do not need to handle costly sensing and computation. In addition, they do not have to transmit information, which typically consumes a lot of power. In particular, an important contribution of our proposal is the use of multiple cameras, which improves the maximum coverage, robustness and scalability with respect to a single-camera setup. Our method is partially distributed, preserving some properties of centralized systems (e.g. more efficient performance than distributed controllers).

The system can be flexibly dimensioned by selecting the appropriate number of cameras for a given number of robots and size of the workspace. Our approach is image-based and, therefore, does not use range information, contrary to position-based or distance based formation control techniques. In addition, we do not need a global reference frame for the robots (which typically requires additional sensors). All the information is measured in the images, the cameras do not share a common coordinate reference, and their motion does not affect the control performance. This work provides several contributions:

- A precise definition of the control method when multiple cameras are used. We discuss specifically aspects of the control units that carry the cameras (UAVs), and define the interactions (established via communications) that need to exist between them to guarantee a correct performance of the global system.
- A formal stability analysis of the multi-camera control method.
- In addition to controlling the motion of the robots, we also address the control of the motion of the cameras. We propose an algorithm that ensures that they maintain the required intersections between their sets of viewed ground robots and thus the desired multi-robot task is successfully carried out.
- The validation of the method via realistic simulations and experiments with multiple cameras and real mobile robots.
- The method can be combined with map merging strategies.

CONTACTS

Youcef MEZOUAR
Youcef.MEZOUAR@univ-bpclermont.fr

FURTHER READING

Feature-based map merging with dynamic consensus on information increments
R. Aragues et al., Autonomous Robots (2015)

Hybrid multirobot control with multiple cameras
M. Aranda et al., in American Control Conference, ACC'13, Washington DC, USA (2013)

Visual Control for Multi-Robot Organized Rendez-vous
N. Lopez et al., IEEE Transactions on Systems, Man and Cybernetics - Part B (2012)

CONTRACTS

Chaire d'Excellence (2011-2014)
Action AVOMNI LabEx IMobS3 (2012-2015)

PhD

R. Aragues, M. Aranda

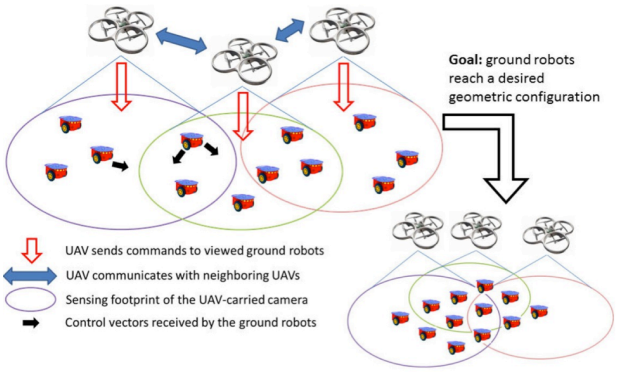

Fig. 1: Overview of the proposed multi-robot control system. Multiple (three, in this example) UAV control units, whose motion is modeled by single integrator kinematics, are used. Each of them has an onboard camera from which it obtains the motion commands for the unicycle robots within the camera's field of view. These take the form of desired motion vectors, and are transmitted to the robots. The robots that are viewed by multiple cameras compound the multiple received commands to obtain their motion input. The UAVs also communicate among themselves in order to control their own motion, with the goal of ensuring appropriate coverage of the robotic team and the successful completion of the control task, which consists in bringing the set of ground robots to a desired geometric configuration.

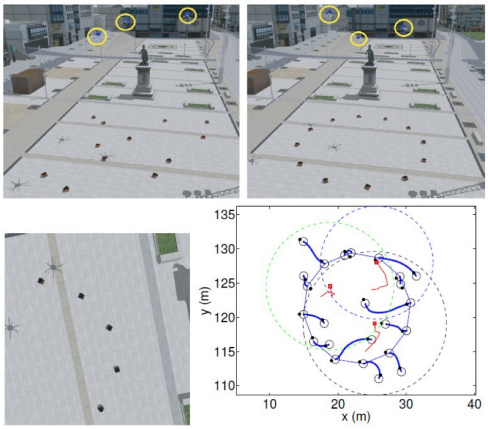

Fig. 2: Realistic simulation example using Cobaye from 4D-Virtualiz. Top: Initial (left) and final (right) views of the simulated scenario, with circles plotted around the UAVs. Bottom: Final image captured by one of the cameras (left). Paths followed by the robots (right). The cameras' paths are displayed in thin lines, and their final positions are marked with squares. The final camera footprints are shown as dashed-line circles.

Scientific achievement #26
Anticipatory representations and dynamic model selection for active perception

Experimental and computational studies conducted on decision-making tasks under ambiguity and heavy time constraints demonstrated that a strong coupling between perception and action through anticipatory representations improve performance. When present at the core of the models required to differentiate situations, such coupling facilitates unsupervised learning (normative representations), makes decisions more robust to noise and uncertainty (population coding and competition dynamics), and allows dynamic selection of relevant information to reach a decision (active perception). The proposed bio-inspired mechanisms apply to object recognition (reproducing human and primate behavioral data), but also to localization (with applications to mobile robotics).

Living beings have to continuously select adequate actions to interact with their environment (originally for the sake of survival). Perception and action are thus naturally bound at the heart of several theoretical frameworks on cognition (embodied cognition, enaction, interactivism...), and are directly modulated by a lot of factors (from the physical to the social). From this perspective, the stable representation of percepts and model based decision-making are required once the complexity of the body, the environment, or their coupling increases beyond a critical threshold. This is of course true for humans, but also for many nowadays artificial systems; especially in robotics, with either a high number of DoFs, open environments to explore, or HRI applications.

To reproduce the near-optimal information sampling and action selection strategies observed in humans, these need to be experimentally studied and generative models designed. Three complementary mechanisms are invoked and combined:

- **Active learning** of statistical regularities from flows of information with hidden structure. Adopting anticipatory and distributed representations (sensorimotor contingencies for interactive systems) increases the state space but enables unsupervised learning and exploration mechanisms (to locally reduce problem dimensionality). Models based on this type of representations are directly testable by interacting with the environment, and can be internally simulated to predict action outcomes (see mental simulations from L.W. Barsalou).
- **Active perception** is the reverse mechanism by which acquired knowledge can help focalizing perception at relevant information (discrimination) through epistemic actions (e.g. covert or overt visual attention, measured through eye-tracking in humans). The obtained information can then infirm/confirm predictions and thus orient pragmatic actions oriented toward a goal (e.g. selecting a response as measured by mouse-tracking in humans) (see D. Kirsh's work for the justification of this distinction). Such a mechanism satisfies temporal and energetic constraints, by balancing parallel sensory processing and sequential action selection.
- **Dynamic model selection** finally corresponds to the integration of information to discriminate between situations (e.g. objects or contexts) by weighting models and corresponding actions. Depending on constraints and parameters, the same competition dynamics may lead to winner-take-all (e.g. categorization in abstract concepts) or probabilistic solutions with spatiotemporal continuity (e.g. navigation or movement generation). Selection car occur between an arbitrary number of models of arbitrary complexity (often involving planning) and must deal with data variability.

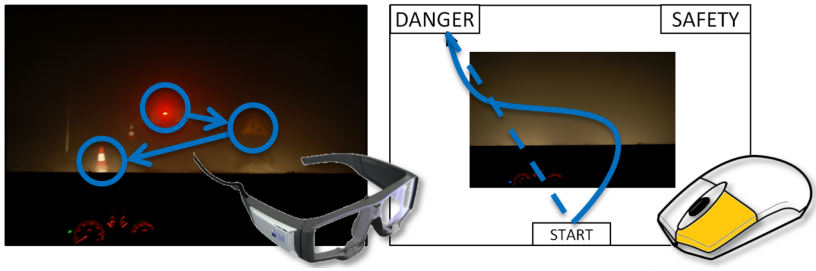

Fig. 1: Illustration of tools used in human experiments to measure active perception strategies. Measures include the recording of dynamic traces reflecting epistemic actions (eye-tracker) and pragmatic actions (mouse-tracking). Pictures were taken in the Fog & Rain platform of the DLCF Cerema.

These mechanisms feedback on each other, mainly positively, but their interaction opens a new problematic, as the sampling of information is biased by existing models, leading to a dilemma between active learning and active perception.

Using various combinations of bottom-up preprocessing steps (e.g. saliency maps), and competition dynamics (e.g. dynamic neural fields, energetic networks...), we consistently demonstrated that using such mechanisms within a predictive coding framework can lead to improved performance for recognition and localization applications. They nevertheless require changes in the way robots and their control architectures are designed, in order to allow low level perception-action coupling.

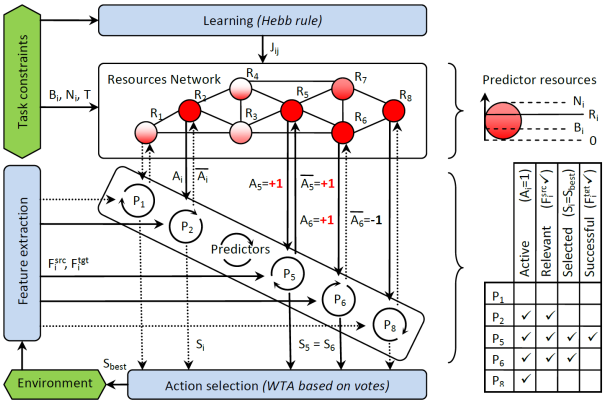

Fig. 2: Attractor Predictors Network (as in Catenacci et al., 2014) modulating the activity of chains of predictors. Those relevant within the current context compete for action, and based on the satisfaction of their predictions, excite/inhibit associated nodes in the network. After only a few iterations, the activity may fall into a basin of attraction and thus converge to a decision.

CONTACTS

Jean-Charles QUINTON
J-Charles.QUINTON@univ-bpclermont.fr

FURTHER READING

The cat is on the mat. Or is it a dog? Dynamic competition in perceptual decision making
J.C. Quinton et al., IEEE Transactions on Systems, Man and Cybernetics: Systems 44, 539-551 (2014)

How active perception and attractor dynamics shape perceptual categorization: a computational model
N. Catenacci et al., Neural Networks (2014)

CONTRACTS

FP7/EUCognition (2011)
Action PEVMA LabEx IMobS3 (2012-2015)
PEPS CNRS M²DyCS (2014-2015)

PhD

N. Catenacci Volpi, L. Lopez, B. Quétard

Scientific achievement #27
Hardware architecture of smart camera

Processing images to extract useful information in real-time is a complex task, dealing with large amounts of iconic data and requiring intensive computation. Smart cameras use embedded processing to save the host system from the low-level processing load and to reduce communication flows and overheads. Field programmable devices present special interest for smart cameras design: flexibility, reconfigurability and parallel processing skills are some especially important features.

Artificial intelligent systems often need to get information about the surrounding environment, in order to adapt their behavior or perform a given task. In much cases, the quality of extracted information determines system's performance. Hence, the sensing system plays an important role in several applications, from intelligent vehicles (autonomous navigation, obstacle detection, assisted driving, etc.) and robotics (visual servoing) to security systems (surveillance, face and behavior recognition, etc.). Image sensors are frequently employed, alone, in network, or in combination with other sensing devices through data fusion techniques. Some interesting features presented by image sensors are their low-cost, easy integration (standard interface protocols such USB, Firewire, GigaEthernet …), and the ability to extract different kinds of information (motion detection and estimation, localization, detection and recognition of a given pattern (face, object), etc.). However, many vision tasks exhibit the following characteristics: first, they rely on real-time operation to extract useful information from a dynamic environment. Second, they involve low-level, time consuming processing of large amounts of iconic data. They therefore place stringent constraints on the computing system, both in terms of communication bandwidth and computing power. Even with recent outstanding advances in microelectronics, standard PC architectures are frequently unable to deliver required performances for such applications. Embedded processing can help to solve these problems by executing low-level tasks within the camera platform, before data transmission to the host system. This way, amounts of data to be transmitted can be strongly reduced, and transmitted data is more pertinent than a raw pixel flow, meaning that received data can be promptly used by the host system, without pre-processing time consuming tasks. Processing resources are added to the camera's hardware in form of FPGA devices, media/streaming processors, DSP's, etc. Cameras with embedded processing resources are known as "Smart Cameras", and are the subject of growing interest.

Field programmable logic presents special interest for smart cameras design. Reconfigurability allows to adapt camera's architecture for a wide palette of applications, and data and task parallelism can be easily and massively exploited to meet real-time constraints. Moreover, FPGA's flexibility allows to interconnect different external devices (memories, ASICs), as well as internal soft-core processors, making possible to exploit mixed hardware/software solutions.

A strength of our hardware platforms is the modularity. Different hardware devices are integrated in different boards. These boards are interconnected, and can be replaced to allow the platform's evolution. Thanks to this feature, this smart camera platform has frequently evolved.

Many FPGA-based smart cameras have been developed during these 10 last years:

- SeeMOS: Active vision-dedicated camera
- BiSeeMOS: High speed stereo smart camera
- Panoramos: Cylindrical panoramic smart camera
- DreamCam is a mature prototype of smart camera. This camera is the core of technology transfer to the Spin-off Wisip.

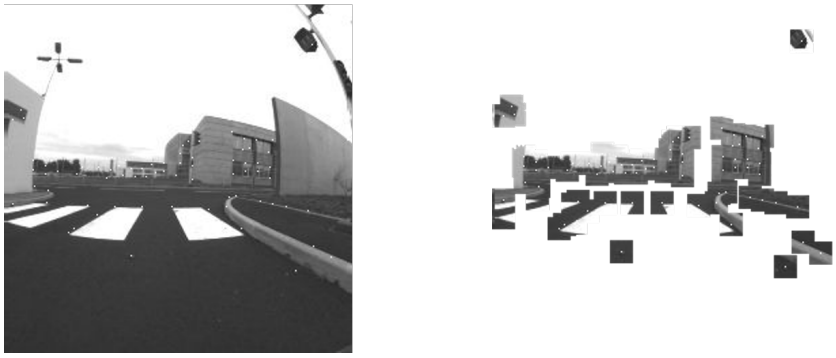

Fig. 2: Output of DreamCam (Harris and Stephen points extraction). Left - classical video streaming. Right – Stream of Harris points described by a grey-level template.

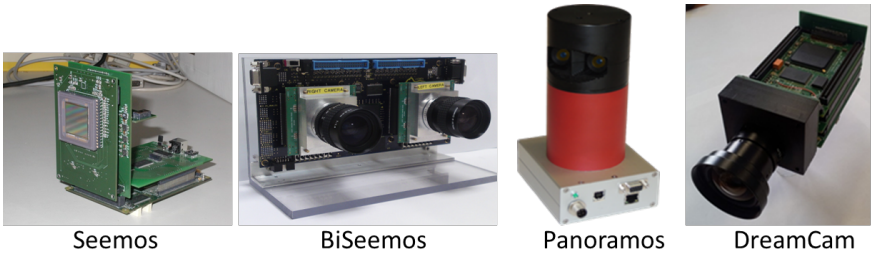

Fig. 1: Hardware architecture of Smart Cameras.

CONTACTS

François BERRY
Francois.BERRY@univ-bpclermont.fr

FURTHER READING

G ??????? g
L. ?????? (2012)

CONTRACTS

ANR Jeunes Chercheurs VIRAGO (2007-2011)
ANR COGIRO (??-??)
Projet EUREKA Euripides Seamoves (??-??)
Action RECIPAS LabEx IMobS3 (2012-2019)

PhD

S. Ahmed, M. Birem, C. Bourrasset, F. Dias Real, N. Roudel

Scientific achievement #28
SCANET: Conjunction of IoT (Internet of Things) and distributed smart camera

Smart Camera Network (SCN) is nowadays an emerging research field promoting the natural evolution of centralized computer vision applications towards full distributed and pervasive systems. Differently from Wireless Sensor Networks (WSN) which are generally supposed to perform basic sensing tasks, SCNs consist of autonomous devices (Embedded Vision Systems), performing collaborative applications and leveraging on-board image processing algorithms optimized in respect of the limited available resources. In this vision, we propose a SCN based on a reconfigurable FPGA-based architecture and inspired by the IoT paradigm. Thus, a future SCN pervasively monitoring and controlling many activities in our daily life is a realistic view.

In the last years, the rapid growth of interconnected objects has triggered new autonomous and smart nodes development. As evidenced by recent surveys, the Internet of Things (IoT) concept is now a highly active trend that is shaping the Information Communication and Technology (ICT) sector.

Highly dynamic and pervasive Wireless Sensor Networks (WSNs) are already deployed in many different scenarii, e.g. environmental monitoring, smart cities, or health-care.

Network nodes now not only measure simple physical events (e.g. light, sound, temperature) but also have basic computing capabilities to extract features from the captured data.

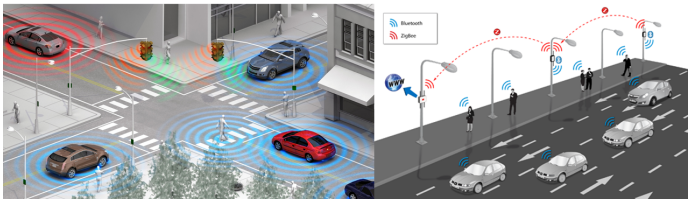

Fig. 1: Example of collaborative smart sensors: Each "road actor" (vehicle, pedestrian, infrastructure) provides, exchanges and consumes data (warnings, map,…) via internet.

In foreseeing a seamless integration of pervasive multimedia sensors, vision-enabled applications are becoming more and more attractive within the IoT scenario. These vision-enabled devices, also known as Smart Cameras (SCs), are nowadays challenging the processing architecture to perform complex, computationally intensive image processing operations in resource constrained embedded systems. In particular SC architectures greatly ease the deployment of applications relying on distributed video processing. This is evidenced, where a wireless, low-power SC platform is used for steady state video-surveillance and in, where a distributed Smart Camera Network (SCN) is used by a traffic tracking application in smart cities.

In order to achieve real-time image processing performance with limited hardware resources, the architecture of SCs are generally custom-designed and, consequently, highly application specific. However, the emergence of pervasive autonomous applications, which have to provide a reliable understanding of quickly varying environmental conditions, requires a degree of flexibility that custom-built hardware cannot provide. To address this issue, several reconfigurable SC architectures, built upon FPGA circuits, have been proposed.

Indeed, hardware architectures offer vast opportunities for applications based upon the IoT concept beacause services provided at the node level are now not only limited to "lightweight" operations implemented in software but can also include intensive image processing operations aimed at improving the high level scene understanding.

The only drawback of using FPGAs is that they are usually featuring dedicated solutions for low level operations, neglecting both the reconfigurability and flexibility issues. These facts are demonstrated in literature when scientists propose non-reconfigurable custom solutions targeted to specific applications only. In many works, the hardware is programmed from scratch to match a specific problem. In order to fit the IoT paradigm requirements, we propose an innovative and reconfigurable FPGA internal architecture based on the System on a Programmable Chip (SoPC) design technique able to overcome these limitations abstracting each functional block as a network resource.

Our envisioned architecture will be featuring: (i) pervasiveness and ubiquitous programming, (ii) real-time image processing, (iii) multi-purpose platforms, (iv) low cost hardware and (v) limited power consumption.

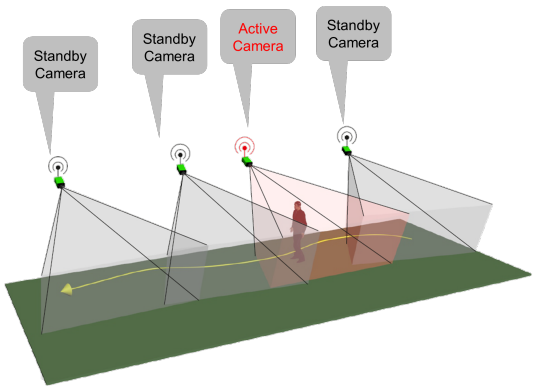

Fig. 2: Tracking application on a distributed network of smart cameras. The system will be based on particle filter which is very common for tracking objects. A first application (HOG) computed in each SC is able to exchange information via any Ethernet network for a re-identification task.

CONTACTS

François BERRY
Francois.BERRY@univ-bpclermont.fr
Jocelyn SEROT
Jocelyn.SEROT@univ-bpclermont.fr

FURTHER READING

FPGA-based smart camera mote for pervasive wireless network
C. Bourrasset et al., 7th Inter. Conf. on Distributed Smart Cameras (ICDSC), 1-6 (2013)

CONTRACTS

Action RECIPAS LabEx IMobS3 (2012-2019)
Collaboration CNIT (Pise-Italie)

PhD

C. Bourrasset, L. Maggiani

Scientific achievement #29

Design and fabrication of many-core ASIC solutions dedicated to embedded smart camera

This action proposes an original flexible MP-SoC (Multi-Processors System on Chip) architecture for image processing applications called HNCP based on parallel algorithmic skeleton. A single core (HNCP-I) has been fabricated using a 65nm CMOS technology then a 16-core and a 64-core ASIC with a software configuration has been designed. Each tile (processor + peripherals) of the network can configure its communication links depending on the most relevant overall parallelism scheme for a targeted application. HNCP-I chip is programmable and testable through an ad-hoc JTAG solution. It turns out to be a tile of a future MP-SoC ASIC design.

Smart sensors today require processing components with sufficient power to run algorithms at the rate of these high-performance image sensors, while maintaining low power consumption. Mono-processor systems are no longer able to meet the requirements of this field. Thus, thanks to technological advances and based on previous works on parallel computers, many-core approaches represent an interesting and promising solution.

Previous works around this topic have used FPGA but results have shown the limits of this target in terms of hardware resources and in terms of performance (speed in particular). This observation leads our team to change the target from FPGA to ASIC. This migration requires deep rework at the architecture level. Particularly, existing IPs (communication, clock management, video management ….) around the method (called HNCP for Homogeneous Network of Communicating Processors) have been revisited.

To take advantage of the performance offered by the ASIC target, proposed many-core systems are based on the flexibility of its architecture. Combined with parallel skeletons that ease programmability of the architecture, the proposed circuits allow to offer systems that support various real-time image processing algorithms. This action has led to the fabrication of the first integrated circuit fabricated in the Institut Pascal (HNCP-I) based on a single processor and its peripheral. HNCP-I chip consists of one open-source 32 bits RISC processor called SecretBlaze supporting FSL instructions with 4KB of local memory, Wishbone bus, peripherals (UART, timer, GPIO and interrupt controller) and clock and reset modules.

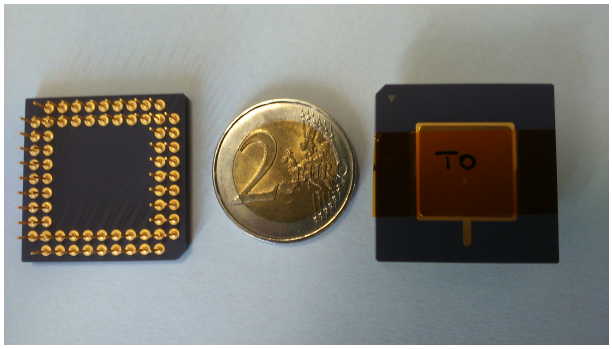

Fig. 1: HNCP-I first ever IC fabricated at Institut Pascal (partnership with CMP institute using technology node from ST-Microelectronics).

It is implemented in ST 65 nm CMOS technology and the die size is 0.906 mm^2. Moreover, two flexible multiprocessor architectures based on the concept of parallel skeletons have been proposed (a 16 cores 65 nm CMOS multiprocessors and a 64 cores 28 nm FD-SOI CMOS multiprocessors) and evaluated regarding executing time, speedup and efficiency for various image processing algorithms (Harris & Stephen, matching etc...).

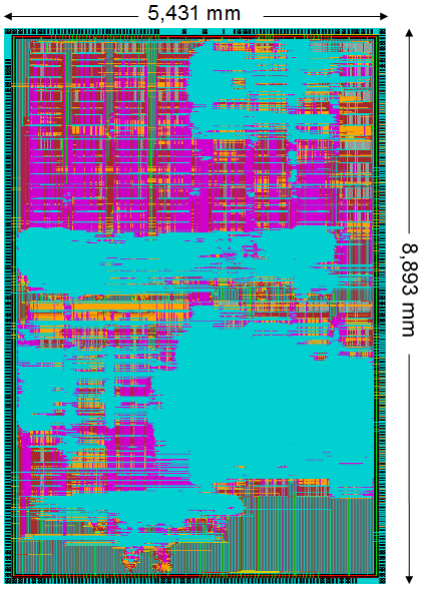

Fig. 2: HNCP-III a 28nm 64-core many-core designed (not fabricated) dedicated to embedded smart camera.

CONTACTS

Alexis LANDRAULT
Alexis.LANDRAULT @univ-bpclermont.fr
Jean-Pierre DERUTIN
Jean-Pierre.DERUTIN@univ-bpclermont.fr

FURTHER READING

A 16-Core microprocessor ASIC for image processing algorithms
M.A. Boussadi et al., *9th International Symposium on Reconfigurable Communication-centric Systems-on-Chip (ReCoSoC2014), Montpellier, France* (2014)

CONTRACTS

CMP: A service organization in ICs low volume production
LIRMM: Definition and fabrication of a ST 28 nm many-core solution

PhD

M.A. Boussadi, H. Chenini

Scientific achievement #30

CAPH: a Domain Specific Language for implementing stream-processing applications on reconfigurable FPGA-based hardware

CAPH (caph.univ-bpclermont.fr) is a high-level, domain-specific language (DSL) dedicated to the implementation of *stream-processing* applications on reconfigurable harware such as FPGAs. *Stream-processing* application are applications operating on the fly on continuous streams of data, such as real- time image processing for example. These applications often require a computing power which still beyond the capacity of general purpose processors (GPPs) but generally exhibit a large amount of fine-grained parallelism, making them good candidates for implementation on FPGAs. However, in the current state-of-the art, programming FPGAs requires expertise in digital design and in practice this limits the applicability of FPGA-based solutions. CAPH allows programmers without this expertise to implement and test applications on FPGAs. Being based on well-defined formal semantics, CAPH does not suffer from the problems of many *ad-hoc* approaches to the high-level synthesis problem.

Digital circuits based upon reconfigurable logic (FPGAs) offer large opportunities for exploiting massive, fine grain parallelism. In many application domains, FPGAs are now promoted as a way out of the restrictions of specific CPU designs on system scalability. This is specially true for smart cameras integrated into wireless networks, for which the low bandwith of the network forces the cameras to pre-process on-the-fly raw image streams into mid-level semantic descriptors. The computing power required for such tasks, in the range of billions of operations per second typically, is generally beyond the capacity of general purpose processors. But most of these computationally demanding tasks exhibit massive, fine-grain parallelism, making them good candidates for implementation on reconfigurable logic such as FPGAs.

However, if the introduction of FPGAs can address some performance issues in smart camera architectures, it raises significant challenges in terms of programmability. In the current state of the art, programming FPGAs is essentially done using low-level hardware description languages (HDLs), such as VHDL or Verilog. Using these languages requires expertise in digital design and in practice this limits the applicability of FPGA-based solutions. High-level synthesis (HLS) have been developed in response to this limitation, in order to allow FPGAs to be used by programmers lacking skills in digital design. But, despite significant advances in this field, these tools still have difficulties in generating efficient circuit implementations from high-level behavioral specifications because of the semantic gap between this level and the gate-level implementations. This, again, is specially true for FPGA embedded in smart camera because of the stringent constraints that the architecture and the applications put on the implementations. The complexity of the target FPGA, for example, is often severily limited by the total power consumption of the platform, thus requiring highly op- timized synthesis. Moreover, real-time processing puts a strong emphasis on precise timing requirements, which are difficult to take into account when resorting to HLS tool.

CAPH pragmatically addresses the challenge of obtaining efficient FPGA implementation from high level specifications by focusing on a specific application domain – within which the synthesis process can rely on application-specific abstractions – and by adopting a purely dataflow model of computation. This model actually fills the gap between the programming and execution models (which is the main obstacle in most of HLS approaches) while being naturally amenable to formally-based transformations, optimizations and proofs.

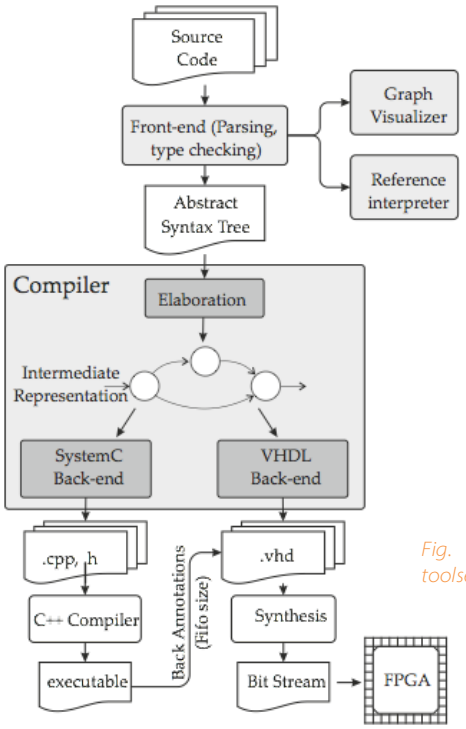

Fig. 1: The CAPH programming toolset.

The current tool chain supporting the CAPH comprises a graph visualizer, a reference interpreter and a compiler producing both SystemC and synthetizable VHDL code. The reference interpreter is based on a fully formalized semantics of the language, written in axiomatic style. The compiler generates a target-independent intermediate representation of programs, which are then processed by specific back-ends. The VHDL back-end is in charge of generating the FPGA configuration for hardware synthesis. The SystemC back-end produces cycle-accurate SystemC code which is used to provide *back-annotations* to customize and optimize the VHDL code.

Several real-time image processing applications have been implemented using CAPH on smart-cameras, FPGA-based, platforms (such as the one described in XXX) : object tracking, MPEG encoding, vehicle and pedestrian detection, *etc,* demonstrating that efficient implementations of complex applications can be obtained with a language whose abstraction level is significantly higher than that of traditional HDL languages such as VHDL or Verilog.

CONTACTS

Jocelyn SEROT
Jocelyn.SEROT@univ-bpclermont.fr

FURTHER READING

High-level dataflow programming for real-time image processing on smart cameras
J. Sérot et al., Journal of Real-Time Image Processing, DOI10.1007/s11554-014-0462-6 (2014)

High-Level Dataflow Programming for Reconfigurable cameras
J. Sérot et al., Inter. Symp. on Computer Architecture and High Performance Computing Workshop, Paris, 72-77 (doi=10.1109/SBAC-PADW.2014.18) (2014)

CONTRACTS

Action RECIPAS LabEx IMobS3 (2012-2019)

PhD

S. Ahmed, C. Bourrasset

Scientific achievement #31
ECOGRAFI project: ECOpromotion of GRAnular and FIbrous materials

Many industrial sectors use, make, transform and transport granular or fibrous materials (food and production of the food-processing industry, aggregates and materials for civil engineering, industrial wastes and residues, pharmaceutical powder). Besides, these materials are also present in the natural state (grounds, woods, …).

Today in a context of research for ecological sustainable technical solutions, these materials of natural (mineral or plant) or industrial (manufactured goods, waste, etc.) origin have to be to enhanced and optimized with the aim of protecting resources and reducing pollution and energy. But only it is necessary to know their behavior: mechanical, thermal and acoustic performances, ageing, assembly, recycling, etc.

ECOGRAFI is a technical center dedicated to research whose goal is the development of new materials or characterization methods for eco-materials and any granular or fibrous materials. Ecografi is also destined to allow the characterization of the behavior of these materials in particular for their use and their promotion in the field of the construction.

This technical center is also destined for the devloppment of a soils and granular materials bank (physical and numerical) unique in France at this present time.

In the end, the objective is to develop techniques or materials which can be industrialized and accentuate partnerships or collaboration with industrial partners.

The global cost of the project is 840 000 Euros divided between building and scientific equipment.

At a local scale, this center focused on the material scale (characterization, identification, instrumentation) is complementary of the civil enginnering technical center which works at the scale of the structure. The latter can thus benefit directly from contributions and from results led by EcoGraFi.

On the other hand, the presence of the Biological technical center Bio'UP ' next to EcoGraFi center will allow to make the link between the physical and mechanical properties of materials and the biochemical properties (particularly for eco-concretes or problems of environment in grounds).

On a regional scale, EcoGraFi will be opened to the other research structures such as the IRSTEA, the BRGM, the Laboratory Magma et Volcans as well as the schools of architecture and will thus be an important experimental tool for these various structures and to introduce common projects between them.

In the inter-regional scale of Massif Central, works can be launched with different structures working on related problems, in particular the technical center of Egletons or the LMGC of Montpellier.

At the national level, the ambition of the ECOGRAFI is to create a center of resources and a research center of national and European visibility for the characterization of granular and fibrous materials.

CONTACTS

Sofiane AMZIANE
Sofiane.AMZIANE@univ-bpclermont.fr
Pierre BREUL
Pierre.BREUL@univ-bpclermont.fr

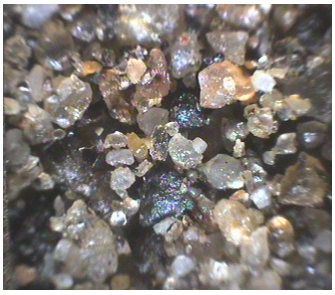

Scientific achievement #32
Settlement prediction of coarse granular materials under vertical loading

The elementary mechanisms of a granular bed under vibrational loading are still unclear and there is presently no established theory or methodology to predict the settlement and its statistical variability. By means of a parametric study, carried out on a full-scale track, and a critical analysis of density relaxation laws, a novel settlement model in coarse granular materials under cyclic loading has been introduced. Experimental data indicate that the settlement process is governed by three independent parameters strongly correlated with the vibration intensity and initial packing fraction. We have showed that the mean settlement is well predicted by the model with its parameter values extracted from experimental data.

Granular materials are both pressure-dependent and density-dependent materials and exhibit a broad range of intricate behaviours due to their discrete nature, dissipative interactions and generic structural disorder. The packing fraction may vary as a result of particle rearrangements induced by shearing or vibrations and it leads to dramatic changes in the structure and mechanical response of a granular material. A long-time logarithmic relaxation law of the packing fraction is systematically observed in experiments. In simple compaction models, this behaviour is attributed to the exponentially increasing time for the particles to reach a new configuration of lower packing fraction. The case of settlement under cyclic loading has, however, been much less investigated. The settlement of granular bed occurs due to both compaction and side-wise spreading. An important industrial example is the railway ballast (figure 1), which undergoes gradual settlement under the static and dynamic overloads induced by train traffics. The readjustment of differential settlements requires costly operations on fast-train railways. For this reason, an improved understanding of the parameters governing the settlement process is a critical technological challenge for new developments in this field.

In this work, we carried out a parametric study on a full-scale ballast track (figure 1) in order to test various models for the prediction of settlement in coarse granular materials under cyclic forcing. The bed was subjected to a sinusoidally varying vertical overload up to 104 cycles for a broad range of amplitudes and frequencies. In the same way, the initial state of the granular bed was varied and a light dynamic penetrometer was used to characterize its packing fraction before each loading test. In order to achieve a better understanding of the penetration process into the coarse granular material, a numerical study was performed by means of contact dynamics simulations (figure2).

Fig. 1: Full-scale track model used in the present work.

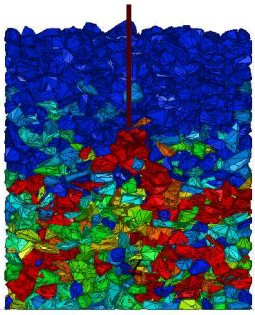

Fig. 2: Modelling of Penetration test in coarse granular materials with Discret Element Methods.

The settlement as a function of the number of cycles occurs in three stages with nearly the same functional dependence but varying with the initial state of the material and vibration amplitude (figure 3). A model based on the Chicago density relaxation law provides an accurate estimation of settlement for a high number of cycles with parameters that reflect the loading parameters and initial mechanical state of the material and can be measured by independent tests (figure 3). This model provides a reliable approach in applications where long-term settlement needs to be estimated in coarse granular materials. Our findings raise also a fundamental question as to the predictability of the mechanical response of granular materials despite their natural variability and complex shapes of ballast grains.

The behaviour is chaotic in the sense that small variations in the initial configuration of a granular packing are expected to be amplified with the number of loading cycles. This is not what we observe although fluctuations are observed between independent tests. This indicates that the fluctuating parts of consecutive incremental settlements average out and the system tends to a well-defined ultimate mechanical state. In other words, the mechanical state of the granular material under vibrations is determined by its distance from the ultimate state.

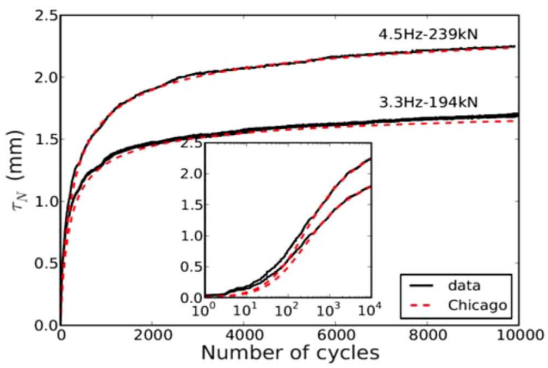

Fig. 3: Prediction of settlement by a logarithmic law in comparison to the experimental data for two tests (frequency of 4.5 Hz and applied load of 2393103 N; Frequency of 3.3 Hz and applied load of 1943103 N). The inset shows the data on a log-linear scale.

CONTACTS

Pierre BREUL
Pierre.BREUL@univ-bpclermont.fr

FURTHER READING

Penetration test in coarse granular material using Contact Dynamics Method
J.C. Quezada et al., Computers and Geotechnics 55, 248 (2014)

Predicting the settlement of coarse granular materials under vertical loading
J.C. Quezada et al., Scientific reports 4, 5707 (doi:10.1038/srep05707) (2014)

Un modèle qui rend les trains moins cahotants
Les cahiers scientifiques du Monde, page 2 (éd. 03/09/2014)

PhD

J.C. Quezada

Scientific achievement #33
Full-field measurements and identification in thermomechanics of materials

The development and use of full-field measurement technique is one of the most recent fields of research in Solid Mechanics. The local team involved in this topic has been active in the last few years in the development and use of various measurement techniques. This has enabled to characterize finely various types of materials ranging from natural to metallic and polymeric materials, favouring the detection and study of localized phenomena in numerous cases.

Full-field measurement techniques are spreading at an accelerating pace in the experimental mechanics community. The local research team on this topic is active in two main fields : 1- the development of image processing tools able to provide displacement strain or heat source fields from images shot by digital and infrared (IR) cameras ; 2- the use of such tools to study the thermomechanical response of materials and structures.

Concerning the first point, two techniques providing displacement and strain maps are currently developed: the grid technique and digital image correlation (DIC). They are complementary in terms of strain or displacement amplitude: the first one is mainly suitable for small strains and displacements, the second one for large deformations. Particular attention has been paid in our recent work on the determination of the metrological properties of these measuring tools, more particularly in terms of bias and noise quantification. Concerning the use of IR thermography, attention has been paid on the heat source reconstruction from temperature change fields in order to determine the calorimetric signature of the mechanical events occurring in the specimens under tests.

These measuring techniques were employed to characterize various types of materials in the recent past, for instance aluminium (pure or alloys), shape memory alloys, wood, concrete, biocomposites and elastomers. « Characterizing » means here first observing phenomena with the metrological tools cited above, second proposing suitable models to describe the observed phenomena, and third identifying the parameters driving these models. Concerning the first point, Figure 1 shows a typical strain and displacement fields measured with the grid method on a shape memory alloy during a tensile test. High gradients due to phase transformation and numerous features such as martensitic bands and needles are clearly visible. The deformed specimen (deduced from measurements though a mesh is employed for depicting deformation in a realistic way) also illustrates its non-conventional mode of deformation.

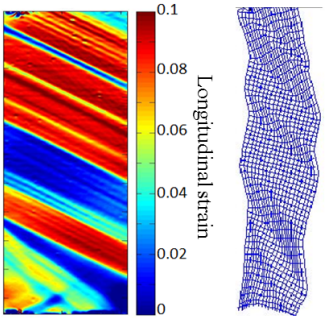

Fig. 1: Typical strain and displacement fields measured with the grid method during a tensile test carried out on a Cu-Al-Be shape-memory alloy specimen.

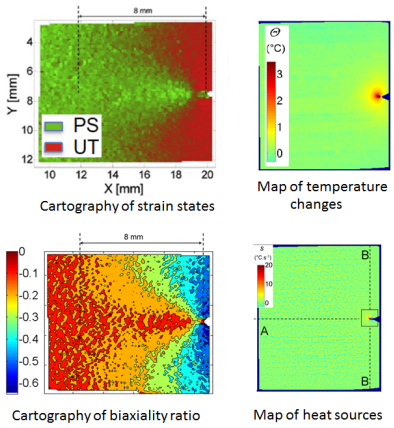

Fig. 2: Cartographies of strain states, biaxiality ratio, temperature changes and heat sources at the crack tip of elastomeric material.

Figure 2 shows the fields obtained around a crack tip in an elastomeric specimen characterized with DIC and IR thermography. This example shows the complexity of the thermomechanical behaviour of elastomeric materials. In particular, the distribution of the strain states corresponding to uniaxial extension and pure shear illustrates the high heterogeneity in the material around the crack tip. Due to the movement of physical points on the surface of the material, heat source fields have been determined by coupling digital and IR cameras and using a motion compensation technique developed in the lab.

Figure 3 finally shows an example of heat source field related to the Portevin Le Châtelier effect in an aluminium-magnesium specimen. Different types of band distributions are revealed by the processing, such as the X-shaped microstructure which is clearly recognizable in this example.

To go beyond the measurements, it is necessary to identify the parameters driving the constitutive laws. For this purpose, the team has been instrumental in the development of one of the techniques introduced to process the wealth of data provided by full-field measurement techniques, namely the Virtual Fields Method.

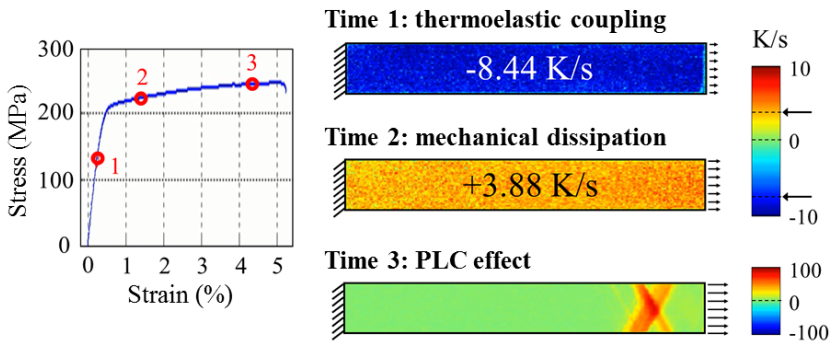

Fig. 3: Typical heat source revealing Portevin Le Châtelier bands during a tensile test performed on an aluminium-magnesium specimen.

CONTACTS

Xavier BALANDRAUD
Xavier.BALANDRAUD@ifma.fr
Benoit BLAYSAT
Benoit.BLAYSAT@univ-bpclermont.fr
Michel GREDIAC
Michel.GREDIAC@univ-bpclermont.fr
Evelyne TOUSSAINT
Evelyne.TOUSSAINT@univ-bpclermont.fr

FURTHER READING

Heat and strain measurements at the crack tip of filled rubber under cyclic loadings using full-field techniques
J.R. Samaca Martinez et al., Mechanics of Materials 81, 62 (2015)

Investigation of martensitic microstructures in a monocrystalline Cu-Al-Be shape memory alloy with the grid method and infrared thermography
D. Delpueyo et al., Mechanics of Materials 45, 34 (2012)

The Virtual Fields Method
F. Pierron and M. Grediac, 517 pages, Springer (2012)

CONTRACTS

ANR Demether (2011-2015)
CIFRE Michelin (2010-2014)

PhD

C. Bubulinca, D. Delpueyo, P. Jongchansitto, J.R. Samaca Martinez, S. Sun

Scientific achievement #34
Methodology of diagnosis of tunnels and underground structures in use

The infrastructure maintenance is of major concern for the management and the development of cities. It is thus essential that the managers can improve their diagnosis techniques and have the adequate tools to better assess the current state of their structures. This project proposes to develop a new diagnosis methodology for this type of structures and a tool for the study of their behaviour that better takes the various components and their interaction into account. The aim is to provide physical and mechanical indicators to managers in order to help them defining and optimizing their maintenance policy, based on a more rational expertise.

The plannified development of the urban areas will imply to build and to spread the infrastructures needed to their good operating. But the infrastructure maintenance is of major concern for the management and the development of cities, in order to ensure good working conditions, security and to optimize the management cost of these structures. It is thus essential that the managers can improve their diagnosis techniques and have the adequate tools to better assess the current state of their structures. However, the methods that they currently have at their disposal are either deficient to give quantitative information of good quality or not adapted to the site constrains, especially for underground structures in use.

This project proposes to develop a new diagnosis methodology for this type of structures and a tool for the study of their behaviour that better takes the various components and their interaction into account (figure 1). The aim is to provide physical and mechanical indicators to managers in order to help them defining their maintenance policy, based on a more rational expertise.

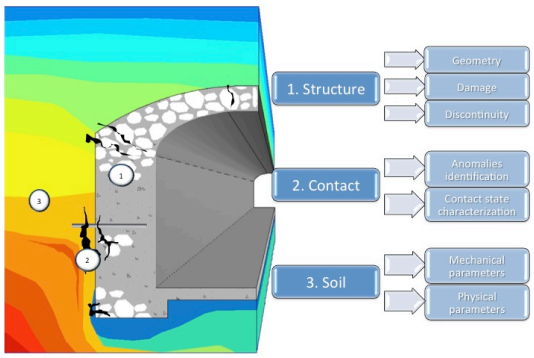

Fig. 1: Different components of an underground structure and parameters to be determined for the diagnosis.

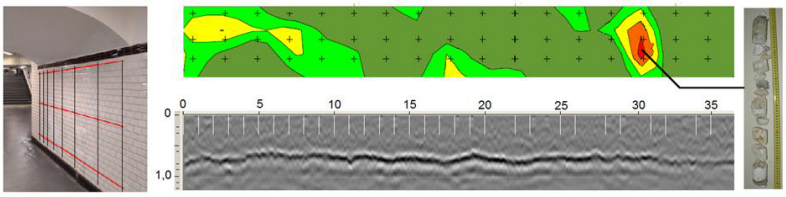

Fig. 2: Exemple of an underground tunnel study (left), impulse-response cartography and radar thickness profile (center) and core sample (right) extracted for analysis.

To a quantitativ characterization of the structure and soil current state by taking into account *the soil and structure variability and their interaction:*

The main goals of the project are:

- the evaluation of the current state of the various components of the structure. Therefore, a set of monitoring tools adapted to the site constrains will be tested and the processing of some tools under development will be improved in order to provide the localization and the importance of the defaults
- the development of a diagnosis methodology containing the unification of the various obtained data in order to provide reliable and realistic input parameters to the models and to obtain a good evaluation of their spatial variability (figure 2).
- the development of a model which incorporates the soil and structure variability and takes really their interaction into account. The model will be characteristic of the problem handled (underground structure, damaged state, urban area), it will be fed by the input parameters developed at the point 2. and will provide an estimation of the global state of the structure portion.
- the development of a basic tool to decision aid and risk analysis for the choice of a strategy of maintenance.

Main results:

- Improvement of the auscultation methodologies (no disturbing methods and estimation of the parameters)
- Improvement of the on site material identification (masonry and soil) and better evaluation of soil deformation modulus from dynamic penetrometric test.
- Improvement of the response of numerical model: by a better evaluation of the input data and by really taking into account soil/structure interaction and data variability.
- Proposition of a maintenance methodology based on amulti criteria analysis.

The Méditoss project is an industrial research project manged by the Institut Pascal (Pierre BREUL). Four partners are involved in this project: two public laboratories (Institut Pascal - Université Blaise Pascal and LGCIE of INSA de Lyon) and two industrial partners (RATP and Sol Solution). The duration of the project would be 4 years with a total cost equal to approximatively 1000 k€ including solicited aid of 500 k€.

CONTACTS

Pierre BREUL
Pierre.BREUL@univ-bpclermont.fr

FURTHER READING

Mechanical investigation of tunnels: risk analysis and notation system
N. Rhayma et al., Structure and Infrastructure Engineering, doi:10.1080/15732479.2015.1019892 (2015)

Characterization of the mansonry lining of an underground structure by geoendoscopy
D. Llanca et al., Tunnelling and Underground Space Technology 38, 254 (2013)

Numerical modeling of the time dependent degradation of the mechanical properties of a metro underground gallery
T. Kamel et al., 1st Eastern European Tunneling Conference (1EECT), Budapest (2012)

CONTRACTS

ANR Villes Durables MEDITOSS (2009-2014)

PhD/Post Doc

D. Llanca/N. Rhayma

Scientific achievement #35
Reliable and optimal repair of damaged structures using composite materials

The project TASSILI established strong international cooperation between French and Algerian researchers through the development of multi-scale behavior models and repair of structures using composite materials. The first stage allowed the modeling of composite material behavior, especially the internal force transfer between fibers and matrix, and between composite and substratum. The natural variability of composite materials and the multi-material interfacing are the main concerns in the joint works. In the second stage, the multi-scale modeling of repair of damaged structures was developed and applied of typical pipelines, aerospace and civil engineering structures. This cooperation has been valorized through 6 PhD theses and 11 papers in international journals.

The maintenance and lifetime extension of existing structures represents a highly challenging field for many industrial sectors, not only because of the unpredictable damage phenomena, but also due to the high sensitivity of the repair technology. The concept of using bonded composite materials, to maintain aging structures in acceptable service conditions, has shown to be performant at the short term in nominal conditions. However, the lifespan of the repair efficiency cannot be guaranteed, especially due to material aging, and uncertainties related to loading and environmental conditions. Technically, bonded repair reduces the stress field in the damaged region (e.g. near the crack tips) by bridging the stresses within the structure, leading to retardation or complete stopping of the structure deterioration.

The scientific cooperation between the Institut Pascal and the USTO aims at developing mechanical and probabilistic models of structures repaired by composite patches. This cooperation has been established through the development of the following two axes:

The first axis concerns the development of mechanical and probabilistic strength models for unidirectional composites made of industrial and natural fibers. Analytical and numerical models have been developed to predict the stress concentration in the neighborhood of the broken fibers, as well as the sequence of breaks in the neighboring fibers. Micromechanical technique with random fiber spacing and irregular diameters is considered for the development of the load sharing patterns. A sequential cracking procedure is developed to simulate the crack propagation along fibers in the composite materials. The randomness of fiber diameters and spacing allows us to determine the probabilistic distribution of composite strength, as well as the sensitivity of various material and geometrical parameters regarding the overall reliability of the composite plates. The applications have been carried out on composite plates and pipes.

The second axis concerns the development of strengthening models for structures repaired with unidirectional fiber composite patches. The optimization of repair patch forms and materials is carried out for both concrete and metal structures. The 3D modelling and the consideration of adhesive interface between the repaired structure and the composite patch are seen as important features of the undertaken developments.

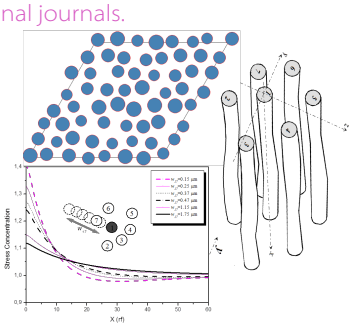

Fig. 1: Randomly distributed composite and stress concentration in the vicinity of broken fibers.

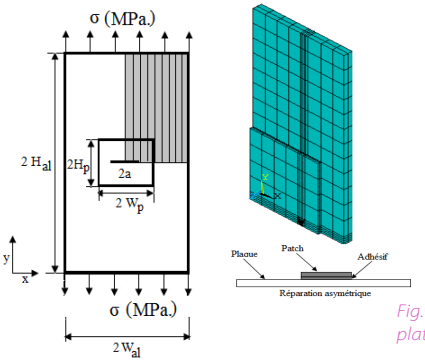

Fig. 2: Optimal repair of cracked aluminium plate using composite patch.

An original model is developed for reliability-based optimization of fatigue of non-uniform crack growth behaviour of a cracked plate repaired with a bonded composite patch.

The developed theoretical and numerical models have been applied to various types of structures:

- Localized break in unidirectional composite plates, with industrial, natural and hybrid fibers.
- Composite pipelines under internal pressure.
- Cracked aluminium plates repaired with one-sided composite patches.
- Repair of reinforced concrete beams in bending.
- Repair of damaged reinforced concrete columns.

The outcome of this cooperation is summarized in the high quality and quantity of the scientific production, in addition to the supervision of six PhD students, in addition to Master students.

Beyond the International project TASSILI, three issues of the International "conferences on Composite Materials" have been jointly organized in the past years. Actually, the cooperation is still actively ongoing with original scientific models in composite material field.

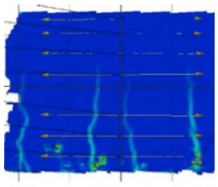

(a) Experimental flexural cracks [5]

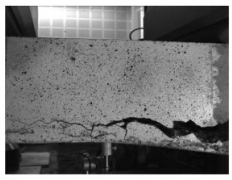

(b) Experimental Cover separation Cracks [5]

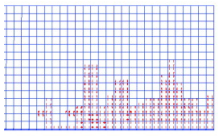

(c) Numerical flexural cracks

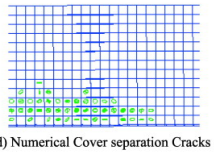

(d) Numerical Cover separation Cracks

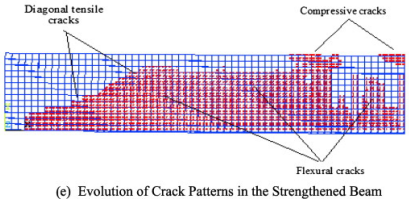

(e) Evolution of Crack Patterns in the Strengthened Beam

Fig. 3: Reinforced concrete beam repaired with composite patch.

CONTACTS

Sofiane AMZIANE
Sofiane.AMZIANE@ univ-bpclermont.fr
Alaa CHATEAUNEUF
Alaa.Chateauneuf@univ-bpclermont.fr

FURTHER READING

Numerical model for optimal design of composite patch repair of cracked aluminium plates under tension
H. Errouane et al., International Journal of Adhesion & Adhesives 49, 64 (2014)

Uncertainties of stress intensification near broken fibers of unidirectional composite with random fiber spacing
B. Bouhamida et al., Theoretical and Applied Fracture Mechanics 65, 1 (2013)

Cohesive zone model for the prediction of interfacial shear stresses in a composite-plate RC beam with an intermediate flexural crack
K. Hadjazi et al., Composite Structures 94, 3574 (2012)

CONTRACTS

TASSILI 08MDU751 (2007-2011)

PhD

M. Bouhafs, B. Bouhamida, M. Bennegadi, H. Errouane, K. Hadjazi, M. Khiat

Scientific achievement #36
Fire resistance of steel-to-timber connections

The thermo-mechanical behaviour of steel-to-timber joints loaded in various directions (0°, 45°, 90° and bending) exposed to fire is analyzed considering the real characteristics of material. The 3D finite element mechanical model is based on nonlinear criteria (von-Mises for steel, Hoffman and Hill for timber). It is validated by comparison with experimental results for mechanical, thermal and thermo-mechanical parameters of joints with real dimensions. The numerical models are applied to evaluate the load distribution among the fasteners. They can be used as general tools to analyze a large variety of joint configurations with the aim to propose reliable analytical approaches for engineering practice design.

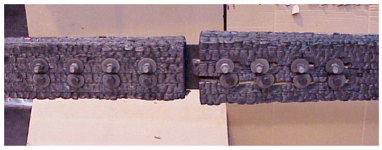

Fig. 1: Steel-to-timber joints in tension parallel to grain.

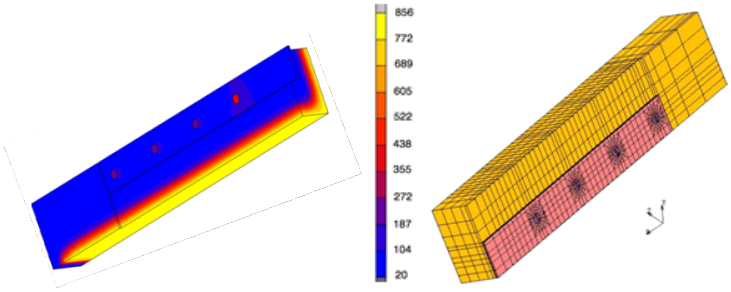

Fig. 2: Temperature fields in a steel-to-timber joint and meshing.

Structural wood members exposed to fire are commonly used by architects in modern buildings. Wood material is combustible but it burns in a controllable way so that it allows the estimation of its stability in fire when the evolutions of its physical and mechanical properties with temperature are known. In fire situation as well as in normal condition, the connections govern the bearing capacity and the mechanical behavior of the structure. Besides, their thermo-mechanical behavior is very complex because of the difficulty to analyze the heat-mass transfer in wood members, the degradation of wood, the cracks formed in the charred wood and the contact evolution between the components. Thus, a 3D finite element model is developed and validated on full-scale experimental results. The thermal and mechanical models are based on two different meshes to take into account their specific high gradient zones.

The mechanical response is calculated under the influence of an external load considering the evolution of the mechanical characteristics of the materials depending on the temperature. The numerical results are then used to analyze the behavior of various dowelled and bolted steel-to-timber joints in fire conditions. The models are refined to take account of the thermal degradation of wood around the fasteners and the thermal and the mechanical interfaces between the steel plate and the wood members. The fire exposure of the joints considered in the tests and the models is based on the common ISO curve.

The thermo-mechanical model shows its capability to represent the resistance of joints exposed to fire. The obtained results show that, for all the considered loading ratios, the fire resistance is always greater than 30 minutes. The final failure mode observed for all the tests is the shear in wood members along the fasteners rows (figure 1). This failure is combined with a source of ductility due to the plastic bending of dowels. The heat transfer modeling gives the distribution of the temperature field on the joint components (figure 2) depending on gas temperature. The thermo-mechanical model showed that the presence of the bolt head, the nuts and the washers increases the surface area exposed to fire. Thus, the heat transfer by conduction along the bolts inside the wood member is more important than dowels. The study showed also the barrier effect of the steel plate limiting the measured temperatures at the metal plate between 80 and 100 °C on a significant period of time. An adaptation of the numerical model allowed representing this observed phenomenon.

The model shows that in real joints, the load distribution among the fasteners governs the distribution of stresses in the joint and can control its failure mode and capacity. The curves representing the evolution of the loads among the fasteners depending on the time duration of fire exposure are shown on figure 3. It can be observed that the bolt carry the main part of load in comparison with dowels and its part decreases with time. This can be explained by the higher temperatures along the bolts due to the higher surfaces exposed to fire.

The numerical model developed in this study can well represent the thermo-mechanical behavior of steel-to-timber joints. It also represents an interesting tool for the analysis of the behavior of joints in fire with several fasteners allowing the access to some characteristics which are very difficult, even impossible, to measure experimentally. The final goal of the model is to understand the behavior of the steel-to-timber joints with the aim to improve their design and propose more realistic analytical models to be used by the engineers to design safely the timber joints in fire. A part of the research is included in the Technical guideline for Europe (Fire safety in Timber buildings).

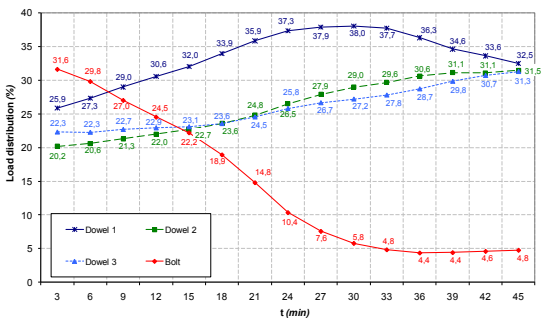

Fig. 3: Load distibution among fasteners in joint exposed to fire.

CONTACTS

Abdelhamid BOUCHAIR
Abdelhamid.BOUCHAIR@univ-bpclermont.fr
Patrick RACHER
Patrick.RACHER@univ-bpclermont.fr
Philippe AUDEBERT
Philippe.AUDEBERT@univ-bpclermont.fr
Mustapha TAAZOUNT
Mustapha.TAAZOUNT@univ-bpclermont.fr

FURTHER READING

Experimental and numerical analysis of timber connections in tension perpendicular to grain in fire
M. Audebert et al., Fire Safety Journal 63, 125 (2014)

Thermo- mechanical analysis of the fire performance of dowelled timber connection
P. Racher et al., Engineering Structures 32, 1148 (2010)

Fire safety in timber buildings (Technical guideline for Europe)
A. Bouchair et al., SP Tratek (Sweden), 211 pages (2010)

CONTRACTS

Européen WoodWisdom-Net research project FireInTimber (2007-2010)
COST - TU0904 - Integrated Fire Engineering and Response (2010-2014)
COST - FP1404 - Fire Safe Use of Bio-based building products (2014-2018)
1 CIFRE PhD : CSTB
1 bourse Département Allier PhD

PhD

M. Audebert, A. Samaké

Scientific achievement #37
Effects of climatic and mechanical variations on the durability of timber structures

The durability of timber structures is an important topic, regarding the climatic and mechanical variations in time and space. The climatic changes will lead to more extreme humidity variations, for which the wood cracking is very sensitive. In addition, the long-term loading of timber leads to creep deformations which are affected by climatic conditions. As the variations of these phenomena are random in nature and in time, the use of stochastic approach is mandatory to assess properly the lifetime of timber structures. The aim of the project ANR CLIMBOIS is therefore to develop a numerical and experimental methodology for predicting accurately the durability of timber structures, considering uncertainties in both climatic and mechanical loading.

The low energy impact of wood material leads to an increase in its use in building constructions. This increase is governed by the understanding of both the mechanical behaviour and the durability of wood structures. Notched beams are usually subjected to both climatic and complex mechanical loadings. These loadings are generally interacting with the heterogeneous behaviour of wood material. In order to ensure effective use in the field of construction, it is important to understand properly the in-service behaviour of wood structures under climatic loading (humidity, temperature, etc.), in addition to mechanical loading.

The project ANR CLIMBOIS aims at investigating the durability of wood structures under variable climatic environment as well as several mechanical loadings. This project leads to a robust methodology for the design of timber structures and wood components under complex climatic and mechanical loadings. During these last years, two French laboratories Institut Pascal (Blaise Pascal University) and GEMH (Limoges University) conducted several studies to investigate material durability under multi-loadings (due to moisture diffusion and mecanosorptif law). The mechanical behaviour of wood becomes more complicated to understand when considering various mechanical properties (anisotropy, viscoelasticity, orthotropic behaviour).

The first objective of this project is to propose efficient methods combining both viscoelastic constitutive laws and uncoupling of fracture mixed-modes for viscoelastic materials subjected to the above mentioned loads. The numerical modelling of these physical phenomena will be also investigated. The development of analytical methods and numerical viscoelastic incremental formulations allows us to separate the mixed-mode cracking in viscoelastic materials.

The second objective of the project is focused on both conducting creep tests, and investigating the randomly spatial distribution of properties/flaw (on notched specimen, undamaged beam, and beam with flaws). These creep tests, conducted for both outdoor and in a climatic chamber, are designed to validate these models and to characterize the spatial variability of properties and defects (cracks on specimen, healthy beams and beams with defects).

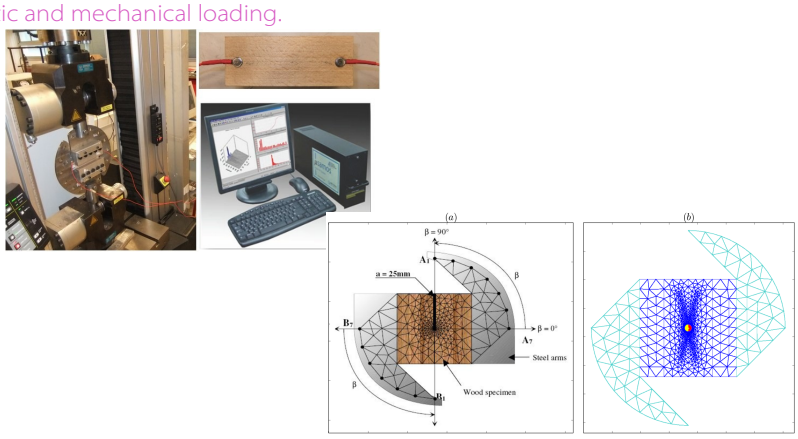

Fig. 1: Mechanical and acoustic emission testing of crached specimen, and finite element model.

The third objective of the project consists in conducting non destructive tests (optical methods, acoustic emission, ultrasonic, etc.) on cracking specimens. The aim is to characterize the mechanical fields during the cracking phase, to measure the water or thermal gradient, to characterize also uncertainties and spatial variability of these gradients with the distribution of defects. Finally, the randomness will be taken into account for study the spatial variability of wood properties and the mechanisms degradation due to environmental actions and measurement errors/model through mechanical couplings with reliability, Fig. 3.

The expected development of nonlinear viscoelastic constitutive laws, will allow reducing time-computation, analyzing field deformations during the cracking process, and determining the effects of model parameters on the lifetime of wood structure members. The coupled approach (analytical, numerical, probabilistic and non-destructive testing), adopted herein, have the ultimate goals of determining the most influential parameters on the service life of timber structures and wood components. In summary, the background and objectives are:

- To expand the use of wood material (characterized by low environmental impact) in the construction of structures.
- To better understand the in-service behaviour of timber structures subjected to both mechanical loads and climatic variations.
- To propose numerical methods that take into account both the viscoelastic behaviour and the failure modes of wood material.
- To develop a damage monitoring method based on the acoustic emission activities recorded during the cracking phases of wood.
- To conduct non destructive testing (optical methods, acoustic emission, ultrasonic, etc.) on cracked specimens.
- To characterize wood behaviour in different physical/mechanical domains, related to changes of properties and behaviour of wood and of wooden.

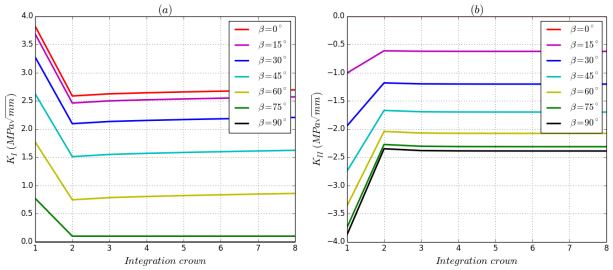

Fig. 2: Independence path domain for temperature variation of ΔT=10°C: part of mode I (a); part of mode II (b).

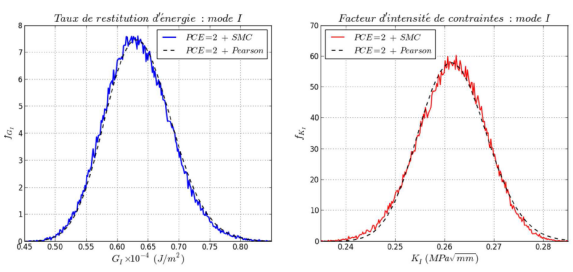

Fig. 3: Probability distributions of energy release rate and FIC in mode I.

CONTACTS

Rostand MOUTOU PITTI
Rostand.MOUTOUPITTI@ univ-bpclermont.fr
Alaa CHATEAUNEUF
Alaa.Chateauneuf@univ-bpclermont.fr

FURTHER READING

On numerical evaluation of mixed mode crack propagation coupling mechanical and thermal loads
H. Riahi et al., Wood Material 5, 21 (2015)

Effects of climatic and mechanical variations on the durability of timber structures: use of acoustic emission tool to evaluate wood mechanical behavior
R. MoutouPitti et al., Project CLIMBOIS, COST Action FP1302 Wood Music, Paris (2014)

CONTRACTS

ANR JCJC CLIMBOIS (2013-2017)

PhD

S.E. Hamdi, H. Riahi

Scientific achievement #38
Plant fibre based composites: Daniel Valentin Award 2011

Karine Charlet won the Daniel Valentin Award in 2011 for her work on natural fibre based composites, whose hydrophilic character is very important. It has been proved that the mechanical properties of the fibre/matrix interfaces are much higher those of fibre/fibre interfaces, without considering any fibre treatment. Thus, fibres have to be elementarised as much as possible within the composites, in order to reach good mechanical properties, notably strength. Moreover, the study of the environmental conditions and of the scattering of the physical properties is essential for modelling the behaviour and the durability of the natural fibre composites.

Each year, the Daniel Valentin Award recognizes a young researcher in the field of composites. In 2011, it has been given to Karine Charlet for her work on plant fibers as composite reinforcements.

The increasing use of composite materials in many areas such as automotive and aerospace is motivated, among others, by lightening the structures aiming at reducing consumption of non-renewable energy resources. With the same objective of sustainable development, renewable materials have been recently used as composite reinforcements instead of fossil reinforcements. In this context, plant fibers were studied under different aspects (morphological, mechanical, physical and chemical ...) and were proved to be good candidates as composite reinforcements; nevertheless some drawbacks still hamper their development.

Plant fibers interest researchers and industrials mainly because of their lightweight, renewability and availability. Flax fiber composites, for instance, possess theoretically specific properties comparable to those of glass fiber composites. Car manufacturers such as BMW or Mercedes-Benz have even used some short natural fibers to make interior elements of cars like rear beaches or interior door. Similarly, in the field of leisure, the impact resistance of tennis rackets or bicycle frames was greatly improved by combining short flax fibers and carbon fibers. However, the use of these natural fibers is usually motivated by their recyclability and only aims at meeting the latest government guidelines; their mechanical and functional performance are often underused. Their integration as long fibres, which would in theory lead to composites with superior mechanical properties, raises several problems, especially in terms of processing or durability under certain conditions.

One of the main obstacles to the widespread use of these long natural fibers as reinforcements of structural parts is their poor compatibility with the majority of organic resins traditionally used. Indeed, fibers are hydrophilic whereas resins are generally hydrophobic. Several treatments have been developed to overcome this problem, but they did not convince of their effectiveness, for economic or ecological reasons. The mechanical properties of the matrix/fiber interface (with or without treatment) are far superior to those of the fiber/fiber interfaces present within a bundle. There is therefore a major interest in dividing the fibers used in composites in order to obtain good properties, before seeking to improve the quality of fiber/matrix interfaces.

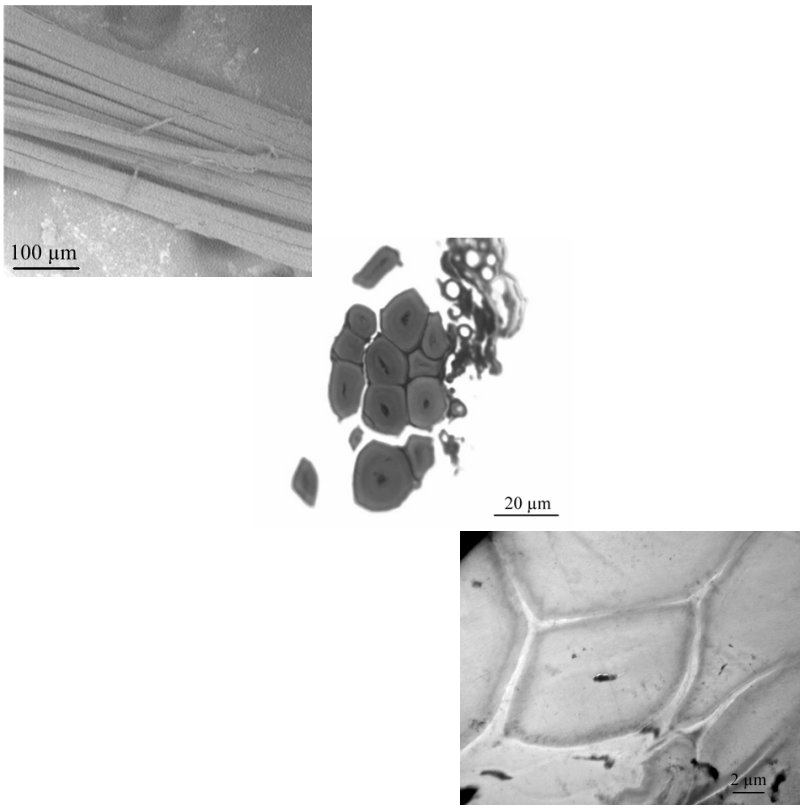

Fig. 1: Flax bundles (top left) scanning electron micrography, (center) optical micrography, (bottom right) transmission electron micrography.

The impact of environmental conditions on the mechanical behavior is also an important point when studying the durability of plant fiber based composites. In fact, their high reactivity towards moisture or temperature can be detrimental both during the composite processing and during its use. Added to the wide dispersion of fiber properties, modeling the fiber or the derived composite behavior is relatively difficult and requires the integration of dispersion laws which are particularly restrictive.

Finally, more work remains to be done to further improve our understanding of the mechanical behavior of composites plant fibers, to further develop their use and convince industry that their disadvantages can be blurred by their numerous benefits.

CONTACTS

Karine CHARLET
karine.charlet@ifma.fr

FURTHER READING

Natural fibres as composite reinforcement materials: description and new sources
K. Charlet, Natural Polymers-Volume 1: Composites, M.J. John, S. Thomas (Eds), RSC Publishing, Londres, 37-62 (2012)

Mechanical properties of interfaces within a flax bundle – Part I: Experimental analysis
K. Charlet et al., International Journal of Adhesion and Adhesives 31, 875 (2011)

Mechanical properties of flax fibres and of the derived unidirectional composites
K. Charlet et al., Journal of Composite Materials 44, 2887 (2010)

Scientific achievement #39
FP7 thinkMOTION: **dmg-lib.org** goes **europeana.eu**, an open digital library of machines and mechanisms

The thinkMOTION project is specialised on gathering specific content in the field of **motion systems**. Different kinds of material are considered (e.g. books, journals, drawings, images, physical models) to establish a digital library which connects historical and recent content from different countries. Content providers are spread over Europe and part of consortium. This project helped to digitize significant books of interest, such as Artobolevski's atlas of mechanisms, and produce a considerable number of reusable parametrized models of mechanisms, suitable for future design methods.

Fig. 1: Collection of 340 mechanisms by Pierre and Alexandre CLAIR, Crozatier museum, Le Puy en Velay (43), that was digitized during the thinkMOTION project.

The thinkMOTION project was supported by programme CIP-ICT-PSP.2009.2.3 - Digital Libraries, with a budget of 4.4M€.

The 6 partners are:

- Ilmenau University of Technology (coordinator)
- University of the Basque Country
- Politechnica University of Timisoara
- RWTH Aachen University
- IFMA / Institut Pascal
- University of Cassino.

The objectives of the thinkMOTION project are:

- To construct one of the biggest digital libraries for machine and mechanisms
- To save European technical heritage, with historical or modern value (Fig. 1)
- To address a wide audience, from students to researchers, companies, historians or lawyers
- To digitize varied contents: texts, photos, videos, real machines… (Fig. 2)
- To provide multi-lingual archiving: English, French, German, Spanish, Italian, Romanian
- To provide a semantic network of metadata
- To guarantee free access for all on **dmg-lib.org** and provide contents for the European digital library europeana.eu.

The French team was in charge of "WP8: Multi-lingual contents and semantic network of metadata". A team was set-up with 3 researchers, 6 engineers, 13 French partners and the educational contribution of 210 students from IFMA and UBP each year [1].

Results of the French team:

- 34055 items (out of the global objective of 76100 items).
- 362 books, for a total of 52425 scanned pages and 1748 graphical pages, including contributions from UBP Central library. The French edition of the famous atlas of mechanisms from Artobolevski (Fig. 3) is now freely available online (7 volumes, 4746 mechanism descriptions).
- 16452 items from CAD re-modelling of machines described in patents and Artobolevski's encyclopedia, including 12229 pictures, 1699 videos, 554 CAD models, also declined in VRML and 3DXML models, 43 PDF 3D models; 42 Geogebra models and 169 patents.

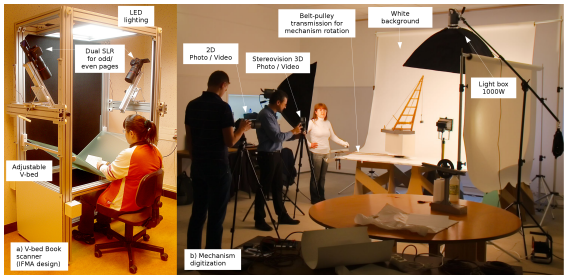

Fig. 2: Digitizing books and real mechanisms.

- 18195 items from real machines coming from the PATSTEC project (www.patstec.fr, [2]), Crozatier, Henri Lecoq and Michelin museums, including 8611 2D photos, 6496 3D stereo-vision photos, 813 2D videos, 337 3D stereo-vision videos.
- The evaluation of the whole project by the European Commission (26 November 2013) was the maximal one: **Excellent** (the project has fully achieved his objectives and has even exceeded expectations).

Future work:

This project provided a strong infrastructure for deploying a knowledge base about machines at the regional level and initiating future research on design methods based on databases, encouraging the re-use not only of mechanical single parts but whole elementary mechanisms. The corresponding CAD software still have to be created [3].

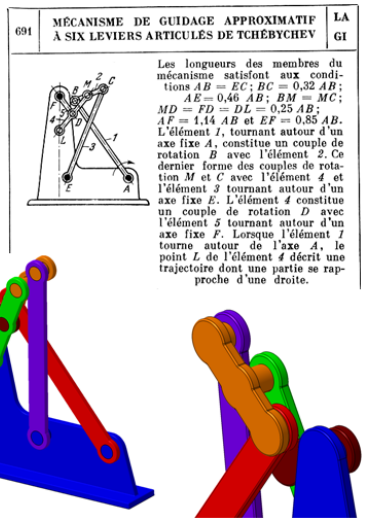
691 MÉCANISME DE GUIDAGE APPROXIMATIF À SIX LEVIERS ARTICULÉS DE TCHÉBYCHEV LA GI

Les longueurs des membres du mécanisme satisfont aux conditions $AB = EC$; $BC = 0{,}32\ AB$; $AE = 0{,}46\ AB$; $BM = MC$; $MD = FD = DL = 0{,}25\ AB$; $AF = 1{,}14\ AB$ et $EF = 0{,}85\ AB$. L'élément 1, tournant autour d'un axe fixe A, constitue un couple de rotation B avec l'élément 2. Ce dernier forme des couples de rotation M et C avec l'élément 4 et l'élément 3 tournant autour d'un axe fixe E. L'élément 4 constitue un couple de rotation D avec l'élément 5 tournant autour d'un axe fixe F. Lorsque l'élément 1 tourne autour de l'axe A, le point L de l'élément 4 décrit une trajectoire dont une partie se rapproche d'une droite.

Fig. 3: Elementary mechanisms: from the kinematic description in a digitized book (Artobolevski's encyclopedia) to a parametrized reusable CAD model.

CONTACTS

Jean-Christophe FAUROUX
Jean-Christophe.FAUROUX@ifma.fr
Belhassen-Chedli BOUZGARROU
Belhassen-Chedli.BOUZGARROU@ifma.fr
Grigore GOGU
Grigore.GOGU@ifma.fr

FURTHER READING

[1] *Pédagogie et recherche pour une bibliothèque numérique de machines et mécanismes au sein du projet européen thinkMotion*
J.C. Fauroux et al., Actes du 20e congrès Français de Mécanique, Bezançon, Paper 676, Colloque Formation et Pédagogie (2011)

[2] *PATSTEC-thinkMOTION, Une riche collaboration entre projets national et européen*
J.C. Fauroux, Conférence invitée à la Journée Nationale de la Mission de Sauvegarde du Patrimoine Sc. et Tech. Contemporain (PATSTEC), CNAM, Paris (2012)

[3] *Using Geometry Sketchers and CAD Tools for Mechanism Synthesis*
I. Prause et al., in Proc. of IFToMM 2015, The 14th World Congress in Mechanism and Machine Science, Taipei, Taiwan (2015)

CONTRACTS

FP7 thinkMOTION (2010-2013)

Scientific achievement #40
ANR FAST project: Fast Autonomous rover SysTem

The ANR FAST project has the ambition to design a Fast Autonomous rover SysTem capable to roll in unstructured environments at high speed (10m/s). Within this project, Institut Pascal developed an innovative concept allowing longitudinal damping of the wheels for a better stability of the vehicle during obstacle crossing at high speed. Nine solutions of suspensions where developed: one serial and eight parallel mechanisms, two with a planar and six with a spatial kinematics. All the solutions were patented. The eighth solution was prototyped and experimented with success.

The FAST project was set-up to design a Fast Autonomous rover SysTem capable to roll in unstructured environments at high speed (10m/s). Institut Pascal participated to this project funded by the French National Agency for research (ANR), with two researchers, one post-doctoral student, and the contribution of seven engineering students from IFMA.

Research objectives :

- Characterize the real behaviour of a vehicle bumping on an obstacle at high speed.
- Find a concept allowing to extend current limitations of all-terrain vehicles.
- Develop and experiment solutions deriving from the concept.

Team results:

- 77 experiments allowed determining the stability limit of a classical vehicle crossing an obstacle at high speed (Fig. 1). The limit speed for stable crossing decreases with the obstacle height [1]. Over this limit, the vehicle pitches-over.
- A concept was proposed: horizontal damping of the wheel reduces the peak damping effort during the shock, decreases the pitching moment of the vehicle and preserves its suspensions.
- A synthesis method based on constraints and progressive enrichment of kinematics was proposed [2].
- It allowed generating 9 solutions (Fig. 2), one serial and eight parallel mechanisms, two with a planar and six with a spatial kinematics.
- The last two solutions (Fig. 3) guarantee four mobilities of the wheel:
  - Longitudinal translation Tx for innovative longitudinal damping
  - Vertical translation Tz for classical vertical damping
  - Rotation Rx for wheel propulsion
  - Rotation Rz for wheel steering
- Damping translations are slightly coupled whereas rotations are completely independent from the other motions.
- The last solution is compatible with the fixtures of a classical vehicle (double triangle or McPherson suspensions).
- The solutions were patented at the French and PCT level [3].
- Active or semi-active control strategies.

Applications: all-terrain vehicles; terrestrial drones for wide area monitoring, agriculture, de-mining and fast intervention in case of natural disasters.

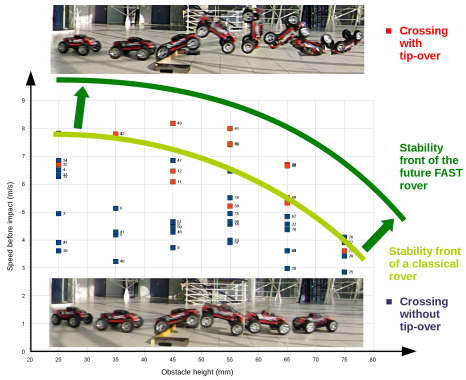

Fig. 1: 77 experimental results show the existence of a stability limit above which a pitch-over occurs. This limit can be extended with advanced suspensions.

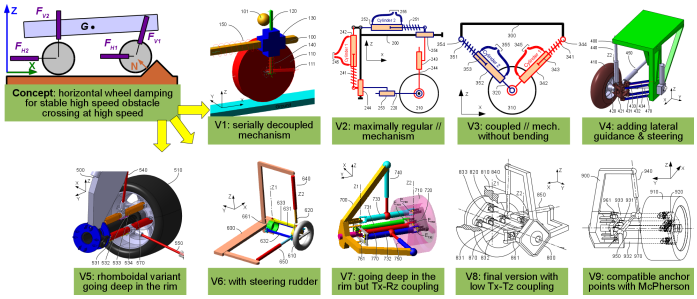

Fig. 2: Initial concept and nine patented [3] derived solutions allowing horizontal damping of wheels during obstacle crossing at high speed.

Acknowledgements
French National Research Agency (ANR) for funding this work through the FAST project (FAST Autonomous Rover).
IFMA students for their contribution to the FAST project : F. Kreit, A. Riesemann, A. Authier, S. Ovazza, R. Cousturier, T. Dejeante & R. Vendrôme.

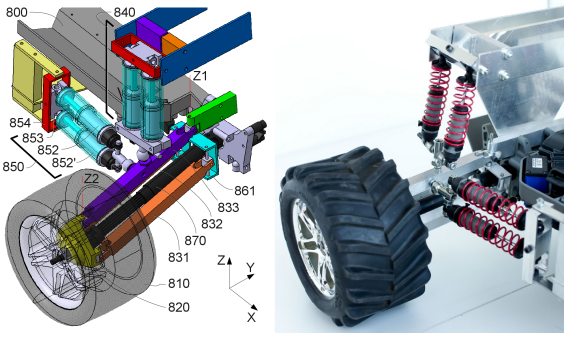

Fig. 3: Detailed CAD model and prototype of the Susp4D suspension from solution V8.

CONTACTS

Jean-Christophe FAUROUX
Jean-Christophe.FAUROUX@ifma.fr
Belhassen-Chedli BOUZGARROU
Belhassen-Chedli.BOUZGARROU@ifma.fr

FURTHER READING

[1] *Dynamic Obstacle-Crossing of a Wheeled Rover with Double-Wishbone Suspension*
J.C. Fauroux et al., in "Field Robotics", World Scientific Publishing, ISBN-13 978-981-4374-27-9, 642-649 (2011)

[2] *Synthesis of spatial parallel mechanisms for a vertical and longitudinal all-terrain suspension*
J.C. Fauroux, TransTech Publications, Vol. 162 of Applied Mechanics and Materials, ISSN 1660-9336,19-28 (2012)

[3] *Dispositif de suspension d'une roue, et véhicule muni d'au moins une roue équipée d'un tel dispositif de suspension*
J.C. Fauroux et al., PCT Patent WO 2013045634, IFMA/UBP (2012)

CONTRACTS

ANR FAST (2007-2010)

Scientific achievement #41
FUI ECOMEF project: Eco-design of harvesting heads for hardwood

The ECOMEF project was created for eco-designing innovative harvesting machines dedicated to hardwood trees. The research work was focused on creativity methods, innovative kinematics and models for tree-head interaction. By addressing the specific problems of hardwood, that include crooked trunks and numerous strong branches, new high performance components and innovative heads were developed to achieve the challenge of a 40% productivity increase.

The ECOMEF project is a pre-competitive research project supported by the French Ministry of Industry, French regions and Europe, endorsed by the competitiveness clusters ViaMeca & Xylofutur, with a total budget of 3.8M€.

The 7 partners are:

- ISI Process (coordinating SME)
- FCBA (technical institute)
- IFMA/Institut Pascal (lab)
- Irstea (lab)
- France Bois Forêt (association of wood professionals)
- Comptoir des Bois de Brive (paper company)
- Lycée forestier Claude Mercier (professional school).

Until 2020, France expects an increase of wood production of around 21 Mm³/year. However, 65% of the wood comes from hardwood trees, of which one third could be harvested with machines. The mechanization level of hardwood is only 4% in France now. Simultaneously, the French forest grows and the lumberjack profession becomes less and less attractive.

The objectives of the ECOMEF project are:

- To develop a new generation of harvesting capable to increase productivity of 40% in hardwood
- To identify the specific problems of hardwood harvesting (Fig. 1)
- To apply creativity methods to bring innovative concepts to the market
- To model and characterize the head-tree interaction during the process (Fig. 2)
- To develop prototypes and experiment them in real conditions (Fig. 3)
- To include sustainable development into the design process.

The research team at IFMA/Institut Pascal gathers 4 researchers, 2 Ph.D. students, 5 engineers and more than 25 students that contributed to the project during their engineering and master's studies.

Team results:

- A knowledge base of more than 200 concepts and innovative solutions, accessible through an original online server at IFMA allowing teamwork and combined with a Product Data Management system at ISI.
- Kinematic synthesis methods based on mobility analysis of mechanisms allowed developing several original concepts of gripping devices [2] and several kinematics of articulated frames suitable to crooked trees (ongoing patents).

Fig. 1: Re-designing harvesting heads for hardwood and crooked trunks [2].

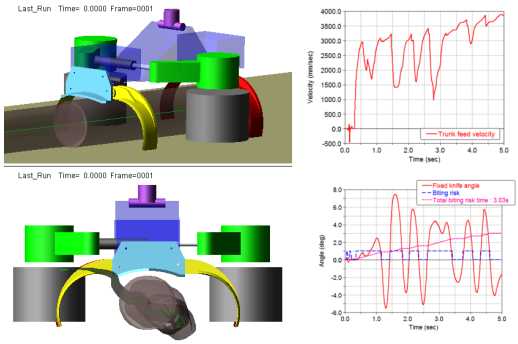

Fig. 2: A multibody model of a harvesting head with Adams, to predict trunk feeding velocity and biting risk of the knives.

- Predictive models of the phenomena occurring during harvesting, such as trunk feeding and branch delimbing. The models allowed to determine cutting forces during delimbing [1] and predict the biting risk of knives on the trunk (Fig. 2).
- Experimental test benches: a slow delimber (Fig. 3), a force pendulum for higher speeds, a feeding test bench with rollers and an instrumented harvesting head.
- Mono-functional mechanisms, at reduced and full scale, capable to feed crooked trees with lower risks of locking and lower energy consumption.
- Innovative high performance components, that were tested on real machines, such as patented ribbed delimbing knives with low cutting force [3].

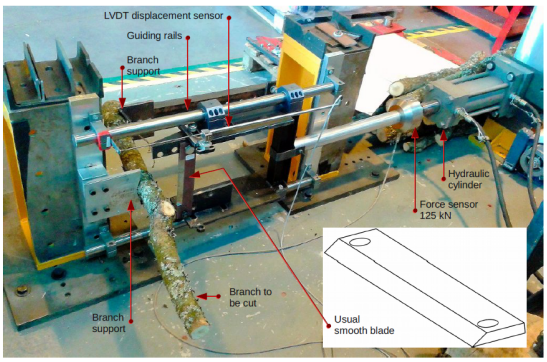

Fig. 3: Test benches to measure the delimbing force [1] and develop high performance patented delimbing knives [3].

CONTACTS

Jean-Christophe FAUROUX
Jean-Christophe.FAUROUX@ifma.fr
Belhassen-Chedli BOUZGARROU
Belhassen-Chedli.BOUZGARROU@ifma.fr
Vincent GAGNOL
Vincent.GAGNOL@ifma.fr
Grigore GOGU
Grigore.GOGU@ifma.fr

FURTHER READING

[1] *Experimental determination of delimbing forces and deformations in hardwood harvesting*
B. Hatton et al., Croatian Journal of Forest Engineering 36, 43 (2015)

[2] *Gripping mechanisms in current wood harvesting machines*
D. Goubet et al., Frontiers of Mechanical Engineering 8, 42-61, Springer, ISSN: 2095-0233 (2013)

[3] *Lame courbe d'ébranchage, son utilisation, tête d'ébranchage et kit de coupe correspondants*
G. Dargnat et al., French Patent, IFMA/ISI (2014)

CONTRACTS

FUI ECOMEF (2010-2015)

PhD

D. Goubet, B. Hatton

Acknowledgements
This research work is part of FUI ECOMEF national project funded by the Fond Unique Interministeriel (FUI) of the French Government, Conseil Régional Auvergne, FEDER – "Europe en Auvergne", Clermont Communauté, Conseil Général 63 Puy-de-Dôme, Conseil Général 03 Allier, Région Limousin, Agglomération de Brive, Région Aquitaine, FEDER Limousin. These organisms are acknowledged for their financial support to this pre-competitive project.

Scientific achievement #42
Structural Synthesis of Parallel Robots – a work in five parts published by Springer

The publication by Springer in 2014 of the book Structural Synthesis of Parallel Robots, Part 5: Basic Overconstrained Topologies with Schönflies Motions marked the end of a series of 5 books with more than 3400 pages written between 2008 and 2014 by Grigore Gogu as a quintessence of his original contributions on this challenging subject. The synthesis methodology and the solutions of parallel manipulators (PMs) proposed in this work represent the outcome of some recent results obtained by the author, partially published in the last years, and mainly developed in these books.

The first two parts of this work have been published in 2008 and 2009 and the last three parts in 2010, 2012 and 2014. Two important contributions of the author made possible this work. They consist in (i) proposing and demonstrating new formulae for the calculation of the degree of mobility, the degree of connectivity, the degree of redundancy and the number of overconstraints of parallel robotic manipulators that overcome the drawbacks of the classical Chebychev-Grübler-Kutzbach formulae, and (ii) developing a new method of systematic innovation in engineering founded on an evolutionary morphology approach.

For more than 150 years, 36 formulas for calculating the mobility of a mechanism have been proposed beginning with some great mathematicians and physicists such as Chebyshev, Sylvester, Koenigs, and several others. These formulas for mobility calculation have been critically reviewed and their limitations have been set up and demonstrated by the author for the first time in the literature. New formulas for mobility, connectivity, redundancy, and the hyperstatism are proposed and demonstrated by the author via an original approach based on the theory of linear transformations. These new formulas are applicable to any parallel mechanisms along with any simple or complex mechanism including the so-called "paradoxical mechanisms" for which the traditional formulas of Chebychev-Grübler-Kutzbach give erroneous results. The author has demonstrated that these mechanisms have nothing paradoxical and that we may call into question the appropriateness of the previous formulas.

The new formulas for the calculation of structural parameters are integrated in an original structural synthesis approach founded on the evolutionary morphology (EM). The main paradigms of EM are presented in a closed relation with the biological background of morphological approaches and the synthetic theory of evolution. The main difference between the evolutionary algorithms and the EM are also discussed. The evolutionary algorithms are methods for solving optimization-oriented problems, and are not suited to solving conceptual design-oriented problems. They always start from a given initial population of solutions and do not solve the problem of creating these solutions. These two original contributions are combined in a unified approach of structural synthesis giving interesting innovative solutions for parallel robotic manipulators. Solutions of coupled, decoupled, uncoupled, fully-isotropic and maximally regular robotic manipulators with various motion types of the moving platform are systematically generated and presented in these five books. Overconstrained non redundant /overactuated/redundantly-actuated solutions with simple/complex limbs are proposed. Many solutions are presented here for the first time in the literature. Some of them are implemented in the innovative parallel robots of Isoglide family developed by Pascal Institute (see for example Fig. 1). The author had to make a difficult and challenging choice between protecting these solutions through patents, and releasing them directly into the public domain. The second option was adopted by publishing them in various recent scientific publications and mainly in these five books (Fig. 2). In this way, the author hopes to contribute to a rapid and widespread implementation of these solutions in future industrial products and new reconfigurable parallel robots [1]-[3].

Fig. 2: The cover pages of the five books on Structural Synthesis of Parallel Robots.

Fig. 1: Isoglide4-T3R1 a parallel robot with decoupled Schönflies motions of Pascal Institute.

CONTACTS

Grigore GOGU
Grigore.Gogu@ifma.fr

FURTHER READING

T2R1-type parallel manipulators with bifurcated planar-spatial motion
G. Gogu, European Journal of Mechanics/A Solids 33, 1 (2012)

Maximally regular T2R1-type parallel manipulators with bifurcated spatial motion
G. Gogu, Journal of Mechanisms and Robotics 3(1), doi:10.1115/1.4003180 (2011)

Bifurcation in constraint singularities and structural parameters of parallel mechanisms
G. Gogu, Meccanica 46(1), 65 (2011)

Scientific achievement #43
Dynamic prediction of machining robot and stability analysis

Robots machining have major advantages over Cartesian machine tools because of their flexibility, their ability to reach inaccessible areas on a complex part, and their important workspace. However, their lack of rigidity and precision is still a limit for precision tasks. Beyond accuracy problems, it is also necessary to quantify the vibration phenomena that may affect, as in machine tools, the quality of machined parts and the tools and spindle lifespan. One of the main limitations to increase productivity is the occurrence of unstable regenerative phenomena known as chatter vibration. The scientific action deals with the dynamics prediction of robot during machining operation and the optimization of the process regarding stability prediction.

Machining with anthropomorphic robotic manipulators is used to increase the flexibility and reduce the costs of production. Industrial robots actually have been developed for pre-machining and the machining of other post-casting applications in the foundry industry. To increase the removal rate, which gives a shorter machining cycle time and higher productivity, cutting volume and cutting speed can be increased. These parameters are limited by the low rigidity of the robot structure and the vibration instability (chatter) in a nonlinear relationship. The dynamic behavior of the robot inside the workspace depends on its configuration therefore each posture of the robot has its own dynamic behavior and stable cutting conditions. Thus a dynamic robot model which correctly takes into account these variations is essential to maintain machining operations within a stable margin by optimizing the cutting parameters.

During the robotic milling process, vibration instability can occur at specific combinations of robot configurations and cutting parameters. Hence, a first way to improve the process regarding stability concerns HSM cutting conditions which enable optimizing the maximum removal rate. A second improvement approach consists of introducing and managing kinematic redundancy. These works are applied to the robotic machining cell (Innov@pole, EquipEx Robotex) made up of two 6-DoF robots with a hybrid architecture (parallelogram closed loop and Tricept PKM) served by a 2-DoF tilting turntable carried by a linear track which adds another DoF (Figure 2).

A simplified dynamics-based robot model using three-dimensional Euler– Bernoulli beam element is developed (thesis Mousavi, RobotEx). The proposed model is calibrated by experimental modal analysis in static configuration and also through operational modal analysis (thesis Mejri, LabEx ImobS3). The calibrated model is used to predict dynamic behavior in different static configurations and also along machining trajectory under machining excitation. Simulation results are compared to experimental characterization and indicate consequent variation of robot dynamics behavior and consequently on the stability margin.

The management of the kinematic redundancies and functional redundancy (reorientation around the spindle axis) can be carried out to optimized tool path and tool trajectory. The objective function allows us to modify the value of weighting of the three criteria Kinematic, mechanical and stiffness with regard to various machining strategies and specifications related to some operations. The current experimentation is designed to validate the paths planning optimization algorithm applied to various strategies (face milling, pocketing, machining contours, etc.) on a set of test part (Figure 3).

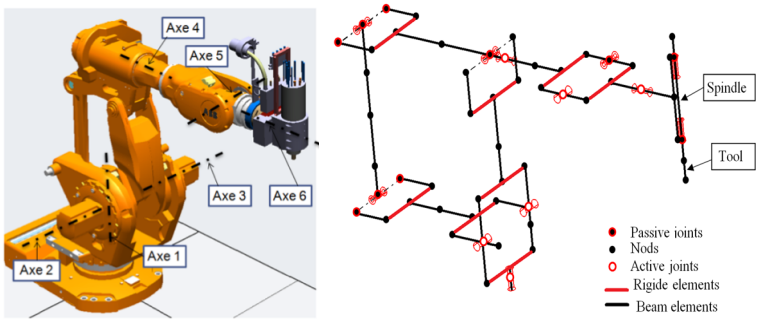

Fig. 1: (left) ABB IRB6660 serial robot. (right) Finite element

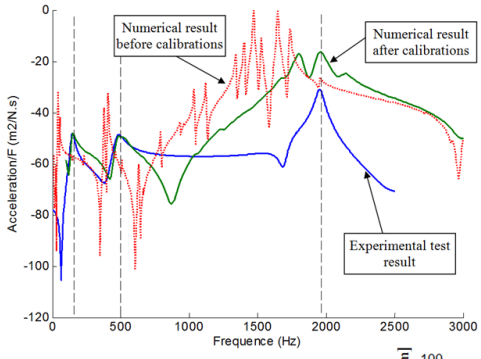

Fig. 2: (left) Model calibration through experimental modal analysis 3D stability lobes diagram. (bottom) 3D stability lobes diagram.

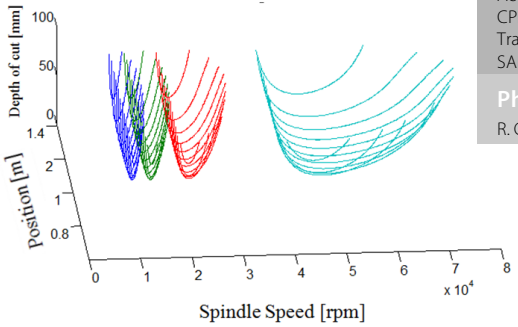

Fig. 3: 3D stability lobes prediction.

CONTACTS

Chedli BOUZGARROU
Chedli.Bouzgarrou@ifma.fr
Vincent GAGNOL
Vincent.Gagnol@ifma.fr
Thien-Phu LE
Thien-Phu.Le@ifma.fr
Laurent SABOURIN
Laurent.Sabourin@ifma.fr

FURTHER READING

Redundancy-based optimization approach to optimize robotic cell behaviour: application to robotic machining
L. Sabourin et al., Industrial Robot: An International Journal 42, 167 (2015)

Dynamic characterization of machining robot and stability analysis
S. Mejri et al., J. of Advanced Manufacturing Technol., accept. publication (2015)

Machining predictions of spindle-self vibratory drilling head
S. Mousavi et al., J. of Materials Processing Technology 213, 2119 (2013)

CONTRACTS

ANR EQUIPEX ROBOTEX RoboTool/ RobProd (2011-2019)
ANR LABEX IMobS3, MASPAR Project, RobDyn Action (2012-2015)
CPER Project Innov@Pôle (2007-2013)
Transfert 2MATech : ABB/Renault ACI, SAFE Metal (2014-2015)

PhD

R. Cousturier. S. Meiri. S. Mousavi. K. Subrin

Scientific achievement #44
Use of the cross-entropy method to tackle the storage location assignment problem

This action covers a combinatorial optimization method called the cross-entropy method. The aim is to show the relevance of this method to solve an optimization problem: implementations of products in order to minimize the total distance traveled by workers during the picking order. After elaborating a state of the art regarding issues that affect the design of logistics warehouses, we develop an overview of methods used to solve and/or optimize this type of problem. The cross-entropy method applied to the shortest path problem is developed, and we show that this method can easily be used to solve an optimization problem in the logistics area.

The primary purpose of managing logistics warehouses is to find the most effective way to ensure the functionality of the warehouse in the supply chain, which may be the distribution-based way to develop other innovative value-added activities. Driven by customer demand for an efficient and high-quality service in a minimal time but with as low a cost as possible, the performance of logistics operations has become critical in today's competitive market.

Order picking –removing the product from storage areas in response to a specific request from a customer–is considered the most expensive process as regards labor and the most critical in terms of time spent. The order picking process therefore has a strong impact on the reactivity of warehouses. In practice, the policies used by manufacturers to control the picking process include policies specific to storage, batch control groups, and path optimization preparer control. This last point is crucial for optimization and it has given rise to numerous studies and research projects. It is a complex combinatorial optimization problem closely linked to other issues such as the implementation of reference picking. However, in all situations, these are combinatorial optimization problems, envisaged by heuristic means and providing more or less optimal results. These problems are solved by well-known algorithms such as Tabu Search, the problem of the shortest path or the TSP (Traveling Salesman Problem). Among these algorithms there exists a more recent optimization method called cross-entropy.

The industrial case is a real warehouse belonging to one of leaders in logistics dedicated to mass-market retailing in France. This warehouse consists of 1071 locations in a pallet storage rack. We have to place 474 products, one product per location and one location per product. These products are grouped into five families. The size of the search space is about $8.35\ 10^{750}$ solutions. The company itself decided on the grouping of products into families, regarding weight constraints and stackable capacity. It also decided on the order of the families: the first family must have the first locations, the second family's locations must follow the first family locations, and so on. The order of the products in each family is then what we have to optimize.

Fig. 2: Picking locations.

The evaluation function is the total distance to satisfy a real set of customer orders (10851 orders). Satisfying an order means building all the pallets on which the ordered goods will be stacked.

This optimization has certain constraints. These constraints are directly taken into account through the probability distribution in the cross-entropy. Indeed, we simply have to associate all possible locations for each product. To solve this problem, we created a C++ program based on the cross-entropy approach. Our approach is able to find an efficient solution in a very large solution space, and the solution found respects the constraints imposed by the enterprise. The gains are significant (-25%), especially when we consider that the profit margins of such companies are low, and that minimizing the distances traveled is of utmost importance. Moreover, it has to be noted that our approach can be directly used for all warehouses under similar constraints.

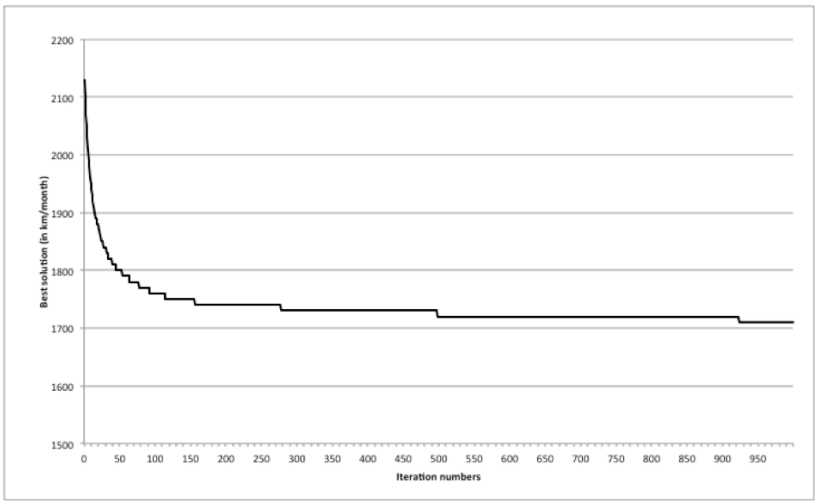

Fig. 1: Evolution of the best solution found at each iteration.

CONTACTS

Olivier DEVISE
Olivier.Devise@ifma.fr
Séverine DURIEUX
Severine.Durieux@ifma.fr
Jean-Luc PARIS
Jean-Luc.Paris@ifma.fr

FURTHER READING

Use of the cross-entropy method to tackle the storage assignment problem in logisitics warehouses
O. Devise et al., Concurrent Engineering: Research and Applications (2015)

Storage assignment problem in logistics warehouses: optimization of picking locations by cross-entropy method
O. Devise et al., IDMME - Virtual Concept, Improve, Ingegraf (2014)

Optimisation combinatoire par entropie croisée : application à des problèmes de grandes tailles dans les entrepôts logistiques
S. Durieux et al., Modélisation, Optimisation et Simulation (2013)

CONTRACTS

INDUSTRY : OptiPick (2011-2014)
INDUSTRY : OptiStock (2014-2017)

Scientific achievement #45
Numerical tools for solving stochastic dynamics problems in structural mechanics

This research work was mainly conducted within the framework of the ANR project CISSSI dedicated to intensive stochastic calculus and its application to the reliability analysis of structural and electronic systems. Three types of numerical tools were developed: special schemes for the numerical solution of stochastic differential equations encountered in structural random dynamics, algorithms for simulating general stochastic processes and fields, and algorithms for identifying modal characteristics of linear random dynamical systems. Many numerical tests and applications showed the practical interest of most of these tools.

Spread over a period of four years (2006-2010), the ANR project CISSSI aimed to participate in the French effort in the field of intensive stochastic calculus, focusing in particular on the development of numerical tools dedicated to the solution of stochastic dynamics problems arising from the reliability analysis of structural and electronic systems. The numerical tools can be classified into three categories. The first focuses on the development of numerical schemes for the solution of stochastic differential equations (SDE) encountered in structural random dynamics. Due to the conservative properties of such SDEs, we brought much attention to schemes suited to these features, as for example the symplectic schemes. We have also developed special algorithms for the multivalued SDEs, or stochastic variational inequations, appearing for example in the analysis of dynamical response of nonlinear structures under seismic excitations (elasto-plastic or hysteretic behavior under random dynamic loads). The second category of numerical tools deals with simulation algorithms for a large class of vector random processes and fields (Gaussian or non-Gaussian, stationary or non-stationary). The proposed algorithms are based on appropriate representations of these random quantities (spectral or integral representation, Markovian representation, Karhunen-Loève representation,...) and are either existing algorithms revisited or new algorithms. This work was supplemented by the development of algorithms for estimating probabilistic characteristics of vector random processes and fields known through a large number of sampled trajectories. Finally, the third category of numerical tools concerns the identification algorithms and more particularly the spectral identification algorithms for linear structures under random dynamic ambient excitations (wind, marine wave, earthquake,...).

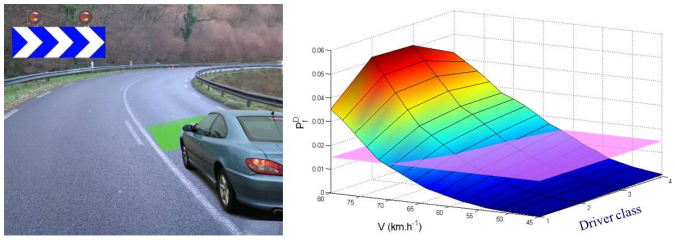

Fig. 1: Evolution of the roadway departure probability with the speed of the car and the driver class.

In this area, we have developed two original identification procedures based on judicious couplings between the Random Decrement Method and the Proper Orthogonal Decomposition Method. Applied to various examples, these two methods showed their relevance and appeared as an attractive alternative to the well-known Random Decrement-Ibrahim Time Domain Method. Several applications of the numerical tools were carried out : nuclear plant subjected to a seismic excitation, construction of seismic fragility curves, vibrations induced by a turbulent flow in the piping network of a nuclear plant, bridge subjected to combined effects of traffic and wind, wind effect on a plane, probabilistic analysis of roadway departure risk for light vehicles, uncertainties propagation in a mechanical system, reflection of radar waves on a random geometry, behavior of an electronic system controller in a disruptive electromagnetic environment,... They showed that most of the proposed algorithms are in good agreement with the project objective: they are effective and can be used in an industrial context. All these algorithms were implemented and are proposed in a free library accessible to all partners and interested users (user agreement). This library is usable either on a single server or in a distributed environment (cluster, computing grid). Some algorithms are also available in the Open TURNS library.

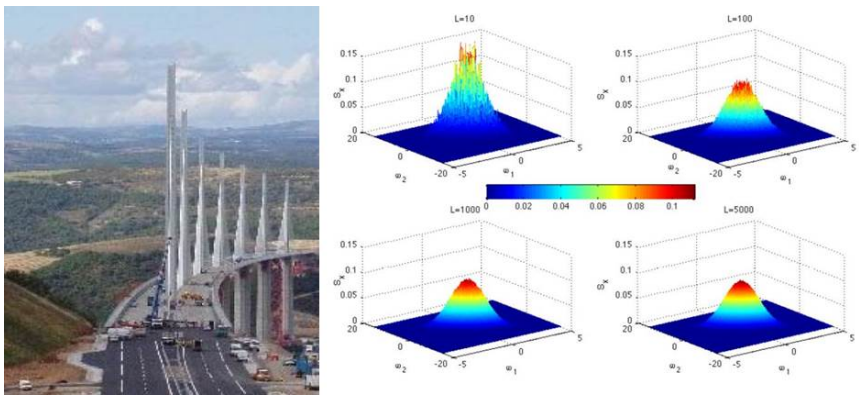

Fig. 2: L-estimates of the power spectral density (PSD) of the stochastic field modeling the wind action on a bridge element.

CONTACTS

David CLAIR
David.CLAIR@univ-bpclermont.fr
Michel FOGLI
Michel.FOGLI@univ-bpclermont.fr

FURTHER READING

Surveillance de Santé Structurale des Ouvrages - Chap. VI : Identification structurale, surveillance structurale
D. Clair et al., Sous la direction de A. Orcési et C. Crémona - Editions du LCPC (2012)

Probabilistic assessment of roadway departure risk
G. Rey et al., Vehicle System Dynamics 49, 1649 (2011)

Reliability analysis of roadway departure risk using stochastic processes
G. Rey et al., Mechanical Systems and Signal Processing 25, 1377 (2011)

CONTRACTS

ANR CISSSI (2006-2010)

PhD

G. Rey

Scientific achievement #46
AK-RM: Active learning and Kriging-based Reliability methods

The important challenge in structural reliability is to keep to a minimum the number of calls to the numerical models. Engineering problems involve more and more complex computer codes and the evaluation of the probability of failure may require very time-consuming computations. Based on the Kriging meta-model, a new family of methods named AK-RM is proposed. Starting from a sampling population (Monte Carlo or importance sampling) to be classified into two categories (acceptable points and unacceptable one), an iterative scheme is constructed to reach accurate and efficient estimation of the failure probability in comparison to the crude simulation of the whole population. AK-RM methods were published in 4 journal articles and cited more than 100 times in the past 3 years.

Applying reliability methods to a complex industrial structure is often delicate for two main reasons. First, such a structure is fortunately designed with codified rules leading to a large safety margin which means that failure is a small probability event. Such a probability level is difficult to assess efficiently. Second, the structure mechanical behavior is modelled numerically in an attempt to reproduce the real response and numerical model tends to be more and more time-demanding as its complexity is increased to improve accuracy and to consider particular mechanical behavior. As a consequence, performing a large number of model computations cannot be considered in order to assess the failure probability.

To overcome these issues, the AK-RM methods propose a solution to reach failure probability of structures in an industrial context. Based on the statement that reliability assessment aims at classifying a population (Monte Carlo or importance sampling, see figure 1 for illustration) into two groups (safe and unsafe one), the AK-RM methods propose a fast classification using the Kriging meta-model, widespread in optimization since more than 20 years. It associates the Kriging meta-model and its advantageous stochastic property to propose an iterative scheme that proposes the only necessary mechanical computations.

The AK-RM methods are shown to be very efficient as the probability of failure obtained is very accurate and this, for only a small number of calls to the mechanical model. Several examples from literature prove its efficiency particularly for problems dealing with high non-linearity, non-differentiability, non-convex and non-connex domains of failure and moderate dimensionality. They were also used for complex industrial problem (figure 2 and 3) in collaboration with SAFRAN Snecma Company.

AK-RM methods gather AK-MCS method for very complex limit state but quit high failure probability level, AK-IS for very small failure probability and AK-SYS for system problems dealing with more than one failure mode. The proposed family of method was published in 4 journal articles and cited more than 100 times in the past 3 years. A partnership with SAFRAN Snecma company starts in 2012 to go in depth after the APPROFI project funded by the ANR national agency.

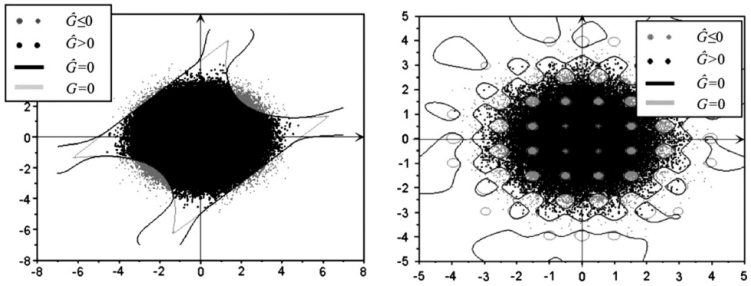

Fig. 1: Examples of 2 dimensions population to be classified.

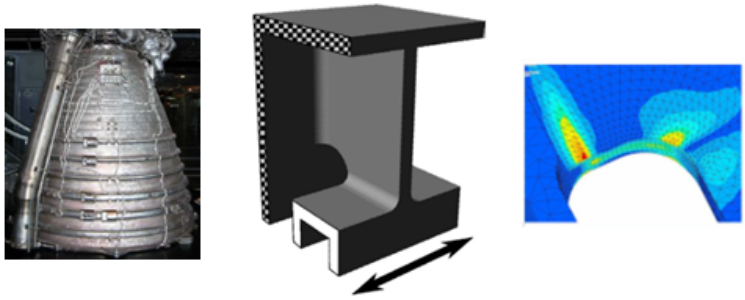

Fig. 2: AK-RM method application on a blade support of the Vulcain motor to assess the probability of fatigue crack initiation.

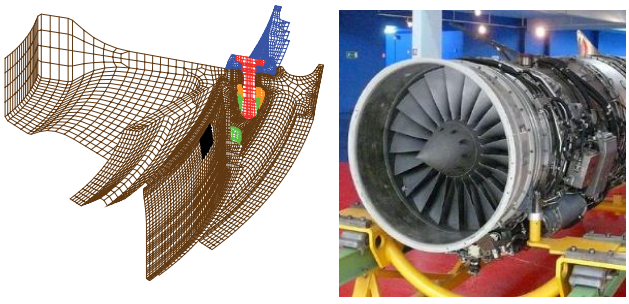

Fig. 3: AK-RM method application on an aeronautic part subjected to potential fatigue crack initiation.

CONTACTS

Nicolas GAYTON
Nicolas.GAYTON@ifma.fr

FURTHER READING

AK-SYS: an adaptation of the AK-MCS method for system reliability
W. Fauriat et al., Reliability Engineering and System Safety 123, 137 (2014)

A combined Importance Sampling and Kriging reliability method for small failure probabilities with time demanding numerical models
B. Echard et al., Reliability Engineering and System Safety 111, 232 (2013)

AK-MCS: an Active learning reliability method combining Kriging and Monte Carlo Simulation
B. Echard et al., Structural Safety 33, 145 (2011)

CONTRACTS

ANR APPROFI (2008-2011)
Research collaboration with SAFRAN Snecma Company (2012-2015)

PhD

B. Echard, W. Fauriat

Scientific achievement #47
FERUM: a Matlab open-source toolbox for uncertainty propagation

The open-source Matlab toolbox FERUM 4.x developed at Institut Pascal and first released in 2009 has become with years a worldwide referenced general purpose code for reliability assessment. This very accessible and easy to use toolbox represents a convenient solution for development and application works of researchers and engineers in many fields., e.g. mechanical and civil engineering, geotechnical engineering, energy, oil and gas, ... This toolbox has been used and cited in many research works including those of the MPMS research group of Institut Pascal.

FERUM 4.x is an open-source Matlab toolbox for uncertainty propagation in numerical models distributed under the GNU General Public License agreement. Initially developed at UC Berkeley until 2003, this toolbox has been improved at Institut Pascal and an enhanced version of this toolbox is now available at http://www.ifma.fr/FERUM.

This toolbox performs uncertainty propagation in numerical models (e.g. finite elements). The implemented methods mainly allow the estimation of probabilities of rare events (structural reliability as known in structural mechanics, see conceptual idea in Fig. 2) but FERUM is also able to perform global sensitivity analysis based on Sobol' indices and reliability-based design with FORM method.

The methods available in FERUM are approximation methods (FORM and SORM) and Monte Carlo-like methods (crude Monte Carlo, importance sampling, directional sampling, subset simulation). Some adaptive strategies based on Support Vector Machine surrogate models are also proposed for reliability assessment and global sensitivity analysis.

This toolbox is immediately comprehensible and easy to use for students and very accessible for researchers in the objective of exploring new solution strategies.

Since its first release in 2009, this toolbox has been downloaded worldwide in more than 60 countries by about 1,200 users (USA: 150, France: 130, China: 120, Iran: 90, India: 80, Germany & Brazil: 50), see Fig. 3. FERUM is used in the following institutions by more than 10 users: Pontificia Universidad Catolica de Rio de Janeiro (Brazil), Aalborg University (Denmark), TU Munich (Germany), Indian Institute of Science Bangalore (India), Amirkabir University of Technology (Iran), TU Delft (The Netherlands), Seoul National University (South Korea), ETH Zurich (Switzerland), University of Akron (USA), UC San Diego (USA), University of Illinois at Urbana-Champaign (USA). FERUM users are mostly academic researchers. About 10% of FERUM users are researchers or research engineers in private companies or research centers.

Fig. 1: FERUM logo.

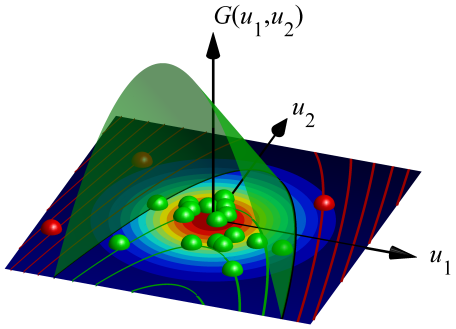

Fig. 2: Conceptual idea of reliability assessment.

Works of PhD students at Institut Pascal in the MPMS research group have benefited from developments brought to FERUM 4.x since 2010. Some of these students have also participated in the implementation of new features of this toolbox in the scope of their PhDs.

A major release of FERUM is planned in 2016. The new version will offer up-to-date and efficient methods with new capabilities. An objective is also to set up a version control platform allowing worldwide collaborations in order to allow selected contributions from FERUM users.

CONTACTS

Jean-Marc BOURINET
bourinet@ifma.fr

FURTHER READING

A review of recent features and improvements added to FERUM software
Bourinet J.-M., Mattrand C., Dubourg V., In: Proc. 10th International Conference on Structural Safety and Reliability (ICOSSAR 2009), Osaka, Japan, September 13–17, 2009. Ed. by H. Furuta, D.M. Frangopol, M. Shinozuka. CRC Press (2009)

PhD

V. Dubourg, C. Mattrand

Fig. 3: FERUM users map.

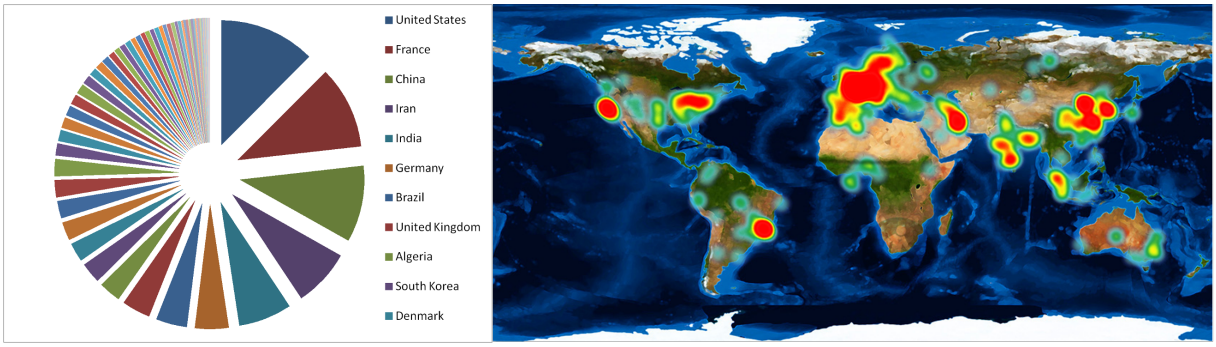

Scientific achievement #48
Summer schools in uncertainty quantification

The French-German summer schools on uncertainty quantification were organized by Institut Pascal and the Karlsruhe Institute of Technology. The first one was held in Pforzheim, Germany, in 2011 with a focus on mechanics and material sciences. The second one (which was also an Ecole thématique CNRS) was organized in Porquerolles, France, in 2014 on the mathematical concepts of uncertainty quantification problems and the related computational/algorithmic methods available to solve them. These summer schools gathered an international audience of researchers and lecturers which demonstrates the growing interest of the scientific and engineering communities in this field.

Uncertainties play a central role in many engineering systems and physical phenomena. Quantifying the impact of these uncertainties on responses of interest has become an active field of research over the past few years in many disciplines such as structural mechanics, material science, fluid dynamics, geophysics, electromagnetics, telecommunication networks, chemistry, ...

Two French-German summer schools were jointly organized by Institut Pascal and the Karlsruhe Institute of Technology in Germany, the first one in 2011 and the second one in 2014.

The first French German summer school organized in 2011 in Pforzheim, Germany, aimed at presenting the theoretical basis of the most common stochastic approaches and demonstrating how these approaches could be applied in the specific fields of structural mechanics and material sciences. The main topics addressed in the given courses were stochastic modeling and identification, stochastic finite elements, reliability and sensitivity analysis and risk assessment. The financial support was brought by the French-German University (UFA/DFH) et Association France de Mécanique (AFM).

The main objective of the second French German summer school (and Ecole thématique CNRS) organized in 2014 in Porquerolles, France, was to address the important mathematical concepts of uncertainty quantification and the related computational/algorithmic challenges arising in the numerous engineering and science disciplines. A focus was placed on reliability assessment by simulation methods in the context of rare events, construction of surrogate models (also known as metamodels) for expensive-to-evaluate computational models with applications to reliability assessment and global sensitivity analysis, spectral methods with the emphasis placed on low rank approximations and reduced basis methods. Additional topics were covered such as stochastic inverse problems, identification by Bayesian methods, stochastic multi-scale analysis, HPC for stochastic analysis, robust optimization and decision under uncertainty. The sponsors were the French-German University (UFA/DFH), CNRS, AFM, Institut Pascal and ED SPI Clermont.

Fig. 1: Sponsors of the 2014 French-German Summer School and Ecole Thématique CNRS.

These summer school gathered an international audience composed of young researchers (PhD students and postdocs) involved in ongoing works in stochastic approaches for most of them and a few researchers and engineers interested in the development and implementation of methods for uncertainty quantification. A total of 38 participants from 6 countries (French: 30%, German: 50%) attended the first summer school and 65 from 15 countries (French: 40%, German: 20%) the second one. The courses were given by 12 additional lecturers, most of them from France and Germany.

A third edition of these French-German summer schools is expected to be organized in 2017.

Fig. 2: 2014 summer school classroom.

CONTACTS

Jean-Marc BOURINET
bourinet@ifma.fr

FURTHER READING

Summer school web sites:
- http://www.ifma.fr/summerschool2011
- http://www.ifma.fr/summerschool2014

Scientific achievement #49
Benchmark of numerical methods for reliability-based design optimization

The Reliability-Based Design Optimization (RBDO) seeks for the best compromise between cost and safety, by considering various types of system uncertainties. A benchmark with different levels of difficulties has been established to offer full-scale comparative platform for various RBDO formulations. By covering a wide range of numerical approaches, the benchmark study offers a comprehensive assessment of the available methodologies, and gives clear ideas about their capabilities and limitations, allowing us to draw useful conclusions regarding their performance and robustness. This work is nowadays considered as a reference for all research works in this scientific area, as indicated by the high citation index of the related paper.

The classical structural optimization takes into account the uncertainties through the use of partial safety factors, leading, in many cases, to over-designed structures. As this approach does not ensure the target reliability level with the most economical design, the probabilistic modeling of uncertainties should be integrated in structural optimization by the mean of specific algorithms.

The probabilistic constraint is the key constraint in Reliability-Based Design Optimization (RBDO), as it requires considerable computation effort and reveals the numerical problems of efficiency, accuracy and stability. Although many works have been developed in the past years, the numerical difficulties still remain a strong barrier for practical engineering applications. Three approaches have been developed to overcome these difficulties:

- The two-level approach considers the probabilistic constraints inside the optimization loop. This approach leads to nested optimization problems, where the inner loop deals with reliability assessment and the outer loop deals with cost optimization.
- The mono-level approach aims at solving the RBDO problem in a single loop procedure, where the reliability analysis is avoided. The probabilistic constraints are replaced by the optimality conditions or by reformulating the RBDO problem in order to obtain a single loop optimization.
- The decoupled approach consists in separating the reliability analysis from the optimization procedure. The RBDO problem is transformed to a sequence of deterministic optimization, where the deterministic constraints are linked to the reliability analysis (or any equivalent analysis) performed after or before the deterministic design. Many RBDO algorithms adopted this concept.

The paper by Aoues and Chateauneuf (2010) consists in a comprehensive study for better understanding of the differences between RBDO formulations and for the definition of the validity domains which are mandatory for the choice of the method to be used for solving engineering structures.

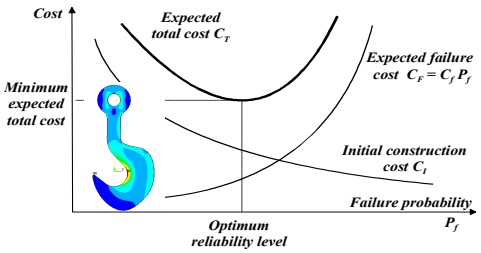

Fig. 1: Expected total cost as function of the failure probability.

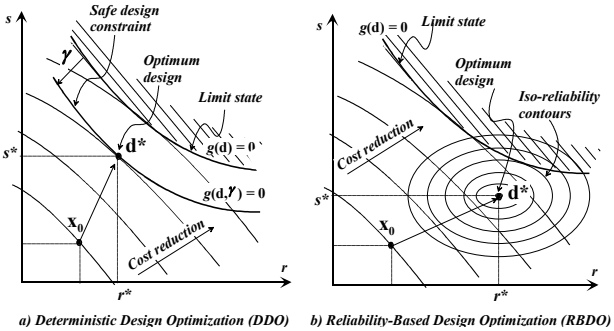

Fig. 2: Comparison of optimal solutions of deterministic and reliability-based formulations.

The developed benchmark, considering mathematical and finite element models, constitutes a large-scale comparison between RBDO approaches, providing useful information about their efficiency, performance and capabilities, allowing us tomake decision on the most suitable method to be applied, depending on the problem configuration and parameters.

The drawn conclusions show that, although the two-level approaches are simple to implement, they are usually inefficient for real structures. The mono-level approaches involve some approximations and could be efficient for specific applications. The decoupled approaches are generally efficient and accurate, but require particular implementation efforts.

Despite the large progress in this field, the application of RBDO to practical engineering structures is still a challenging issue because of the high computation cost, compared to deterministic optimization. The future works in this field should allow for significant improvements of the numerical efficiency, in order to integrate more realistic reliability problems, such as system and time-variant reliability assessment.

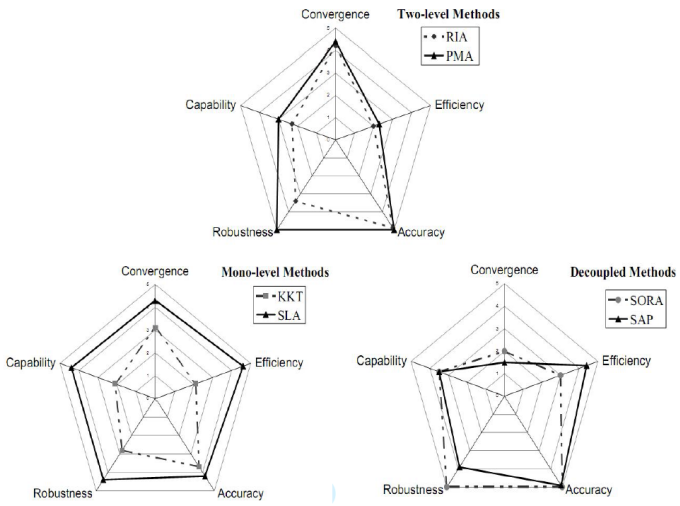

Fig. 3: Performance of the RBDO methods: Two-level, Mono-level and Decoupled approaches.

CONTACTS

Alaa CHATEAUNEUF
Alaa.Chateauneuf@univ-bpclermont.fr

FURTHER READING

Optimal design of new deteriorating timber components under climate variations
E. Bastidas-Arteaga et al., ICASP12, Vancouver, Canada (2015)

Optimal design under uncertainty of reinforced concrete structures using system reliability approach
Y. Aoues et al., International Journal for Uncertainty Quantification 3, 487 (2013)

Benchmark study of numerical methods for reliability-based design optimization
Y. Aoues et al., Journal of Structural and Multidisciplinary Optimization 41, 277 (2012)

PhD

Y. Aoues

Scientific achievement #50
Reliability-based multi-scale assessment of seismic vulnerability of buildings

The simulation of real dynamic behavior of buildings requires multi-scale approaches involving nonlinear mechanics and probabilistic analysis. This type of modeling is particularly challenging due to highly nonlinear energy dissipations under random excitations, material properties and structural joints. The scientific activities in this field are mainly performed in the framework of national projects, namely the ANR SISBAT, the participation to normative groups on seismic vulnerability and the in-situ expertise on countries affected by large-scale seismic damage. In the multi-scale approach, the experimental and numerical characterization starts from the elementary components (materials and joints), to go to the scale of constitutive components (walls, frames and trusses), and then to the scale of the whole structure.

Fig. 1: Building damage induced by seismic loading.

In most cases of industrial and individual buildings, the combination of the nonlinear behavior and the ductility of joints and components inevitably generates energy dissipation phenomena during the seismic loading. This is particularly the case of timber structures which are composed of wood members joint with connectors made of steel plates. Unfortunately, a part of this major advantage (i.e. dissipation capacity) is omitted or underestimated in many design codes, as it is not appropriately taken into account in the calibration of the safety factors. Mostly, the failure of many construction materials is considered to occur due to brittle fracture. In timber structures, the mechanical behavior of joints is highly nonlinear, mainly due to the metal fasteners (plates and dowels) which ensure the connection between the timber members.

The assessment of the structure reliability subjected to seismic hazards requires various knowledge levels, namely: the coupled mechanical and probabilistic behavior, which implies highly complex and time consuming modelling, the randomly applied seismic loading, the mechanical properties of components and their variability in space and time, the design standards and the construction conditions and associated uncertainties.

In the ANR SISBAT project, the application to timber roofs and houses has been performed, and supported by real-scale testing of house system. A probabilistic methodology has been developed to assess the behavior of timber joints under seismic loading, including variations and uncertainties. The considered hysteresis anisotropic behavior law allows us to describe the behavior of the punched metal plate fasteners in timber joints. Its originality lies in taking into account the damage under cycles of constant amplitude and in describing the bidimensional behavior of timber joints. The parameters of the proposed hysteresis law are determined from experimental results, which are then used to validate the numerical model.

In order to take account for uncertainties, the univariate decomposition method, combined with sensitivity analysis, has been developed to compute the statistical moments (i.e. mean, standard deviation) of 3-D timber roof under seismic loading. Due to the large number of random variables (several hundreds), a selection procedure is proposed in order to identify the most significant random variables and vectors. The reliability analysis is conducted by considering the randomness of the peak load at each joint in the structure. The numerical application is carried out for an industrial timber joint with hysteresis anisotropic behavior. The failure is obtained by the increase of the applied seismic loading until reaching the resisting capacity of the roof. The overall failure is considered when a significant number of joints fail. It is observed that the failure probability strongly decreases with the increase of the joint capacity. The sensitivity analysis allows us to identify the role of the most important joints regarding the structural performance. It is shown that the proposed methodology has reasonable time consuming behavior since the convergence is well achieved using a limited number of finite element analyses.

Works on timber horizontal diaphragms and vertical bracings illustrate deterministic approaches in order to define the mechanical parameters integrated in the whole modeling. The coupled large scale experiment and multiscale FEM modeling allows us to extrapolate results to more complex diaphragm shapes and compositions. Torsion impact on bracings constitutes a link between scientific research and simplified method integrated in standards. The work performed in this field during the last years is integrated in the future simplifed standard for simple buildings and individual houses. These studies and developments are carried out as well as in the research institute, in collaboration in DHUP and french association on seismic engineering and also in French and European standard committees. Finally in order to complete real-scale testing of houses, post earthquake mission feedbacks give the complete dimension of the topic of seismic building reliability.

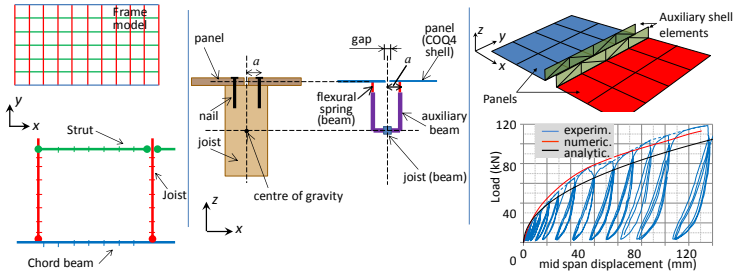

Fig. 2: Multiscale horizontal diaphragm modeling and comparison with experimentation and new analytical proposal.

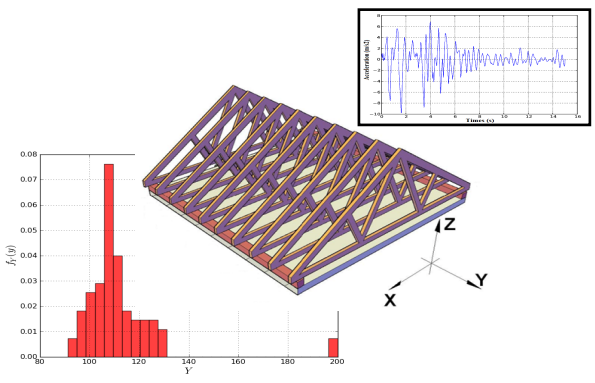

Fig. 3: Probabilistic distribution of timber roof seismic resistance.

CONTACTS

Philippe BRESSOLETTE
Philippe.BRESSOLETTE@ univ-bpclermont.fr
Alaa CHATEAUNEUF
Alaa.Chateauneuf@univ-bpclermont.fr
Eric FOURNELY
Eric.FOURNELY@univ-bpclermont.fr

FURTHER READING

Experimental study of the in-plan stiffness of timber floor diaphragms
S. Fuentes et al., European J. of Environmental and Civil Engineering 18(10) (2014)

Reliability analysis of nonlinear timber roofs under seismic loading
H. Riahi et al., The 11th ICOSSAR, New York (2013)

Evaluation of accidental eccentricity for buildings by artificial neural networks
M. Badaoui et al., Structural Engineering and Mechanics 41, 527 (2012)

CONTRACTS

ANR SISBAT (2010-2014)
Contract FCBA (2014)
Contract DHUP-AFPS/IP : RSPB
Contract DHUP-AFPS-CSTB/IP : CPMI
COST FP1402, Basis of structural timber design - from research to standards
AFNOR/CN/PS, Règles de construction parasismique
BNTEC/P21A, Programme de normalisation des structures en bois
Scientific and technical groupe - Nouvelles réglementations parasismiques AFPS
Organizations of AFPS post-seismic missions (2007-2012) in Kashiwasaki, L'Aquila, Haïti, Chili Cauquenes, Lorca, Tohoku and Emilie-Romagne.

PhD

M. Badaoui, S. Fuentes, H. Riahi, T.K. Vu

Scientific achievement #51
Slow light self-collimation in photonic crystal superlattices

Photonic band gap materials, also known as photonic crystals, bring a powerful control over light that has permitted significant progress in nanophotonics. With the advent of metamaterials, novel photonic crystals combining positive and negative refraction have pushed further the frontier of electromagnetics. In the framework of a French project funded by the ANR, we have developed a new concept of laser cavities based on photonic crystal superlattices that simultaneously beat light diffraction and slow down the speed of light.

The self-collimation effect discovered in the 80's by H. Kosaka suppresses the natural the natural spreading of light due to diffraction when a beam propagates in a nano-structured semicondutors. These periodic optical refractive index materials, known as photonic crystals, present particular photonic dispersions that force light to follow strait paths but without the use a traditional waveguides. In the framework of a French project CLAC for "cavité laser à autocollimation", novel laser cavities based on such self-collimation effect have been explored in particular for generating large laser beams of controlled width. However, we rapidly face to several problems due to the large number of air holes required to get the selfcollimation regime. Indeed, high filling factors in air decrease the amount of gain material that hinders a good heat transfer and finally prevents observing the lasing effect. To solve this problem, we have proposed new structures that reduce dramatically the number of air holes drilled in the GaAs membrane and present a mesoscopic self-collimation effect, Fig.1. The considered structures, named photonic crystal superlattices, are patterned at two scales: at the micro-scale, 2D photonic crystal layers that mimic metamaterials are periodically alternated with unprocessed regions, Fig. 2a. In the nano-structured layers, a carefully crafted array of holes is drilled through the semiconductor to provide a negative refraction effect that exactly compensates diffraction in the consecutive homogeneous layers. Moreover, our new approach allows for the first time this self-collimation to be combined with slow light giving unprecedented control over both light speed and light diffraction. Photonic crystal superlattices designed by Photon and fabricated by the LAAS-CNRS have demonstrated a lasing effect showing the viability of our concept, Fig. 2b-c.

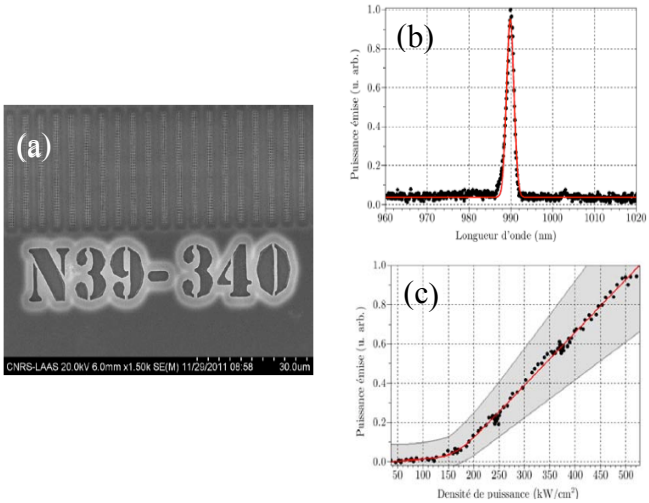

Fig. 2: (a) SEM image of a GaAs photonic crystal superlattice fabricated by the LAAS-CNRS (Toulouse). (b) Photoluminescence spectra. (c) Power laser emission as a function of the pump power.

By combining slow light with non-diffracting propagation, photonic crystal superlattices pave the way towards unprecedented control over light-matter interaction, a key process in many opto-electronic and photonic devices.

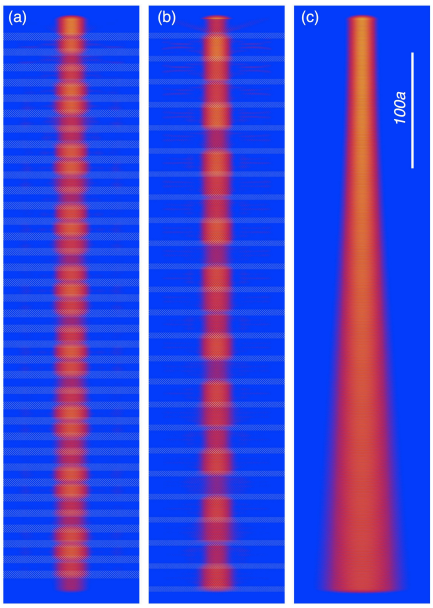

Fig. 1: (a) and (b), FDTD simulations of a Gaussian beam propagation (λ=1μm) through photonic crystal superlattices of respectively filling factor in air of 6% and 3%. (c) Propagation of the same Gaussian beam in the nonpatterned semiconductor.

CONTACTS

Emmanuel CENTENO
Emmanuel.CENTENO@univ-bpclermont.fr

FURTHER READING

Mesoscopic self-collimation and slow light in all-positive index layered photonic crystals
J. Arlandis et al., Phys. Rev. Lett. 108, 037401 (2012)

Self-collimation and focusing effects in zero-average index metamaterials
R. Pollès et al., Optics Express 19, 6149 (2011)

CONTRACTS

ANR BLANC Cavité Laser à Auto-Collimation (2009-2012)

PhD

J. Arlandis, R. Pollès

Scientific achievement #52
A new numerical modal method based on Gegenbaueur polynomial expansion

Optical umerical modal methods are well suited to investigate rigorously wave propagation in optical structures. They consist in describing the electromagnetic field in terms of eigenfunctions and eigenvalues of an operator. In the particular case of the Fourier modal method, the eigenfunctions are approximated by a finite Fourier sum. This approximation can lead to a poor convergence and also to spurious modes. In the case of plasmonic structures it is absolutely necessary to investigate other basis functions that may represent the fields more accurately. That is the reason why we have revisited modal methods using Gegenbaueur polynomials expansion.

Rigorous analysis of diffraction or propagation by metalic-dielectric structures becomes a mandatory step for a lot of applications in optics and photonics. Among rigorous methods, modal methods and mode matching techniques are well established methods to solve wave guide and scattering problems. One of their interesting features is that they easily allow understanding and giving some physical insight into the physical phenomena. Numerical modal methods differ in the choice of expansion and test functions. One can distinguish full domain function or sub-domain function according to weather they are defined on the whole period or only on some part of it. In the well known Fourier Modal Method expansion and test functions are pseudo periodic functions. Hence, the various lateral boundary conditions that define the eigenvalue problem are automatically satisfied without writing them explicitly. However many structures consist of piecewise homogeneous media which allows to use sub- domain polynomial expansions. The main advantage of such an approach is that continuity relations can be written in an exact manner at the border of the different sub-domains. Indeed polynomials modal methods outperform the Fourier modal method in term of speed of convergence and we never observed suprious modes. In the field of plasmonics, we have to analyse structures whose real part of the permittivity jumps from a positive value to a negative one. As a consequence, some field components also exhibit large jumps both in amplitude and phase. For such cases, the advantage of polynomial expansion is crucial because they allow to match in an exact manner the tangential components of the field at the border of two sub-domains. In our most recent work, we have combined the flexibility offered by Fourier basis with the advantage of polynomials for taking into account transversal boundary conditions.

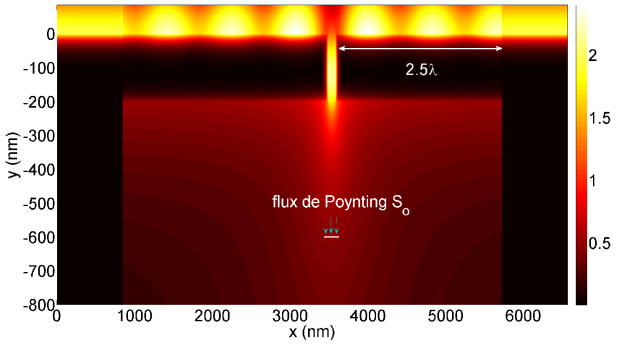

Fig. 1: Gap plasmon inside a single slit in a silver film and enhanced transmission. Note the presence of perfectly matched layers at the border of the computational domain.

The numerical scheme consists of defining a set of polynomial basis functions called modified polynomials that rigorously describe the transversal boundary conditions. These polynomials are themselves constructed from orthogonal polynomials. To the best of our knowledge, the above approach has proven to be the most effective one for metallic crossed grating. We have also extended the use of polynomial expansions for diffraction by cylinders with arbitrary cross sections. In addition, polynomials expansions have been combined with perfectly matched layers and curvilinear coordinates. Figures 1 and 2 illustrate two typical possible applications of our modal method. At present, we have an original numerical modal method well adapted for plasmonic structures. In the next future we plan to developp it for 3D particules.

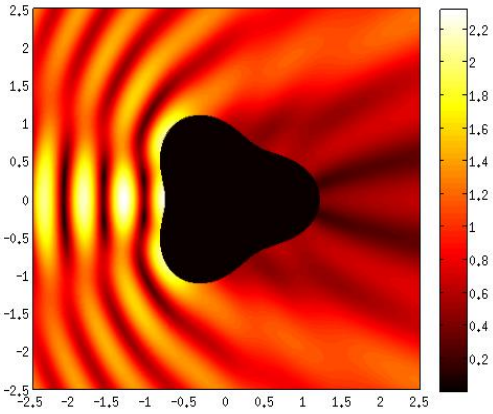

Fig. 2: Diffraction by a cylinder with arbitrary cross section. The problem is solved by using simultaneously curvilinear coordinates and polynomial expansion.

CONTACTS

Koffi EDEE
Koffi.EDEE@univ-bpclermont.fr
Gérard GRANET
Gerard.GRANET@univ-bpclermont.fr

FURTHER READING

Numerical scheme for the modal method based on subsectional Gegenbauer polynomial expansion: application to biperiodic binary grating
K. Edee et al., JOSA A 32, 402 (2015)

Modal method based on subsectional Gegenbauer polynomial expansion for lamellar gratings: weighting function, convergence and stability
K. Edee et al., Progress in Electromagnetics Research 133, 17 (2013)

Modal method based on subsectional Gegenbauer polynomial expansion for lamellar gratings
K. Edee et al., JOSA A 28, 2006 (2011)

CONTRACTS

LabEx IMobS3 Défi 3

PhD

M. Abboud

Scientific achievement #53
Extremely efficient light absorption by nanocube-based resonators

Nanocubes coupled to a metallic film are able to absorb light very efficiently because of the excitation of very peculiar resonances that can be easily tuned. It is a very simple and cheap way of building a metamaterial surface, filled with deeply subwavelength resonators. Potential applications are numerous because of the intrinsic sensitivity of the device and the physical phenomenon that may occur (extreme light concentration, Purcell effect).

Nano-antennas are nano-sized metallic resonators, like nanoparticles, that allow to concentrate, and then to absorb or scatter light. Until recently, the performances of nano-antennas were rather poor. A collaboration between Institut Pascal and Duke University has shown that nanocubes (75 nm large) randomly scattered on top of an extremely thin (a few nanometers) transparent layer, itself deposited on a metallic surfaces behave as extremely effficient light absorbers. Light sneaks into the extremely small gap between a cube and the metallic film, and is thus concentrated in a tiny volume. The resonance frequency depends on the geometrical parameters of the structure, so that it can be easily tuned, and is especially sensitive to the width of the gap below the cubes.

The absorption cross-section of a nanocube can be as large a 30 times the section of the nanocube itself. Theoretically, only 3 % of the surface needs to be covered with nanocubes to absorb 100 % of the incoming light, just as if the cubes were able to suck up the light. A very important point here is that the structure does not need to be fabricated using lithography : the cubes can be chemically synthesized and then randomly deposited. The whole process is uncredibly fast, simple and cheap compared to any lithographic process, opening up totally new perspectives.

These resonators actually belong to the larger class of gap-plasmon resonators, whose resonances are based on the existence of a nanometric gap in the structure (like a nanoslit in a metallic film). These resonators, with so small gaps, need a more accurate electromagnetic description than the classical Drude model, and they can be used to scatter light as well as to enhance the fluorescence by Purcell effect.

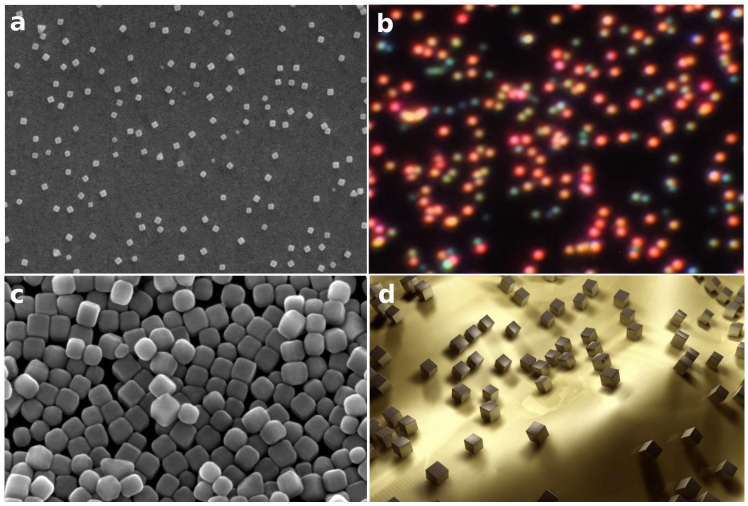

Fig. 2: (a) The nanocubes once they have been deposited. (b) As seen in a dark field microscope. (c) Nanocubes as synthesized. (d) Artist's view of the surface.

An ANR project has recently begun whose aim is to explore the physics of gap-plasmons and to setup modelization and simulation adapted techniques. Potential applications are numerous, including ultra-sensitive detection of biomolecules, light extraction, or ultra-fast optoelectronic devices.

Fig. 1: Geometry of the resonators.

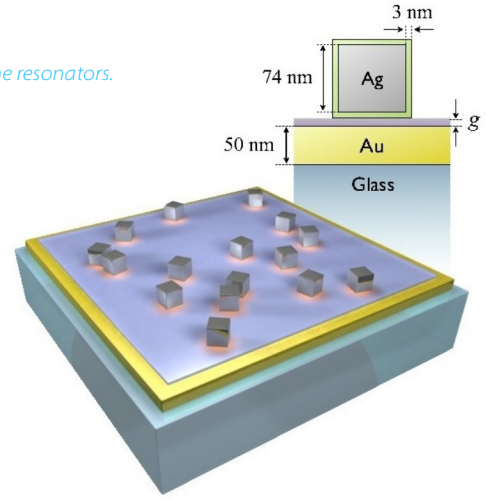

CONTACTS

Antoine MOREAU
Antoine.MOREAU@univ-bpclermont.fr
Emmanuel CENTENO
Emmanuel.CENTENO@univ-bpclermont.fr
Gérard GRANET
Gerard.GRANET@univ-bpclermont.fr

FURTHER READING

Controlled-reflectance surfaces with film-coupled colloidal nanoantennas
A. Moreau et al., Nature 492, 86 (2012)

Impact of nonlocal response on metallodielectric multilayers and optical patch antennas
A. Moreau et al., Physical Review B 87, 045401 (2013)

CONTRACTS

ANR Jeune Chercheur PGP (2012-2016)

Scientific achievement #54

Exciton-Polariton condensates in low dimensionality systems, polariton circuits and devices

Since 2009, the LPN developped unique etching techniques of planar microcavities in the strong coupling regime, keeping intact the optical and electrical properties of the system. This has allowed the realization of 1D wires, 0D pillars, coupled pillars, 1D and 2D lattices, and polariton circuits and devices of different geometries. This has allowed a very deep experimental and theoretical study of coherent phenomena in these systems which led to the publication of 2 Nature Physics, 2 Nature Communications, and 5 Phys. Rev. Lett. and several other articles which have all acquired a high citation rate . The main results of these works are listed below.

In [Nature Physics, 6, 860, 2010], cited 200 times, a 1D cavity was excited non resonantly by a focused excitation spot which created a local excitonic reservoir. The polariton condensate created in the pumping area has been accelerated by the repulsive potential created by the exciton reservoir and was then found to flow ballistically and keeping its coherence all along the 1D sample (fig. 1a). This experiment was the first demonstration of extended spatial for a spontaneous polariton condensate. It also demonstrated the possibilities of manipulating polariton flows by non-resonant optical excitations. When the density of the flowing condensate is large enough, it can develop parametric instabilities while it is flowing, which surprisingly was found to dramatically reduce the flow depletion induced by the structural disorder (Backscattering suppression) [Phys. 108, 036405, (2012).]. Similar experiments have been repeated time resolved [PRL 109, 216404 (2012)], in pillars [PRL 106, 126401 (2011)], and double pillars [PRL 108, 126403 (2012)], and 1D Lattices [Nature Com, 4, 2313 (2013).]. In this last case, the spontaneous condensation in Gap solitons bound or unbound to the potential induced by the exciton reservoir, as well as the study of their motion in real space have been reported. Detailled theoretical studies of polariton Bloch Oscillations have been performed as well [PRB 83 045412, PRB 84 125314 (2011).]. These papers have brought a much better understanding of the role of the interactions between the reservoir and the condensate on the energy relaxation as shown on the figure 1 where one can see on the three panels the ballistic propagation on polariton on the left of the reservoir, and its energy relaxation on the right, where the condensate is confined between the reservoir and the structure edge and relax its energy. This has allowed the development of a new model describing Bose Einstein Condensation in opens systems. This model which has been presented in details in [PRA 89, 033626, (2014).] demonstrated that a driven dissipative condensate can show a superfluid behavior, an aspect which is presently widely debated. Following our 2008 theoretical proposal, the resonant pulsed excitation of double pillar structure has allowed the study of Non-linear Bosonic Josephson Oscillations, and of one of its main manifestation, the Self trapping effect [Nature Physics, 9, 275, (2013).]. Finally a polariton Mach Zehnder interferometer [Nature Com., 5, 3278, (2014)] (figure 2) and of a polariton resonant tunneling transistor [PRL 110, 236601, (2013)] have been fabricated and studied. In both cases the modulation of the transmission of the circuit is induced by the energy shift of the states induced by a local non-resonant optical excitation. This energy shift induces a phase shift in the Mach Zehnder and put a 0D state in or out of resonance of a propagating state in the tunneling transistor. In both cases, the huge strength of the polariton-exciton interaction has allowed record compacities for the designed devices.

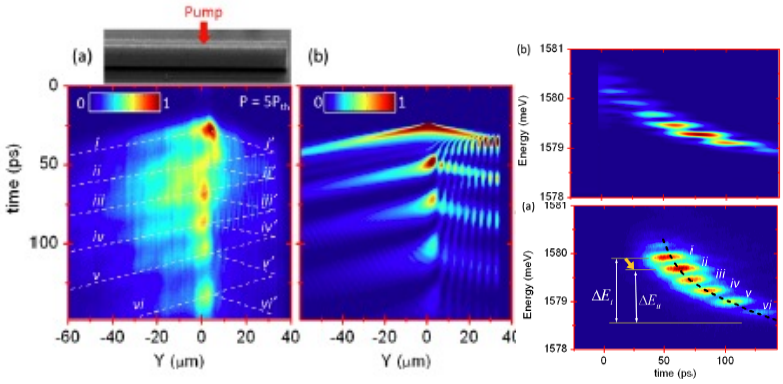

Fig. 1: ***Ballistic propagation versus relaxation of a polariton condensate.*** *a, experiment, b theory. A non resonant pulse creates an immobile excitonic reservoir at t=0 and condensates propagating on each side. On the left the propagation is quasi-ballistic. On the right the polariton condensate is reflected by the edge of the sample and comes back in the reservoir region. It re-stimulate the creation of a condensate and dissipates energy because of polariton exciton interaction. The energy dissipation is evidenced on the panels shown on the right (b theory, a experiment).*

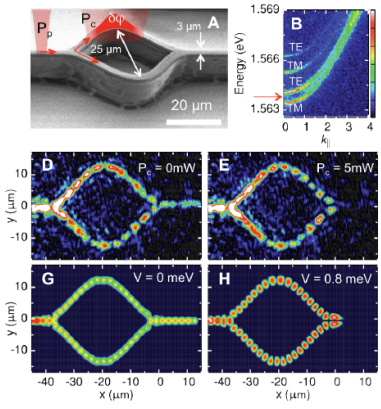

Fig. 2: ***Polaritonic Mach-Zehnder interferometer.*** *A: SEM image of a etched microcavity fabricated at LPN. The light is injected from the right (Pp) and propagates in the 2 arms of the interferometer. A laser placed on one arm (Pc) induces a phase shift. B energy dispersion in the wire part of the structure. The arrow shows the energy of excitation. (D, G): Constructive interference case for (experiment, theory). (E,F) Destructive interference case for (Experiment, Theory).*

CONTACTS

Guillaume MALPUECH
Guillaume.MALPUECH@univ-bpclermont.fr
Dmitry SOLNYSHKOV
Dmitry.SOLNYSHKOV@univ-bpclermont.fr

FURTHER READING

Macroscopic quantum self-trapping and Josephson oscillations of exciton-polaritons
M. Abbarchi et al., Nature Physics 9, 275 (2013)

Polariton condensation in solitonic Gap states in a one dimensional periodic potential
D. Tanese et al., Nature Comm. 4, 2313 (2013)

Spontaneous formation and optical manipulation of extended polariton condensates
E. Wertz et al., Nature Physics 6, 860 (2010)

CONTRACTS

ITN SPINOPTRONICS (2009-2013)
ANR QUANDYDE (2011-2015)

PhD

H. Flayac, D. Visnevskii

Scientific achievement #55

Topological excitations in spinor quantum fluids of light: magnetic monopole behavior and collective properties

We described theoretically and demonstrated experimentally in collaboration with LPN and LKB that the topological excitation of spinor exciton-polariton fluids (half solitons, half vortices) behave as emergent magnetic monopoles which can be accelerated by effective magnetic fields. We studied the collective behavior of a half soliton ensemble. We demonstrated that it can form a Wigner Crystal made out of photonic excitation. We also studied magnetricity, namely the conductivity of the monopole gas under the action of an external field and found a record mobility own thanks to the photonic character of the system.

Cavity exciton-polaritons (polaritons) are photonic quasi-particles strongly mixed with the excitonic resonances of semiconductor nanostructures. As it they behave as strongly interacting photonic particles with two spin projection. Moreover, cavity polaritons are characterized by spin-anisotropic interaction, and some specific spin-orbit interaction based on the energy splitting between the TE and TM polarized eigen modes, spin-orbit interactions which allowed us to describe theoretically and observed in collaboration with LKB the Optical Spin Hall Effect about a decade ago [PRL 95, 136601, (2005), Nature Physics 3, 628, (2007)]. Observation of polariton superfluidity, vortices, oblique solitons has been reported as well. Thanks to the great flexibility offered by the experimental study of cavity polaritons, this system has appeared as an ideal platform to study spinor quantum fluids made out of photonic excitations.

Since 2010, we described theoretically topological defects in Spinor quantum fluids with spin anisotropic excitations which are the so-called half vortices and half solitons. In [PRB, 83 1933055, 2011], we proposed to consider a flow of linearly polarized polaritons, hitting a defect, in presence of photonic spin-orbit interaction. Further, [PRB 85, 073105, (2012); NJP14 085018 (2012)] we demonstrated that half solitons and half vortices can be described in terms of emergent magnetic monopoles which are accelerated in the presence of effective magnetic fields associated with linear polarization splittings. This monopole acceleration has been demonstrated experimentally in collaboration with the LKB and the LPN [Nature Physics 8, 724, (2012)]. The figure 1 shows a simulation demonstrating the monopole separation induced by the action of an effective magnetic field. A flow of polaritons linearly polarized hits a defect. The circularly polarized emission σ^+ (fig 1a) shows the formation of two oblique solitons at the wake of the defect which are accelerated to the left by the effective field whereas the σ^- is deviated in the opposite direction. The trajectories of the resulting four solitons can be visualized on the fig 1-c which shows the circular polarization degrees. We have also demonstrated theoretically that half solitons can be formed when a radial flow of linearly polarized interacting polaritons is created in presence of a TE-TM effective magnetic field [PRL 110, 016404 (2013)]. In this non-linear regime the current induced by the Optical Spin Hall effect are strongly focused. In a next step we consider the properties of a 1-Dimensional gas of effective magnetic monopoles (half solitons). We have first shown that half solitons are fermionic quasi-particles and we derived the interaction potential between them.

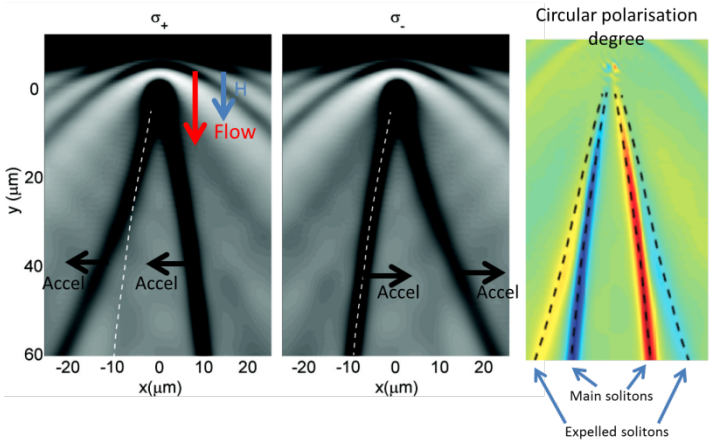

Fig. 1: ***Effective magnetic monopole acceleration.*** *Numerical solutions of the spinor Gross Pitaevskii equation including pumping and decay and TE-TM splitting. A flow of polariton linearly polarized is resonantly excited by the pump. It hits an impenetrable circular defect at y=0. a,b) Density plot of the σ^+ and σ^- components respectively. The dark traces shows the half soliton trajectories. c) Circular polarization degree.*

We have shown that despite of the relatively short range interactions, half solitons can form the analog of a Wigner Crystal [PRL 110, 035303, (2013)], which to our knowledge is the first description of a Wigner Crystal made out of photonic excitations. We then considered the behavior of such gas in presence of an effective magnetic field providing an accelerating force. We have analyzed the different conductivity regime for the magnetic charges [PRL 113, 036403 (2014).]. A remarkable aspect which was first pointed by S.T. Bramwell in a news and Views of Nature Physics [Nature Physics 8, 703, (2012)] is that these effective charges are made of light which allows a very fast motion and a record mobility as we calculated.

CONTACTS

Guillaume MALPUECH
Guillaume.MALPUECH@univ-bpclermont.fr
Dmitry SOLNYSHKOV
Dmitry.SOLNYSHKOV@univ-bpclermont.fr

FURTHER READING

High Speed DC Transport of Emergent Monopoles in Spinor Photonic Fluids
H. Terças et al., Phys. Rev. Lett. 113, 036403 (2014)

Topological Wigner Crystal of Half-Solitons in a Spinor Bose-Einstein Condensate
H. Terças et al., Phys. Rev. Lett. 110, 035303 (2013)

Half-solitons in a polariton quantum fluid behave like magnetic monopole
R. Hivet et al., Nature Physics 8, 724 (2012)

CONTRACTS

ITN SPINOPTRONICS (2009-2013)
ANR QUANDYDE (2011-2015)

PhD

H. Flayac

Scientific achievement #56
Polariton Z topological insulator

We have studied theoretically and experimentally (together with LPN) the effects of the spin-orbit coupling of polaritons in topologically nontrivial systems with hexagonal symmetry. A polaritonic benzene molecule was shown to exhibit a circular spin-current under polariton condensation because of the TE-TM spin-obrit coupling. We have shown that this coupling has a dramatic effect for polariton graphene, where it leads to trigonal warping of the Dirac point of the dispersion. Together with an applied magnetic field giving rise to Zeeman splitting for excitons, the spin-orbit coupling leads to the opening of a non-trivial gap at the Dirac point with topologically protected one-way (chiral) surface states inside the gap. We demonstrate that these states are indeed protected from backscattering.

Exciton-polaritons are the quasiparticles formed from strong coupling of cavity photons with quantum well excitons. Confined structures with polaritonic modes have become the laboratory for many insightful experiments. The first studies of polaritonic molecules [PRL 108, 126403 (2012)] consisting of just 2 coupled pillars have demonstrated the importance of the polarization effects: the splitting between the lowest modes was largely defined by the polarization splitting. In larger molecules, such as the polariton benzene molecule [PRX 5, 011034 (2015)] which has a hexagonal shape, the effects of the spin-orbit coupling become even more dramatic: it affects the condensation which occurs not on the ground state, but on an excited state carrying a circulating nonzero spin current. This is because the whole structure of the eigenstates becomes modified, because the field couples the eigenstates with different angular momentum. In this situation, it is the excited state which obtains the largest overlap with the reservoir.

It is natural that a ring-like structure exhibits nontrivial topological properties in presence of a spin-orbit coupling. The topological insulators are not ring-like, but periodic structures, where the topological non-triviality is obtained by opening an "inverted" gap. In this case, the surface states of the structure are topologically protected: their presence in the gap is guaranteed, and their chiral nature makes possible for particles to propagate in only one direction.

After demonstrating the appearance of Dirac points and a flat band in the polariton graphene [PRL 112, 116402 (2014)], and studying condensation on the states in the scalar case (neglecting spin), we have analysed the effect of the ubiquitous TE-TM splitting of planar cavities on such hexagonal lattices of pillars [PRL 114, 026803 (2015)]. We have shown that the 2-fold structure of the TE-TM field at the Gamma point is transformed to a 1-fold structure at the Dirac point due to the reduced symmetry of the Dirac points, making appear an effective Dresselhaus field, which can be viewed as a non-Abelian gauge field. This transformation can be evidenced by the typical pattern of the optical spin Hall effect [PRL 95, 136601, (2005)], changing from 4 domains to 2, which has been published on the cover of Physical Review Letters. Other effects include a trigonal warping leading to appearance of 3 supplementary Dirac cones around each Dirac point, and a transformation of the band topology at high values of the spin-orbit coupling

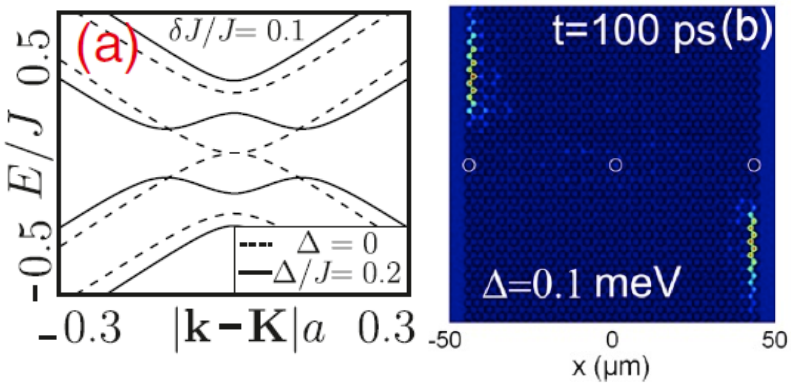

Fig. 1: ***Band gap opening and chiral edge states.*** *a) The band structure of polariton graphene at the Dirac point in presence of the spin-orbit coupling (dashed line) and magnetic field (solid line), calculated in the tight-binding model, demonstrating the opening of the gap. b) A snapshot of a numerical simulation demonstrating one-way propagative surface states 100 ps after the localized excitation (marked by circles). The contours of the honeycomb potential are plotted with black lines.*

Photons are not charged, and therefore they are insensitive to the magnetic field, which prevents the observation of their Landau levels and quantum Hall effect. Polaritons are also uncharged particles, but their excitonic fraction gives rise to a Zeeman splitting. We have shown [PRL 114, 116401 (2015)] that this Zeeman splitting, combined with the spin-orbit coupling discussed above, opens a gap at the Dirac point. The band structure is characterized by Chern numbers ±2. Moreover, the gap is inverted in the two different Dirac points of the Brillouin zone, which creates chiral (one-way) propagative states on the surface. Such states are robust against perturbations. We demonstrate that even when a pillar is removed from the surface, the backscattering of the particles propagating on the surface does not occur because the counter-propagating state simply does not exist.

CONTACTS

Guillaume MALPUECH
Guillaume.MALPUECH@univ-bpclermont.fr
Dmitry SOLNYSHKOV
Dmitry.SOLNYSHKOV@univ-bpclermont.fr

FURTHER READING

Polariton Z Topological Insulator
A.V. Nalitov et al., Phys. Rev. Lett. 114, 116401 (2015)

Spin-Orbit Coupling and the Optical Spin Hall Effect in Photonic Graphene
A.V. Nalitov et al., Phys. Rev. Lett. 114, 026803 (2015)

Spin-Orbit Coupling for Photons and Polaritons in Microstructures
V.G. Sala et al., Phys. Rev. X 5, 011034 (2015)

CONTRACTS

ITN SPINOPTRONICS (2009-2013)
ANR QUANDYDE (2011-2015)

PhD

A. V. Nalitov

Scientific achievement #57
Room temperature polariton condensation based on ZnO and GaN microcavities

We report the first observation of room temperature polariton lasing in ZnO and GaN planar microcavities grown on silicon. These recent results are very promising for the future electrically injected polariton devices. Moreover polariton condensation is obtained in an unprecedented excitonic fraction from 17 to 96% in a bulk ZnO microcavity with dielectric mirrors. Thus we observe a variation of the exciton-polariton mass, lifetime and interaction constant by one order of magnitude. Furthermore, polariton mode switching is demonstrated simply by controlling the optical pumping or by changing the photonic part of the polariton.

Polaritons are bosonic quasiparticles resulting from the strong coupling between photons and excitons. Due to their mixed nature, polaritons have unique properties: a very low effective mass but a strong interaction with their environment. These key parameters allow polaritons to undergo Bose-Einstein condensation (BEC) up to room temperature (RT). Based on this specific behavior, a new generation of optoelectronic devices such as polariton laser, polariton switch and polariton circuit could be realized. Indeed, for classical laser diodes (LDs) a population inversion is required to reach the threshold but the situation is different for polariton lasers since polaritons are stimulated from the final state (BEC mechanism) thus the threshold for a coherent emission of photon is very low, two order of magnitude smaller than LDs. In this framework, wide bandgap semiconductors like ZnO and GaN appear as ideal candidates since their exciton are still robust at room temperature. Moreover the lasing threshold may be decreased with a larger Rabi splitting and a longer photon lifetime. The first parameter is mainly controlled by the oscillator strength, which gives the advantage to ZnO, and the second is obtained with a high quality factor resonator.

Planar microcavities, made of a semiconductor layer embedded between two high reflectivity mirrors, permit to tune the ratio between photonic and excitonic properties of the polariton by introducing a thickness gradient in the active layer. The excitonic fraction is a direct estimation of this ratio: this quantity varied from zero percent for a pure photon to one hundred for a pure exciton. An illustration is given in figure 1 for a GaN microcavity grown on Si: from left to right, the excitonic fraction decreases from 56% to 11%, changing the curvature of the energy versus wavevector dispersion. In other words, the polariton effective mass is divided by a factor of 2 but interactions between polaritons are also strongly reduced. Figure 2 highlights the appearance of polariton lasing when the number of optically injected carrier is increased. Indeed, the drastic reduction of linewidth above threshold combined to a marked non-linearity is a proof of the bosonic stimulation. Remarkably, this microcavity is grown on silicon substrate with a 30 pair crack-free DBR leading to a very low photonic disorder and a large quality factor up to 3500. Such a structure appears as an ideal building block for future electrically injected room temperature polariton devices.

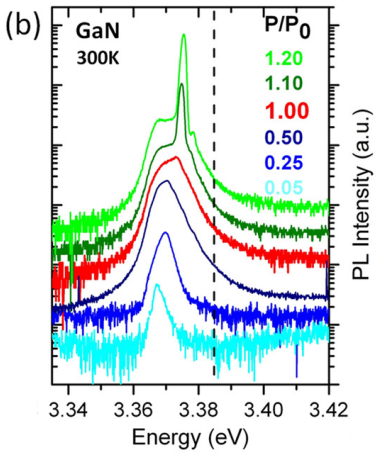

Fig. 2: Polariton at normal incidence is reported as a function of the number of optically injected carriers; power densities are normalized to threshold. The dashed line indicates the energy of the bare cavity mode.

In another approach, a ZnO substrate is thinned and placed between two dielectric DBRs. This structure combines very high optical quality and a large cavity quality factor. Polariton condensates have been observed up to RT for an excitonic fraction from 17% to 96%. The deep polaritonic trap allows condensation of the quasi-exciton like polaritons while the LO phonon assisted relaxation helps polaritons with high photonic fraction to relax into the fundamental state. For each temperature the minimum threshold is determined by the trade-off between thermodynamic and kinetic regimes.
In the thicker region of the sample, several lower polariton branches are present simultaneously. At threshold, polariton condensation occurs on the branch closed to the optimal detuning then the increase of the optical pumping enhances the polariton-polariton scattering processes and allows polariton condensation to a lower state. This optical switch operates through a non resonant optical pumping and could be easily transposed at RT.

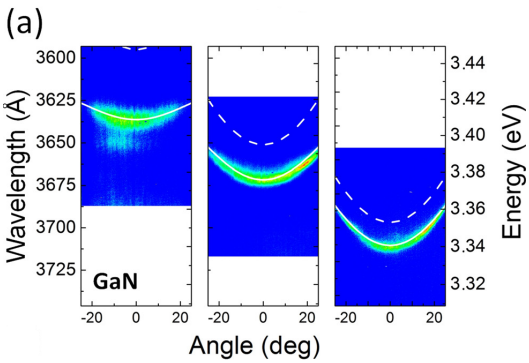

Fig. 1: Dispersion curves illustrating the effective mass variation of the low polariton branch as its excitonic fraction changes: 56% (left panel), 23% (central panel) and 11% (right panel). The simulated photonic mode (dashed line) and polariton (solid line) are both shown.

CONTACTS

Pierre DISSEIX
Pierre.DISSEIX@univ-bpclermont.fr
Joël LEYMARIE
Joel.LEYMARIE@univ-bpclermont.fr
Martine MIHAILOVIC
Martine.MIHAILOVIC@univ-bpclermont.fr
François REVERET
Francois.REVERET@univ-bpclermont.fr

FURTHER READING

Patterned silicon substrates: A common platform for romm temperature GaN and ZnO polariton lasers
J. Zuniga-Perez et al., Appl. Phys. Letters 104, 241113 (2014)

Fabrication and characterization of a room-temperature ZnO polariton laser
F. Li et al., Appl. Phys. Letters 102, 191118 (2013)

From excitonic to photonic polariton condensates in a ZnO-based microcavity
F. Li et al., Phys. Rev. Letters 110, 196406 (2013)

PhD

O. Jamadi, E. Mallet, L. Orosz

Scientific achievement #58

Accurate determination of excitonic parameters of GaN and ZnO by linear and non-linear spectroscopies

We report an extensive study of the excitonic properties of GaN and ZnO bulk samples with an accurate determination of the excitonic parameters from linear and non-linear spectroscopies. It is shown that in GaN due to microscopic disorder the inhomogeneous broadening prevails over the homogeneous one at low temperature, while the situation is opposite in ZnO, where the interaction of excitons with acoustic phonons is noticeable. This comparative study also allows to highlight the influence of oscillator strength values on spectrally-resolved-four-wave mixing and time- integrated-four-wave-mixing.

In the past three decades, wide band gap semiconductors GaN and ZnO have been intensively investigated for their potential applications in new optical devices emitting in the near UV region. Recent developments in polaritonics have shown that these materials are interesting to obtain a low threshold coherent light-emitter at room temperature, namely the polariton laser. Thus, the accurate knowledge of excitonic parameters is of a particular importance for an optimized design of these new optical components. In addition to continuous-wave reflectivity (CW-R) and autocorrelation reflectivity (AR), time-integrated degenerate-four-wave mixing (Ti-DFWM) and spectrally-resolved-DFWM experiments has been carried out in bulk GaN and ZnO at various temperatures. The advantage of the Ti-DFWM, combined with the CW-R and AR experiments lies in the fact that the inhomogeneous and homogenous excitonic broadenings can be accurately measured together with the oscillator strength. The excitonic parameters for GaN and ZnO are compared in table 1: the GaN oscillator strengths are found smaller than those of ZnO and no dissymmetry is observed between the oscillator strengths of A and B excitons. Concerning the broadening of the excitonic lines, the inhomogeneous broadening (σ) is larger than the homogeneous one (γ) in GaN while the situation is reversed in ZnO. In GaN, the inhomogeneous broadening is due to weak fluctuations of strain which induce variations of the excitonic energy. It has been shown that the homogeneous broadening at low temperature in both materials comes from the interaction of excitons with impurities. The higher homogeneous broadening in ZnO with respect to GaN is due to the higher group velocity of excitons induced by the larger oscillator strength (see figure 1). The SR-DFWM spectra displayed in this figure show three excitonic lines for ZnO while only two peaks are in evidence for GaN. It is worth noting that the emission occurs near the light dispersion curve with a sufficient density of states. The higher oscillator strength of ZnO with respect to GaN explains the existence of these three lines resulting from the light-matter coupling giving rise to the low polariton branch (LPB), middle polariton branch (MPB) and upper polariton branch (UPB). In GaN, the LPB and MPB lines are mixed up.

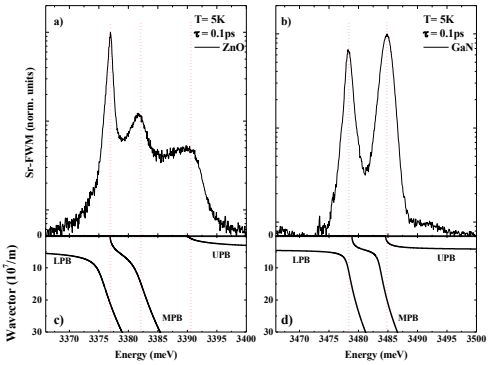

Fig. 1: Sr-DFWM obtained experimentally at 5K for ZnO and GaN. The pulse energy is centered between A and B exciton energies. For a better comprehension of peak positions on Fig.1c and d are reported polariton dispersions. An increase of the peak linewidth is observable when energy peak increases.

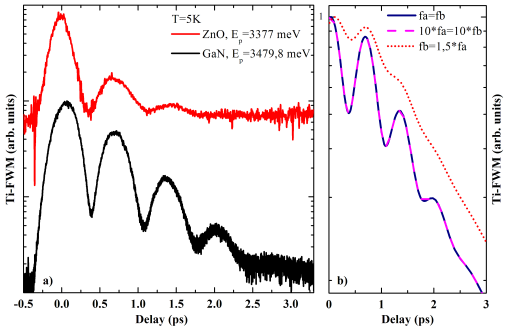

Fig. 2: (a) Ti-DFWM obtained experimentally at 5K for ZnO (black solid line) and GaN (red solid line). (b) On solid blue line and dashed pink line, Ti-DFWM calculated with A oscillator strength equal to the B one. In blue line oscillator strengths are ten times smaller than in pink line. To compare contrast beat the two spectra are normalized. On red dotted line B oscillator strength is 1.5 larger than the A one.

In fig. 2a, Ti-DFWM spectra recorded for a pulse energy centered between A and B excitonic transitions are plotted respectively for ZnO (black line) and GaN (red line). For the sake of clarity, the spectra have been normalized. It appears that the quantum beats (QBs) are more defined in the case of GaN than for ZnO. This behavior is explained in terms of oscillator strengths. Calculations displayed in fig. 2b clearly show that the oscillator strength asymmetry between A and B excitons affects the contrast of the QBs. The lower contrast for ZnO (with respect to GaN) is then attributed to the strong asymmetry between A and B excitons which does not exist in GaN.

In a near future, DFWM experiments will be carried out in wide bandgap microcavities to evaluate the dephasing time of cavity polaritons along their dispersion curve. These delicate experiments will also allow to measure the polariton-polariton interactions.

Table 1 *Data at T=5K*

		Oscillator strength (meV^2)	Polarisability	γ (meV)	σ (meV)	Energy (meV)
GaN	XA	40 000	$3.33.10^{-3}$	0.4	0.8	3478.1
	XB	39 000	$3.21.10^{-3}$	0.65	0.8	3483.5
ZnO	XA	155 000	$1.36.10^{-2}$	0.55	0.20	3375.2
	XB	250 000	$2.19.10^{-2}$	1.35	0.25	3380.7

CONTACTS

Pierre DISSEIX
Pierre.DISSEIX@univ-bpclermont.fr
Joël LEYMARIE
Joel.LEYMARIE@univ-bpclermont.fr
François REVERET
Francois.REVERET@univ-bpclermont.fr

FURTHER READING

Influence of excitonic oscillator strengths on the optical properties of GaN and ZnO
E. Mallet et al., Phys. Rev. B 90, 045204 (2014)

Accurate determination of homogeneous and inhomogeneous excitonic broadening in ZnO by linear and nonlinear spectroscopies
E. Mallet et al., Phys. Rev. B 87, 161202 (2013) (R)

PhD

E. Mallet

Scientific achievement #59

Optical properties of AlGaN/AlGaN heterostructures for the realization of a solid-state Vertical Surface Emitting Laser operating at 280 nm

Optical UV emission at 280 nm has been demonstrated by using AlGaN/AlGaN quantum wells grown on a relaxed AlGaN buffer on AlN template by Metal Organic Vapor Phase Epitaxy. The aluminium compositions for the buffer, barriers and quantum wells were optimized from envelope function calculations and ***k.p*** formalism in order to obtain an emission around 280 nm with a reasonable TE/TM polarisation ratio for surface emission. These heterostructures are now suitable for the realization of a Vertical Cavity Surface Emitting Laser operating in the deep UV region. This work is carried out within an ANR project VESUVE with a national consortium of four laboratories (LPN, Gorgia Tech UMI, SUPELEC-Metz, Institut Pascal).

Nitrides based laser diodes are compact alternatives, potentially low-cost, and more stable than common UV lamps, and their applications are numerous: spectroscopy, imaging, lithography, purification... An interesting configuration consists of a laser emission through the surface of a vertical cavity (Vertical Cavity Surface Emitting Laser - VECSEL) but the extension to wavelengths lower than 300 nm (UV-B) remains a major challenge in terms of materials and of the realization of the laser cavity. The study of AlGaN based deep UV lasers is challenging because it has to overcome growth issues of high Al-content AlGaN heterostuctures and lack of understanding in gain characteristics of the quantum wells (QW) employed for deep UV laser. Moreover, in AlGaN/AlGaN heterostructures, a crossover from TE to TM polarization at short wavelengths is an obstacle for light extraction from top emitting UV devices grown on the c-plane because light that propagates along the c-axis must have TE polarization. It was, therefore, necessary to engineer the active region so that TE polarization is preserved. To achieve emission at a wavelength of around 280 nm, the Al composition in the wells and barriers were chosen to be x_{Al} = *0.37* and *0.57* respectively. The well and barrier thicknesses used in the calculations were 1.7 nm and 10 nm. The calculated values of the relative oscillator strengths for E perpendicular to c axis (TE polarization) are displayed on figure 1 as a function of the Al composition in the barriers. The uppermost valence bands of würtzite nitrides are formed out of p orbitals with wave functions combining |X>, |Y> and |Z> symmetries. The anisotropic strain mixes these valence band states and the polarization properties of the interband transitions are thus modified. When the biaxial stress increases with the increase of Al content in the barriers, the band-to-band oscillator strength of the fundamental transition involving Γ_7-valence band (crystal field splitt-off hole band (CH)) increases up to *0.5*, which corresponds to the value of the oscillator strength of the transition involving the Γ_9-valence band (heavy hole).The CH valence band is no longer purely governed by p_z states but arises from a mixing between p_x, p_y and p_z states and is therefore not forbidden for TE polarization. The compressive strain increases the weight of p_x, p_y-like states at the expense of p_z-like states.

Figure 2 shows the macro-transmission measurements (E-field⊥c configuration) at 5K and 77K together with photoluminescence results. The transmission spectra reveal the absorption edge of the barriers at 260 nm, while a 30% drop of transmission is observed around 290 nm due to the absorption in the wells. The absorption coefficient in the wells is found to be as high as 3.10^5 cm^{-1} from the fit of the transmission spectrum, which implies that the oscillator strength is preserved in the QWs despite the high aluminium composition.

These results represent a significant step towards the development of solid-state deep-UV VECSEL. We have now to implement the extended vertical cavity by incorporating two dielectric mirrors, one deposited on the front face of the epitaxial structure and the other on the back face of the thinned sapphire substrate (LPN, Marcoussis). The lasing should be demonstrated at IP in a near future with an optical in-well pumping (λ_{exc}=266 nm).

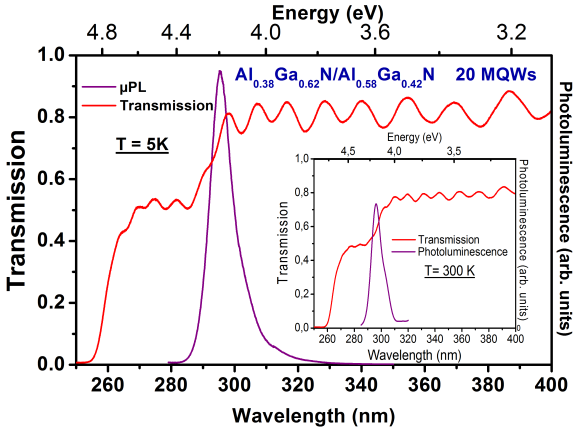

Fig. 2: Macro-transmission measurements of ten AlGaN/AlGaN MQWs together with photoluminescence spectra recorded at low temperature (T=5K) and room temperature (T=300K).

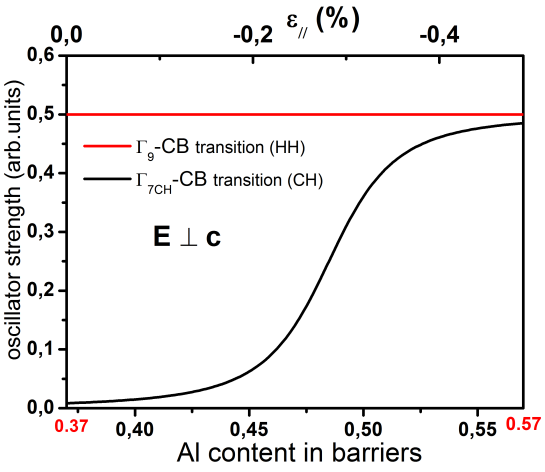

Fig. 1: Relative oscillator strengths for the optical transitions between the valence bands (Γ_7 (CH) and Γ_9 (HH)) and conduction band (CB) in an AlGaN/AlGaN quantum well as a function of the Al composition in the barriers, with Al content in the well fixed to x_{Al} = 0.37. The corresponding strain in the well is also reported in the top axis.

CONTACTS

Pierre DISSEIX
Pierre.DISSEIX@univ-bpclermont.fr
Joël LEYMARIE
Joel.LEYMARIE@univ-bpclermont.fr
François REVERET
Francois.REVERET@univ-bpclermont.fr

FURTHER READING

AlGaN-based MQWs grown on a thick relaxed AlGaN buffer on AlN templates emitting at 285 nm
X. Li et al., Opt. Mater. Express 5, 380 (2015)

Effect of strain and barrier composition on the polarization of light emission from AlGaN/AlN quantum wells
J.E. Northrup et al., Applied Physics Letters 100, 021101 (2012)

CONTRACTS
ANR Blanc VESUVE (2011-2015)

Post Doc
G. Legac

Scientific achievement #60
Ultralong defect-free single crystal phase GaAs and GaN nanowires

Record crystal phase GaAs and GaN nanowires (NWs) were grown by catalyst-assisted vapor-liquid-solid growth implemented in a HVPE reactor. High mass inputs of chloride III-Cl and hydride V-H3 gaseous growth precursors as used by the HVPE process, provide high axial growth rate of NWs up to 200 μm/h. The high Ga concentration in the liquid catalyst droplets decreases their surface energy which ensures the nucleation of a single phase and prevents polytypism, regardless of the NW radius. HVPE-grown NWs then exhibit record aspect ratio and polytypism-free crystalline structure.

III-V semiconductor nanowires (NWs) are synthesized by catalyst-assisted vapor-liquid-solid (VLS) growth and catalyst-free selective area growth, mostly by molecular beam epitaxy (MBE) and metal-organic vapor phase epitaxy (MOVPE). The control of the morphology and crystalline phase of NWs is still a challenging task. NWs feature spontaneous polytypism beyond critical small diameters (<30 nm), and stacking faults can form along the axis of the nanowires. Efforts are made to reach phase perfection and control the phase axial swapping. That is obtained for a limited range of experimental growth parameters, on length of several microns with tapered morphology quite frequently. In that context, the *forgotten* hydride vapor phase epitaxy (HVPE) technique, known for its fast growth rate property, provides interesting results. HVPE is carried out with completely different thermodynamic conditions with respect to MBE and MOVPE, in terms of temperature and precursors (GaCl, V-H_3) with a particular H_2/chlorine ambient pressure. This peculiar experimental environment yields the growth of NWs with record aspect ratio and crystalline structure.

Figure 1 shows the TEM and HRTEM images of zincblende (ZB) GaAs NWs grown by Au-assisted VLS-HVPE. NWs exhibit a rodlike shape with a constant radius over length ranging from 10 to more than 100 μm. When the radius is decreased down to 11 nm and 5-6 nm, NWs keep displaying a perfect ZB phase, which is unexpected. Polytypism and conversion to wurtzite (WZ) should take place in the 5-15 nm radius range as predicted by equilibrium formation energy. The competition between the ZB and WZ phases is actually driven by the difference in the corresponding nucleation barriers rather than equilibrium energies of fully formed NWs.

VLS-HVPE is carried out at high temperature for which NW growth preferentially occurs via the adsorption of As and GaCl species on fully liquid Au-Ga-As droplets, followed by the fast decomposition and desorption of the Cl atoms in the H_2 ambient atmosphere.

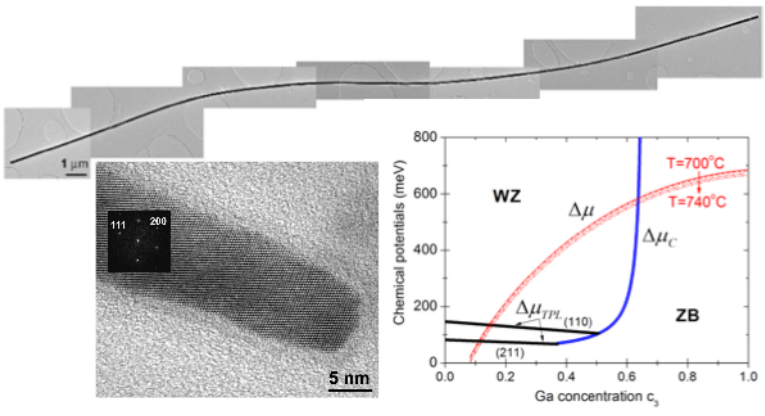

Fig. 1: GaAs NW 50 μm long, diameter 120 nm, grown by VLS-HVPE at 715°C (top image). HRTEM of a zinc-blende GaAs NW 12 nm in diameter (bottom left image). Chemical potential of GaAs in a liquid Au-Ga-As droplet showing the ZB phase area in the right side for high Ga concentration (bottom right figure).

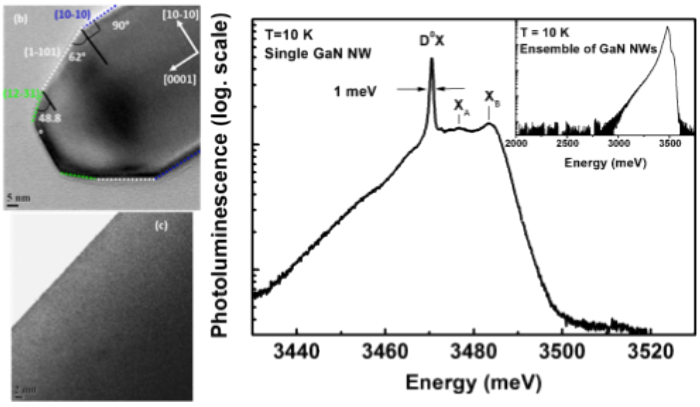

Fig. 2: (left) HRTEM images of GaN nanowires grown by Au-Ni assisted VLS-HVPE: (top) near the top of the NW; (bottom) NW sidewall. (right) Micro-PL spectrum of a single GaN NW. Inset: micro-PL spectrum of a set of GaN NWs.

High mass inputs (300 Pa for GaCl) yield high axial growth rate (more than 100 μm/h) and high supersaturation in the catalyst droplets. High Ga concentration in the droplets (>0.6) increases chemical potential ($\Delta\mu$) which suppresses nucleation at the triple phase line thus preventing the formation of the WZ phase regardless of the NW radius (see Fig. 1, bottom right curves).

Same features are observed for GaN NWs. Figure 2 displays HRTEM images of GaN NWs grown by Au-Ni assisted VLS-HVPE at a rate of 130 μm/h. GaN NWs crystallized in the hexagonal wurtzite structure along the [0001] orientation. Microphotoluminescence (micro-PL) showed a narrow and intense neutral-donor bound exciton emission line with a narrow 1 meV line width.

Free A and B exciton recombinations indicate that the GaN NWs are strain-free. VLS-HVPE GaN NWs demonstrate state of the art optical properties comparable to those of NWs obtained by the catalyst-free MBE process.

Neither Au or Ni were detected in the NWs by EDX. As another evidence of GaN crystal purity, no yellow band is observed in contrast to MOVPE-grown GaN. As for GaAs NWs, a continuous and rapid Ga incorporation takes place into liquid Au-Ni-Ga catalyst droplets, yielding a high axial growth rate.

The HVPE group focuses now on the growth of GaAs NWs by Ga-assisted (auto-catalysed) VLS-HVPE on Si substrate, and on the growth of GaN/AlN core-shell NWs on various substrates including Si.

CONTACTS

Yamina ANDRE
Yamina.ANDRE@univ-bpclermont.fr
Evelyne GIL
Evelyne.GIL@univ-bpclermont.fr
Agnès TRASSOUDAINE
agnes.trassoudaine@udamail.fr
Dominique CASTELLUCI
Dominique.CASTELLUCI@univ-bpclermont.fr

FURTHER READING

Ultralong and defect-free GaN nanowires grown by the HVPE process
G. Avit et al., Nano Letters 14, 559 (2014)

Record pure zinc-blende phase in GaAs nanowires down to 5 nm in radius
E. Gil et al., Nano Letters 14, 3938 (2014)

Fast growth synthesis of GaAs nanowires with exceptional length
M.R. Ramdani et al., Nano Letters 10, 1836 (2010)

CONTRACTS

CPER Project Innov@Pôle (2007-2013)

PhD

G. Avit, Z. Dong, K. Lekhal, M.R. Ramdani

Scientific achievement #61
HVPE growth of (In,Ga)N structures with controlled morphologies

The versatile HVPE process implementing III chloride precursors was developed to grow (In,Ga)N structures with controlled morphologies. GaN rods with high optical quality and high aspect ratio were grown by selective area growth (SAG). Then hybrid HVPE GaN core/MOVPE InGaN shell structures for LED's manufacturing, exhibiting high optical quality without yellow luminescence, were successfully synthesized. On silicon substrates, various GaN morphologies were grown without any surface treatment. HVPE revealed a high potential for monolithic integration of GaN nanostructures on a Si platform. Today InGaN nanowires growth is investigated.

Recently, 1D c-axis InGaN core/ GaN shell rods have emerged as good candidates for LEDs. Heteroepitaxy on highly mismatched substrates allows strain relaxation, enhanced by the wire morphology. Crack and dislocation densities can be drastically reduced, inducing less non-radiative recombinations and exalting light emission. Particularly, high aspect ratio columns offer a larger active zone per substrate unit area than planar layers. The fabrication of such structures is mainly performed by self-assembled metal organic vapor phase epitaxy (MOVPE), which is the standard industrial technique. But for this process, issues appear such as non-uniformity of the rods in their diameter or density. In order to improve GaN rod morphology and distribution, selective area growth (SAG) is developed. In SAG, the growth selectively occurs on patterned substrates in the precisely defined apertures of an inert dielectric mask, ideally without addressing the filling factor (opening/mask pattern ratio) or the pattern periodicity. Chloride precursors, applied in hydride vapor phase epitaxy (HVPE) are so volatile that they provide the most suitable environment for implementing selective and localized growth without any adsorption on the dielectric surface. This growth process is ruled by surface kinetics that is, by the intrinsic growth anisotropy of crystals. The facet growth rate can be set by varying the experimental parameters of temperature and vapor phase composition. SAG-HVPE and MOVPE processes were coupled for the synthesis of high quality c-axis InGaN/GaN core/shell structures. The core consists in high aspect ratio and high optical quality GaN rods grown by SAG-HVPE on patterned AlN-Npolar/Si(100) substrates (Figure 1a). The shell is then grown by MOVPE. The silane free HVPE process ensured the whole lateral cladding of the core. The hybrid HVPE core/MOVPE shell structures (Figure 1b) exhibit high optical quality without yellow luminescence.

The growth of GaN nanowires (NWs) on silicon has drawn much attention because it provides a unique way for the monolithic integration of high-quality GaN structures on a Si platform for producing low-cost devices. Today, growers use an intermediate AlN to bridge the mismatch between the GaN material and the substrate. Here again, the HVPE process appears to be powerful: hexagonal individual, tripod and hyperbunched GaN nanorods (NRs) were grown on silicon (Figure 2) without performing any intentional pretreatment in a short growth process (<1h). The obvious effect of the temperature and the element V gas flow on the NRs size distribution was demonstrated. The crystal symmetry of the nuclei imposes the final NRs structure.

The high potential of SAG-HVPE process for the synthesis of dense GaN rod arrays and the direct growth on silicon is today harnessed. A work combining the (In,Ga)N NWs synthesis on patterned silicon (111) substrates and their optical characterization is performed. Growth conditions were first determined via a semi-empirical approach based on thermodynamical calculations. A partial pressure of only 10^{-7} atm of $InCl_{3g}$, the selected III precursor, was necessary to achieve InGaN NWs growth with high indium incorporation (50%). The next step is to address the full range In composition (0-100%).

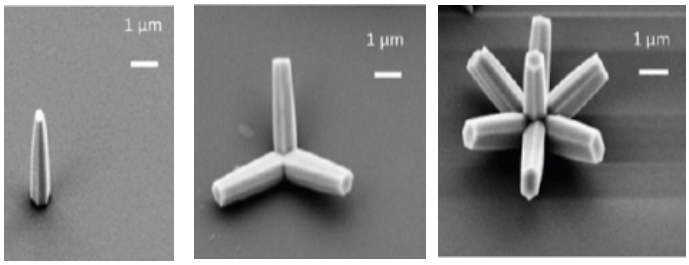

Fig. 2: SEM images of perfectly crystal-defined nanorods grown by HVPE on silicon (111) substrate exhibiting several morphologies: one nanorod perpendicular to the substrate, 3- and 7-bunched GaN nanorods.

CONTACTS

Agnès TRASSOUDAINE
agnes.trassoudaine@udamail.fr
Yamina ANDRE
Yamina.ANDRE@univ-bpclermont.fr
Evelyne GIL
Evelyne.GIL@univ-bpclermont.fr
Dominique CASTELLUCI
Dominique.CASTELLUCI@univ-bpclermont.fr

FURTHER READING

GaN rods grown on Si by SAG-HVPE towards GaN HVPE/InGaN MOVPE core/shell structures
G. Avit et al., Nano Letters (2015)

Exceptional Crystal-Defined Bunched and Hyperbunched GaN Nanorods Grown by Catalyst-Free HVPE
K. Lekhal et al., Crystal Growth and Design 12, 2251 (2012)

CONTRACTS

ANR P2N FIDEL (2012-2015)
LABEX GANEX (2012-2019)

PhD

G. Avit, K. Lekhal, E. Roche

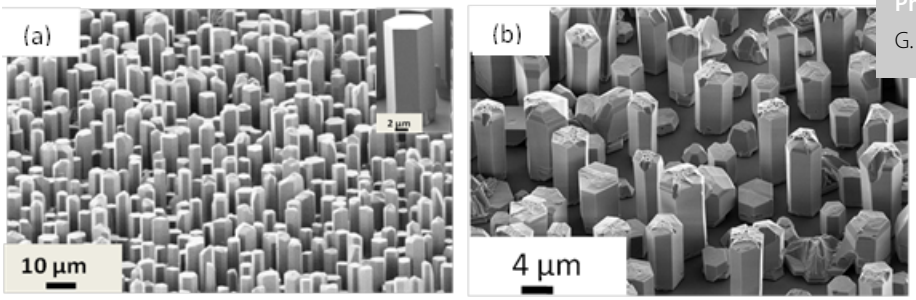

Fig. 1: SEM image of dense array of GaN rods grown by SAG-HVPE on Si(100)/AlN /SiO_2 substrate on a zone with 0.7 µm diameter holes. As an insert a single GaN rod. (b) MOVPE InGaN/GaN MQWs grown on HVPE GaN rods for LED device.

Scientific achievement #62

Elaboration of nitrided III-V thin films, under ultra high vacuum conditions. Nanostructured surfaces and their passivation

High quality GaN thin layer formation on a GaAs surface is carried out by using a low power glow discharge nitrogen plasma source under UHV conditions. This rare type of plasma source allows the growth of stoichiometric and As-free GaN ultrathin film on GaAs surfaces by means of the inter-diffusion of As and N atoms. In situ electronic spectroscopies associated with models are used to monitor surface composition and to estimate the GaN thickness. The possibility of crystallizing the amorphous GaN layer by annealing at 620 °C in a cubic structure with a lattice parameter close to that of c-GaN is evidenced by means of TEM and LEED measurements. In addition, the passivating effect of the GaN ultra-thin film to protect the GaAs surface is proven by monitoring the surface oxidation using XPS over several days of air exposure.

Nitridation is generally used to protect surfaces in the field of metallurgy. This process has been transferred to III-V materials where surfaces and interfaces play a key role in electrical properties. Under UHV conditions, GaN thin layers have been elaborated on GaAs surfaces with different crystallographic orientations.

The necessary removal of ion-implantation damage has led to use of a glow discharge nitrogen plasma source, which has the specificity of working at low power (5-10 W) and low pressure (10–1 Pa). A small quantity of active nitrogen species is created. This distinctiveness allows the growth of stoichiometric and As-free GaN ultrathin films on GaAs surfaces. In parallel theoretical studies using DFT (density functional theory) and Car Parinello simulations have be developed in order to better understand the diffusion of nitrogen atoms into the GaAs matrix.

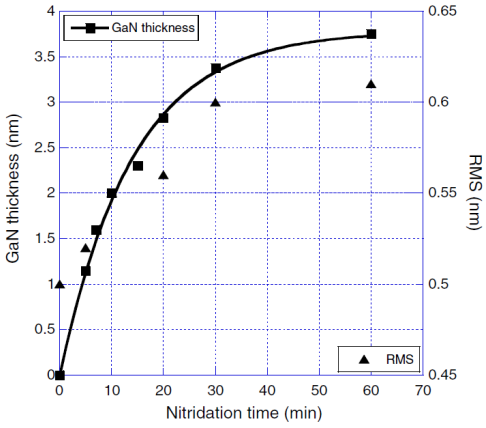

Fig. 1: GaN thickness on GaAs(100) and surface roughness (RMS) evolutions versus nitriding time.

The thickness of GaN thin films created on GaAs(001) substrate was studied versus the nitriding time by electronic spectroscopies (XPS, EELS).

Results of the comparison between experimental spectra and our theoretical model of XPS peak intensities, taking into account a stoichiometric description of the GaN layers grown on the GaAs(001) substrate are shown figure 1. The nitriding time evolution of the GaN thickness is coherent with an inter-diffusion of N and As atoms. Recently, real-time FTIR measurements were performed to follow the atomic bond creations during the nitriding of GaAs.

These results supported by DFT calculations of the vibration frequencies of the GaN/GaAs structure will be published.

TEM and LEED measurements have been carried out after an annealing at 620 °C of the system and a cubic structure with a lattice parameter close to that of c-GaN is achieved (figure 2). The passivating effect of the GaN ultra-thin film, due to high thermal and chemical stability of Ga-N bonds, to protect the GaAs surface is proven by monitoring the surface composition under high temperature and under air oxidation. Indeed, an increase up to 640°C of the surface stability temperature with only 2 GaN monolayers on GaAs is observed. Moreover surface oxidation of the c-GaN/GaAs structure during several days of air exposure is widely reduced. Electrical characterizations I(V) and C(V) were also performed to investigate the metal/GaN/GaAs Schottky diode.

This high quality thin film of GaN may also allow the creation of a buffer layer to initiate the growth of cubic-GaN structure but also the elaboration of the nanostructured nitride surfaces, such as nano-pores, nano-dots and nanowires.

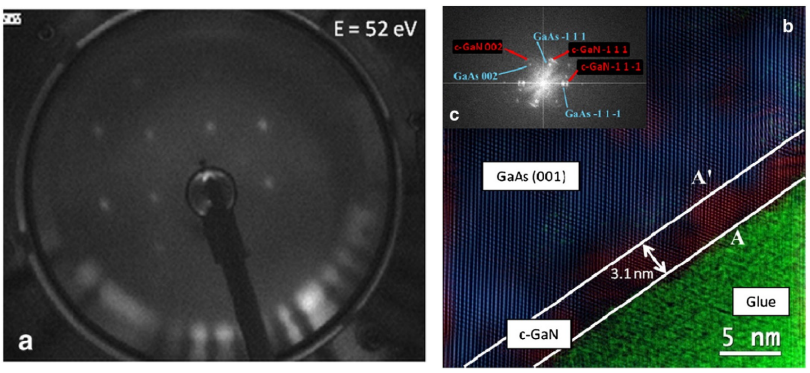

Fig. 2: (left) Low Energy Electron diffraction (LEED) on c-GaN elaborated. (right) Transmission electron microscopy (HR-TEM) of GaN/GaAs interface.

CONTACTS

Luc BIDEUX
Luc.BIDEUX@univ-bpclermont.fr
Philip HOGGAN
Philip.HOGGAN@univ-bpclermont.fr
Guillaume MONIER
Guillaume.MONIER@univ-bpclermont.fr
Christine ROBERT-GOUMET
Christine.ROBERT-GOUMET@univ-bpclermont.fr

FURTHER READING

Passivation of GaAs(001) surface by the growth of high quality c-GaN ultrathin film by using low power glow discharge nitrogen plasma source
G. Monier et al., Surf. Science 606, 1093 (2012)

Study of the characteristics Current-Voltage and Capacity-Voltage of Hg/GaN/GaAs structures
K. Ameur et al., Sensor Letters 9, 2268 (2011)

CONTRACTS

SOLEIL Synchr. (SMIS beamline) (2010, 2014)
DARI Project (2014, 2015)
PEPS GaN Act (2014)
Marie Curie (UE) FUNPROB (2010-2015)

PhD

G. Monier

Scientific achievement #63

Multi-Mode Elastic Peak Electron Spectroscopy (MM-EPES): experimental measurements combined with Monte Carlo simulations

The Multi-Mode Elastic Peak Electron Spectroscopy analysis is a very sensitive technique to the near-surface using electron elastic scattering at low energy (200-2000eV). However, for quantitative interpretation, this method needs a Monte Carlo simulation of elastic electron trajectories in the material. A new approach, taking into account the surface plasmon, the atomic arrangement and the surface roughness was developed allowing the penetration depth of the electrons to be calculated. The knowledge of this parameter is crucial to precisely probe the material by varying the primary energy. For instance, different nanoscale surface parameters have been estimated by comparison between experimental and theoretical results.

The Elastic Peak Electron Spectroscopy (EPES) is a non destructive method. This unconventional spectroscopy determines the elastic electron reflection coefficient which is the percentage of primary electrons leaving the solid without energy loss. Modulating the primary energy of the electrons (200-2000eV), EPES proved to be a very sensitive method for surface investigations. Indeed, the percentage of elastic backscattered electrons is dramatically influenced by the atomic number, the primary electron energy and the incidence/collection angles (Figure 1).

However, to obtain the quantitative interpretation of the experimental spectra, MM-EPES method must be coupled with Monte Carlo (MC) simulations describing the path of the elastic electrons inside the material. To go further in the quantitative interpretations, the development of this simulation required the introduction of several parameters such as the surface effects (i.e. surface plasmon), the crystallographic orientation of the substrate and the surface roughness. Figure 2 summarizes the different events occurring to the electrons inside the material.

EPES and MC simulations allowed estimating surface concentration of alloys or semiconductors, growth and reconstruction surfaces. However, recently, EPES put in evidence the influence of surface roughness at micro- and nano-meter scale. The use of an original Monte-Carlo method was fruitful for the simulation of different silicon surfaces: Si surface having micro saw-tooth shape and Si nano-porous surfaces prepared with alumina templates and argon bombardment in UHV conditions.

By comparison between experimental and theoretical results, the dimension of the saw-tooth, the diameter, the depth of the pores and the covering rate can be estimated. These different results highlight the ability of the EPES together with MC simulations to determine the morphology of the pores in real time without any other techniques.

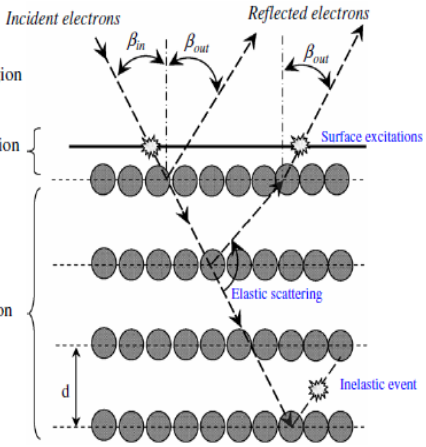

Fig. 2: Atomic layered model and scheme of the different events occurring to the electrons inside the material.

Moreover other nanoscale arrangements as nanodots or buried layers have been investigated with this non-destructive method. In parallel a new method has been developed to better use the hemispherical electron analyzer, necessary instrument to obtain precise by EPES measurements.

In perspective, this work is the basis for the development of a new 3D electronic imaging allowing exploring any nano-patterning surfaces in ultra high vacuum conditions. Indeed, the ability of simultaneous imaging of the specimen surface and of the sample bulk can have important applications in many research fields related to materials physics.

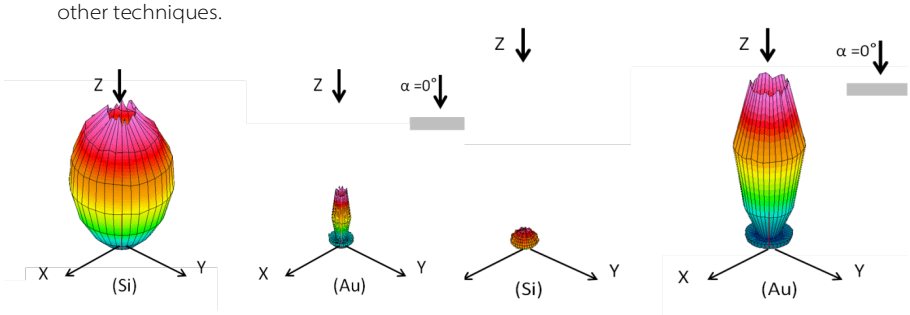

Fig. 1: 3D representations of elastic backscattered electrons from Si and Au surfaces for an incident angle of 0° at 200 eV (left) and 1200 eV (right).

CONTACTS

Luc BIDEUX
Luc.BIDEUX@univ-bpclermont.fr
Bernard GRUZZA
Bernard.GRUZZA@univ-bpclermont.fr
Guillaume MONIER
Guillaume.MONIER@univ-bpclermont.fr
Christine ROBERT-GOUMET
Christine.ROBERT-GOUMET@univ-bpclermont.fr

FURTHER READING

New method for the determination of the correction function of a hemispherical electron analyser based on elastic electron images
M.A. Majhoub et al., J. Electron Spec. and Related Phenomena 197, 80 (2014)

Development of Monte-Carlo simulations for nano-patterning surfaces associated with MM-EPES analysis
C. Robert-Goumet et al., Surface Science 618, 72 (2013)

MonteCarlo simul. for MultiMode Elastic Peak Elec. Spec. of crystalline materials
B. Gruzza et al., Surface Science 604, 217 (2010)

CONTRACTS

CPER Project Innov@Pôle (2007-2013)

PhD

S. Chelda, M.A. Majhoub

Scientific achievement #64
Organic/mineral hybrid nanomaterials for gas sensing applications

By the development of new organic/mineral hybrid nanomaterials highly reactive with gases, the "Chemical Sensor Microsystems" group opens a new way to innovative sensing devices and application fields. Compared to raw materials, the enhancement in sensing performances performed with such hybrid nanomaterials is clearly established and supported by experimental results. The high value of their specific surface area (SSA) enables the structure of original gas sensors with great sensitivity as well as selective gaseous filtering units with high durability. Relevant sensor-systems dedicated to the selective metrology of gaseous pollutants have been successfully achieved.

The scientific activities of the "Chemical Sensor Microsystems" group from MINAMAT is focused on the achievement of gas sensors and sensor-systems enabling the quantification of gaseous species at very low concentrations in complex gaseous phases. Special application is the accurate monitoring of indoor and outdoor air pollutants in the context of air quality control. In the scientific field of gas sensors, the main challenges that we want to overcome are the sensitivity, the threshold of detection as well as the selectivity.

The nature of the sensitive material is the key point of a chemical gas sensor, as it represents the interaction site with the analytes. To take advantage of the high specific surface area of nanostructured materials, specific organic/mineral hybrid nanomaterials have been synthesized. The extended interaction surface provides a high number of active sites available for gas adsorption while the insertion of functional groups on nanocarbons target specific gases. Thus, non-covalently functionalized nanocarbons by organic molecules such as macrocycles are investigated for both the development of very sensitive gas sensors and efficient gaseous filters.

Carbon nanotubes functionalized by substituted metallophthalocyanine, namely ttb-CuPc/CNTs (see fig. 1a), have been synthesized as sensitive material for the detection of aromatic hydrocarbons. Layered on quartz crystal microbalance, experimental results emphasize its high sensitivity towards toluene as compared to phthalocyanine and carbon nanotubes separately (see Fig. 2). The influence of specific surface area of the sensitive material on sensor response is so manifest. The low working temperature (room temperature) must be also pointed out.

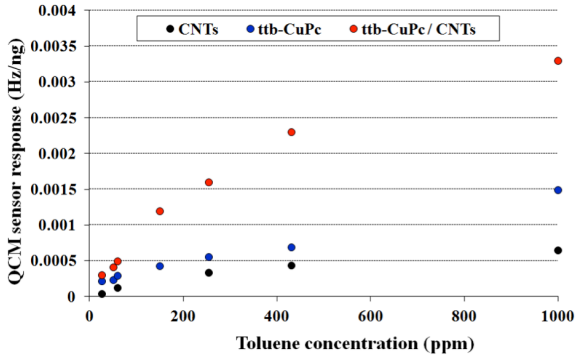

Fig. 2: Intercomparison of QCM-based sensor responses at room temperature for carbon nanotubes (CNTs), tetra-tert-butyl copper phthalocyanine (ttb-CuPc) and hybrid nanomaterial (ttb-CuPc/CNTs) as sensitive layer towards toluene in the 25-1000 ppm concentration range.

Functionalized multi-wall carbon nanotubes by indigo nanoparticles, namely indigo/MWCNTs (see fig. 1b), exhibit both a selective removal of ozone from air and a high durability. Quantitatively, the durability of indigo/MWCNTs hybrid nanomaterials is 4 times and 7 times greater than that relative to indigo and MWCNTs respectively. Implemented as in-line input filtering unit into a sensor-system including copper phthalocyanine-based chemiresistor as sensing device, the selective monitoring of nitrogen dioxide was successfully performed with a high level of performance: threshold of detection close to few ppb, low dispersion of measurements, resolution higher than 10 ppb, linear response in the 20–200 ppb concentration range and repeatable measurements during several months without service.

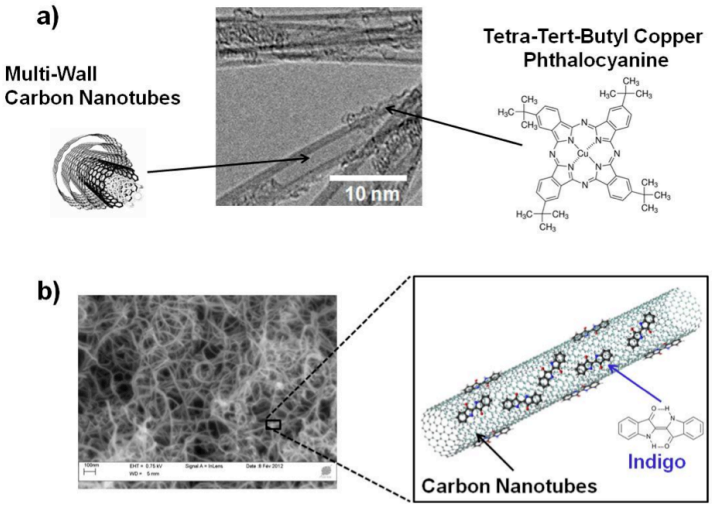

Fig. 1: TEM and SEM pictures of two organic/inorganic hybrid nanomaterials; a) ttb-CuPc/CNTs, b) indigo/ MWCNTs.

CONTACTS

Jerôme BRUNET
Jerome.BRUNET@univ-bpclermont.fr
Alain PAULY
Alain.PAULY@univ-bpclermont.fr

FURTHER READING

Improved selectivity towards NO_2 of phthalocyanine-based chemosensors...
J. Brunet et al., Talanta 127, 100 (2014)

Noncovalent functionalizations of single wall carbon nanotubes...
A. Ndiaye et al., J. of Physical Chemistry C 117, 20217 (2013)

An innovative gas sensor system... Part II: Interpretations of O_3 and NO_2/nanocarbons interactions
A. Pauly et al., Sensors and Actuators B 173, 652 (2012)

CONTRACTS

ANR BLANC CAP-BTX (2010-2013)
COST (UE) EuNetAir (2012-2016)
CPER Project Innov@Pôle (2007-2013)

PhD

A. Kumar, L. Spinelle

Scientific achievement #65

Highly selective NO_2 sensor system for air quality control: towards a technology transfer

An original gas sensor system dedicated to the selective monitoring of nitrogen dioxide in air has been successfully developed. This device involves a sensor implementing an organic layer exhibiting a great sensitivity and a chemical filter providing the removal of the interfering species while preserving NO_2 in air flow. This innovative sensor-system is now protected by patents allowing us to work within the framework of the technology transfer. Projects are now initiated to reach an industrial valuation in a middle term.

The monitoring of atmospheric pollution using common commercial chemical gas sensors (SnO_2, electrochemical cells,..) remains a challenge due to the lack of selectivity of most existing devices. This drawback is at the origin of the poor number of ready-use sensing structures devoted to pollution measurements in environmental or industrial context. In the field of air quality control an original gas sensor system dedicated to the selective monitoring of nitrogen dioxide (NO_2) in air has been successfully developed by the *"Chemical Sensor system and micro-system"* group. This device involves the great sensitivity and the selectivity towards oxidizing gases of a molecular organic semiconductor (copper phthalocyanine, CuPc): among all gases present in atmospheric air, only NO_2 and O_3 induce a significant modulation of electronic conductivity of this semiconductor and so, electrical responses when associated to a resistive transduction. Consequently, these organic materials provide to sensing devices a first level of selectivity.

A perfect selectivity towards nitrogen dioxide is achieved by the association of the CuPc chemiresistor with a porous nanocarbonaceous filter devoted to the removal of ozone in air, keeping the NO_2 concentration in its integrity. The carbonaceous material was developed in order to achieve a very high selectivity to NO_2 and preserves the benefits of semiconductor sensors in terms of sensitivity.

Chemical and physical analysis and spectroscopies (IR, Raman, NEXAFS, RPE, XRD,..) were undertaken in order to emphasis gas/nanocarbonaceous materials interactions.

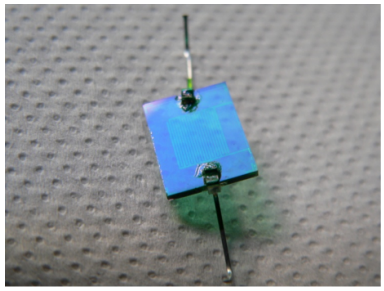

Fig. 1: CuPc sensing layer deposited onto an insulating substrate.

In our, finalized sensor system, the NO_2 selective detection is achieved associating a mixture of carbon nanodiscs and nanocones as ozone chemical filter inserted through the gas flow. The morphology at the nanoscale of the selected carbonaceous materials enables the gas diffusion within the filter to be improved. Their moderate specific surface area limits the interaction with NO_2 while being sufficient to ensure a strong reactivity with O_3. A methodology of measurements is associated to the sensing structure to reach the real-time monitoring of NO_2.

Patents (French patent (n°08 03006 au 11/06/2010), european patent (n° 2291230 au 06/08/2014), US patent (n° 8507228 au 13/08/2013) entitled "*use of carbon nanomaterials as a filtration material impervious to ozone*", A. Pauly, M. Dubois, J. Brunet, K. Guérin, C. Varenne, A. Hamwi, B. Lauron) are deposited to obtain an industrial protection in order to work in the field of technology transfer. A project is now in investigation with SATT Grand-Centre to improve technical aspects of our sensing system.

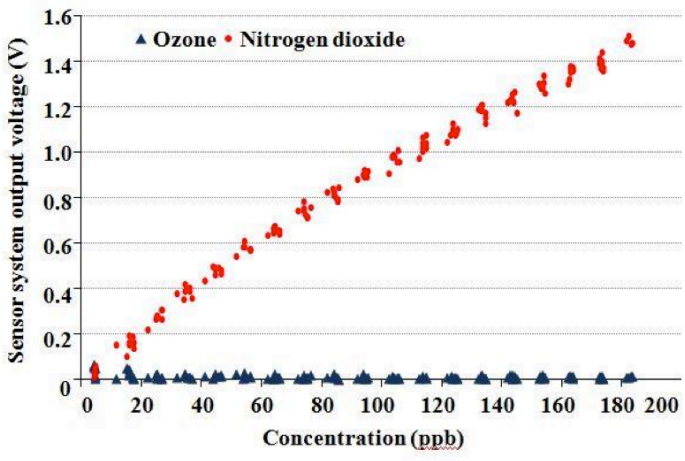

Fig. 2: Calibration curves of nanocarbons/CuPc sensor-system towards ozone and nitrogen dioxide.

CONTACTS

Jerôme BRUNET
Jerome.BRUNET@univ-bpclermont.fr
Alain PAULY
Alain.PAULY@univ-bpclermont.fr

FURTHER READING

A carbonaceous chemical filter for the selective detection of NO_2 in the environment
M. Dubois et al., Carbon 52, 17 (2013)

An innovative gas sensor system... Part I: Development of a nanocarbon filter for the removal of ozone
J. Brunet et al., Sensors and Actuators B 173, 659 (2012)

An innovative gas sensor system... Part II: Interpretations of O_3 and NO_2 /nanocarbons interactions
A. Pauly et al., Sensors and Actuators B 173, 652 (2012)

CONTRACTS

ANR BLANC POLLCAP (2006-2010)
COST (UE) EuNetAir (2012-2016)
CPER Project Innov@Pôle (2007-2013)

PhD

L. Spinelle

Scientific achievement #66
Uncertainty Quantification and Propagation for Computational and Experimental ElectroMagnetic Compatibility (EMC) Reliability

In the electromagnetic compatibility (EMC) literature, designing electronic large systems is mostly based upon "worst" cases approaches while security margins exist to ensure the system safety. In accordance with standards, this mainly sets two problems: the need for precise and efficient tools to quantify more realistic EMC margins, jointly with trustworthy reliability levels. Basically, some environmental parameters (geometry, material, sources) are not deterministically known and some random variations lead to uncertainties. For the last decade, EMC group has applied and developed advanced and original techniques to assess the quantification and propagation of uncertainties for complex EMC systems.

The purpose of EMC is to study the unintentional / intentional generation; propagation and reception of electromagnetic (EM) energy with reference to related undesired effects (EM interference, EMI). In this context, the development of a simple and clear methodology to integrate randomness into EMC modeling is crucial since the EMC of complex systems within critical devices cannot rely on the sole use of deterministic approaches. Quantifying the effects of uncertainties on the overall system behavior becomes nowadays of great importance in regards to EMC standards and this field of research has gained a growing interest over the past few years. Non-exhaustive state-of-the-art electromagnetic (EM) stochastic issues contain different philosophies to integrate this problem for instance involving printed circuit boards (PCBs), cable coupling, dosimetry (bio-electromagnetics), propagation (antenna) and effects of uncertain High Intensity Radiated Fields (HIRFs).

EMC group from Institut Pascal (IP), Université Blaise Pascal (UBP), was a pioneer in the integration of uncertainties for EMC applications (F. Diouf Phd thesis, 2008). The gradual insertion of the stochastic techniques for different issues from antennas characterization (R&T CNES 2015), EM diffraction and time-reversal (B. Jannet PhD thesis, 2014), bio-electromagnetic purposes [1] and EMC measurements ([3], REI PRINCE 2011) has broadly validated these methods in computational [2;3] and experimental electromagnetics (Figure 2, [3]). Moreover, the use of relevant sensitivity analysis tools allows ranking accurately the different random parameters. The transdisciplinary collaboration initiated 10 years ago with mathematicians and colleagues from mechanics is still active. It reinforced for a couple of years with stochastic and safety EMC analyses for wires and bundles of cables.

Parallel to the growing interest of EMC actors for accurate and trustworthy approaches to ensure functioning safety in electrical engineering, different stochastic techniques (inspired by mechanical reliability: FORM, SORM, subset simulations; polynomial chaos and stochastic finite element expansions for instance) are promising and were successfully applied to uncertain EMC configurations (Figure 3) to rank most influential random variables and compute systems' probability of failure. Combining improved stochastic approaches and reliability techniques may be crucial in the future to properly design complex electronic systems and provide more realistic margins (but reliable) for standards.

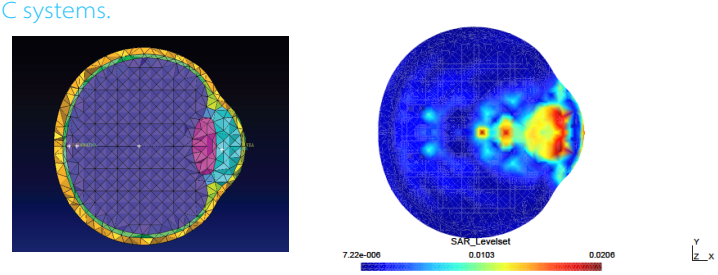

Fig. 1: (left) Human eye electromagnetic model and (right) Specific Absorption Rate (SAR, z-plane, impact of relative permittivity from cornea) induced by plane wave with power density 10 W/m² at frequency 6 GHz: first order sensitivity analysis through coefficient of variation.

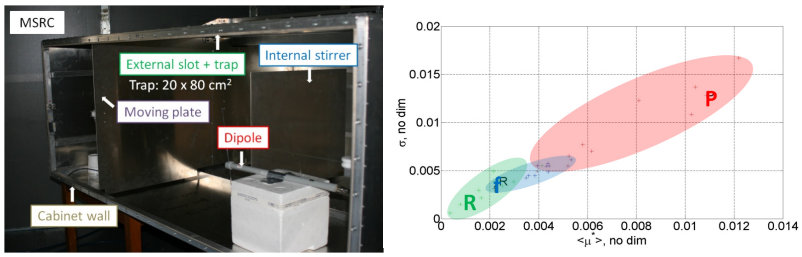

Fig. 2: (left) Inner view of the experimental stochastic cabinet (141x197x77cm³) including trap, moving plate and stirrer. Its design and achievement was the result of a fruitful collaboration between EMC group (IP) and Polytech'Clermont Physics department (2-years student project) funded by REI "PRINCE" French DGA program (CEG Gramat, 2008-2011). (right) Experimental model reduction from Morris' sensitivity analysis (ranking of the random variables R, f and P): from measurement achieved in stochastic cabinet (a), a weaker EMC (shielding due to enclosure) impact of rotating unit R is observed relatively to variations of frequency f and external trap P.

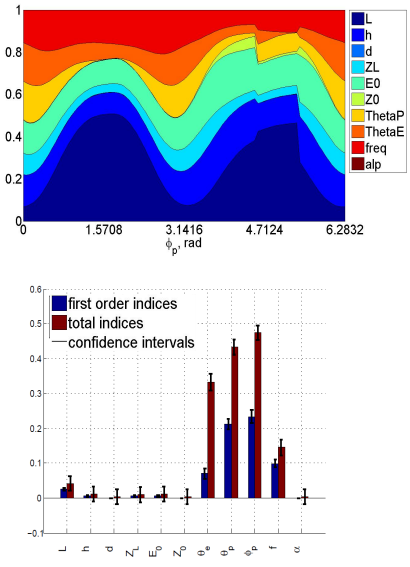

Fig. 3: (top) Local sensitivity analysis from importance factors in case of a random (length L, terminal loads Z0 and ZL, height h above ground plane, diameter d, attenuation coefficient α) transmission line illuminated by an also random (electric field magnitude E0, polarization θe, incidence "elevation" θp) plane wave source in function of incidence "azimuth" φp. (bottom) Global sensitivity analysis from Sobol index (first order and total) showing the importance of the effect of plane wave source illuminating random transmission line (top).

CONTACTS

Pierre BONNET
Pierre.BONNET@univ-bpclermont.fr
Sébastien LALLECHERE
Sebastien.LALLECHERE@univ-bpclermont.fr

FURTHER READING

[1] *Stochastic sensitivity of the electromagnetic distributions inside a human eye modeled with a 3D hybrid BEM/FEM edge element method*
H. Dodig et al., Engineering Analysis with Boundary Elements 49, 48 (2014)

[2] *Electrical stochastic modeling of cell for bio-electromagnetic compatibility applications*
S. Lallechere et al., Annals of Telecommunications 69 (5-6), 295 (2014)

[3] *Numerical simulation of a Reverberation Chamber with a stochastic collocation method*
P. Bonnet et al., C. R. Physique 10, New approaches in Electromagnetic Compatibility, 54-64 (2009)

CONTRACTS

ANR CISSSI (2006-2010)
R&T CNES (2012-2015)
REI PRINCE (2011-2017)

PhD

F. Diouf, B. Jannet, A. Kouassi, A. Pagnetti

Scientific achievement #67
Matrix Pencil Method applied to Smart Monitoring, ElectroMagnetic Compatibility and Ultra Wide band RADAR

Matrix Pencil Method (MPM) is an a high-resolution technique to identify deterministic signals based on either simulation or measurement. It can identify non-stationary signals, even in the presence of numerical or measurement noise, respectively. The basis functions are complex exponentials with a damping factor. The method is applied either in time domain, in frequency domain or in space domain allowing one to identify the original signal (electromagnetic waves, distributed currents or termination currents) by means of a limited number of singular values, poles and residues. This technique is suitable in EMC, Radar, Load monitoring, grounding system...

The MPM is based in eigenvalue decomposition (EVD) and singular value decomposition (SVD) . From original signal, Hankel data matrix is constructed. After some arrangements of this matrix and using Singular Value Decomposition (SVD) we can determine the number of poles and theirs values. The number of significant poles M should be estimated from the ratio of singular values to the largest one. We present three application of MPM.

The MPM in the time domain (MPMTD) to treat the problem of Non Intrusive Appliance Load Monitoring (NIALM) is introduced, the main goal is to monitor load appliances in residential home and without intrusion. This technique takes the advantage from the transient and steady state analysis to improve monitoring efficiency. In particular, it allows us to extract active and reactive power for fundamental and harmonic frequencies. This new approach has been integrated into an energy meter with the collaboration of EDF, Landis + Gyr and the Institut Pascal (Fig. 1). Identification signal based on poles and residues is used not only for slow or fast transients, but also for the steady state. The result is successful and has been patented both in Europe and overseas [1].

The second application deals with the radar target identification and classification by using MPM in the frequency domain (MPMFD) and in the complex plane. The method is applied to Ultra Wide Band (UWB) backscattered signal from canonical targets (thin wire, sphere, and cylinder), complex targets thin wire structure, human, lamp, tree… In frequency domain, the Matrix Pencil Method could be applied to extract the features of different targets.

With this new method (MPMFD), the separation between the early time and the late time is not necessary (difficult task), contrary to users of MPM in time domain [3]. The field scattered from the object is obtained from Ultra Wide Band radar acting as both transmitter and receiver (Fig. 2).

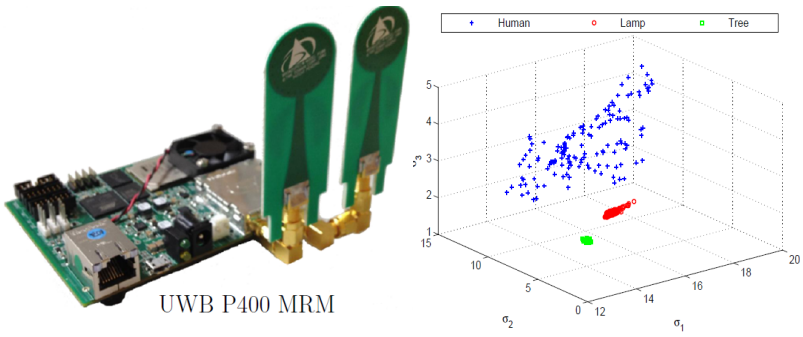

Fig. 2: RADAR setup and target classification based on singular values.

For MPMTD and MPMFD, the accuracy of three different classifiers: Naïve bayes (NB), K-Nearest Neighbor (K-NN), and Support VectorMachine (SVM) have been compared.

The third application of the MPM applied in space domain (MPMSD) and deals with the radiation from a wire antenna in near, intermediate and far zone [2]. For a given current distribution measured or calculated, the proposed model calculates the radiated field by using the magnetic potential vector.

The distributed current is expressed as a finite sum of damped sinus based on MPM identification in space domain. Then the total magnetic potential vector is expressed as a sum of partial vector potentials $\overrightarrow{A_h}$ with $1 \leq h \leq M$.

To verify the validity of the proposed model, we compare the radiated field obtained from MPMSD with the radiated field provided by Feko software. It is applied to the case of an antenna in free space energized with a source positionned in the middle of the line. The application of Matrix Pencil Method to three different cases has been demonstrated. it shows several advantages:

- Robustness against measurement noises.
- Less data required to identify the original signal by using reduced number of poles and residues.
- Application in the real axis (time domain) or in the complex plane (the frequency and space domains).

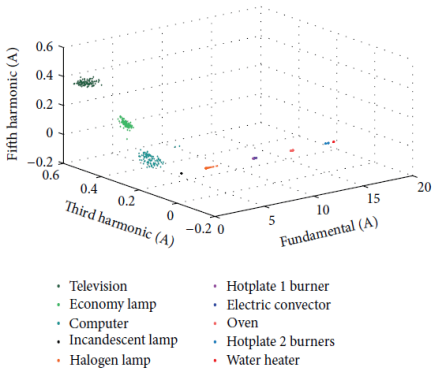

Fig. 1: NIALM measuring system and appliances classification.

CONTACTS

Khalil EL KHAMLICHI DRISSI
drissi@univ-bpclermont.fr
Claire FAURE
Claire.FAURE@univ-bpclermont.fr
Christophe PASQUIER
Christophe.PASQUIER@univ-bpclermont.fr
Kamal KERROUM
Kamal.KERROUM@univ-bpclermont.fr

FURTHER READING

[1] *Method and device for the non-intrusive determination of the electrical power consumed by an installation, by analysing load transients*
A. Diop et al., World Patent, WO 2010037988 A1 (2010)

[2] *An Efficient Computational Method Based on Current Measurements for Fields Radiated by a Thin Antenna or a PLC Line*
M. Chaaban et al., Progress In Electromagnetics Research Symposium, PIERS, Marrakesh, 1845-1849 (2011)

[3] *Comparison of Matrix Pencil Extracted Features in Time Domain and in Frequency Domain for Radar Target Classification*
M. Khodjet-Kesba et al., Int. Journ. of Antennas and Propagation, Vol. 2014 (2014)

CONTRACTS

EDF, Landys+Gyr
BRI Corée du Sud
Marie Curie FP7-People
PHC Cedre, PHC Toubkal

PhD/Post Doc

M. Chaaban, M. Khodjet-Kesba, A. Liakouti, H. Najmeddine / V. Arnautovski-Toseva, K. Chahine

Scientific achievement #68

Novel modulation of dual-vsi fed open-end motor to enhance efficiency for electrical and hybrid vehicles applications

Recently, due to global warming concerns, electric/hybrid vehicles have attracted more attentions over the internal combustion engine. Based on modern embedded systems, it is predicted that these highly competitive vehicles will become common transport, in the near future. Conventionally, in order to respect battery safety/efficiency concerns, low input dc voltage has been preferably used. Therefore, the total efficiency is further deteriorated due to presence of passive components in a DC/DC converter. In this project, new power structure and corresponding modulation strategy is developed to construct pure sinewave output current, to enhance efficiency and to respect EMC standards.

The open-end motor can be driven with dual-VSI at both ends by simply making six terminals of stator windings available. Dual-VSI, due to low input-voltage level feature, is particularly suitable for electrical/hybrid vehicle applications. Single dc-link dual-VSI driven open-end motor, shown in Fig. 1, eliminates needs of a boosting stage (i.e., a DC/DC converter) which suffers from size/price penalty, and low efficiency. The principles of the proposed method are outlined from the standpoint of modulation, switching loss, and voltage/current THD. Conventional space vector modulation (CSVM) is modified by avoiding null-vector utilization to achieve switching loss and Common Mode Voltage (CMV) mitigation. By equally dividing the null-vector duty cycle α_0 into those of the two nearby active vectors, not only the CMV but also the effective switching frequency, which corresponds to switching losses, is suppressed. The above-discussed modification transfers the original circular reference into a discontinuous-line reference at the surface of hexagon.

An Angular Modulation Index (AMI) based on variable phase angle displacement between two references is proposed, in order to minimize the commutation numbers while having full range modulation index. The *AMI* demonstrates non-linear (sin-shaped) dependence on the phase shift. The equivalent dropped space voltage across the load based on [3], at the same hexagon frame, for $\Delta\Theta$=90° is shown in Fig. 2.

In dual-VSI circuit configuration, each VSI imposes individual switching loss related to the angle between the output current and corresponding reference voltage vector Φ_1 and Φ_2 in Fig.2. The highest loss percentage, $1/\pi$, can be obtained at full inductive/capacitive load situation. However, switching losses still reach 50% reduction. Fig. 2 shows 3D curve of equivalent for dual-VSI facilitated by the proposed method versus AMI and load power factor cos(Φ). Switching losses are highly reduced by 50-86.6%, in comparison with that of a single VSI modulated by CSVM. This 3D curve indicates that three peaks in switching loss curve can happen when system operates either at low AMI and high power factor or at high AMI and low power factor.

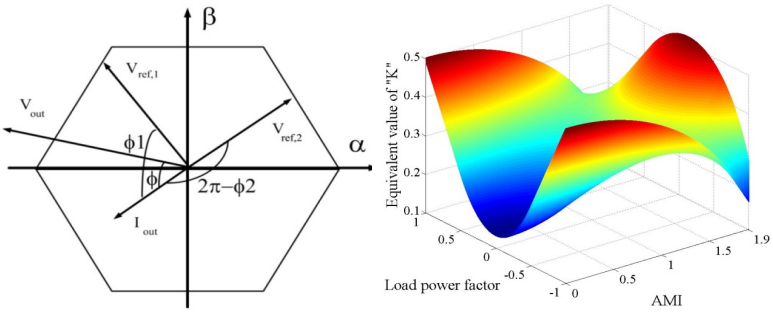

Fig. 2: Decoupled controlling VSIs to synthesize desired output voltage (left); equivalent value of 'K' versus AMI and load power factor (right).

A prototype consisting of dual three-phase two-level VSI produced by ARCEL, open-end squirrel-cage medium-power induction motor coupled to dc-motor as shaft load, and rectifier as dc source are assembled. The proposed algorithm for dual-VSI is implemented in a full digital system by programming Digital Signal Processor (DSP), model RSF562TAADFH. Also the simulation results are carried out based on the same system parameters through MATLAB/Simulink environment. The proposed method assures lower values for THDV of the phase voltage. One of the most important characteristics of VSIs especially for electrical/hybrid vehicle applications is conversion system efficiency. Efficiency of the proposed method is experimentally evaluated for open-end squirrel-cage induction motor hence operating at nominal power, 1.5 kW. The efficiency of the proposed method is measured around 95%, whereas that of the conventional method is around 90%.

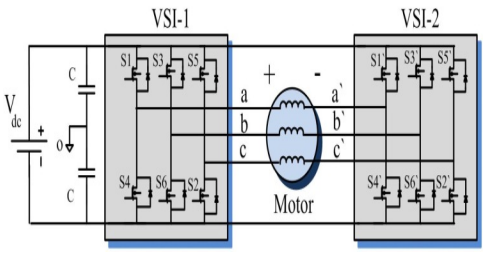

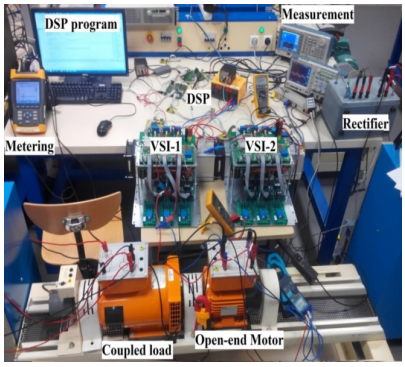

Fig. 1: Single-DC link dual-VSI fed open-end motor (left); power structure experimental setup (right).

CONTACTS

Khalil EL KHAMLICHI DRISSI
drissi@univ-bpclermont.fr
Christophe PASQUIER
Christophe.PASQUIER@univ-bpclermont.fr

FURTHER READING

[1] *Discontinuous Random Space Vector Modulation for Electric Drives: A Digital Approach*
H. Khan et al., IEEE Transactions on Power Electronics 27, 4944 (2012)

[2] *Procédé de commande d'un onduleur triphasé par modulation vectorielle aléatoire discontinue évolutive*
H. Khan et al., World Patent, WO 2013182781 A1 (2013)

[3] *Procédé et dispositif de conversion de courant et véhicule comportant un tel dispositif*
K. El Khamlichi Drissi et al., FR 15 50045 (2015)

CONTRACTS

IFPEN, Sattgc, PHC Tassili

PhD/HDR

A. Dehghani-Kiadehi, H. Khan, M. Melit / N. Boudjerda

Scientific achievement #69
Evaluations of screening performance for new generation braided cable shields

The protection of electronic devices and quality of transmission signals from electromagnetic disturbances is a key issue in most of industrial contexts (such as automotive, aircraft, industrial process and also in medical device). One of the most common solutions used to prevent those problems is to introduce shielding cables and especially braided cables. The recently industrial demand and constraint let us consider the development of a new generation of braided cables. A strong relationship has been created with Tresse Industrie and has led to the creation of new electromagnetic braided shields as well as the development of new electromagnetic measurement methods.

Designing the shields of cables is one of the most important fields in electromagnetic compatibility design. Nowadays an important electromagnetic pollution is found everywhere and can produce a large amount of electromagnetic interference on electronic equipment. This can result in some dysfunction, loss of transmission signal, unwanted event… Electromagnetic interference can be absorbed into conductive materials such as shielding placed around individual conductors within a cable assembly or wire harness. Common braids can be used for shielding material with very good results on efficiency.

In this context, a strong relationship with Tresse Industrie has been created and led to the invention of the EMI-PHY family braided shielding that well answered all the key selection factors. This braid is a mix between high conducting wires (for high screening performance) and polymer PET wires (for high flexibility). This new product is patented and is declined for variable wire diameters. The insertion of PET material in braid needs to reconsider the electromagnetic measurements methods to well define the shielding effectiveness (SE). For electromagnetic interferences, the transfer impedance measurement represents the most objective methodology to estimate the SE of cables. Based on measurement standards, we developed a triaxial measurement bench providing a huge frequency covering range (from DC to 300 MHz) and a very good sensitivity and reliability. This device is depicted in figure 1. It has been developed to support variable shielding cable diameters (not exclusively braid) as well as connectors.

For electromagnetic interferences coming up from unwanted electromagnetic fields, the determination of the SE of cable in Mode Stirred Reverberation Chamber (MSRC) has been developed.

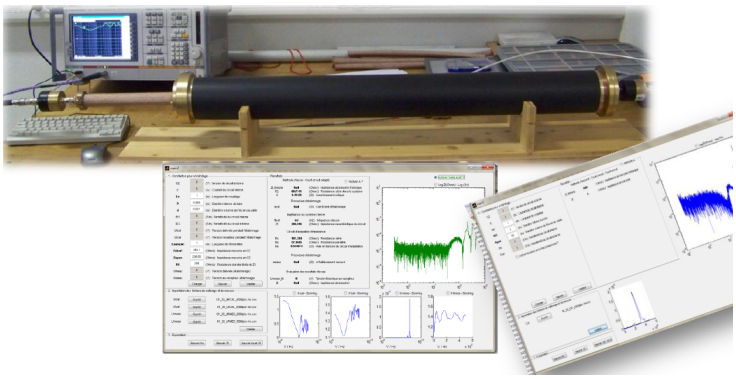

Fig. 1: Triaxial bench image showing the experimental injection tube mounted with a EMIPHY braid and the measurement vector network apparatus (upper part), the homemade measurement and post treatment software (down part).

This new determination method presents most of the advantages of reverb chambers such has high repeatability and reproducibility, high precision measurements (below 1 nW for power estimation), no dependency of the cable position and length. The frequency coverage of this measurement setup starts from 80 MHz and rises up to 6 GHz. This allows us to cover the entire radiated field spectrum.

This strong industrial relation gave the opportunity to explore several research interests in both experimental and simulation contexts. Some master students were also integrated in this project to look forward some special points of interest.

In 2011, Tresse Industrie was awarded from *Trophée de l'innovation* during CIEN fair (Carrefour de l'Industrie Electronique et Numerique) with EMI-PHY.

This project led Tresse Industrie to embed braided shielding sleeve EMI-PHY in Renault electrical vehicle, Kangoo-Z.E., SM3-Z.E., ZOE, in Daimler SMART Fortwo Electric-Drive (Fig 2) and lately in BMW i3 and i8 Plug-in Hybrid cars. EMI-PHY sleeve interests aeronautics industry too. The MSRC showed good shielding performances, associated to light weight and mechanical resistance; it makes this product very interesting for future developments in aeronautics electrical harnesses. All these industrial applications led to 25 employment creations in Tresse Industrie in the area of Ambert (63).

Last but not least it is a beginning of a new huge business for Tresse Industrie and a great success for a partnership between university and industry.

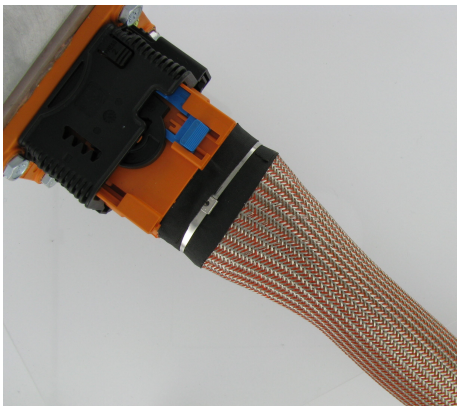

Fig. 2: Integration of the EMI-PHY braid into vehicle.

CONTACTS

Sébastien GIRARD
Sebastien.GIRARD@univ-bpclermont.fr
Françoise PALADIAN
Francoise.PALADIAN@univ-bpclermont.fr
Gilles CLEMENT
g.clement@tresse.com

CONTRACTS
8

Scientific achievement #70
BIOEM Research Laboratory Corresponding partnership

BioEMC can be seen as a branch of electromagnetic compatibility (EMC) where the equipment under test is a biological system. The scientific question is then: do non-ionizing weak electromagnetic fields have effects and if any, what are the coupling mechanisms? To address this complex multidisciplinary problem, the EMC group has developed for the last decade original research areas on the exposure set-ups and on specific biological markers. Pioneer works on high frequency expositions, either for continuous or pulsed waves, have lead to numerous well-cited papers. Since four years these researches mainly take place in the framework of a Research Laboratory Corresponding.

The previous century witnessed an explosion of technological applications that produce electromagnetic fields (EMF). High frequency electric fields are now a vital part of our daily life and are present everywhere in our environment. A wide variety of studies were performed to enhance our understanding of the potential, positive or negative, effects of EMF on living organisms.

Starting from series of experiments on tomato plants (Lycopersicon esculentum) original researches, both for the organism as a whole or at molecular level, were published jointly with biologists from Blaise Pascal University. For the first time a mode stirred reverberation chamber that allows EMF exposures as found in urban environments but protecting the experiment from unwanted external EMF was used. We demonstrated that tomato plants perceive and respond to low-level (non-thermal) EMF as if it were injurious [1].

First April 2011, EMC group from Institut Pascal (formerly known as LASMEA) was appointed Research Laboratory corresponding (LRC BIOEM) of the French Alternative Energies and Atomic Energy Commission (CEA), with the military applications division (DAM), center of Gramat. This partnership, scheduled for an initial term of four years and recently extended for two more years, is the formal framework where take place most of our Bioelectromagnetics researches. A highly important point of these studies comes from its close collaborations with biologists. Pr. Alain Vian (University of Angers) assumes the biological leadership and plays a key role by providing original ideas and critical analyses.

Two findings can be highlighted. The first is that radiated ultrawideband electromagnetic pulses with high amplitude and short duration affect several aspects of cultured murine cell physiology. We have showed, using an original experimental setup (Figure 1), that this electromagnetic field is able to trigger a rapid release of ATP (Adénosine triphosphate) in cultured murine cells.

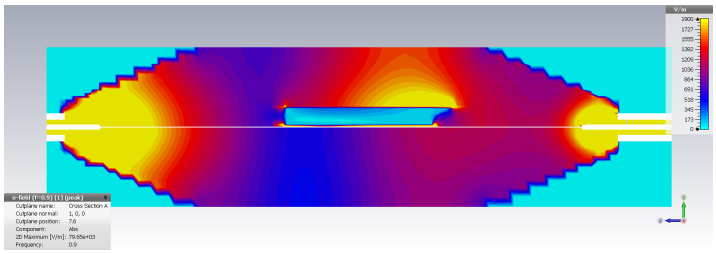

Fig. 2: Simulation of the electric field in the TEM-Cell with 30 mL of yeast inoculum in a flask (frequency=900 MHz, Specific Absorption Rate = 1.03 W.kg^{-1}).

This effect was concomitant with a drop of intracellular adenylate energy charge. Despite this rapid and strong response, we found that cell viability and clonogenicity were only slightly affected by the EMF exposure [2].

The second finding concerns *Saccharomyces cerevisiae* inoculum exposed to a continuous 900 MHz wave in non-thermal conditions in order to examine the still putative effect of high frequency EMF on organisms (Figure 2). Growth dynamics and survival rates of the yeast were not affected by this EMF exposure. We also exposed a transformed strain, which presents increased membrane fluidity in order to test the putative role of this parameter in EMF perception, and the response of this strain was identical to that of the wild type. Thirdly, we exposed a strain bearing a fluorochrome-labeled protein that allows the observation of stress granules. EMF treatment did not induce the formation of stress granules [3].

By sharing material, funding and competences, the LRC BIOEM allows a suitable environment for original and complex BioEMC researches achieved in close collaboration with specialists in electromagnetics and biologists.

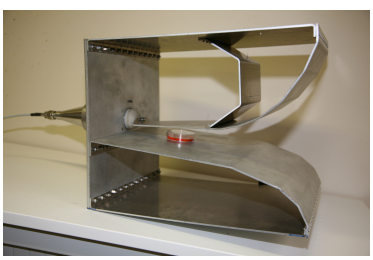

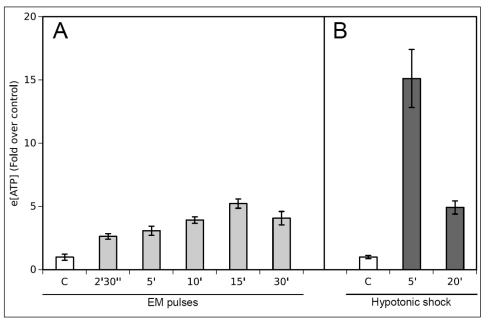

Fig. 1: (left) Koshelev antenna detail showing the position of the Petri dish containing the B16F10 murine melanoma cells exposed to radiated ultrashort high-power electromagnetic pulses (60,000 pulses, rise-time 0.25ns, peak-intensity 930 kV.m^{-1}). (right) A: Extracellular ATP concentration after UWB radiation exposure. B: ATP released after hypotonic shock. Each value is the mean of three independent experiments ± se.

CONTACTS

Pierre BONNET
Pierre.BONNET@univ-bpclermont.fr
Sébastien LALLECHERE
Sebastien.LALLECHERE@univ-bpclermont.fr
Françoise PALADIAN
Francoise.PALADIAN@univ-bpclermont.fr
Sébastien GIRARD
Sebastien.GIRARD@univ-bpclermont.fr

FURTHER READING

[1] *Intercellular communication in plants: evidence for an EMF-generated signal that evokes local and systemic transcriptional responses in tomato*
A. Vian et al., in Long-Distance Signalling and Communication in Plants, ed. by F. Baluska, Springer Verlag (2013)

[2] *Radiated Ultrashort High-Power Electromagnetic Pulses Induce ATP Release in B16F10 Murine Melanoma Cells*
S. Maquaire et al., Journal of Electromagnetic Analysis and Applications 7(3), 66 (2015)

[3] *Mesure du DAS et de l'impact physiologique induits par un champ électromagnétique haute fréquence appliqué à des cultures de levures*
T.C. Durand et al., CEM2014, Clermont-Ferrand, Juin 2014

CONTRACTS

Research Laboratory corresponding (LRC BIOEM) between CEA/DAM (Service des Effets Radiatifs et Electromagnétiques du Département effet des Armes) and Institut Pascal (EMC group) (2011-2017)

Post Doc

T. Durand, R. Filgueras, S. Maquaire

Scientific achievement #71
Redundancy-based optimization approach to optimize robotic cell behaviour

The robotic architectures offer interesting capabilities in terms of workspace and kinematics, but suffer from a lack of stiffness for applications with high loading (machining and polishing operation, meat cutting, deboning, etc.) The proposed solution is to introduce a set of redundancies for the overall improvement of different capabilities. The scientific action concerns the management of redundancy associated with the definition of a set of kinematic, mechanical and stiffness criteria witch enables the placement of the task and optimized path planning.

The proposed solution is to introduce a set of redundancies for the overall improvement of different capabilities of robotic cells. The management of redundancy associated with the definition of a set of kinematic, mechanical and stiffness criteria enables path planning to be optimized. The resolution method is based on an objective function constructed by aggregating the weighted criteria. Kinematic, mechanical and stiffness criteria are defined for each architecture. Optimized redundancy management is applied to the 7, 8, 9-DoF robotic cells including turntable and/or linear track.

First application concerns the meat cutting. The first operations of interest concern the quartering of beef carcasses and ham boning, which are considered as critical and priority operations in the transformation process. The first part involves on in-depth study of operators' expertise, so as to translate their actions into automatable operative tasks and to identify the constraints of robotization. The analysis of the cutting and task constraint parameters involves the use of a cutting strategy using a bone as a guide and a kinematically redundant robotized cell with force control (thesis Guire, Subrin). This work fulfils an identified need to study the beef quartering which is a high variability operation and ham deboning which is a high precision operation (Figure 1). The present work is part of the SRDViand project (FUI) supported by ADIV (Meat Institute Development Agency) and combines a group of industrial partners, manufacturers of equipment for the slaughter, cutting and processing of meat products.

Second application concerns robotic machining. In fact, compared to 5-axis machine tools, robots offer a larger workspace and a lower investment. Unfortunately, the cutting phenomenon causes diverse loadings of variable amplitude, frequency and direction. The lack of static and dynamic stiffness of serial robotic architecture results in a deformation of the structure and causes tool vibration, leading to geometrical defects.

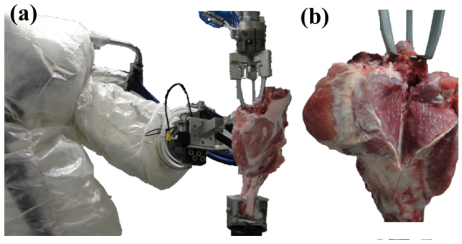

Fig. 1: (a) Robotized deboning along the 2nd fat vein, (b) Results of the cutting of the 2nd fat vein.

Manufacturers now offer high-load robots which better match however. However, these robotic architectures have a strongly anisotropic behaviour in their workspace, which reduces the useful space for machining tasks with high loads. Our improvement approach consists to introduce and manage kinematic redundancy. A first application of methods and simulation tool developed concern an efficient placement of kinematic redundancies. These works are applied to the robotic machining cell (Innov@pole, EquipEx Robotex) is made up of two 6-DoF robots with a hybrid architecture (parallelogram closed loop and Tricept PKM) served by a 2-DoF tilting turntable carried by a linear track. The second concerns the management of the kinematic redundancies to optimized tool machining path and tool trajectory. The objective function allows us to modify the value of weighting of the three criteria kinematic, mechanical and stiffness (Thesis Surin, Cousturier) with regard to various machining strategies and specifications related to some operations. The current experimentations are designed to validate the paths planning optimization algorithm applied to various strategies (face milling, pocketing, machining contours, etc.) on a set of test part (Figure 2).

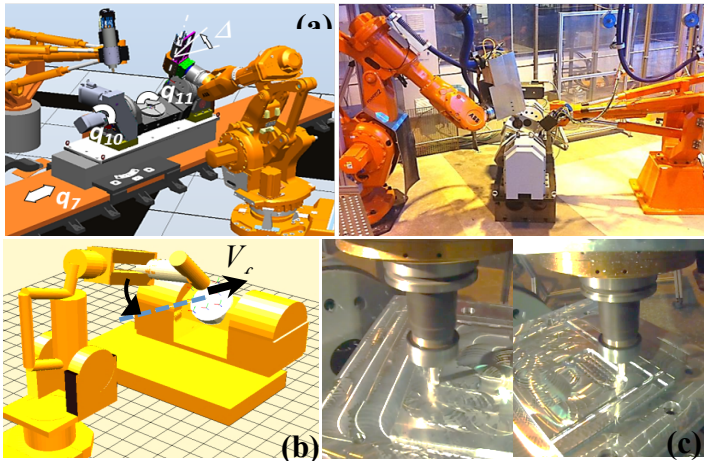

Fig. 2: (a) Studied machining robotic cell, (b) paths planning optimization, (c) various strategies validation.

CONTACTS

Laurent SABOURIN
Laurent.Sabourin@ifma.fr
Grigore GOGU
Grigore.Gogu@ifma.fr
Youcef MEZOUAR
Youcef.Mezouar@univ-bpclermont.fr

FURTHER READING

Redundancy-based optimization approach to optimize robotic cell behaviour: application to robotic machining
L. Sabourin et al., Industrial Robot: An International Journal 42, 167 (2015)

Analysis of the human arm gesture for optimizing cutting process in ham deboning with a redundant robotic cell
K. Subrin et al., Industrial Robot: An International Journal 41, 190 (2014)

Robotic cell for beef carcass primal cutting and pork ham boning in meat industry
G. Guire et al., Industrial Robot: An International Journal 37, 532 (2010) (Outstanding Paper Award 2011, Emerald Literati network)

CONTRACTS

FUI SRDViand Systèmes Robotisés de Découpe de Viande (2007-2011)
ANR RoboTool volet RobProd dans le cadre du projet *EquipEx Robotex* (2011-2019)
CPER Project Innov@Pôle (2007-2013)
UMT 08-02 Mécanisation/Robotisation dans les Filières Viandes et Produits Carnés (2009-2014)
UMT 14.02 Mecarneo (2014-2019)
Action de transfert : 2MATech (Contrats : ABB/Renault ACI - SAFE Metal) (2014-2015)

PhD

R. Cousturier, G. Guire, V. Robin, K. Subrin

Scientific achievement #72
The **C³Bots** project: **C**ollaborative **C**ross & **C**arry mobile ro**Bots**

The C³Bots project aims to design Collaborative Cross & Carry mobile roBots to transport payloads of any shape & mass (*removal man* task). Several *mono-robots* catch the payload on the ground & use it as a connecting part in the resulting *poly-robot*. Two architectures are proposed: (i) C³Bots DGP (Dorsal transport of General Payloads), carries the payload on its top platform & achieves optimal positioning maximizing both stability margin & Force Closure Grasping condition. (ii) C³Bots AT/VLP (All-Terrain / Ventral transport of Long Payloads), carries long payloads between its wheels & performs stable obstacle crossing by re-configuring its shape during an 18-step process.

The C³Bots project is a research project of LabEx IMobS³, involving 4 researchers, a Ph.D. student and a post-doctoral student.

Research objectives:

- Design several Collaborative Cross & Carry mobile roBots (C³Bots) with a simple architecture, called *mono-robots*, capable to co-manipulate and transport payloads of any shape.
- The resulting *poly-robot*, using the payload as a frame, will be capable to solve the so-called "removal-man task" (Fig. 1) to transport any object.
- Reconfiguring the poly-robot by adjusting the number of mono-robots allows manipulating heavy objects and managing objects with any shape, particularly if they are wider than a single mono-robot.
- Obstacle crossing is addressed and stability of the poly-robot and the payload permanently guaranteed.

Two sub-project are developed at Institut Pascal:

Sub-project 1: C³Bots DGP (Dorsal transport of General Payloads) (Fig. 2)

This type of mono-robot evolves on regular grounds and transports the load on its back, whatever its shape and mass (Dorsal General Payload). It is capable to position the mono-robots around the payload (Fig. 2a) to optimize the stability margin (Fig. 2b) and the Force Closure Grasping condition (Fig. 2c). The payload is held by a universal contact gripper capable to adapt its shape to the payload shape. A parallelogram lifting mechanism (Fig. 2d) can bring the payload on the mono-robot top platform. The poly-robot can have a unique centre or rotation thanks to coordinated steering on all the mono-robots.

Applications: logistics, reconfigurable assembly lines

Sub-project 2: C³Bots AT/VLP (All-Terrain / Ventral transport of Long Payloads) (Fig. 3)

This type of mono-robot is capable to evolve in All Terrain (AT) and to transport Ventral Long Payloads (VLP, Fig. 3b). This patented architecture [3] is capable to catch the payload on the ground, to lift it and to transport it over obstacles with an 18-step process that guarantees permanent stability (Fig. 3d). It uses up to four mobilities to allow the motion of one mono-robot along and around the payload. Redundant mobilities are used for postural optimization.

Applications: transport of long parts for civil engineering (pylons, poles, tubes, bunches of metallic reinforcement bars for concrete), for forestry (tree logs), heavy industry (aerospace, naval industry, tube manufacturing), civil safety (transport of people on stretchers or delicate objects).

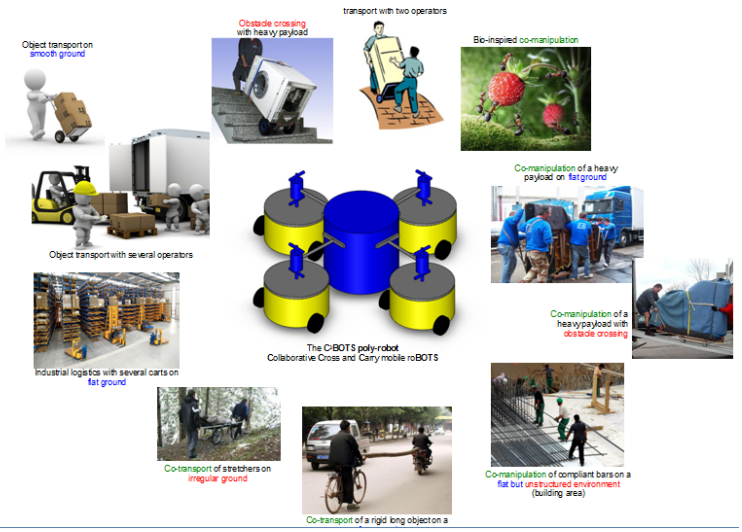

Fig. 1: Examples of "removal-man task" solved by one operator or several co-manipulating operators, on smooth grounds/slopes/obstacles, for standard or long payloads.

Acknowledgements

LabEx IMobS³ Innovative Mobility: Smart and Sustainable Solutions, the French National Centre for Scientific Research (CNRS), Auvergne Regional Council and the European funds of regional development (FEDER) are gratefully acknowledged. This work has been sponsored by the French government research program "Investissements d'avenir" through the RobotEx Equipment of Excellence (ANR-10-EQPX-44), by the European Union through the program Regional competitiveness and employment 2007 – 2013 (ERDF Auvergne Region), by French Institute for Advanced Mechanics and by the Auvergne Region.

CONTACTS

Jean-Christophe FAUROUX
Jean-Christophe.FAUROUX@ifma.fr
Lounis ADOUANE
Lounis.ADOUANE@univ-bpclermont.fr
Belhassen-Chedli BOUZGARROU
Belhassen-Chedli.BOUZGARROU@ifma.fr
Youcef MEZOUAR
Youcef.MEZOUAR@ifma.fr

FURTHER READING

[1] *Lifting mechanism for payload transport by collaborative mobile robots », in "New Trends in Mechanism and Machine Science*
B. Hichri et al., Springer, Mechanisms and Machine Science 34, 157, ISBN 978-3-319-09410-6

[2] *Cooperative lifting and transport by a group of mobile robots*
B. Hichri et al., Int. Symp. on Distributed Autnomous Robotic Systems, DARS 2014, Korea (14 p.)

[3] *Unité robotique de transport de charges longues*
J.C. Fauroux et al., PCT Patent, IFMA (2015)

CONTRACTS

ANR LabEx IMobS³ > Défi 1 > RobDyn > C³Bots
ANR RobotEx EQUIPEX

Invited Professor

Ioan DOROFTEI (Tech. Univ. Gh. Asachi, RO)

PhD/Post Doc

B. Hichri/M. Krid

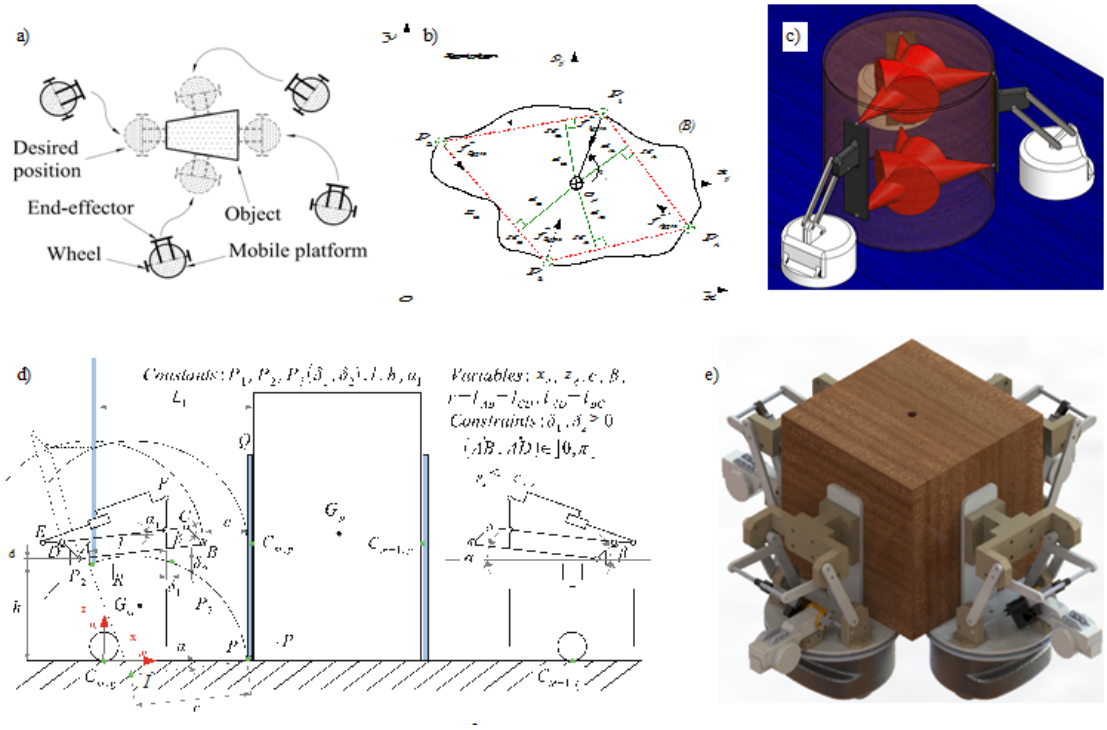

Fig. 2: The mono-robots C³Bots DGP surround the payload (a) to maximize the stability margin (b) and the Force Closure Grasping condition (c). A lifting parallelogram mechanism was designed to bring the payload on the mono-robot top platform (d). CAD view of four mono-robots carrying a box (e).

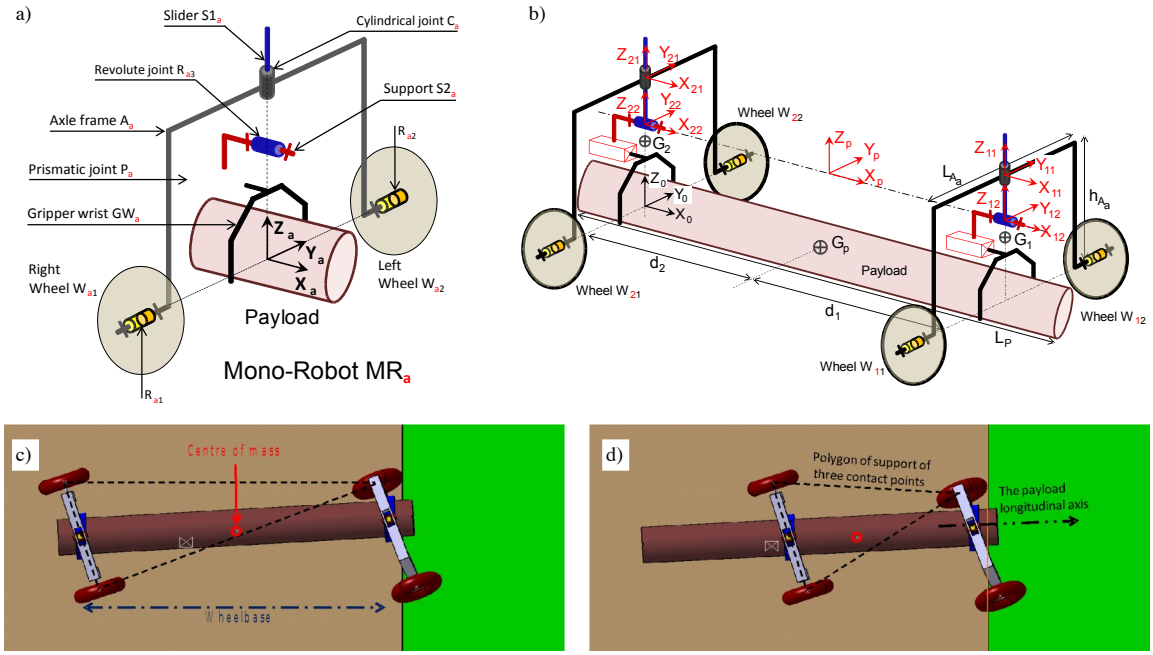

Fig. 3: a) The patented structure of a mono-robot C³Bots AT/VLP [3]. b) A poly-robot using two mono-robots transporting a long payload. c) Unstable configuration due to the centre of mass on the edge of the support triangle. d) Stability improvement thanks to the translation of the rear mono-robot along the payload longitudinal axis.

Scientific achievement #73

Detection of acetic acid using electrochemically modified electrodes based on metallophthalocyanines and porphyrins derivatives

Electroanalytical properties of macrocycles modified electrodes towards acetic acid detection were investigated by cyclic voltammetry. The modified electrodes are obtained by means of electrodeposition technique. The modified electrodes were analyzed by cyclic voltammetry and square wave voltammetry (SWV) and, additionally, deposited films are analyzed using Raman characterization technique. Under CV investigation, the sensors reveal one oxidation and reduction peaks which are shifted in the presence of acetic acid. These shifts are concomitant with an increase of the acetic acid concentration.

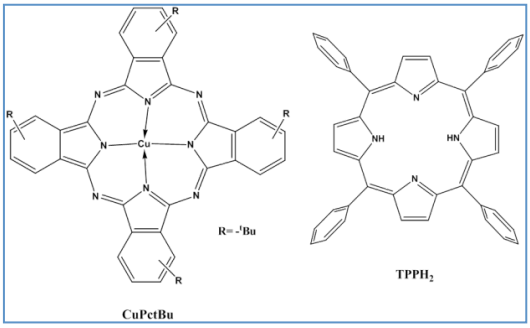

Fig. 1: Structure of the macrocycles investigated.

In the research of new methods for monitoring Volatile Fatty Acids (VFAs), biochemical approaches using electrochemical transduction are really challenging. The use of biosensors is mainly based on the grafting of enzymes or biomolecules able to induce a reaction with the VFAs or to produce significant changes attributed to the presence of VFAs. In literature, biosensors based on the modification of electrodes using enzyme have been reported. In contrast, sensors able to oxidize or reduce directly acetic acid have not been reported. Our strategy consist of developing chemically modified electrodes with sensing materials able to generate different electrochemical response in the presence of acetic acid. Keeping in mind this idea, we have focused our efforts on the development of modified electrodes for acetic acid detection. The modification is based on the use of macrocycles such as metallophthalocyanines (MPc) and porphyrines (Por) as sensing materials. These macrocycles are electron rich systems which offer interesting electronic features. Here we investigated a gold and carbon electrodes as substrates for the electrode modification. The electrochemical modifiers selected are the copper tetratertbutyl phthalocyanines (CuPctBu) and the metal-free tetraphenyl porphyrin (TPPH2) derivative which have been deposited by electrodeposition using Cyclic Voltammetry (CV). In a typical procedure of electrodeposition, the electrodes were immersed in solution containing PcH2-tBu (0.5 mM) material solution in CHCl3/ACN with tetrabutylammonium tetrafluoroborate TBAB (0.1M) and the deposition was carried out by scanning within a predefined potential window at a scan rate of 0.1V/s. The electrodes consist of a screen-printed electrodes (SPEs) elaborated according to the all-in-one configuration system i.e. working, counter and reference electrode on the same electrode support. The working electrodes (WE: 4mm in diameter) are made of carbon or gold while a carbon and gold counter electrode (CE), and a Ag pseudo-reference electrode (RE) complete the three-electrode configuration system. Raman spectroscopies have been used to characterize the coating on the modified electrodes. The coated electrodes present bands which are the superimposition of the electrode bands and CuPctBu or TPPH2 bands highlighting that the coating is effective. We have demonstrated the ability of these macrocycles-based modified electrodes to detect acetic acid by CV and Square Wave Voltammetry (SWV). Under CV investigation, the phthalocyanines and porphyrins reveal one oxidation and reduction peaks which are shifted in the presence of acetic acid. These shifts are concomitant with an increase of the acetic acid concentration. We observed a shift on the SWV potential peak upon increasing the acid concentration. The SWV results are concomitant with those observed in the acetic acid detection using CV. For $TPPH_2$, we have pointed out a Limit Of Detection (LOD) value between 39 and 44 mM at ca. 0.12V. Even if the detected concentrations are currently higher, if we compared them to others electrochemical sensors, these results open a new window on the utilization of macrocycles based material for acid acetic detection and later for VFA detection.

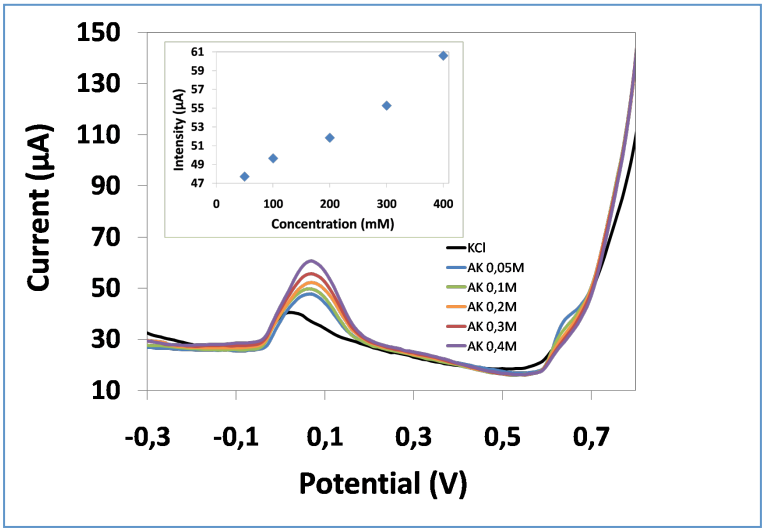

Fig. 2: SWV curves of Au SPE-$TPPH_2$ with addition of the acetic acid. Potential step=10mV; potential pulse=60mV; frequency=15Hz.

CONTACTS

Amadou NDIAYE
Amadou.NDIAYE@univ-bpclermont.fr
Alain PAULY
Alain.PAULY@univ-bpclermont.fr
GePEB
?.?@univ-bpclermont.fr
GePEB
?.?@univ-bpclermont.fr

FURTHER READING

Detection of acetic acid using electrochemically modified electrodes based on metallophthalocyanines and porphyrins derivatives
A.L. Ndiaye et al., submitted to Electrochimica Acta (under review) (2015)

Electrodes modification based on metal free phthalocyanine: example of electrochemical sensors for the detection of acetic acid
A.L. Ndiaye et al., submitted to Journal of Sensors (under review) (2015)

CONTRACTS

ANR LabEx IMobS3, Challenge 3, Action Bioenergy Production Processes (2012-2016)
Invited Professor M.L. Rodriguez-Mendez for VFAs detection issues

Post Doc

S. Delile, A. Ndiaye

Scientific achievement #74
Bioprocesses intensification with high frequency electromagnetic fields

The bi-compartmented experimental device was designed to evaluate the effects of high frequency, high intensity electromagnetic waves in eukaryotic cells (*Saccharomyces cerevisiae)*. Dielectric properties were measured during the cultivation and an electromagnetic simulation code allows the determination of the electromagnetic field inside the reactor. These simulations indicate that the shape of the reactor has a major influence on both attenuation of the electromagnetic waves in the culture medium and the orientation of the field. Tests performed in anechoic or reverberant environments did not show any significant intensification with respect to the production of ethanol.

The recent collective report on radiofrequencies (ANSES October 2013) stressed the need for experimental systems enabling a robust determination of the electromagnetic field impacting cellular cultures.

An exposure chamber designed around a Faraday cage to achieve an either anechoic or reverberant environment was used. A bi-compartmented was developed (Fig 1).

The measurements of two cultivation media dielectric properties from 0.5 to 2.4 GHz indicate that the medium generally behaves like an aqueous ionic solution. During the cultivation, substrates consumption (glucose, amino acids, and ammonium) and biomass and metabolites production (ethanol, acetate and glycerol) continuously modify the medium dielectric properties (decrease permittivity and increased conductivity). These changes are related to the production of metabolites and not to the presence of the yeasts themselves. These results are necessary to initialize realistic numerical simulations.

An electromagnetic computation code based on the moment's method was used to estimate the evolution of the electromagnetic field impacting the yeasts. The geometry, type and thickness of the secondary compartment materials have been investigated numerically in order to estimate the impact of the reactor's shape. Simulations conducted with plane waves and normal incidence indicates that only 30% (at 900MHz) and 18% (at 2.4 GHz) of the incident electromagnetic waves amplitude is effectively propagated inside the reactor. Mode Stirred Reverberant Chamber (MSRC) simulations reveal an electric field mostly oriented along the longest dimension of the reactor (vertical axis in Fig. 2 right). New numerical searches on the reactor's geometry could be investigated to overcome the situation.

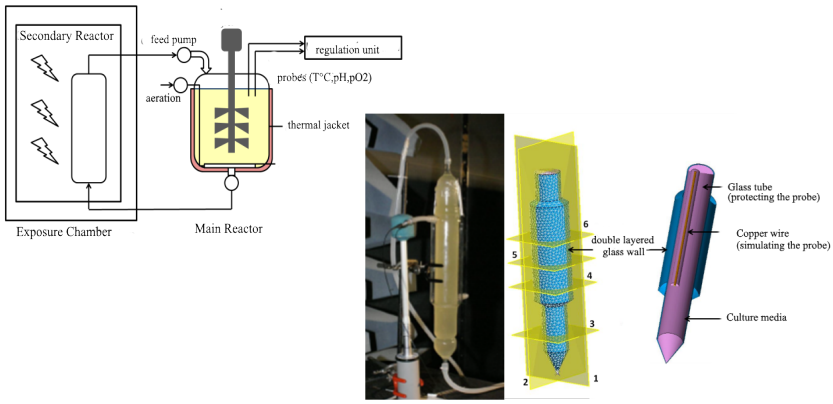

Fig. 1: (up left) Schematic overview of the experimental device. (bottom right) Photograph and mesh of the secondary reactor placed inside the exposure chamber.

To conclude, it is possible to meet the technical requirements necessary for bio-electromagnetism studies conducted in a liquid medium. It includes the production of a perfectly well defined electromagnetic field as well as the control of the yeasts environmental conditions despite the impossibility of introducing the regulatory elements directly into the exposition chamber. However it entails three major limitations: (i) the exposure time is limited in comparison to the total cultivation time (about 25%). (ii) The transmitted electromagnetic field intensity undergoes a significant loss with respect to the incident intensity (30% by plane wave at 900 MHz, less than 20% at 2.4 GHz). (iii) Due to the reactor's shape, the isotropy of the electromagnetic field within the reactor is lost.

To biological effects were observed in this study at frequencies ranging from 900MHz to 2.4 GHz with an emitted intensity at the antenna of approximately 170V.m-1. Whether it shall be associated with a protective effect of the liquid cultivation medium that significantly reduce the level of exposure or to the lack of interactions between the high frequency electromagnetic fields studied with the Saccharomyces cerevisiae metabolism remains an opened question.

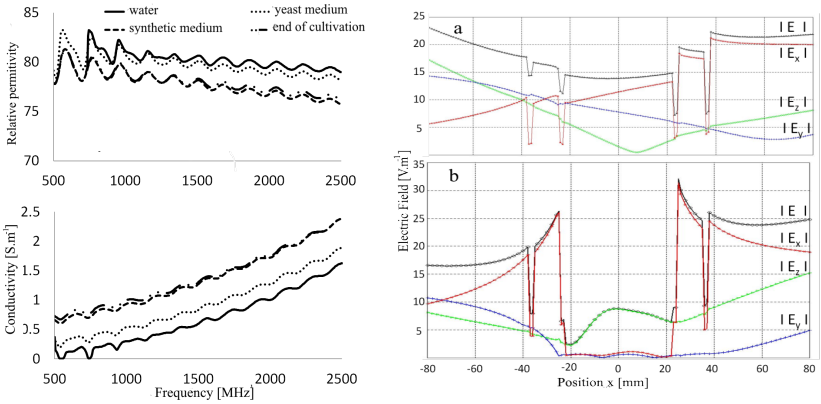

Fig. 2: (left) Culture medium relative permittivity and conductivity during the cultivation of Saccharomyces cerevisiae. (right) Cartesian decomposition of the simulated electric field in the secondary reactor at 900 MHz according to the main sectional plane z = 0. (a) Empty reactor, (b) reactor filled with the culture medium.

CONTACTS

Catherine CREULY
Catherine.CREULY@univ-bpclermont.fr
Agnès PONS
Agnes.PONS@univ-bpclermont.fr
David DUCHEZ
David.DUCHEZ@univ-bpclermont.fr
Christophe PASQUIER
Christophe.PASQUIER@univ-bpclermont.fr
Sébastien GIRARD
Sebastien.GIRARD@univ-bpclermont.fr

FURTHER READING

Design d'un bioréacteur permettant de suivre des cultures de microorganismes soumises à un champ électromagnétique
A. Pons et al., Récents Progrès en Génie des Procédés 104, Ed SFGP, Paris (2013)

Caractérisation d'un bioréacteur pour la culture de Saccharomyces cerevisiae soumis à des champs électromagnétiques en environnements anéchoïques et réverbérants
E. Bertrand et al., In Proceedings du 17ème Colloque International et Exposition sur la Compatibilité Electromagnétique, Clermont-Ferrand (2014)

CONTRACTS

ANR LabEx IMobS3, Challenge 3, Action BioEM (2012-2014)

Post Doc/Master 2

E. Bertrand/R. Zao, T. Zhang

Scientific achievement #75
The Aperiodic Fourier Modal Method for computing micro-organisms cross sections

In order to investigate the light scattering properties by arbitrary shaped particles we developed and implemented a new code based on the Fourier Modal Method equipped with Perfectly Matched Layers. The code was successfully validated by comparison with results from the literature.

Nowadays, our society is facing numerous ecological challenges. Cultivation of photosynthetic micro-organisms within controlled environments such as photobioreactor processes is recognized as a serious alternative to contribute to the CO_2 capture and to produce bio-diesel and bio-hydrogen.

In order to optimize conversion of light energy into chemical energy within the process of photosynthesis, we have to predict the light scattering properties, such as the absorption, scattering and extinction cross sections as well as the scattering diagrams.

Based on the rigorous solution of Maxwell's equations, Lord Rayleigh and Wait introduced respectively the first formalisms to describe the interaction of a monochromatic plane wave with an isolated infinitely long circular cylinder at normal incidence and oblique incidence. In 1908, Mie derived the exact solution for an homogeneous spherical particle for a very wide range of parameter values. This theory is involved in several applications e.g. in photobioreactor processes, in environmental monitoring and so on.

However, most micro-organisms are not spherical and differ by their size and shape parameters. Their scattering properties are significantly different from those of spherical scatterers.

Since it is much more difficult to obtain the exact solution when the scatterer loose the spherical symmetry, a number of approximations have been made in order to calculate the light scattering and absorption properties of non-spherical particles.

Among the most prevalent approximations are Waterman's extended boundary condition method also called T-matrix method, the finite-difference time-domain method and the finite-element method. Asano and Yamamoto obtained solutions for homogeneous prolate and oblate spheroidal particles by solving Maxwell's equations in the spheroidal coordinate system. The main disadvantage of this method is that the vector spheroidal wave functions are not easily calculated, especially for complex arguments that occur with absorbing particles. Nevertheless, a number of numerical results are available. Asano has calculated the scattering and absorption efficiencies and the angular scattering for oriented prolate and oblate spheroids. He obtained results for particles with size parameters up to 30 and axial ratios up to 5. Most of the results are for refractive index of 1,33 and of 1,5 although some calculations have been made for absorbing particles with complex refractive index of 1,5-i0,1.

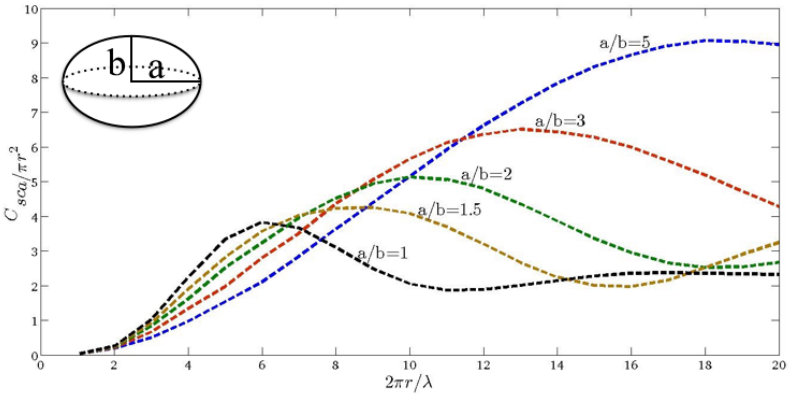

Fig. 1: Scattering cross sections of oblate spheroids normalized by the area πr^2 of the same volume as a function of the size parameter of the sphere $2\pi r/l$ for oblate spheroids with refractive index n=1.33 and a/b=1.5, 2, 3 and 5. Our results and those of Asano are indistinguishable.

Our goal is to develop a general although rigorous code for computing the optical properties of particles with arbitrary shapes and large aspect factor. It is our opinion that the Aperiodic Fourier Modal Method meets the above mentioned criteria. We have implemented a code based on this approach and our numerical results were successfully compared with those obtained by Asano (see Figure 1).

CONTACTS

Kofi EDEE
Kofi.EDEE@univ-bpclermont.fr
Gérard GRANET
Gerard.GRANET@univ-bpclermont.fr
Jean-François CORNET
J-Francois.CORNET@univ-bpclermont.fr
Jérémie DAUCHET
Jeremie.DAUCHET@univ-bpclermont.fr

FURTHER READING

Computation of spheroidal micro-organisms cross sections using the Aperiodic Fourier Modal Method
M. Abboud et al., PIERS Proceedings, Prague (2015)

CONTRACTS

ANR LabEx IMobS3, Challenge 3, Action Bioenergy Production Processes (2011-2020)

Post Doc

M. Abboud

Scientific achievement #76
Mechanical-probabilistic modeling of a compression test on food

The subject focused on the study of the influence of the (large) variability found in industrial food both in terms of geometry as mechanical characteristics. For this, two aspects were developed: one concerning the mechanical modeling (FEA) of a compression test, taking into account the damage to the sample and, secondly, the study of the sensitivity of the probabilistic model to uncertainties in the input data (geometrical and mechanical), the statistical characteristics will be estimated from the results of tests conducted during the work.

The subject, presented as part of the transversal action "probabilistic methods" combining GePEB and MMS axes of the Pascal Institute, focused on the study of the influence of the (large) variability found in industrial food both in terms of geometry as mechanical characteristics, application involving pet dry food (for cats). For this, two aspects were developed: one concerning the mechanical modeling (FEA) of a compression test on food croquettes, taking into account the damage to the sample and, secondly, the study of the sensitivity of the probabilistic model to uncertainties in the input data (geometrical and mechanical), the statistical characteristics will be estimated from the results of tests conducted during the work.

On the first point, we found that the application of conventional mechanical testing methods on an unusual material is not easy. Indeed, the test mechanisms are not adapted to the resistance and the sample size, and it was sometimes necessary to couple the results of two devices to be able to exploit them. It is the nature of the material that has conditioned the techniques used to characterize the random variables of the model input. It was thus possible to implement a method for rapid and accurate measurement by image analysis, tailored to the particle size and an inverse analysis method for non-directly measurable parameters.

The identification of parameters and croquettes behavior allows us to build a simulation model by finite elements, using the damageable elastic model of Mazars. The analyses showed that the model is not dependent on the mesh parameters, thanks the regularization with the cracking energy, and that the slenderness of the finite elements is great. The study focused on the stages of pre and post-neighborhood fracture but the behavior in large deformation of the kibble (in compression) seems to correspond to a viscoelastic behavior and could be included in a future study to use a realistic model to the complete crushing of the sample.

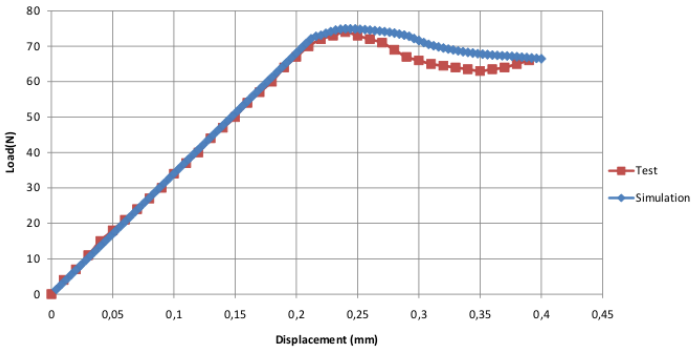

Fig. 1: Comparison between calculation and experiment.

The model was then used to implement stochastic analysis methods that, combined, allowed one hand to identify the respective influence of the input parameters, and also to characterize the variability of output parameters. The underlying laws and the associated parameters were identified by statistical tests. The application of the Morris method allowed for a qualitative analysis of the sensitivity of the model to these variables, that is to say to prioritize them according to their influence on the output variables of interest. The low cost in computation time of this method permits to select the most influential variables on the output of the model and then to implement more expensive methods. Identification of laws and parameters of the model output variables was performed through the application of the stochastic collocation method. The estimation of the response surface model thus created was used as an analytical model for Monte-Carlo simulations to determine the distributions of the output variables.

To highlight the many opportunities offered by stochastic methods, surface response calculated by collocation has also been used as an analytical model for the calculation of Sobol indices.

These indices are used to quantify, for each input variable, the variability from one output variable due to him. The combination of these methods also highlight the complementarity of the methods used, as Sobol indices cannot be used without analytical model: calculation time would be prohibitive. Finally, because the value of the Sobol first order index corresponds to the individual contribution of each of the input variables, it was possible to compare the results with those obtained by the Morris method. This helped to clearly identify and quantify the variables affecting the compression behavior.

A paper is currently being finalized: "Analysis of the variability of food texture properties: application to dry pet food."

CONTACTS

Philippe BRESSOLETTE
Philippe.BRESSOLETTE@univ-bpclermont.fr
Christophe VIAL
Christophe.VIAL@univ-bpclermont.fr

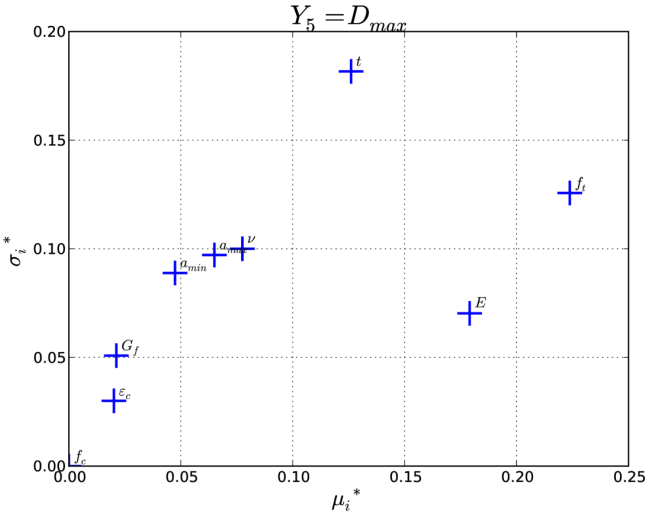

Fig. 2: Results of the Morris method for each control variable.

Scientific achievement #77
Electromagnetic compatibility integrity of cables in complex stochastic environments

Quantifying the effects of uncertainties on the behavior electronic systems becomes nowadays of paramount importance in regards to electromagnetic compatibility (EMC) standards and this field of research has gained a growing interest over the past few years. Knowledge and use of the most efficient techniques of uncertainty propagation is often of practical importance for the analysis and design of systems in the EMC framework. A series of explorative works is being conducted in order to apply the most efficient stochastic methods to reliability assessment and sensitivity analysis of EMC problems under uncertainty.

Cables in modern electronic systems such as aircraft or vehicles are used to transmit both power and signals. For practical reasons of space limitation, such cables generally consist of a large number of electrical lines grouped into strands. Electromagnetic fields in the confined spaces result in interactions between lines, which induce noise signals in adjacent channels. The resulting crosstalk issues may cause dramatic damages on circuits located at line ends. Quantifying electromagnetic interferences (EMI) is therefore a major challenge in electromagnetic compatibility (EMC) of electronic systems.

Several models are available for the analysis of embedded electronic systems threatened by electromagnetic interferences, including high accuracy efficient numerical techniques. The proper functioning of such systems is however prone to uncertainties that may arise at several levels: polarization and angles of incidence of EM waves, system configuration such as placement of electronic devices and routing of cables (lengths, positions and clearance above ground plane), material electric parameters, magnitudes drift over time, pure absence of knowledge,... These uncertainties may seriously impact the performances of the developed systems (loss of information, overcurrents,...). Quantifying how these uncertainties propagate through simulation models and how much they impact a given output or several ones (also known as observables) is of practical importance in EMC of electronic systems.

The ongoing research works carried out in collaboration between PHOTON and MMS aim at exploring the most efficient and available methods to use for the analysis of electronic systems in an EMC uncertain framework. These works are benefitting from the experience gained by the MMS research group in the field of structural reliability. Several objectives are pursued, such as the quantification of the statistics of an output of a model, the assessment of the probability of rare failure event or the sensitivity analysis of a model with random inputs. Polynomial chaos expansions have been explored for evaluating the statistics of EMC problems under the assumptions of smooth physical models and low stochastic dimensionality. Reliability assessment of cables with uncertainties has also been investigated either based on analytically-defined or numerical EMC models. The probability that a current in a given component exceeds a prescribed level (e.g. requirements imposed by governmental or regulatory agencies) is assessed.

Several techniques developed in structural reliability have been applied, such as the FORM and SORM approximation methods and an efficicient variant of the Monte Carlo method known as subset simulation.

Sensitivity analysis, either global or local at failure has been applied in order to quantify the most influential inputs and their respective roles on the output of interest or the system failure. These sensitivities have been interpreted in light of physical interpretations of the system behaviors.

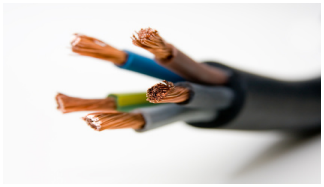

Fig. 1: Cable with electric lines grouped in five strands.

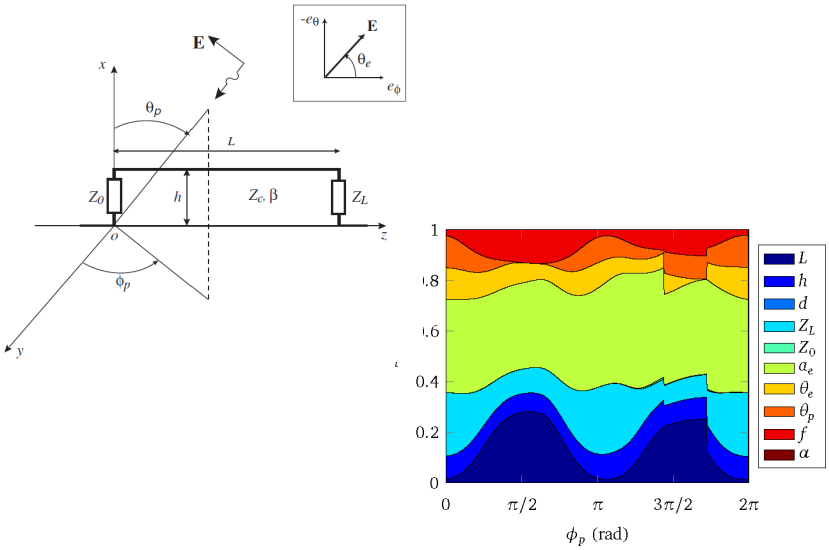

Fig. 2: Reliability assessment of a transmission line above a ground plane illuminated by a linearly polarized plane wave with an incidence angle Φ_p (10 random input parameters) - Relative probabilistic importance measures vs. Φ_p.

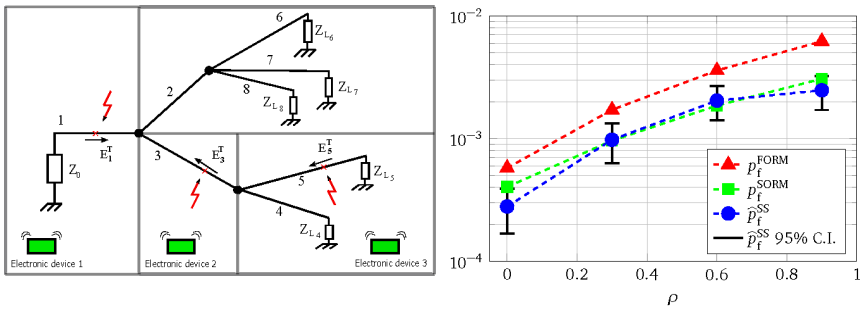

Fig. 3: Reliability assessment of a transmission line network with 3 localized shielding effectiveness deficiencies (failure due to a current in Z_{L8} impedance above a prescribed level) - Failure probability estimates vs. correlation between amplitudes of tangential EM fields E_1^T and E_3^T.

CONTACTS

Michel FOGLI
Michel.FOGLI@univ-bpclermont.fr
Jean-Marc BOURINET
jean-marc.bourinet@ifma.fr
Pierre BONNET
Pierre.BONNET@univ-bpclermont.fr
Sébastien LALLECHERE
Sebastien.LALLECHERE@univ-bpclermont.fr

FURTHER READING

Safety assessment of a transmission line with EMC requirements
A. Kouassi et al., URSI GASS XXXIth, Beijing (2014)

Fiabilité de fonctionnement et sensibilité CEM pour un problème de transmission
A. Kouassi et al., In Proceedings du 17ème Colloque International et Exposition sur la Compatibilité Electromagnétique, Clermont-Ferrand (2014)

Uncertainty assessment of a coaxial line's capacitance in a stochastic context
A. Kouassi et al., ICEAA 2015, Int. Conf. on Electromagnetics in Advanced Applications, Turin (2015)

PhD

A. Kouassi

Scientific achievement #78
Reliability-based optimization of energy performance of buildings

The performance of building insulations depends on the material properties and thickness, on one hand, and on the efficiency of heating and cooling systems, on the other hand. However, the performance is subjected to various types of uncertainties related to material conductivity, insulation geometry, climate predictions, workmanship errors and occupant profiles. In practice, these uncertainties affect the insulation system and leads to unexpected additional costs. The developed research activities aims at considering the uncertainties related to the materials, climate changes and occupant behavior. A new formulation of the total energy cost is provided and applied to design optimization under reliability constraints, in order to allow for better retrofitting decisions.

The improvement of the energy performance of buildings is nowadays of main concern as the building sector represents around 40% of the total primary energy consumption in Europe. Thermal insulation is known as the most effective way of building energy conservation for cooling and heating, by reducing the rate of heat transfer through the building envelope. However, the energy performance is subjected to large uncertainties related to material properties, climate changes and human activities in retrofitting and in use conditions. Moreover, it is approved that there are large uncertainties associated with the future performance of buildings due to changes in regional- and local-scale climatic impact.

The developed methodology aims at taking into account the uncertainties in the energy performance model. These uncertainties are modeled by probabilistic distributions for material and geometrical properties, and by stochastic processes for climate scenarios and occupant behavior. The uncertainties related to the degradation of insulation materials are also taken into account through the development of a probabilistic aging model, where the climate-induced cumulated humidity increases the insulation conductivity. In addition to uncertainties related to model input data, the developed methodology considers environmental and social criteria corresponding to the owner and regulation requirements.

Although the designer interest is mainly focused on insulation and energy costs, many other environmental and social factors have significant impact on retrofitting decisions. For this reason, we have developed a new cost formulation that considers indirect costs related to insulation; the proposed cost formulation is given as:

$$C_{tot} = C_{inv} + C_{ad} + C_{enr} + C_{mat} + C_{Laying} + C_{comfort} + C_{CO_2} + C_{surf}$$

where C_{inv} is the insulation material cost, C_{ad} is the implementation cost, C_{enr} is the energy cost for cooling and heating, C_{mat} is the cost of construction materials, C_{Laying} is the construction cost, $C_{comfort}$ is the comfort induced cost defined by the additional energy to recover the setpoint comfort temperature, C_{CO2} is the pollution consequence in terms of carbon tax, and C_{surf} is the cost of the lost indoor surface.

The optimal design parameters are then obtained by solving the reliability-based optimization problem, where the expected total costs is minimized under reliability constraints:

$$under \begin{cases} P_f(d,X) \le P_f^T \\ g(d) \ge 0 \end{cases}$$

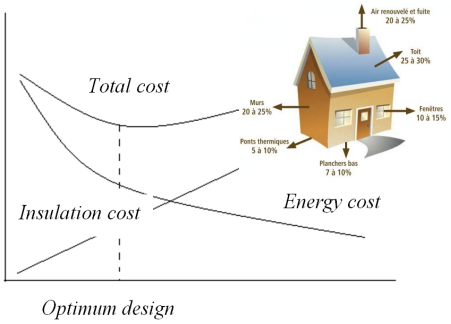

Fig. 2: Optimal cost components considering uncertainties.

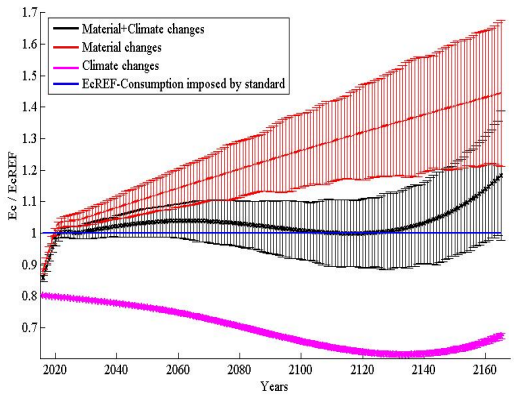

Fig. 3: Expected and confidenc intervals of energy consumpti according to uncertainty considerations.

where C_{tot} is the total cost of the wall insulation, d is the vector of design variables, X is the vector of random variables, $P_f(d,X)$ is the failure probability of the insulation, P_f^T is the admissible failure probability, which describes the acceptance level of the designer regarding the non-conformity regarding energy performance and g(d) is the vector of deterministic geometrical and material constraints. Including a reliability constraint enables the control of the search domain of the design parameters. This is done by comparing the annual failure probabilities obtained all over the lifetime to the admissible failure probability P_f^T imposed by the designer. This constraint brings out the parameters that ensure the reliability desired by the designer despite the variations and uncertainties related to environmental, energetic and social factors affected by the insulation.

The obtained results show the high impact of materials and climate uncertainties, as well as the proposed cost formulation, on the optimal retrofitting decisions. The consideration of insulation degradation shows that the performance becomes sensitive to climate prediction uncertainties when high performance insulation materials are applied. Ongoing works are actually focused on occupant's behavior through the development of multi-agent models based on Markov stochastic processes.

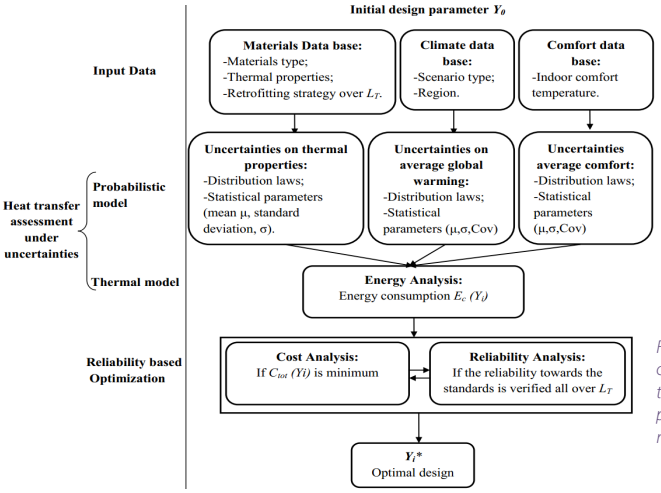

Fig. 1: Propagation of uncertainties in the energy performance model.

CONTACTS

Alaa CHATEAUNEUF
Alaa.CHATEAUNEUF@univ-bpclermont.fr
Jean-Pierre FONTAINE
j-pierre.fontaine@univ-bpclermont.fr

FURTHER READING

Cost model for optimum thicknesses of insulated walls considering indirect impacts and uncertainties
A. Aïssani et al., Energy and Buildings 84, 21 (2014)

Reliability-based design optimization of insulation systems considering climate change and workmanship
A. Aïssani et al., ICASP12, Vancouver (2015)

Impact of the different life cycle cost models on design decisions for insulation
A. Aïssani et al., ESReDA, Reliability Assessment and Life Cycle Analysis of Structures and Infrastructures, Turin (2014)

PhD

A. Aïssani, W. Belazi

Scientific achievement #79
A coupled model for a hydrogel diffraction grating used in pH-sensing

pH-sensitive hydrogels are networks of polymers that can imbibe a solution and swell. They are used in many smart engineering devices. One of such applications is a diffractometric biochemical sensor. This sensor is composed of a hydrogel grating fixed on a hard substrate that can swell due to pH changes. The aim of the present study is to develop a numerical model of such a bi-material device to measure pH value of a solution.

A new diffractometric biochemical sensing device using smart hydrogels has recently been reported. It is based on a hydrogel reflective diffraction grating on a hard substrate which can be used for a precise measuring of pH. The aim of our work is to propose a coupled mechanical and photonic model of such a smart device, based on recent advances in mechanical modeling of hydrogels. A pH sensitive hydrogel grating is a functional part of the sensor. This grating is situated on a hard substrate and can swell or shrink as pH changes. The hydrogel is characterized by a free-energy function taking into account the stretching of the network, mixing the solvent with the network, mixing ions with the solvent, and dissociation of the acidic groups. First, an analysis is performed of the hydrogel grating's deformation as a function of the pH. Also, we provide a comparison between the numerical model and experimental measurements of the real system from the literature. Then, we determine the photonic properties of the studied system and analyze the diffraction intensities for different hydrogel grating deformations. Finally, we show how the reflected beam measurement can be related to the measured pH value using the developed model of the mechanical and photonic response of the smart hydrogel grating.

Let us explain briefly how such a smart device can be used for pH-detection. The hydrogel grating with its changing height acts as an optical element. This periodic structure transforms the incident beam into reflected and several diffracted beams.

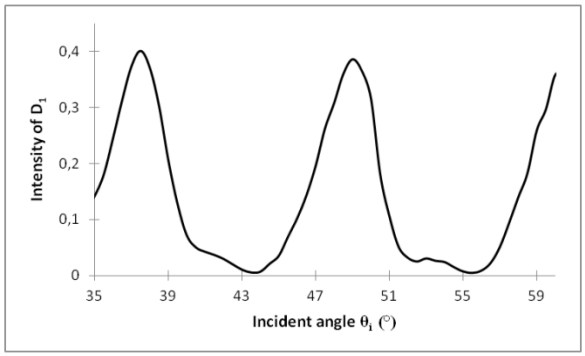

Fig. 3: Plot of (D1) intensity measurements for different values of incident angle θi.

The reflected beam measurements can be analyzed to measure the corresponding pH value. When an incident light beam is applied on the diffraction grating with different incident angles, for each incident angle, the diffracted intensity (D_1) is measured (see e.g. Figure 3). In the presented exemple, the period of oscillation of the reflected beam intensity (D_1), measured between two minimum, is equal to 12°. According to our calculations, this corresponds to a grating height change of 3.6 µm, and the solution pH value is determined as pH=5.

CONTACTS

Yuri LAPUSTA
Yuri.Lapusta@ifma.fr

FURTHER READING

Modeling of a hydrogel diffraction grating used fo pH-sensing
M. Marchant et al., Comptes Rendus Mécanique 342(12), 706 (2014)

CONTRACTS

LabEx IMobS3

PhD

M. Marchant

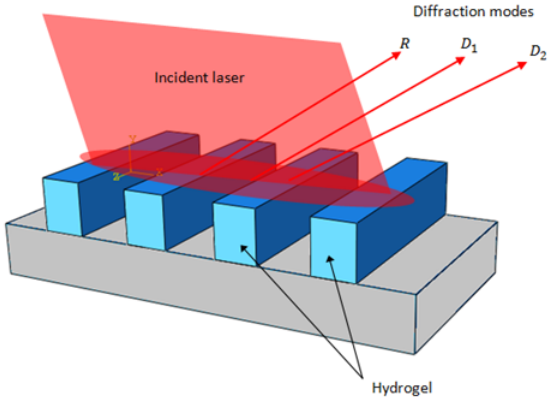

Fig. 1: A hydrogel diffraction grating used for pH-sensing.

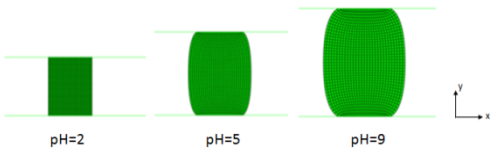

Fig. 2: Each hydrogel stripe swells with increasing pH and changes the optical response of the system.

Scientific achievement #80
Modeling of active piezoelectric composite structures with cracks

In this work, a smart system composed of an aluminum beam with two macro-fiber composites (MFC) patches used in detecting and suppressing of undesired vibrations is analyzed. The influence of defects like cracks is studied. First, a model for a system without cracks is developed. Then, a crack is introduced between MFC and the aluminum beam, and the influence of this crack on the amplitude of beam is studied. Also, a model for a crack in a fixed part of the beam is developed.

Piezoelectric materials have the capability to serve in both sensors and actuators. That's why these materials are used in different feedback control systems. High performance, flexibility and durability are some major properties of the piezoelectric macro-fiber composite (MFC) sensors and actuators. These devices, able to couple efficiently electrical and mechanical fields, can find interesting applications in e.g. robotics, mobility and aircraft industry. One of the important tasks is detection and suppressing of undesired vibrations. Applications of active piezoelectric devices in this field of intelligent control are numerous. For example, in the industry of mobility, many robots use two link flexible arms. One arm can move slowly, the other arm can move faster. As a result, an undesired vibration of the system can be produced. Similar undesired and even excessive vibrations can occur in aeronautics applications caused by specific combinations of the air flux and the parameters of the flying system, or in sport due to the impacts (for example, during the tennis racquet and ball interaction). These effects and vibrations can affect negatively the performance of the whole system, and therefore, they have to be detected and suppressed using some devices of smart control. Note that the performance of such smart systems depends on the state and integrity of their constituents and interfaces between them. Therefore, accounting for the existence of defects and possible appearance of cracks is very important in such applications in order to assure a correct functioning of the whole system.

In this work, an intelligent system consisting of an aluminum beam with two patches "macro-fiber composite" (MFC) based on piezoelectric materials (Fig. 1) is analyzed. The influence of defects and cracks is studied.

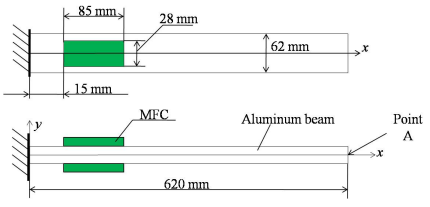

Fig. 1: Schematic of aluminum beam controlled by two MFC patches.

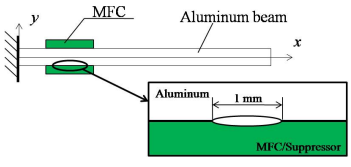

Fig. 3: Studied system with a crack.

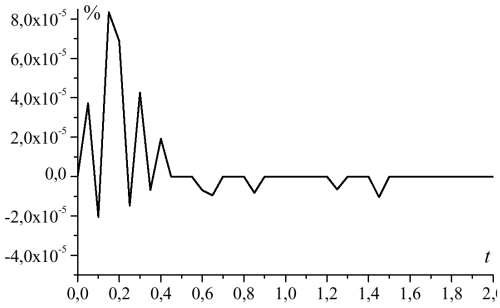

Fig. 4: Amplitude difference in point A for a system with and without interface crack.

First, a crack is introduced between the MFC and the aluminum beam and the influence of the crack on the amplitude of the beam is studied. Also, the effects of a crack in a fixed part of the beam on the system performance were analyzed.

Let us explain briefly how such a smart device, controlled by two MFC patches, acts. The MFC actuators consist of polyamide films with electrodes that are glued on the top and bottom of piezoelectric fibers (Fig. 2). The electric field required to activate the piezoelectric effect in the fibers is created by the electrodes. The system of electrodes can be like a periodic structure of positive and negative conducting plates, and like a completely positive and completely negative plates. The shape of piezoceramic fiber also can be different. The response of the fibers creates displacements of the free end of the controlled structure which is, in our case, a rectangular aluminum beam.

Two MFC patches are glued to the top and the bottom of the beam. The latter can move (bend) under electric stimuli. One of MFC detects an undesired movement or vibration of the beam, and the other one suppresses it. In the modelling, the polyamide film outside the active region and the epoxy bond between the MFC actuator and aluminum beam were ignored. The beam is fixed only at the left end. A finite element model of the system was developed using ABAQUS software. The aluminum beam is modeled as a plate. A 4-node bilinear plane strain elements was used. MCFs are modeled like piezoelectric plates, and 8-node linear piezoelectric elements were used. We applied the boundary conditions corresponding to the experimental conditions by restraining the left nodes of the beam in the model from movements in all directions. First, the beam was excited using MCF attached on it. The vertical displacement of the point A at the end of the aluminum beam was calculated and compared to experimental results from Kovalovs et al. (2007) for a system without cracks. We observe that the amplitude of vertical displacement of the beam decreases when the voltage increases like in experiment and note that the FEM results are slightly smaller than experiment results for the studied system without cracks. Then, a system with a crack, which represents a gluing defect at the interface between the MCF and the beam, was analyzed, as presented in Fig. 3. The difference of the amplitude at the point A for MFC with crack and without crack is presented on Fig. 4.

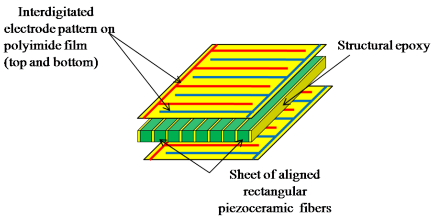

Fig. 2: MFC structure consisting of electrodes, piezoelectric fibers and epoxy.

CONTACTS

Yuri LAPUSTA
Yuri.Lapusta@ifma.fr

FURTHER READING

Modeling of active piezoelectric composite structures with cracks
O. Viun et al., Research in Mechanics of Composites, Paderborn, Germany (2013)

CONTRACTS

LabEx IMobS3

PhD

O. Viun

Scientific achievement #81
Shape-from-Template (SfT)

Shape-from-Template is a single-image 3D reconstruction technique. It uses a visual memory represented by templates containing prior knowledge on the objects to be reconstructed. Shape-from-Template is specific to textured objects whose shape cannot be statistically learnt. It first detects the objects visible in the image by registration and then infer their 3D shape by geometric reasoning. Shape-from-Template has a strong potential for applications in augmented reality and human-computer interaction. ALCoV pioneered Shape-from-Template, and matured the case of objects undergoing isometric deformations, such as a piece of paper or cloth.

The 3D reconstruction problem is to resolve the 3D shape of the observed environment from images. The main difficulty arises from the fact that the environment's 3D shape is 'flattened' when the 2D images are formed by a camera. The first type of approach to 3D reconstruction is Shape-from-Motion, which uses multiple images. It is very mature and successful but makes a fundamental limiting assumption which is that the observed environment is rigid. The world is however made of objects which move and undergo deformations rather than remaining rigid. The second type of approach to 3D reconstruction exploits visual cues extracted from a single image. An example is shading, which establishes the relationship between the environment's light sources, shape and the input image and leads to the Shape-from-Shading technique. Single-image reconstruction from visual cues is tremendously difficult and generally requires unrealistic assumptions which hinder its applicability to real-world problems.

Shape-from-Template is a new type of technique which achieves 3D reconstruction from a single image using a visual memory, as shown in figure 1. The latter is represented by a set of object templates containing prior information, including the objects' appearance represented by texture-map images. Similarly to the human visual system, Shape-from-Template relates image observations to past experience and prior knowledge on the objects' characteristics such as shape and color. It is thus also related to object detection. Shape-from-Template is specific to objects whose appearance is matchable and whose shape space cannot be learnt statistically but may be modeled physically. Technically, Shape-from-Template has two internal steps: 1) registration and 2) inference. In the first step, the input image is tentatively matched to the texture-map from the object template. The outcome of matching indicates if the object may be present in the image. Registration is a difficult problem, as the object may be deformed and partly occluded, and may be visible at very different scales. Existing tools such as the fundamental matrix and homographies break down because of deformations. We have proposed to use local consistency of the motion field to solve registration automatically. In the second step of Shape-from-Template, the registration is used to infer 3D shape. This is a complicated nonlinear problem. The early approaches tried to solve for the global surface in a single step by approximating the constraints. In contrast, we recently proposed a local approach, based on the theory of non-holonomic solutions of partial differential equations. These solutions are very fast to compute and do not require one to approximate the problem's constraints.

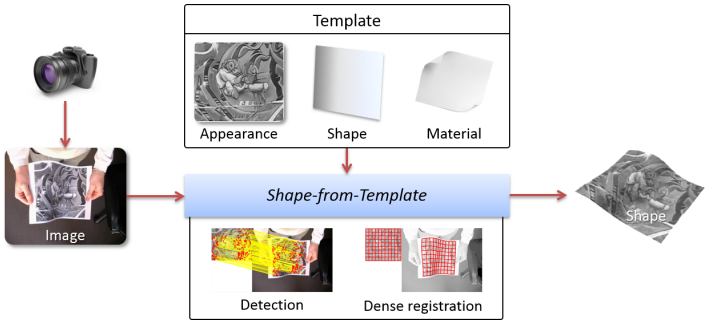

Fig. 1: Shape-from-Template, under the hood. The template represents the visual memory, containing object specific prior knowledge. In this example, the template contains the object's appearance, shape and material. The latter constrains the object's deformation space. The 3D shape is reconstructed automatically from a single input image.

Shape-from-Template and the concept of using a visual memory and geometric constraints to aid 3D reconstruction has emerged over the past decade thanks to the work of mostly two research groups, including ALCoV.

Shape-from-Template has matured in several respects, essentially for thin-shell objects which deform isometrically, such as a piece of paper or cloth, as illustrated in figure 2. This is important as many real-world objects are rigid or deform almost isometrically. Much is however left to do for non-isometric objects and to integrate Shape-from-Template more deeply with object recognition.

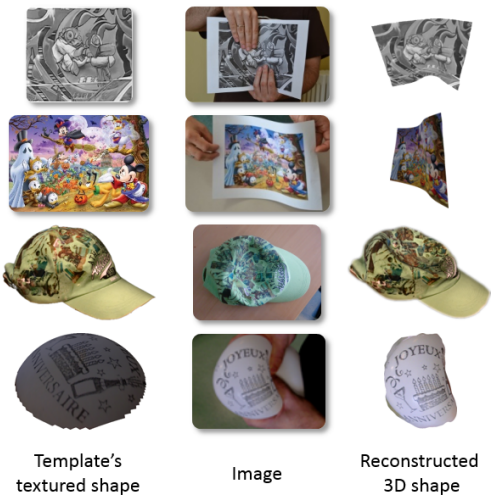

Fig. 2: Shape-from-Template in action. Four examples showing Shape-from-Template applied to different types of objects and materials. For all four examples the reconstruction error with respect to ground-truth was around a few millimeters.

CONTACTS

Adrien BARTOLI
Adrien.Bartoli@udamail.fr

FURTHER READING

Shape-from-Template
A. Bartoli et al., IEEE Transactions on Pattern Analysis and Machine Intelligence (2015)

Monocular Template-Based 3D Surface Reconstruction: Convex Inextensible and Nonconvex Isometric Methods
F. Brunet, A. Bartoli and R. Hartley, Computer Vision and Image Understanding, 125:138-154 (2014)

Feature-Based Deformable Surface Detection with Self-Occlusion Reasoning
D. Pizarro and A. Bartoli, International Journal of Computer Vision, 97(1):54-70 (2012)

CONTRACTS

ERC Starting Consolidator Grant FLEXABLE (2013-2017)

Scientific achievement #82
Seeing in 3D in monocular laparoscopy

Almost all laparoscopes in use are monocular. This means that the surgeon sees the patient's abdominal cavity on a standard 2D monitor and cannot exploit their full 3D vision capabilities. Existing solutions to 3D laparoscopy change the hardware by adding a second sensor, capturing a second viewpoint. They are costly and do not allow one to implement new view synthesis. We have proposed a dedicated Shape-from-Shading method as a pure software solution to 3D laparoscopy. Our method runs in realtime and produces quality reconstructions in challenging conditions. It is compatible with all existing monocular laparoscopes.

Laparoscopy is a minimally invasive surgery technique which consists in introducing an optics fiber and surgical instruments through small incisions in the patient's abdomen. The optics fiber is directly connected to a camera, allowing the surgeon to see the patient's abdominal cavity. Laparoscopy has many advantages over open surgery but also some limitations. One of these limitations is the absence of 3D vision, which is important when the surgeon has to precisely locate the tip of an instrument in the working space for suturing, for instance. The problem of 3D laparoscopy has two main types of approach. The first one is to change the hardware to stereo laparoscopes. Technically they may be made by using two cameras or two optics fibers. The two images can then be directly displayed to the surgeon's eyes, as in the Da Vinci robot. An obvious drawback is its cost. The second type of approach is based on reconstructing the missing third dimension by software using computer vision and rendering two images from the reconstructed 3D model which will be displayed to the surgeon's eyes. This solution does not require one to change the existing hardware but is much more complex to achieve. However, if effective, it has a clear advantage. In the hardware solution, the laparoscope-computer system does not compute 3D, as it simply carries two images to the surgeon's eyes, and 3D is then inferred by the surgeon's brain as if they were observing the surgical site directly. This means that the amount of processing which can be done is quite limited. In the software solution however, the computer reconstructs 3D, and may thus do processing such as new-view synthesis in a very simple manner. It can also synthesize images which will fits the surgeon's sight perfectly.

We have proposed a software system which performs 3D reconstruction in realtime from the laparoscope's video stream. This is a tremendously difficult problem, as the observed environment is highly deformable and may be subject to occlusions, blur, smoke and bleeding, as figure 1 illustrates.

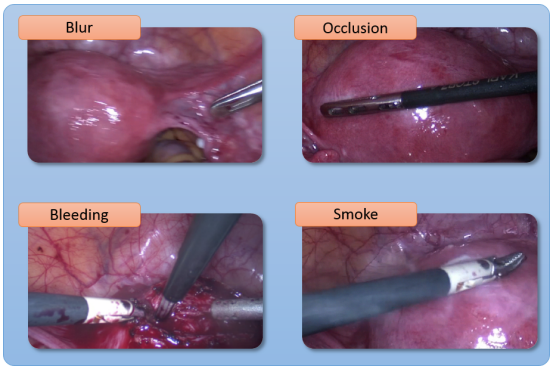

Fig. 1: These images from a laparoscopic surgery of the uterus show how applying computer vision may be tremendously difficult.

Our system's strength is that each image of the video stream is processed independently. It uses shading as the main visual cue. This basically relies on the relationship modeling the interaction between the light, the surface and the camera. Laparoscopy is a very well-adapted setup to using shading. The main reason is that the light source is fixed with respect to the optics fiber's tip. Therefore, their relative position, as well as the light's characteristics can be precalibrated. We have proposed a new non-parametric light model which captures, for each voxel in the working space, the amount of incoming light. This is tremendously important, as Shape-from-Shading tends to yield convex-concave shape ambiguities. With our light model, we can exploit light fall off, the property that voxels placed further away from the laparoscope's tip receive less light. Modeling light fall off increases accuracy compared to previous algorithms but also resolves most of the usual ambiguities.

Figure 2 illustrates the type of reconstruction we obtain and the system in use with 3D visualization glasses. Our system was implemented to run at 25-30 frames-per-seconds on a GPU for high definition laparoscopes. This work received the best paper award at the 2012 IPCAI conference.

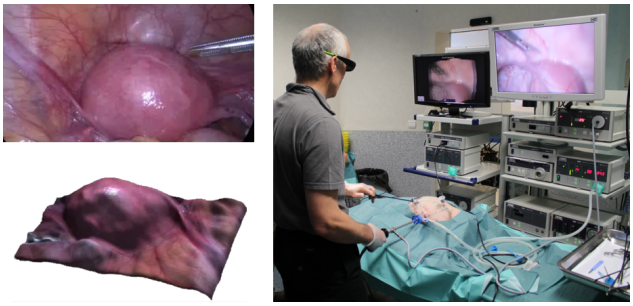

Fig. 2: The proposed system upgrades a monocular laparoscope to enable full 3D visualization in realtime. The example of input image shown top left is reconstructed to give the 3D surface shown bottom left. In our working system shown right during testing with porcine surgery, the 3D surface is used to render two images displayed directly to the surgeon's eyes using a 3D screen.

CONTACTS

Adrien BARTOLI
Adrien.Bartoli@udamail.fr
Toby COLLINS
Toby.Collins@gmail.com

FURTHER READING

Computer Assisted Minimally Invasive Surgery: Is Medical Computer Vision the Answer to Improving Laparosurgery?
A. Bartoli, T. Collins et al.,
Medical Hypotheses, 79(6):858-863 (2012)

3D Reconstruction in Laparoscopy with Close-Range Photometric Stereo
T. Collins and A. Bartoli
MICCAI - International Conference on Medical Image Computing and Computer Assisted Intervention, Nice, France (October 2012)

Towards Live Monocular 3D Laparoscopy using Shading and Specularity Information
T. Collins and A. Bartoli
IPCAI - International Conference on Information Processing in Computer-Assisted Interventions, Pisa, Italy (June 2012)

Scientific achievement #83
Computer-Aided Uterine Laparosurgery with Augmented Reality

An important and growing research topic in medical imaging is to develop surgical guidance systems in laparoscopic Minimally Invasive Surgery (MIS) with Augmented Reality (AR). This involves registering data from another modality and fusing it with the laparoscopic video. The main open challenge is registering the modalities automatically, robustly and in realtime. We have lead the field in developing methods for fully-automatic realtime AR in uterine laparoscopic MIS, and published papers for solving the main sub-problems, including segmentation, registration and tracking. Many of the ideas extend to AR for other organs, so have a broader impact beyond uterine surgery.

We illustrate our AR system applied to assisted myoma localization in figure 1. The system fuses data from a pre-operative MRI and works as follows. First the MRI is segmented, to give 3D models of the uterus and the myomas. This process is done before surgery, and therefore does not need to be realtime. During surgery, our system determines the deformable 3D transform that maps the uterus and the myomas to the laparoscope's 3D coordinate frame. Once the transform is determined, the 3D myoma models are transformed to the laparoscope's coordinate frame and then rendered using the laparoscope's camera projection function. Finally the render is fused with the real laparoscopic image, to show the myoma positions. In [1] we presented a robust, semi-automatic solution to the registration problem. In [2] we developed methods to make it fully-automatic. In relation to previous works, our work is the first to register an organ between an MIS videos and a 3D pre-operative image in realtime and without needing any manual input by the surgeons.

The registration problem is difficult and ill-posed when using a single laparoscopic image. In [1] we showed that accurate solutions can be obtained by decomposing the problem into an initial registration (done once) and an update registration (done at every subsequent frame. Because the initial registration is done just once, only the update registration needs to be realtime. The decomposition exploits the fact that during intervention the uterus moves quasi-rigidly (until resection begins). Therefore the update registration is approximately rigid. We solve it at approximately 27fps on standard workstation hardware.

Our core idea for solving the initial registration was to use multiple laparoscopic keyframe images simultaneously. We achieved this using rigid Structure from Motion (SfM) to give 3D registration constraints, which significantly improved tractability. The reconstruction also aligned the keyframe images in 3D space, which meant we could constrain the problem using occluding contours in all keyframe images, see figure 2.

Fig. 3: Example images from the test dataset and segmentations from [2]. The segmented uterus is highlighted in green. Two failure modes are presented in the right-most images. The first is when a surgical tool fully bisects the uterus and the second is when most of the uterus is occluded by the laparoscope's optical ring.

By combining 3D and occluding contour constraints from multiple images, the problem could be solved accurately and quickly (usually taking less than 10 seconds).

In [2] we presented a method to automatically detect and segment the uterus in laparoscopic images completely automatically. Our main idea was to use a trained patient-independent uterus detector to roughly localize the uterus, which was then used as a supervisor to train a patient-specific organ segmenter. The segmenter used a physically-motivated organ boundary model designed specifically for illumination in laparoscopy, which was fast to compute and gave strong segmentation constraints. Segmentation was solved globally with a lightweight conditional random field with a single graphcut. On a dataset of 220 images our method obtained a mean DICE score of 92.9%, and took approximately one second on a standard desktop PC (without GPU optimization).

We have also researched other techniques for 3D reconstruction of organs in laparoscopic image using active and stereo sensors [3]. The goal of this work was to survey all potential techniques and quantifiably evaluate them in real clinical conditions.

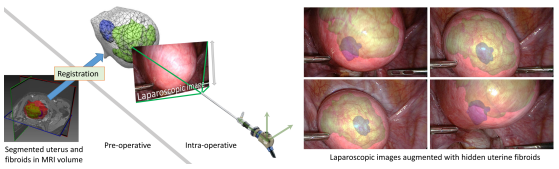

Fig. 1: Our AR-based laparoscopic surgical guidance system for assisted localization of hidden myomas.

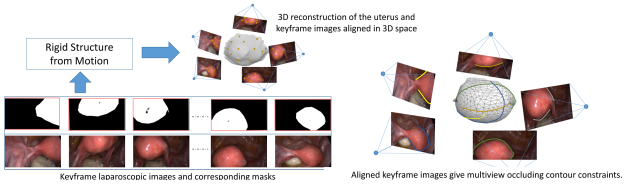

Fig. 2: 3D reconstruction of the uterus in laparoscopic images using rigid SfM (left) and multiview occluding contour constraints (right).

CONTACTS

Adrien BARTOLI
Adrien.Bartoli@udamail.fr
Toby COLLINS
Toby.Collins@gmail.com
Michel CANIS
mcanis@chu-clermontferrand.fr

FURTHER READING

Segmenting the Uterus in Monocular Laparoscopic Images without Manual Input
T. Collins et al., MICCAI'15 - Proceedings of the International Conference on Medical Image Computing and Computer Assisted Intervention, Munich, Germany (Oct. 2015)

Computer-Aided Laparoscopic Myomectomy by Augmenting the Uterus with Pre-operative MRI Data
T. Collins et al., ISMAR'14 - Proceedings of the IEEE International Symposium on Mixed and Augmented Reality, Munich, Germany (Sept. 2014)

Comparative Validation of Single-shot Optical Techniques for Laparoscopic 3D Surface Reconstruction
L. Maier-Hein et al., IEEE Transactions on Medical Imaging, 33(10):1913-1930 (2014)

CONTRACTS

Industrial contract with Almerys (2014-2016)

Scientific achievement #84
Laparoscopy-like operative vaginoscopy

We developed a new endoscopic technique which allows to do vaginal surgery with a perfect vision although exposure is difficult to achieve with conventional instrument for vaginal surgery as these meshes induce a severe retraction of the tissues. This new technique was reported in several endoscopic meeting and a video paper. This technique was reported for the first time in the world by our group. A communication on 3D teaching from our department received the price of the best poster in the European Society of Gynecologic Endoscopy in Brussels in October 2014.

Event 1

Study objective

Mesh erosion through the vagina is the most common complication of synthetic mesh used for pelvic organ prolapse repair. However, conventional transvaginal mesh excision has many technical limitations. We aimed at creating and describing a new surgical technique for transvaginal removal of exposed mesh that would enable better exposition and access, thus facilitating optimal treatment.

Design

A step-by-step video showing the technique.

Setting

A university tertiary care hospital.

Patients

Five patients previously submitted to pelvic organ prolapse repair using synthetic mesh, presenting mesh erosion through the vagina.

Interventions

Mesh excision using a laparoscopy-like operative vaginoscopy in which standard laparoscopic instruments are used through a single-incision laparoscopic surgery port device placed in the vagina.

Measurements and main results

In all cases, a very good exposure of the mesh was achieved, a minimal tissue traction was required, and the procedures were performed in a very ergonomic way. All the patients were discharged on the same day of the surgery and had a painless postoperative course. So far, there have been no cases of relapse.

Conclusion

This seems to be a simple, cheap, and valuable minimally invasive technique with many advantages in comparison with the conventional approach. More cases and time are necessary to access its long-term efficacy. It may possibly be used for the management of other conditions.

Event 2

Three-dimensional (3D) vision appears as an important factor influencing the quality of a controlled gesture. The purpose of this prospective and randomized study is to obtain subjective and objective data on the contribution of the 3D vision in laparoscopic surgery training.

Seventy-eight naïve medical students were randomly assigned to group A (2D vision, n = 39) and group B (3D vision, n = 39). They were trained for 3 consecutive days to achieve intra-corporeal sutures on pelvitrainer. Every day, the making of a stitch with the right and the left hand was recorded on video. On the last day, after their third day evaluation, the same exercise was recorded with the other vision system. Following each suture, students gave their impression on the two techniques through questionnaires and two experts evaluated blindly the gesture (operating time and technical scores).

Results A significant increase of performance in terms of time and score was observed in both groups. There was no time difference between them (p=0,23). The technical score of both subjective and objective evaluation of video were significantly higher in group B at each assessment (p<0,001). As the group A switched to 3D, their operating time and scores were similar to those of group B on day 3 (p= 0,51 and p=0,78 respectively). And vice versa when group B switched to 2D (p = 0,27 and p =0,98 respectively). Participants considered the suture technique to be significantly easier in 3D. Eighty- three percent of students preferred 3D to 2D. However the group B showed significantly more visual strain (46% vs 21% at day 1, p =0,01). This study confirms that 3D vision facilitate complex tasks execution by novices and is superior to last generation 2D HD systems. Further studies in clinical practice are necessary in order to translate these results to experienced surgeons.

Fig. 1: The surgical installation. The new endoscopic approach allows for a perfect vision of the deeper part of the vagina. Moreover, this vision may be shared by assistants which is unusual for vaginal surgery.

CONTACTS

Prénom NOM
prénom.nom@udamail.fr
Prénom NOM
prénom.nom@gmail.com

FURTHER READING

Laparoscopy-like operative vaginoscopy: a new approach to manage mesh erosions
Billone V, Amorim-Costa C, Campos S, Rabischong B, Bourdel N, Canis M, **Botchorishvili R.**
J. Minim Invasive Gynecol. 2015 Jan;22(1):10. doi: 10.1016/j.jmig.2014.09.004. Epub 2014 Sep 11.

Interest of a three-dimensional vision system in laparoscopic suturing on pelvi- trainer: a prospective comparative study among naïve medical students
C. Compan, B. Rabischong, J.L. Pouly, M. Canis, R. Botchorishvili
Service de Gynecologie Obstétrique et Reproduction Humaine, CHU Estaing, Clermont-Ferrand, France

Scientific achievement #85
Analysis of intracoronary prosthesis by Optical Coherence Tomography

Our work permitted us to develop semi automatic and automatic tools in analysis of intracoronary prosthesis images obtained in vivo by OCT (optical coherence tomography). They concerned the automatic detection of struts of metallic stent and bioresorbable scaffold, the analysis of struts coverage and quantification (with mapping) in case of eventual malapposition. The analysis of 2 exams (immediately after implantation and follow up control) permitted to develop images registration tools to assess the possible stent deformations (and resorption of strut in case of bioresorbable).

The first step of the work was to develop an algorithm to detect automatically, on images obtained in vivo by coherence tomography, the struts of metal stents by separating the arterial lumen and shadow cones created by the strut of the stent. The second step was to quantify the possible stent malapposition (strut not in contact with the arterial wall) and create a malapposition map with simple color codes (figure 1).

We then had to design a new algorithm for detecting bioresorbable scaffold strut (image appearance by Optical Coherence Tomography is different from metallic stent). From these data, a three-dimensional reconstruction of scaffold (figure 2) has been possible (useful application for the interventional cardiologist).

The second part of our work is the development of algorithms for images registration (with manual method as reference) on OCT exams couples (first performed immediately after stent implantation and second during systematic control several months later). The aim of that work is to evaluate the longitudinal and radial deformation of stents (and polymer resorption in case of bioresorbable scaffold).

Finally, in collaboration with the Thoraxcenter of Rotterdam (Holland), we began a work concerning OCT analysis of coronary arterial wall (3 layers). The objective of that project is to detect automatically pathological and normal areas of analysed segments (Figure 3).

Then, when a pathological segment is recognised, the algorithm has to define which sort of abnormality is detected: lipid plaque, fibrous plaque vs calcified plaque. Again, manual analysis is considered the gold standard.

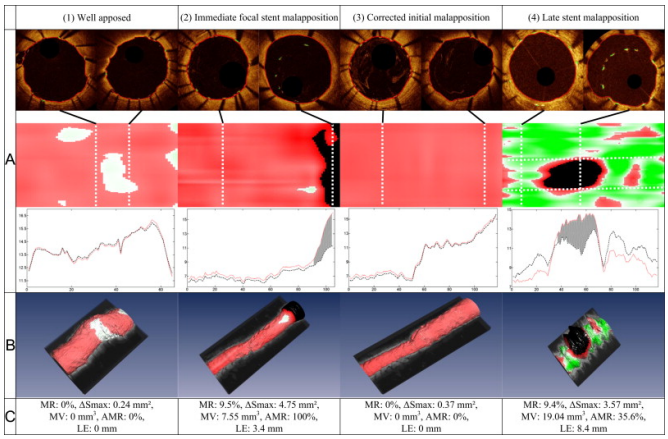

Fig. 1: A: segmented slices (lumen wall in red and detected struts in green), distance color map (positions of the slices are given by the vertical white dotted lines) and plots of the surface areas of lumen (red continuous line) and stent (black dotted line) vs. slice number z; B: volume rendering of the OCT sequence with superimposition of the segmented lumen wall colored by the distance map; C: quantification of malapposition rate (MR), max of the difference of surface (ΔSmax), volume of malapposition (MV), angular malapposition rate (AMR) and longitudinal extension (LE).

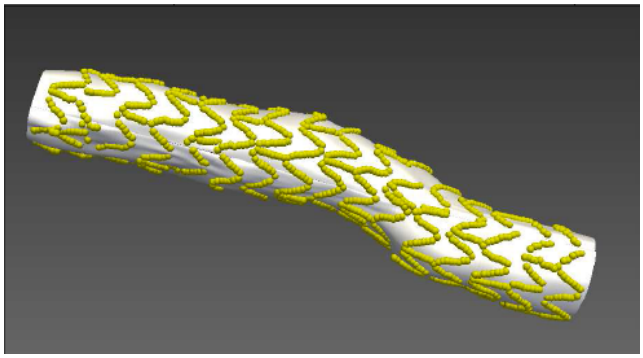

Fig. 2: 3D reconstruction of a bioresorbable scaffold from the data from of the semi-automatic struts detection algorithm.

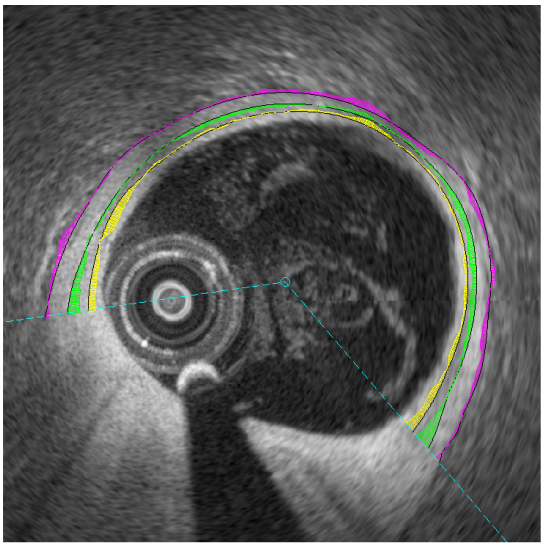

Fig. 3: Example of OCT frame showing atheromatous plaque (left bottom quadrant) and detection of 3 layers of arterial wall in the normal part.

CONTACTS

Pascal MOTREFF
pmotreff@chu-clermontferrand.fr
Emily PERY
emilie.pery@udamail.fr

FURTHER READING

Automated peroperative assessment of stents apposition from OCT pullbacks
F. Dubuisson et al., Comput Biol Med 59, 98 (2015)

Bioresorbable scaffolds on the bench
Ormiston J et al., EuroIntervention 11 Suppl (2015)

CONTRACTS

Industrial support of SainJude Medical and Terumo

PhD

N. Combaret, F. Dubuisson, P.Y. Menguy, P. Motreff, G. Souteyrand

Scientific achievement #86
Interventional Planning and Assistance for Ascending Aorta Dissections

Our works concern the planning and assistance of clinicians gestures within the framework of aortic dissections endovascular treatment. The first theme is about segmentation of aortic dissection features from a pre-operative 3D scan and the 3D/2D registration of them onto a per-operative 2D angiographic sequence. The main goal of the second topic is the virtual simulation of medical images and operating environment both using external sensors' data in order to assist the medical staff to position the imaging system and to track instruments. The third theme deals with gesture simulation in virtual reality with force feedback and extension to the surgery robotisation.

Our works concern the planning and assistance of clinicians gestures within the framework of aortic dissections endovascular treatment. Three themes are studied.

The first theme concerns image processing of aortic dissections images. The first work deals with segmentation of aortic dissection features (lumens, flap) by using digital topology and mathematical morphology approaches ; it led us to materialize a virtual feature : tears in a vascular wall. The second work deals with the 3D/2D registration of these features onto a per-operative 2D angiographic sequence : a direct initialization, based on aortic dissection shapes, allowed us to propose a more fast registration framework (Fig. 1).

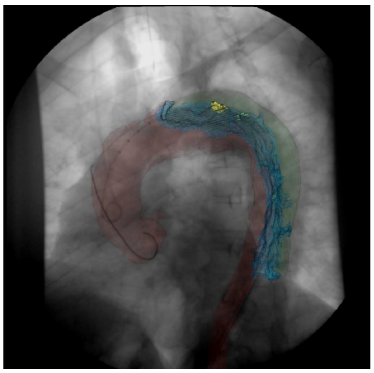

Fig. 1: Aortic dissection features (true lumen in red, false lumen in green, intimal flap in blue, intimal tear in yellow) – segmentation from a 3D scan then registration onto an angiographic sequence [from P. Lubniewski's Ph.D. thesis, under the guidance of C. Lohou].

The second topic deals with online per-operative assistance. The main goal is to virtually simulate medical images and operating environment both using external sensors' data (cameras, depth sensors) in order to assist the medical staff to position the mobile C-arm imaging systems and to track instruments inside the body. Some works have been done : the conception of a 3D model of the innovative hybrid operating room IMABLOC recently set up in the University Health Center at Clermont-Ferrand and the development of a simulation software tool of operating room applied to the IMABLOC (modelling, sensor's data simulation). This tool allows the validation of the developped algorithms for intervention assistance as well as a virtual reality device for medical team training (Fig. 2).

The third theme deals with gesture simulation in virtual reality with force feedback and extension to surgery robotisation. Three works have been developped. The first work leads to define mechanical models of the TX40 6-axis robot (this robot should be used as a force measurement arm to fit gesture models and is also the support of the surgery robotisation study), the set up of a simulator for this study requiring the use of geometric, kinematic and dynamic models. The second work concerns the modelling of the gesture and the surgical tools, the goal is to define mechanical models (geometry and forces transmission) based on robotic technics in order to simulate and study the forces felt by the surgeon during the intervention. The third work deals with merging the robot and surgical instrument models. In order to study the robot behavior during the catheter insertion into the aorta, the geometry of the aorta should be adapted from results of the first theme and relocated with respect to the robot. A catheter model is defined by considering it as a set of universal joints moving along the centerline of the aorta. This allows for studying the catheter insertion by the robot (Fig. 3).

CONTACTS

Christophe LOHOU
christophe.lohou@udamail.fr

FURTHER READING

Interventional planning and assistance for ascending aorta dissections
C. Lohou et al., IRBM 34, 306 (2013)

PhD

N. Fetnaci (fail), P. Lubniewski (defended)

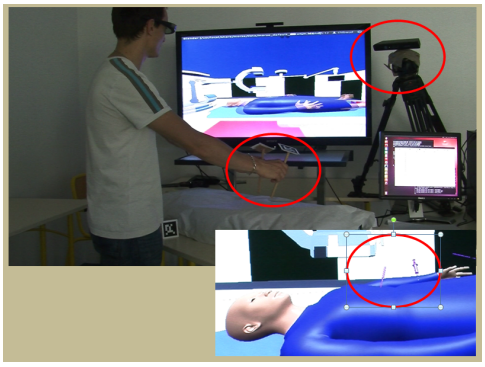

Fig. 2: Real/Virtual interactions [from T. Pilorin's engineer's report, under the guidance of J. Courbon].

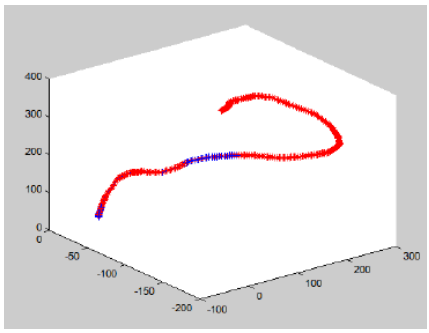

Fig. 3: Catheter tracking inside an aorta [from Inigo Cortés's engineer's report, under the guidance of F. Paccot].

Scientific achievement #87
Standardization of transcatheter arterial chemo-embolization of the liver

Our work is dedicated to develop a physiological model to evaluate the liver distribution of Cisplatin (CDDP) according to the route of administration in a healthy liver model. To achieve this goal we have used a two-step approach: 1- pharmacokinetics evaluation on an animal model, 2- computer analysis of tumor vascularization based on CT scan or MRI studies.

After a preliminary toxicity study, we compared the plasmatic and parenchymal concentrations of CDDP in four groups of healthy pigs according to the route of administration: the drug was injected by intravenous or intra-arterial route without embolization or intra-arterial followed by partial or complete embolization of hepatic arteries. The plasmatic pharmacokinetic shows a decrease of the half-life and the plasmatic exposure to CDDP when the drug was administrated by chemo-embolization as compared to intra-arterial or intra-venous route (figure 1 a&b). The parenchymal pharmacokinetic shows an increase of the half-life and the hepatic exposure to CDDP after chemo-embolization as compared to intra-arterial or intra-venous administration (figure 1 c&d).

In a second step, to achieve a precise measure of the pharmacokinetic of tumoral regions, we have developed a novel segmentation algorithm of liver lesions based on the selection of a region of interest. After using a noise reduction and edge preserving algorithm (smoothed shock filtering), we combined fuzzification and defuzzification phases for this purpose. The first step aims at calculating a categorization of pixels into two classes (tumor vs. background), by attributing them a percentage of membership to each class. From this fuzzy clustering, we then applied a binary crisp segmentation by integrating this fuzzy information, together with geometrical features represented as Zernike moments.

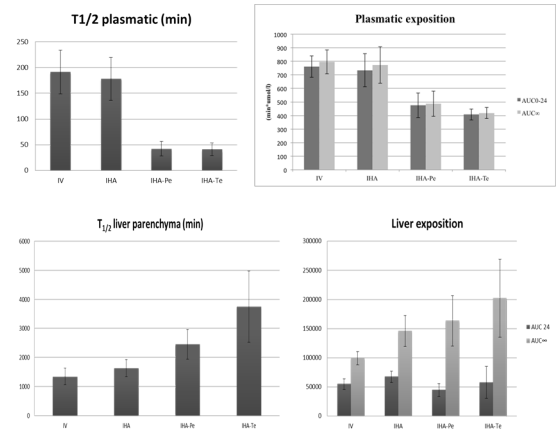

Fig. 1: Decrease of plasmatic half-life and exposure after chemo-embolization: comparison of the intra-arterial or intra-venous administration (figure 1a & b). Increase of parenchymal half-life and liver exposure after chemo-embolization as compared to intra-arterial or intra-venous administration (figure 1c & d).

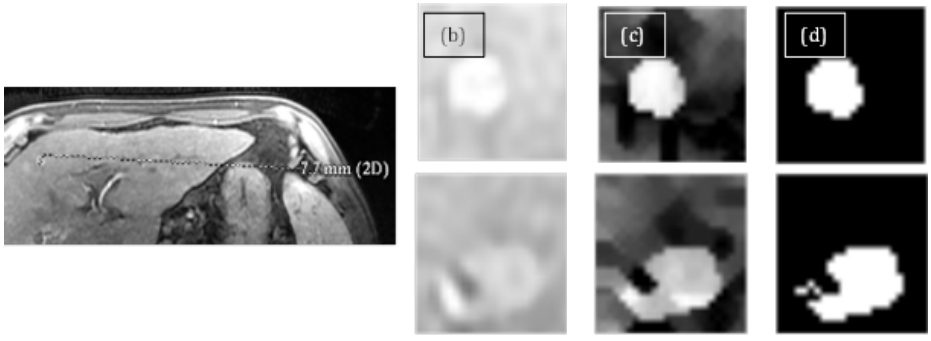

Fig. 2: The region of interest (b) selected during a diagnosis routine (a) is processed with our algorithm by first applying a noise reduction algorithm (c), then by segmenting it thanks to a combination of a fuzzifier and a defuzzifier integrating fuzzy and geometrical features.

CONTACTS

Pascal CHABROT
pchabrot@chu-clermontferrand.fr
Armand ABERGEL
aabergel@chu-clermontferrand.fr
Antoine VACAVANT
antoine.vacavant@udamail.fr

FURTHER READING

Cisplatin Pharmacokinetics in Nontumoral Pig Liver Treated With Intravenous or Transarterial Hepatic Chemoembolization
P. Chabrot P et al., Cardiovasc Intervent Radiol 35, 1467 (2012)

A Novel Fuzzy C-Means Based Defuzzification Approach with an Adapted Minkowski Distance
A.-R. Ali et al., Computer Vision Winter Workshop 2014. February 2014, Krtiny, Czech Republic.

Fast Smoothed Shock Filtering
A. Vacavant et al., IEEE International Conference in Pattern Recognition 2012. November 2012, Tsukuba, Japan.

CONTRACTS

PHC/WTZ MARIA (2014-2015)
Projet Région Nouveau chercheur (2014-2017)
Industrial support of Celo Nova ®.

PhD

A.R. Ali (thèse Sciences pour l'Ingénieur), F. Bouculat (thèse de Médecine), P. Chabrot (thèse Sciences de la Vie), P. Guibert (thèse de Médecine)

Scientific achievement #88
Joint estimation of myocardial strain and contraction phase from data assimilation

We have designed a generic formalism for regional tracking of the left ventricle (LV) from 3D+t cardiac imaging modalities used in clinical routine (echocardiography, gated-SPECT, cine-MRI). The displacement field is estimated from a variational data assimilation framework and is used to assess regional myocardial function in 3D from the computation of deformations (strain). Phase of the cardiac contraction is also estimated as a state variable parameterizing the dynamical model. Comparison to state-of-the-art methods from tagged MRI and to expert wall motion scoring showed promising results to help diagnosing contraction abnormalities.

The alteration of left ventricle systolic function is shared by most cardiac pathologies. This is due to necrosis, tissue ischemia (ischemic cardiopathy) or myocyte degradation (dilated or hypertrophic cardiomyopathy, etc.). Dynamic imaging enables early detection of a decrease in regional myocardial deformation (strain). Strain indices have the advantage of being quantitative, operator-independent, unrelated to charge conditions and better correlated with complex contraction processes during systole. Prognostic value of these indices is better than the Left Ventricular Ejection Fraction (LVEF) or the Wall Motion Score (WMS) in case of slightly altered LVEF.

For the estimation of a dense displacement field from the image sequences, we use data assimilation techniques that seek to recover a system state vector $\boldsymbol{\chi}(\mathbf{x},t)$ conforming to a dynamical law that governs system evolution. The dynamical system is defined by a non-linear operator M depending on state variables. The measurements $\boldsymbol{\gamma}$ (commonly known as observations) are assumed to be available at some discrete times and are measured through a non-linear operator H that links the system state variables to the observation function. $\boldsymbol{\chi}$ is defined at every pixel/voxel and every time of the image sequence and contains the displacement vector $\mathbf{v}$, the phase φ and the asymmetry factor a (depending on the systole-to-diastole ratio) of the contraction cycle. The observation operator H for $\mathbf{v}$ is based on the optical flow constraint equation combined with a non-linear regularizer. The dynamic model is designed with enough degrees of freedom to not hide defects in cardiac kinetics due to various pathologies: it is built from a transport equation, assuming the invariance of the state variables with displacement, that is parameterized with an asymmetric square wave function accounting for the sign of myocardium contraction (positive in systole and negative in diastole).

The differentiation of the estimated dense displacement field gives access to the deformation tensor, and projection onto a local coordinate system provides radial, circumferential and longitudinal components of strain. With phase and asymmetry, they are complementary information to fully diagnose myocardial function. Preliminary results obtained in 2D from cine MRI are very promising with a good estimation accuracy on simulated image sequences (Figure 1 top), and a good agreement with strain computed from tagged MRI with the inTag Osirix plugin (CREATIS, Lyon) (Figure 1 bottom). Moreover, the informational value of the estimated strain and phase values was high enough to discriminate among three of the four clinical WMS (1=normal, 2-3=moderate or severe hypokinesia, and 4=akinesia) and between dyskinetic and non dyskinetic myocardial sectors.

All the methods and software framework have been extended to 3D image sequences to process SPECT and US exams (Figure 2).

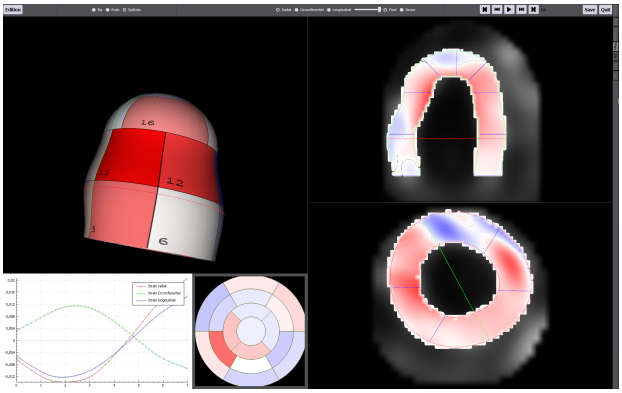

Fig. 2: Software interface for 3D strain estimation: left, 3D interactive model for endocardial and epicardial walls; right, long-axis and short-axis slices at the selected 3D point; and bottom, bull's eye representation for the standard AHA divisions and temporal variations of strain components for the selected division.

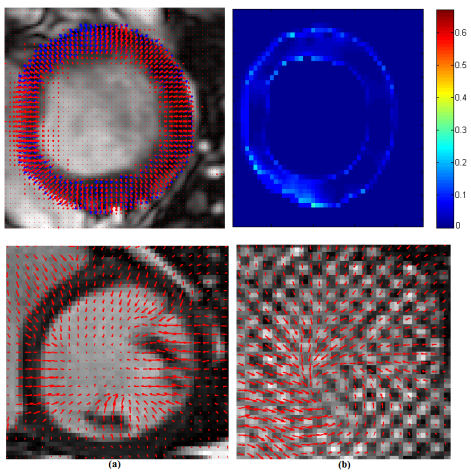

Fig. 1: Comparison between the displacement field estimated with our method and: a synthetic displacement field used to simulate a deformed MRI sequence and the corresponding error in percents (top); the displacement field computed by a tracking method (inTag OsiriX plugin) from MRI tagging.

CONTACTS

Laurent SARRY
laurent.sarry@udamail.fr

FURTHER READING

Variational Myocardial Tracking from Cine-Mri with Non-Linear Regularization.
V. Tuyisenge et al., Proc. ISBI (2013)

Multimodal quantification and validation of 3D regional myocardial function.
C. Beitone et al., IRBM 36, 70 (2015)

Estimation of Myocardial Strain and Contraction Phase from Cine MRI using Variational Data Assimilation.
Tuyisenge et al., IEEE Trans Med Imaging (2015)

CONTRACTS

ANR TecSan *3DStrain* (2011-2015)

PhD

K. Bianchi, L. Cassagnes, V. Tuyisenge

Scientific achievement #89
4.7-Tesla Magnetic Resonance Imaging Atlas of Human Deep Brain

Human brain stereotactic atlases are widely used in stereotactic neurosurgery for indirect anatomical targeting, when medical imaging cannot reveal directly the spot. Following a 4.7-Tesla MRI acquisition of the deep brain of an anatomic specimen, we contoured and labeled 100 anatomic objects, lending to an extended anatomical 3D MRI atlas. This is the first 3D anatomic atlas detailing the deep brain. An Industrial transfer is ongoing. Since 2013 we are developing the analysis of the upper brain stem notably the tegmental region, showing complex anatomical structure such as reticular nuclei for future clinical studies (e.g. gait control).

Context

Human Brain Stereotactic Atlases are widely used in stereotactic neurosurgery for indirect anatomical targeting of deep brain structures. They are dedicated to probabilistic targeting when medical imaging cannot reveal directly the anatomical target. Atlases are buildup of histological slices with fixed and irregular inter-slice distances and orientation of sections. The Talairach and al's (1957; & Tournou, 1988, coplanar) is well-known because it was the first used for non-medical applications (Talairach Daemon) and often used as reference for other non-medical atlases (e.g. MNI atlas). For medical applications, the Schaltenbrand and Bailey (1959, 1977) and the Mai-Assheurer-Paxinos (1977) are nowadays the most well-known and used.

Scientific achievement

In 2004 we have performed a very high field MRI acquisition of the deep brain of an anatomic specimen (collaboration JM Bony, Inra; Saint Genès Champanelle) for the analysis of the deep brain (T1-weighting; isotropic cubic voxels of 250µm side). Anatomical structure was contoured and labeled, showing that MRI contrast is favorably comparable to histology dyeing. This lent progressively to an extended anatomical 3D MRI atlas of about 100 anatomic objects. This is the first 3D anatomic atlas detailing the deep brain and enabling slice reconstruction along any trajectory (Iplan, BrainLab, Germany); it is used in clinical condition in our institution, and as stereotactic tool for collaborative research works (anatomical location of complex anatomic structures). An Industrial transfer is ongoing. This advanced anatomic study enabled to propose a new clinical ontology of thalamic nuclei and an indirect location of hypothalamic nuclei. Since 2013 we are developing the analysis of the upper brain stem notably the tegmental region, showing complex anatomical structure such as reticular nuclei (ongoing study and application), for future clinical studies (e.g. gait control).

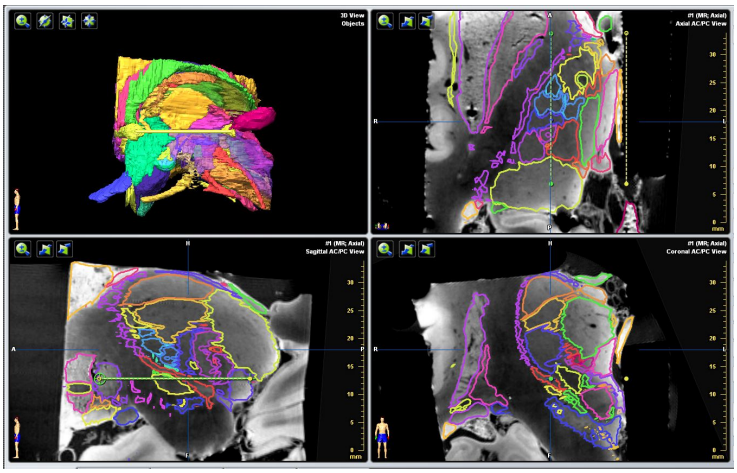

*Fig. 1: **4.7-Tesla MRI atlas centered on the thalamus;** clock-wise from left-top (Iplan software, BrainLab, Germany), 3D display of anatomic objects (medial view; anterior-posterior line or ACPC line, is projected), horizontal (axial) slice, vertical-frontal (coronal) slice and vertical-sagittal slice, going through the nucleus ventrointermedius of thalamus (Vim, blue); (yellow, pulvinar; lateral and medial ventro-lateral nuclei, dark and light pink; centromedian (red); ventro-oral nuclei, blue).*

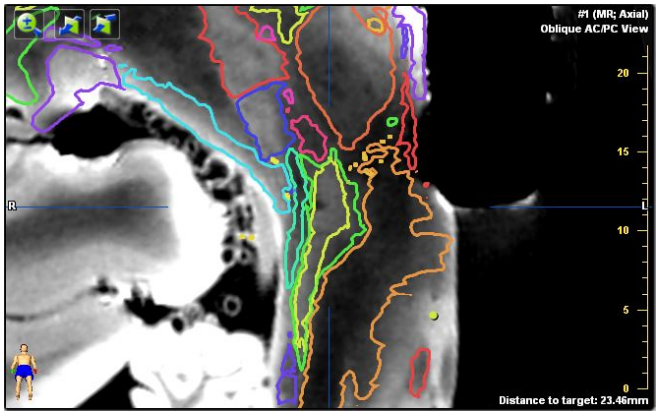

Fig. 2: 4.7-Tesla MRI atlas centered on the nucleus tegmental pedunculopontine; reconstructed pseudo-coronal slice (Iplan software, BrainLab, Germany) along the line perpendicular to the vertical line of Paxinos & Huang and going through the nucleus tegmental pedunculopontine of the lateral reticular system (ppn, yellow); (brachium conjunctivum, orange; medial and lateral lemniscuses, light and dark blue; spino-thalamic fascicle, light green).

CONTACTS

Jean-Jacques LEMAIRE
jjlemaire@chu-clermontferrand.fr

FURTHER READING

Fontaine D et al., Brain. 133:1214 (2010)

Lemaire JJ et al., Neurosurgery 66: ons161 (2010)

Lemaire JJ et al., NeuroImage 37 : S109 (2007)

CONTRACTS

Industrial Partnership *Human Brain MRI Atlas* (2007-2008)
Industrial Partnership *Human Brain MRI Atlas* (2012-2015)

PhD

F. Caire, F. Vassal

Scientific achievement #90
3D MRI reconstruction based on transfinite approximation

Our method, based on transfinite interpolation, aims at reconstructing high resolution isotropic volume from three anisotropic volumes with different orientations. The main idea is to register all data slices in the same space and use transfinite interpolation in convex cells to fill the output grid. The formula is based on projection on surrounding structures containing data and blend them taking into account the data geometries. In the general case, some projections belong to several slices which we manage to regularize data during the interpolation procedure. We manage to reconstruct volume high resolution isotropic volume improving resolution compared to raw data. Our reconstructed volume can serve as a basis for semi-automatic segmentation algorithms in the deep brain.

Some MRI sequences like the White matter Attenuated Inversion Recovery (WAIR) are technically restricted to anisotropic acquisition. To overcome this drawback, we propose a method to merge three anisotropic volumes of the same healthy subject, one of each orientation, onto a high resolution isotropic volume. This method is inspire from transfinite interpolation, used in Computer Assisted Design (CAD), which read data value into projection on all surrounding structures like faces, edges, and vertices and blend them based on their geometries. In order to express a point coordinate relatively to its local data shape, the transfinite formula uses barycentric coordinates which weight each vertex of the structure relatively to the point spatial position within the shape. On our case, the geometrical shape is defined by the intersection between all data slices from the three volumes. Since it is define only by planes, all empty space are convex polytopes where edges and vertices respectively correspond to the intersection of two and three slices. Therefore, it is impossible to read a single value on this structures due to a non-smooth data transition among them. In order to keep raw data unmodified, projections are limited to be orthogonally on two dimensional faces.

A comparison between one of the original volume and the reconstruction show the benefits of isotropy on the information visualization against anisotropy. The contrast displays by the reconstruction is similar to the contrast of a raw. Concerning the resolution, the original WAIR volumes have voxel resolution of 0.52 x 0.52 x 2 mm^3 and the reconstruction grid has a resolution of 0.26 x 0.26 x 0.26 mm^3. Through the improving resolution, the ability of the WAIR sequence to display deep brain structures and the ability to use the reconstruction in all directions, this method simplifies manual segmentation task due to better capacity to follow fine structures and allows us to create an atlas using WAIR MRI.

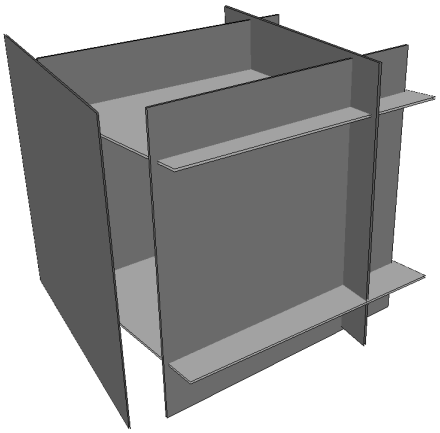

Fig. 1: Example of the spatial organisation of our data, each plane corresponding to a slice.

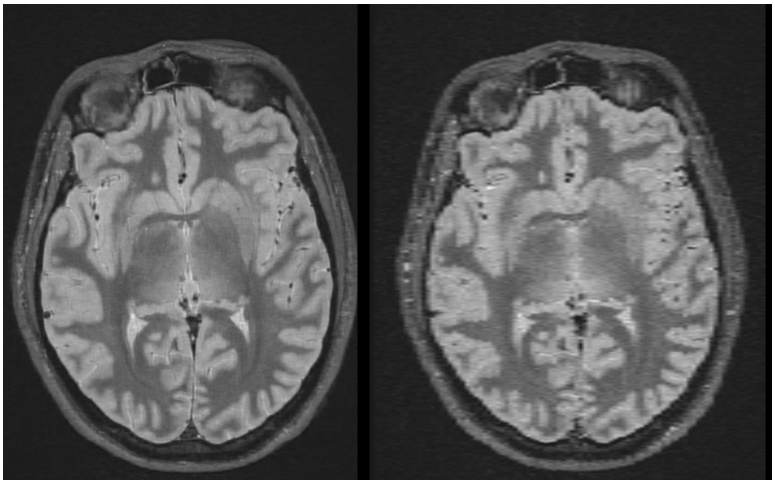

Fig. 2: Superior view of the reconstructed axial slice of TFI volume (left) and the reconstructed sagittal raw volume (right).

CONTACTS

Fabien FLESCHET
fabien. fleschet@u-auvergne.fr
Jean-Jacques LEMAIRE
jjlemaire@chu-clermontferrand.fr
Quentin DANIEL
quentin.daniel@udamail.fr

FURTHER READING

On transfinite interpolations with respect to convex domains
M. Randrianarivony, CAGD 28(2), 135–149 (2011)

Direct stereotactic targeting of the ventrointermediate nucleus of the thalamus based on anatomic 1.5-t mri mapping with a white matter attenuated inversion recovery (wair) sequence
F. Vassal, J. Coste, P. Derost, V. Mendes, J. Gabrillargues, C. Nuti, F. Durif, J.J. Lemaire, Brain Stimulation 5(4), 625–633 (2012)

Mean value coordinates in 3d
M.S. Floater, G. Ks, M. Reimers, CAGD 22, 623–631 (2005)

CONTRACTS

Financement ministériel (2014-2017)

PhD

Q. Daniel

Scientific achievement #91

Variation Maps of ^{18}F-fluorodesoxyglucose Pet-Scans of Severe Brain Injured Patients: Individual Comparison of Deep Brain Stimulation in On and Off Conditions

^{18}F-**f**luoro**d**esoxy**g**lucose(F-FDG) **p**ositron **e**mission **t**omography (Pet-Scan) is used for the exploration of brain disease metabolism. In **d**eep **b**rain **s**timulation (DBS), FDG Pet-Scan enables to detect metabolic variations, prior and after DBS[1], using group comparison analysis (e.g. SPM). We developed an original individual comparison of FDG Pet-Scan, in severe brain injured patients with extensive brain tissue lesions making statistical parametric approach useless.

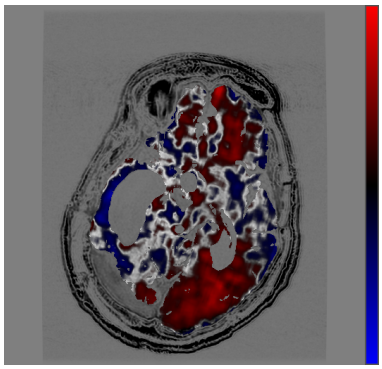

Fig. 2: Patient 3: Variation map overlaid on T1.

Materials

Patients:

We analysed three **severe brain injured patients** of clinical ongoing study:
Patient 1: 32 yo, traumatic, vegetative;
Patient 2: 62 yo, spontaneous haemorrhage, minimally conscious state (MCS);
Patient 3: 24 yo, traumatic, (MCS);
All suffering of extended brain tissue lesions.

Imaging Data:

For each patient were acquired:
A **T1** weighted MRI (SIEMENS Avento 1.5 tesla machine; 0.47x0.47x0.7mm^3);
Two 18 F-FDG **Pet-Scan** in DBS **On** and **Off** conditions (GE Discovery Pet-Scan; resolution of 2.34x2.34x3.27mm^3).

Methods

An individualized **manually contoured mask** of brain tissue (skull and cerebrospinal spaces removed) was realized from patient T1 weighted MRI (T1-mask) using Iplan software (Iplan, BrainLab, Germany).
Both DBS **On** and **Off** conditions 18 F-FDG Pet-Scans were **co-registered** with T1 weighted MRI and re-sliced using Slicer (Slicer, USA; automatic rigid co-registration, 6 degrees of freedom).
^{18}F-FDG Pet-Scans were **normalized** using the **c**erebral **g**lobal **m**ean (CGM)[3] computed using T1-mask. Individual CGM and normalized results, presented as a red (above CGM) and blue (below CGM) map, were automatically generated using an internally developed ITK (Insight Segmentation and Registration Toolkit) based software.
Metabolism variations between On and Off conditions were then automatically compared and **variation maps** computed by a voxel based approach. The method uses a logarithmic function between normalized Pet-Scans (On condition versus Off condition). [insuring that stability is zero].

Results

Masks, normalized CGM Pet-Scans, and variation maps, were generated for the three patients.

Each individual variation map revealed pertinent pathophysiologic mechanisms on consciousness disorders:

- Within the attentional network (occipital cortex).
- Within the behavioural control network of the frontal lob (notably medial and basal cortex).

Conclusion

The proposed automatic method to compute individualized comparison of brain metabolism between DBS On and Off conditions for severe brain damage patient showed pertinent metabolic variations which should be useful to analyse disorders of consciousness, still relying on manual mask contouring (specific for these severe brain injured patients). This method paves the way for further individualized analysis of variations of 18 F-FDG Pet-Scans.

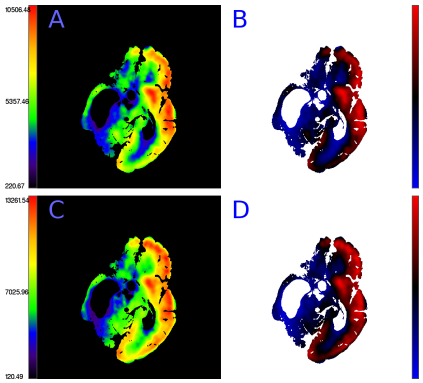

*Fig. 1: Patient 3: Pet-scans. DBS condition **A**. On, **C**. Off; DBS condition (CGM Normalized) **B**. On, **D**. Off.*

CONTACTS

Basile ROCHE
basile.roche@udamail.fr

FURTHER READING

Brain energization in response to deep brain stimulation of subthalamic nuclei in Parkinson's disease
Garraux G. et al. , Journal of Cerebral Blood Flow & Metabolism, 31[7], 1612- 1622 (2011)

Study of Conscious Behavior Under Low-frequency Deep Brain Stimulation in Chronic and Severe Post-coma Disorders of Consciousness. (Post-coma DBS)
ClinicalTrials.gov , NCT01718249

SPM-Based Count Normalization Provides Excellent Discrimination of Mild Alzheimers Disease and Amnestic Mild Cognitive Impairment from Healthy Aging
Yakushev I. Et al. , NeuroImage 44[1], 43-50 (2009)

PhD

B. Roche

Scientific achievement #92
Set-up of combined accelerometry, electrophysiology and clinical assessments during DBS

In this study, we have evaluated the contribution of the acceleration measurement to aid in the optimal location of anatomical structures during deep brain stimulation surgery. Our primary objective in this pilot study, therefore, is to determine the characteristics of this method. The contribution can be dual: (1) Support for positioning using accelerometry with objective assessment of tremor or rigidity; (2) Improving the understanding of the physiopathology mechanisms and effect of chronic stimulation by correlating the accelerometer measurements with electrophysiological measurements and the patient's individual anatomy.

In collaboration with Dr Simone Hemm-Ode, Ashesh Shah (PhD student) and Prof Erik Schkommodau, head of the School of Life Sciences, Institute for Medical and Analytical Technologies, FHNW University, Switzerland.

Project background and objectives

The optimal electrode placement for deep brain stimulation (DBS) critically depends on clinical observation of the patient during surgery. The choice of the final implantation sites of electrodes is based on microelectrode recordings (MER) that are performed intra-operatively along the trajectory down to the target to detect neuronal activities. In parallel to MER, acute intraoperative stimulation tests (IST) are realized using progressive electric current increments at each step to assess the clinical effects. The evaluation of the different effects is done by semi-quantitative subjective clinical rating scales applied by the physician. Intraoperative quantitative measurement of the motor manifestations of Parkinson's disease has rarely been proposed in routine. The aim of the project is to analyse the feasibility to perform objective evaluations of rigidity and tremor during IST using accelerometry and to couple accelerometer data with intraoperative MER recordings in order to provide new objective relevant functional data facilitating and optimizing the choice of the electrode positioning.

Results

In the first year of the project, the equipment to measure acceleration (Fig. 1) during the DBS surgery was developed including the hardware and the software. Using this equipment, a bachelor thesis was performed by Dagmar Gmünder to evaluate feasibility of acceleration measurements in real condition. Ashesh Shah (PhD student) has added a synchronization TTL signal from the accelerometer recording system to the electrophysiology system and further software modifications allowing online visualization of data in the operating room.

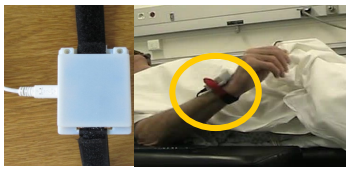

Fig. 1: Patient during DBS surgery with accelerometer on his wrist.

As a part of the clinical research project, 20 patients were included in the clinical trial. The data analysis has done post operatively using Alpha Omega Studio (Alpha Omega Eng.) and Matlab (Mathwork Inc.). The data is filtered and then statistical features are extracted from it (Fig 2A). These statistical features are used to identify stimulation amplitudes at which the patient symptom was reduced considerably (threshold) (Fig 2B). A significant change in acceleration measurements could be identified during IST compared to the semi-quantitative subjective clinical evaluations performed by the neurologist (Fig 2C). The results show that the acceleration measurements are sensitive to the changes in the patient's symptoms and that they can be used to quantify the changes.

Conclusions and Outlook

The data has successfully demonstrated that changes in the symptoms of movement related disorders can be quantified using acceleration measurements of the patient's or the neurologist's arm.

This research was funded by the Swiss National Science Foundation and partly by the Germaine de Staël program of the Swiss Academy of Engineering Sciences.

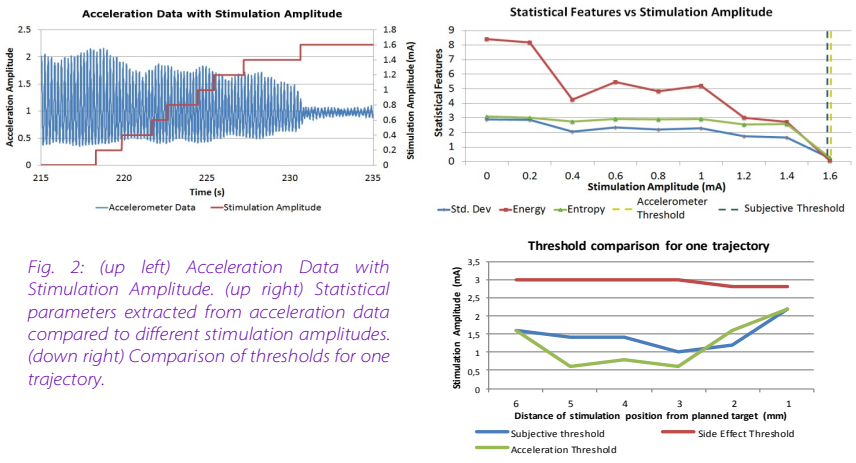

Fig. 2: (up left) Acceleration Data with Stimulation Amplitude. (up right) Statistical parameters extracted from acceleration data compared to different stimulation amplitudes. (down right) Comparison of thresholds for one trajectory.

CONTACTS

Jérôme COSTE
Jerome.Coste@udamail.fr

FURTHER READING

Correlation analysis between quantitatively analyzed stimulation effects and anatomical position during deep brain stimulation surgery
Shah A et al., Stereotactic and Functional Neurosurgery 92 (suppl.2): 167 (2014) (proceedings)

Acceleration measurements to quantify changes in rigidity during deep brain stimulation surgery
Shah A et al., Movement Disorders 29 (suppl.1): S30 (2014) (proceedings)

Using acceleration to quantify symptoms during deep brain stimulation surgery
Shah A et al., Biomedical engineering 58(Suppl 1-A): 4007 (2013) (proceedings)

CONTRACTS

Germaine de Staël, partnership Hubert Curien franco-swiss (2011-2012 ; 24737VA)

Swiss National Foundation (2011-2014; Project funding n°135285) *Investigation of extended intraoperative data recording for safer and improved target selection for deep brain stimulation in Parkinson's disease*

Swiss National Foundation (2014-2015; Interdisciplinary project n°153370) *Investigation of the mechanism of action of deep brain stimulation by combining intraoperative patient-specific electric field simulations and acceleration measurements*

Clinical trial number 2011-A00774-37 *Evaluation de l'apport de l'accélérométrie à la localisation et la compréhension des mécanismes physiopathologiques pendant et après l'implantation d'électrodes de stimulation cérébrale*

PhD

A. Shah

Scientific achievement #93
Contribution of the recording of local field potential during deep brain stimulation

In this study we have analyzed the relationships between magnetic resonance imaging (MRI) anatomy and local field potential (LFP) done during surgery for 10 patients with Parkinson's disease. Percentage of power spectral density for main physiological LFP frequency range was considered for thalamus, ZI, STN and Forel (Figure). We have shown LFP allow to discriminate between structures in the subthalamic region using exploration electrode with patient at rest during electrode implantation surgery.

Introduction

The subthalamic nucleus (STN) is the main target for deep brain stimulation (DBS) in Parkinson's disease. We analyzed the relationships between magnetic resonance imaging (MRI) anatomy and electrophysiology (local field potential, LFP) done during electrodes implantation surgery. We hypothesized that the contribution of LFP to neuronal firing rate with detailed MRI anatomy should allow to explore finely anatomo-electrophysiological relationships and also to determine precisely functional surgical targets.

Patients, material and methods

Ten patients with Parkinson's disease underwent bilateral STN DBS procedure. A stereotactic MRI was performed with a White matter Attenuated Inversion Recovery sequence. Direct targeting of STN region was performed using stereotactic software (Iplan, BrainLab, Germany). Under local anesthesia, after recording of neuronal activity and LFP, an acute stimulation was performed with a MicroGuide Pro system (Alpha Omega, Israel). Then an electrode (DBS 3387, Medtronic, USA) was placed on the selected area. Postoperative clinical assessments showed a mean improvement of 63.6% of motor control (part III of UPDRS). 693 LFP recordings in MRI-outlined anatomical structures (Thalamus [Thal], Zona Incerta [ZI], Forel Field [Forel] and STN) were analyzed: Power spectral densities (PSD) from 0 to 100Hz; 1024 frequency values; Normalization: % of total PSD; Calculation for delta (0-4 Hz), theta (4-7 Hz), alpha (7-13 Hz), beta (13-30 Hz), gamma (30-50 Hz, 50-100 Hz) frequency range. Non-parametric Kruskal-Wallis ANOVA tests were performed followed by pairwise comparisons with adjusted p-value.

Results

The most frequently encountered structures were STN (n=192), Thal (n=178), ZI (n=139) and Forel (n=132).

Delta band power spectral density (PSD) of LFP was significantly different between structures (K-W: p = 0.0002). Post hoc tests (pairwise comparisons: adjusted p-value = 0.004) showed differences between thalamus and ZI (p = 0.003), between Forel and thalamus (p = 0.00005) and between STN and Forel (p = 0.0004). Alpha band PSD was significantly different between structures (K-W: p = 0.04). STN had higher α band activity than Forel (p = 0.003). Gamma band PSD was significantly different between structures (K-W: p = 0.0001). Thalamus γ activity differed from all other structures (thalamus-ZI: p = 0.00001; thalamus-STN: p = 0.0005; thalamus- Forel: p = 0.0005) with higher γ activity in thalamus than in others structures. 50-100Hz band power spectral density (PSD) of LFP was significantly different between structures (K-W: p = 0.02). 50-100Hz band activity in Forel was statistically lower than in the thalamus (p = 0.002).

Theta and Beta bands PSD failed to discriminate between the structures of the subthalamic region (K-W: p = 0.09 and p = 0.08 respectively; data not shown).

Conclusion

This study suggests the interest of LFP, which is at least as effective as extracellular neuronal activity (Coste et al., EJN, 2009), to discriminate between structures in the subthalamic region using exploration electrode with patient at rest during DBS surgery. Contrary to previous studies reporting an increase in β band when entering the STN (Chen et al., Exp Neurol, 2006), no significant difference was shown between structures concerning the β band.

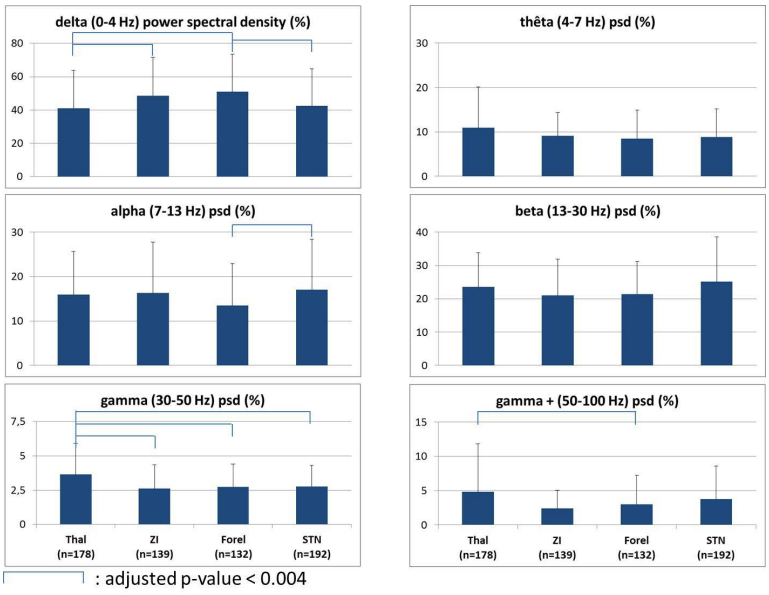

Fig. 1: Local field potential power spectral density analysis.

CONTACTS

Jérôme COSTE
Jerome.Coste@udamail.fr

FURTHER READING

Contribution of local field potential to subthalamic nucleus deep brain stimulation in Parkinson's disease
Coste J et al., 1st International Symposium on Deep Brain Connectomics, Clermont-Ferrand, France (Sept 28-29, 2012) Contribution of local field potential to subthalamic nucleus deep brain stimulation in Parkinson's disease (Poster)

Contribution of local field potential to subthalamic nucleus deep brain stimulation in Parkinson's disease
Coste J et al., 20th World Congress on Parkinson's Disease and Related Disorders, Geneva, Switzerland (Dec 8-11, 2013) Contribution of local field potential to subthalamic nucleus deep brain stimulation in Parkinson's disease (e-Poster)

CONTRACTS

Fondation de l'Avenir (projet ET7-455, 2007) *Développement d'outils d'électrophysiologie pour aider à la localisation et à la compréhension des mécanismes physiopathologiques durant l'implantation d'électrodes de stimulation cérébrale : mesure de conductivité et enregistrement du potentiel de champ local*

Clinical trial number 2007-A01201-52
Evaluation d'un outil d'électrophysiologie pour l'aide à la localisation et à la compréhension des mécanismes physiopathologiques durant l'implantation d'électrodes de stimulation cérébrale: enregistrement du potentiel de champ local

Scientific achievement #94
Mapping the Structural Connectivity of Language with DTI Tractography

We used functional-based DTI tractography to map the subcortical connectivity of language in healthy subjects. We provided new insights into the location and inter-subject variability of eight white matter fascicles involved in language. This body of knowledge was transposed to brain tumor surgery, by using patient-specific tractography images incorporated into an intraoperative navigation to localize the functional limits of resection. The combination with transient language deficits induced by subcortical electrical stimulation mapping allowed accurate, real-time anatomofunctional correlations. The findings enhanced our comprehension of brain language organization.

There is much debate about which white matter (WM) fascicles specifically contribute to language, their spatial extent, as well as the functions they subserve during language processing. First, we conducted a preclinical study in twenty healthy subjects, combining DTI tractography and fMRI to yield connectivity associated with language. We explored eight fascicles that have been proposed as putative candidates for language, to which we associated functionality by tracking their connections to the fMRI-derived clusters (Figures 1 and 2). We generated a database of morphological and anatomical characteristics for each fascicle, such as volume, length, cortical terminations and their intra- and inter-subject variations. By using this construct, we provided in explicit details the structural map of the language connectome. Second, this body of knowledge was transposed to brain tumor surgery. Patients were operated on under local anesthesia (i.e. awake surgery) in order to perform intraoperative language mapping (object naming task). Essential language sites were localized through direct electrical stimulation (DES) and anatomically characterized thanks to navigated tractography images (Figure 3). This intraoperative protocol allowed maximum tumor resection while preserving language functions. Furthermore, it gave us a unique opportunity to perform reliable, real-time structure – function relationships, determining the role of 5 WM fascicles in the different subcomponents of language (i.e. phonology, lexical – semantics, initiation and selection, articulatory planning). In summary, beyond a better understanding of the structural and functional organization of language in the human brain, our results are directly applicable to optimize brain tumor surgery outcomes. In a more forward-looking perspective, deeper understanding of language connectivity also paves the way for precise positioning of future brain-computer interfaces in aphasia patients, by targeting the residual functional connectivity spared by the lesion, thereby improving symptoms.

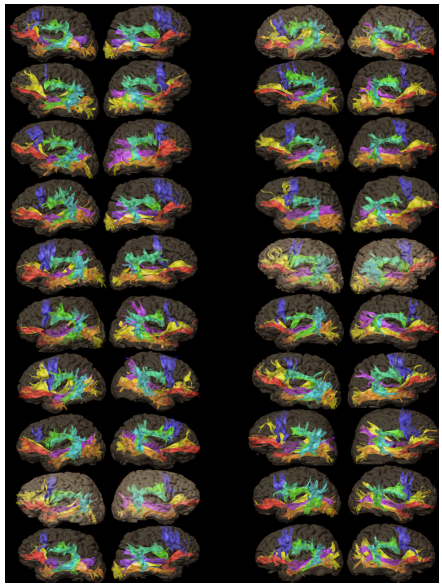

Fig. 1: DTI tractography reconstruction of the language connectome in 20 healthy subjects: (blue) frontal aslant fascicle; (green) arcuate fascicle; (turquoise) anterior and (light blue) posterior segments of the superior longitudinal fascicle; (red) uncinate fascicle; (yellow) inferior fronto-occipital fascicle; (orange) inferior longitudinal fascicle; (purple) middle longitudinal fascicle.

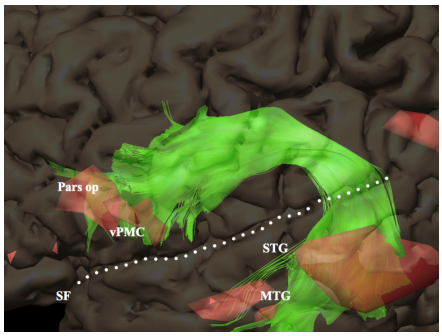

Fig. 2: 3D rendering of fMRI clusters (red) following reading comprehension task (individual brain): fibers of the arcuate fascicle (green) directly connect the frontal and temporal language-related areas. Pars op: pars opercularis of inferior frontal gyrus; vPMC: ventral premotor cortex; STG and MTG: superior and middle temporal gyrus; SF: Sylvian fissure.

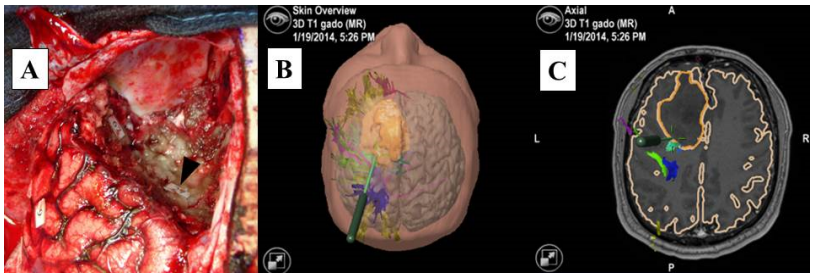

Fig. 3: Example of anatomofunctional correlation. (A) Intraoperative photograph during the removal of a left frontal glioma. Tag 27 (arrowhead) indicates the subcortical site where DES induced delayed speech planning (initiation disorder). (B and C) Intraoperative screen shot: the green cursor indicates the location where such a response was obtained, showing good correspondence with the subcortical course of the frontal aslant fascicle (turquoise).

CONTACTS

Jean-Jacques LEMAIRE
jjlemaire@chu-clermontferrand.fr
François VASSAL
francoisvassal@wanadoo.fr

FURTHER READING

New insights into the functional significance of the frontal aslant tract. An anatomofunctional study using intraoperative electrical stimulation combined with diffusion tensor imaging-based fibre tracking
F. Vassal et al., Br J Neurosurg 28, 685 (2014)

Intraoperative visualization of language fascicles by diffusion tensor imaging-based tractography in glioma surgery
F. Vassal et al., Acta Neurochir 155, 437 (2013)

Extended Broca's area in the functional connectome of language in adults: combined cortical and subcortical single-subject analysis using fMRI and DTI tractography
J.J. Lemaire et al., Brain Topogr 26, 428 (2013)

PhD

F. Vassal

Scientific achievement #95
Processing of speech with graduated emotional charge: an fMRI study to detect residual capacity in patients with disorders of consciousness

A fMRI protocol was developed to detect residual cognitive capacities in patients with severe brain injuries associated with disorders of consciousness. Auditory processing of speech is assessed using passive listening of narratives, with graduated emotional charge. Emotional charge is modulated by voice familiarity (unknown person or relative) and content (general knowledge with no relation to the patient or autobiographical memory recollections). Results in a control group show graduated cerebral activation, with a more widespread recruitment of regions for the highest emotional charge. The case of a patient in persistent vegetative state is shown.

Clinical assessment of awareness in severely brain-damaged relies on observations of overt voluntary behavioral responses to visual, auditory, tactile or noxious stimuli. Thus, in unresponsive brain-damaged patients with underlying function impairments such as apraxia, agnosia or aphasia, observational clinical approach underestimates the level of consciousness in case of covert conscious activity. Functional brain imaging can identify covert residual cognitive function, like speech or emotional processing. We designed an fMRI study with passive listening of narratives with graduated levels of emotional charge: (i) low, unknown person telling general knowledge with no relation to the subject; (ii) mean, relative telling the same general things and (iii) high, same relative telling autobiographical memory recollections. From a clinical perspective, we assessed auditory processing of speech by contrasting narratives with low, mean and high emotional charge versus silence. During passive listening of narratives with low emotional charge, the control group showed significant left-dominant brain activation in bilateral middle and superior temporal gyri. In addition to those activations, narratives with mean emotional charge elicited slight activity in bilateral premotor cortices and left inferior frontal gyrus. Narratives with high emotional charge triggered a large pattern of activation encompassing bilateral middle and superior temporal gyri, temporopolar areas, posterior cingulate and retrosplenial cortices, medial temporal lobes, medial frontal lobes, middle frontal gyri, inferior frontal gyri, thalami, cerebellum; left inferior frontal gyrus and left angular gyrus (figure 1). We investigated the case of a 32-year-old man, who has sustained severe traumatic brain injury 12 years before. According to clinical testing, the patient was considered to be in persistent vegetative state (i.e. absence of awareness of self or the environment). No activation was provided in the patient's brain by listening to general narratives, whether the voice was familiar or not. Yet, a familiar voice telling autobiographical memories triggered activation in medial prefrontal cortex, cingulate cortex, primary visual cortex, hippocampi, right basal ganglia and left supramarginal gyrus (figure 2). In summary, contrary to the diagnostic criteria defining the vegetative state, the patient showed a cerebral activity in response to autobiographical narratives, in regions known to be involved in memory retrieval. The present study provides further evidence of possible residual cognitive functions in the vegetative state, and highlights the importance of emotional charge to pass through an attentional filter, of which selectivity might be altered by cerebral lesions. These findings may have implications in neurorehabilitation programs.

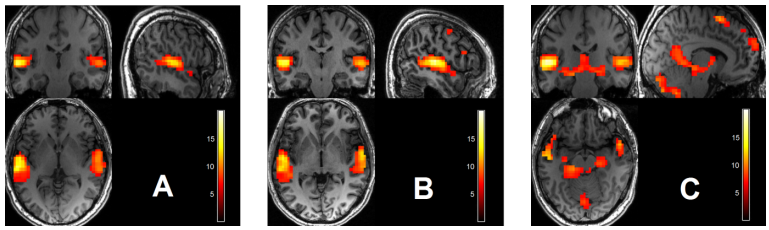

Fig. 1: Cerebral activation in the control group during passive listening of narratives with low emotional charge (A), mean emotional charge (B) and high emotional charge (C), compared to silence.

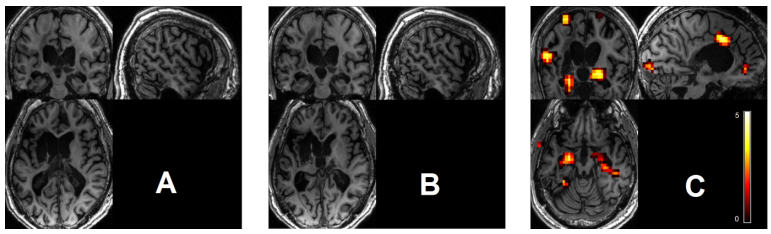

Fig. 2: Cerebral activation in a patient diagnosed in persistent vegetative state during passive listening of narratives with low emotional charge (A), mean emotional charge (B) and high emotional charge (C), compared to silence.

CONTACTS

Jean-Jacques LEMAIRE
jjlemaire@chu-clermontferrand.fr
Anna SONTHEIMER
asontheimer@ chu-clermontferrand.fr

FURTHER READING

New insights into the functional significance of the frontal aslant tract. An anatomofunctional study using intraoperative electrical stimulation combined with diffusion tensor imaging-based fibre tracking
F. Vassal et al., Br J Neurosurg 28, 685 (2014)

Electrical modulation of neuronal networks in brain-injured patients with disorders of consciousness: A systematic review
J.J. Lemaire et al., Ann Fr Anesth Reanim 33(2), 88 (2014)

Selective cerebral response to autobiographical memory in the permanent vegetative state: an fMRI case study
A. Sontheimer et al., Poster, 1st International Symposium on Deep Brain Connectomics (2012)

CONTRACTS

Bourse Legs Deroche, Fondation de l'Avenir (2015-2018)

PhD

A. Sontheimer, F. Vassal

Scientific achievement #96
DBS Targeting in Brain Injured Patients with Severe Anatomical Lesions

We have developed an original technique of pure direct anatomical mapping of the deep brain, enabling to determine accurately all common targets in stereotactic neurosurgery, as well as their whole neighborhood, and this in 3D. Brain distortion precludes mixed or indirect targeting when anatomical lesions are severe, e.g. after traumatic head injury or intra cerebral hemorrhage. In such conditions (clinical research protocol) we have used advanced direct targeting for the implantation of electrodes according to anatomical landmarks following our direct method of anatomical mapping, extended with several structural MRI sequences and Pet-Scan metabolic data.

Context

DBS stereotactic targeting relies on indirect targeting or direct targeting depending on hospital imaging facilities and target. When the target is visible on MRI imaging, teams use more and more direct targeting, however they rely mostly on mixed technique, using indirect atlas-based coordinates, plus one or more dedicated MRI sequence allowing identifying the target. This technique is efficient for patients without important anatomical lesions whether acquired or congenital. We have developed an original technique of pure direct anatomical mapping of the deep brain, enabling to determine accurately all common targets in stereotactic neurosurgery, as well as the whole neighborhood of the target, and this in 3D. Brain anatomical distortion preclude mixed or indirect targeting when lesions are severe, e.g. after traumatic head injury or intra cerebral hemorrhage.

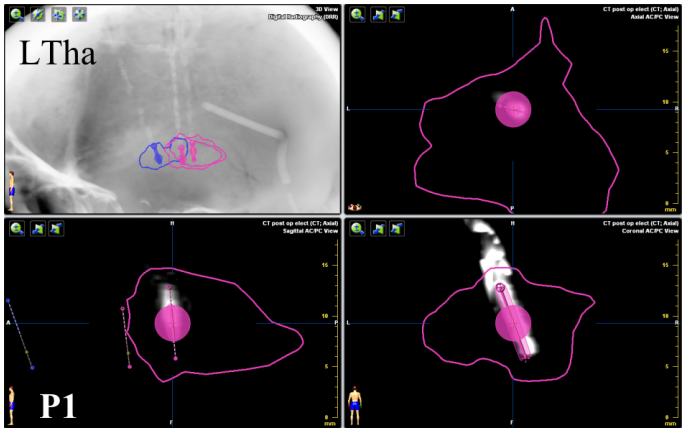

Fig. 1: ***Post-operative location*** *(pink dot)* ***of the left thalamic*** *(pink contours)* ***electrode*** *(white; CTScan artefact)****:*** *top left, X-ray like display with 3D objects overlaid; clock-wise from top right, axial, frontal and lateral views.*

Scientific achievement

We have used advanced direct targeting in brain injured patients suffering of severe consciousness troubles in the frame of a clinical research protocol (NCT01718249). For the first time patients were implanted according to anatomical landmarks following our direct method of anatomical mapping, extended with several structural MRI sequences (WAIR and DTI) and Pet-Scan metabolic data. Electrodes were implanted bilaterally within the pallidum and the central thalamus after identification of targets. Clinical and biological postoperative data are in favor of accurate spotting technique.

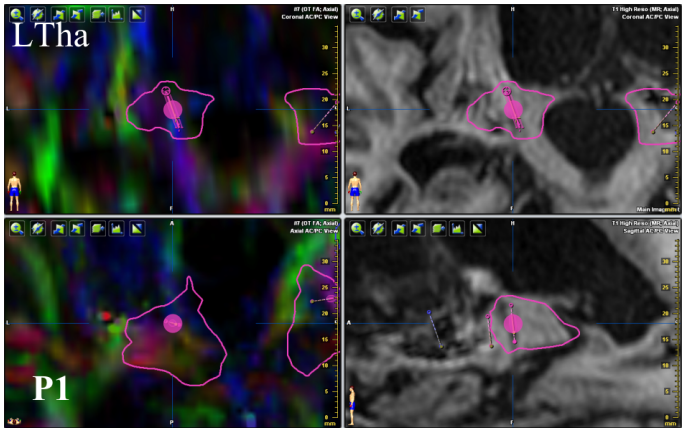

Fig. 2: ***Position of the left electrode*** *(pink dot)* ***within the thalamus*** *(pink contours)****:*** *clock-wise from top left, coronal color-code DTI slice, coronal WAIR slice, sagittal WAIR slice, and sagittal color-code DTI slice.*

CONTACTS

Jean-Jacques LEMAIRE
jjlemaire@chu-clermontferrand.fr

FURTHER READING

Lemaire JJ et al., NeuroImage 37 : S109 (2007)

PhD

B. Roche, A. Sontheimer

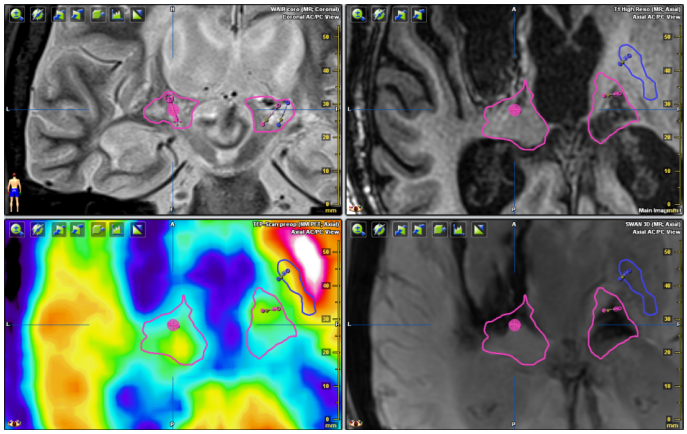

Fig. 3: ***Position of the left electrode*** *(pink dot)* ***within the thalamus*** *(pink contours): clock-wise, from top left, coronal, coronal WAIR slice, axial WAIR slice, axial SWI slice, and axial PetScan slice.*

Scientific achievement #97
Time-course of myelination and atrophy on MRI in *PLP1*-related disorders

We studied the natural time-course of hypomyelinating *PLP1*-related disorders on cerebral MRI in 35 patients followed over 7 years. Patients were classified according to best motor function acquired before 5 years into 5 categories. We determined myelination and atrophy scores, corpus callosum area, volumes of cerebellum, white matter (WM) and grey matter (GM) on 63 MRI. Severe patients had higher severity atrophy scores and smaller corpus callosum area than mild and moderate patients. Myelination increased until 12 years and was correlated with clinical severity in anterior regions. Atrophy worsened in most patients whereas GM and WM compartments did not change with aging.

Introduction: Pelizaeus-Merzbacher disease (PMD) and spastic paraplegia type 2 (SPG2) are X linked defects of central nervous system (CNS) myelin formation caused by mutations of the *PLP1* gene and belonging to the clinical continuum of *PLP1*-related disorders. PMD is characterized by hypotonia before 6 months. Neurological signs modify as the CNS matures. Progressive SPG and cognitive decline are observed in adults. Brain MRI shows typical diffuse hypomyelination of white matter (WM). Cerebral atrophy has also been reported. However, there is still a dearth of MRI data on the natural time-course of PMD/SPG2. We set out to identify pertinent MRI biomarkers of disease evolution.

Material and Methods: 35 *PLP1*-mutated males (age: 0.7 to 43 years) were prospectively enrolled over 7 years and classified according to the best motor function achieved before 5 years: no acquisition (PMD0), head control (PMD1), sitting (PMD2), walking with aid (PMD3) or without aid (PMD4). First MRI was called MRI-1. 17 patients had repeat MRI. Atrophy and myelination scores, corpus callosum (CC) area, volumes of cerebellum and WM/grey matter (GM) were explored. Total intracranial volume (TIV) was used as denominator in ratios to account for brain growth. Multivariate statistical analysis was performed with age-adjusted factor.

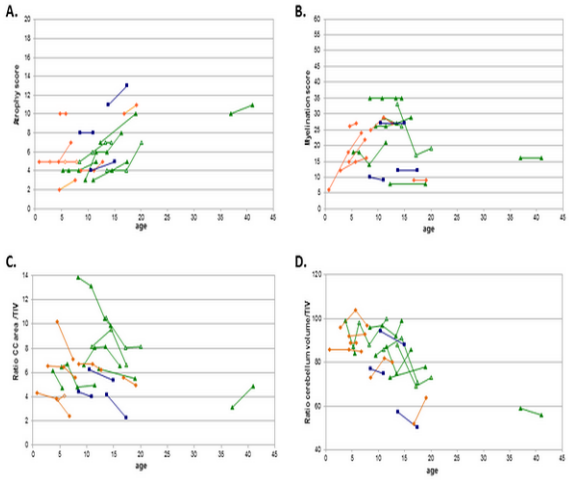

Fig. 2: ***Inter- and intra-individual MRI evolution over time in the subgroup of 17 patients with successive MRIs.*** *Atrophy scores (A; y-axis; from 0, no atrophy, to 21, maximal atrophy) and myelination score (B; y-axis; from 0, no myelination to 60, achieved myelination) according to age (x-axis; years); atrophy tends to increase over time, and myelination tends to increase until 12 years before stabilizing as patients get older. CC area/TIV ratios (C; y-axis) according to the age (x-axis; years); note inter- and intra-individual progressive CC atrophy over time. Cerebellum volume/TIV ratios (D; y-axis) according to age (x-axis; years); note inter- and intra-individual progressive cerebellum atrophy over time. Blue squares: PMD0-1; orange diamonds: PMD2; green triangles: PMD3-4. Several patients are represented with empty symbols for visibility.*

Results: 63 MRI were available. 35 MRI-1 were compared between 3 groups: PMD0-1 (n=9), PMD2 (n=16) and PMD3-4 (n=10). Global myelination was not statistically different between the groups. Global atrophy was more severe in PMD0-1 than PMD2 (p=0,033) and PMD3-4 patients (p=0.040). On the subgroup of patients with successive MRI, atrophy increased in 82%. Progressive atrophy was never observed before 5 years but increased by 8.72% at adolescence. Myelination improved in 41% of patients after 2 years, age of normal complete myelination. After 7 years, myelination remained stable. Among 10 WM regions, only the frontal WM (PMD0-1/PMD3-4, p=0.029), the internal capsule (PMD0-1/PMD3-4, p=0.045) and the U fibres (PMD0-1/PMD2, p=0.046; PMD0-1/PMD3-4, p=0,045) were significantly different. CC area/TIV was statistically smaller in PMD0-1 than PMD3-4 patients (p=0.017). Both CC area/TIV and cerebellum volume/TIV decreased in 88% and 76%, respectively, over time. No statistical difference and no change over time were found for WM and GM volumes.

Discussion: In our series of *PLP1*-mutated patients, clinical severity is correlated with the atrophy score. Myelination scores in the anterior regions partially segregated the different severity groups. Myelination improve until 12 years. At adolescence, atrophy clearly increases. These results might be of upmost importance for interpretation of myelination in young patients in future therapeutic trials. CC area is correlated with clinical severity that would be a good morphological marker both for severity and for disease progression. Cerebellum atrophy tends to occur over time. The WM compartment, despite its defect, tends to remain stable compared to GM compartment. These results suggest a mechanism of both neuronal and myelin atrophy in PMD/SPG2 whereas *PLP1* is mainly expressed in oligodendrocytes, the cells that product myelin. This is coherent with data in patients and animal models that showed a clear involvement of neurones in the physiopathology of *PLP1*-related disorders.

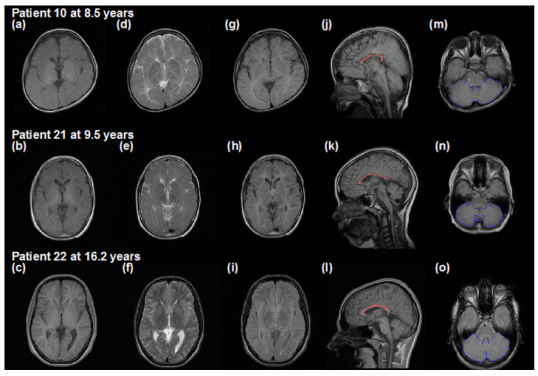

Fig. 1: ***MRI of PMD/SPG2 patients; severe (PMD0; top row), intermediate (PMD2; intermediate row) and mild (PMD4; bottom row) forms.*** *T1-weighted (**a-c**), T2-weighted (**d-f**), and FLAIR (**g-i**) axial slices, showing different degrees of hypomyelination according to clinical severity. CC segmentation on midline FLAIR (**j-k**) and T1-weighted (**l**) sagittal slices. Segmentation of cerebellum on FLAIR axial slices (**m-o**) through the middle cerebellar peduncle.*

CONTACTS

Catherine SARRET
csarret@chu-clermontferrand.fr

FURTHER READING

Time-course of myelination and atrophy on cerebral imaging in 35 patients with PLP1-related disorders
C. Sarret et al., Dev Med Child Neurol (2015)

CONTRACTS

PHRC local, CHU-Clermont-Ferrand (2002-2009), autorisation CPP Sud-Est VI No. AU788, CNIL No. 1406552, AFSSAPS No. B90298-60

Scientific achievement #98
Perinatal databases: monitoring and evaluation

Within the Peprade team some researchers are in charge of 3 databases which are namely AUDIPOG database, database of the perinatal network in Auvergne and the CEMC-Auvergne registery. AUDIPOG database is a data bank from volunteer maternity units all over France that provide at least 1 month of their perinatal results (delivery files) each year. The perinatal network comprises all healthcare facilities managing pregnant women in Auvergne. The CEMC-Auvergne registry is a regional, population-based, malformation-monitoring registry. These databases with full access allow numerous publications.

Audipog database

AUDIPOG (computerized pediatric, obstetric and gynecologic records users association) is a nonprofit organization. AUDIPOG's first objective was to develop a national consensus about the contents of perinatal files, in preparation for the computerization of maternity unit data. Since 1980, the catalogue of files available at our printer includes 16 paper files to meet the needs of perinatal professionals. A common structure for paper and computer files promotes coordination of care and facilitates clinical audits for the evaluation of professional practices, evaluation that is now mandatory for physicians in France.

In 1994, AUDIPOG first created a data bank from volunteer maternity units that provide at least 1 month of their perinatal results (delivery files) each year. This is now known as the AUDIPOG sentinel network. It makes possible the regular production of annual national data, directly accessible to members on the association's web site (http://audipog.inserm.fr). Numerous publications are based on these annual data.

Since 1996, AUDIPOG has also worked to facilitate self-evaluation of professional practices, as some of its publications attest. This involves in particular benchmarking with diverse tools. Accordingly, the professional members of AUDIPOG can interrogate the data bank 24 h a day for answers to questions they may ask themselves in their own practice (for example, what is the national rate of induction for nulliparas?) and then compare it with their own rates. A tool available on the site also makes it possible to compare one's own global cesarean rate with the expected cesarean rate, given the population characteristics and risk factors of the women delivering at that maternity ward. It is also possible to have (for the maternity units that provide a full year of data) a table with selected indicators, including for women at low risk (this 4-page "score card" is also accessible on the internet). A global table, including fewer indicators, will be sent free-of-charge in 2007 to the maternity units furnishing a year's worth of data.

More recently, in order to aid the evaluation of professional practices for colleagues who do not participate in the sentinel network, we have developed simpler tools for such evaluations in various topics.

Database of the perinatal network of Auvergne

The RSPA comprises 14 healthcare facilities, of 4 types: one level III, 6 level II including one private maternity hospital, 3 level I and four local perinatal centres (where babies are not delivered); these account for 100% of the healthcare facilities managing pregnant women or new-borns in the region of Auvergne. There are fewer than 14,000 deliveries each year in Auvergne. Since 2008, the network has sent each maternity unit annual feedback on several indicators (rates of caesareans, episiotomies, etc.) together with the comparison of its own rates with those of the network.

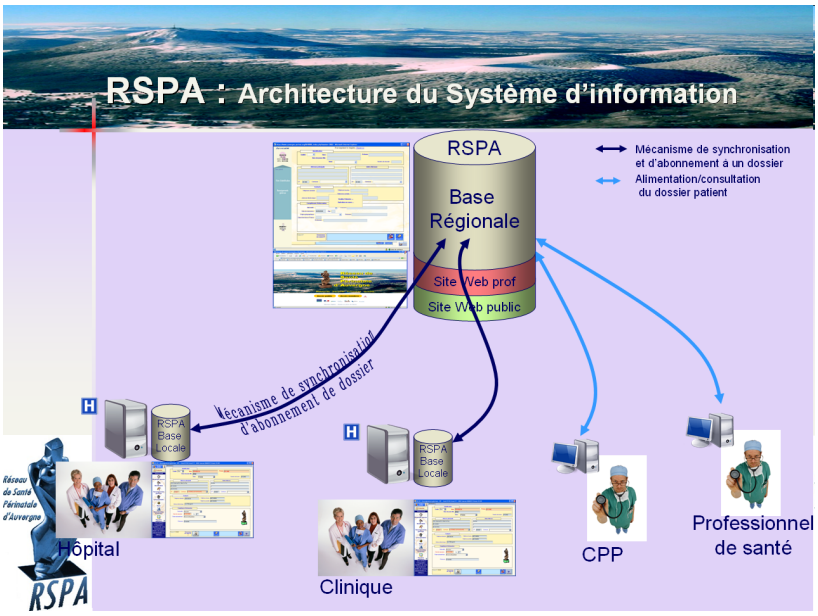

The regionally based shared perinatl file concept.

The CEMC-Auvergne registry

The CEMC-Auvergne registry is a regional, population-based, malformation-monitoring registry currently covering some 13 500 annual births. Terminations of pregnancy are included, regardless of term. Stillbirths are registered at a gestational age of 22 weeks+0 day or later. Live born infants with malformations are identified up to age of 1 year through voluntary reporting from the hospitals in the region and searches of the medical records of the maternity and pediatric units in the area. Regardless of the child's vital status, confirmation of the malformation (or malformations) is obtained after birth, by any means (including pathology examination of fetus or child, in case of death), before it is included in the CEMC-Auvergne database.

CONTACTS

Françoise VENDITTELLI
fvendittelli@chu-clermontferrand.fr
Isabelle PERTHUS
iperthus@chu-clermontferrand.fr

FURTHER READING

How singleton breech babies at term are born in France: a survey of data from the AUDIPOG network
Lansac J. et al., Eur J Obstet Gynecol Reprod Biol. 2015 May;188:79-82

Appropriateness of elective caesarean deliveries in a perinatal network: a cross-sectional study
Vendittelli F. et al., BMC Pregnancy Childbirth. 2014 Apr 9;14:135

Prenatal diagnosis of the VACTERL association using routine ultrasound examination
Debost-Legrand A. et al., Birth Defects Res A Clin Mol Teratol. 2015 Jun 2

Scientific achievement #99

Reliability of health professionals' visual estimate of blood loss in the immediate postpartum period: a didactic training tool

In France, postpartum hemorrhage (PPH) (blood loss ≥ 500 mL in the first 24 hours postpartum) is the leading direct obstetric cause of maternal mortality. In French practice, PPH is mainly diagnosed by a quantitative assessment of blood loss, performed by subjective methods such as visual estimates. Various studies have concluded that visual estimates are imprecise, tend to underestimate blood loss, and thus to delay diagnosis of PPH. We created on online questionnaire with photographs of various volumes of simulated blood loss as a didactic training tool to improve the accuracy of visual estimates of blood loss of health professionals.

In France, obstetric hemorrhages were responsible for 18.1% of maternal deaths between 2007 and 2009 (46/254 deaths), including the 8.3% associated with postpartum hemorrhages (PPH) due to uterine atony (21/254); PPH was thus the leading direct obstetric cause of maternal mortality here. Audits have found that 83.9% of the deaths from hemorrhages were avoidable and that the diagnosis of hemorrhage was non-optimal in 74% of these avoidable deaths.

Immediate PPH is defined by the World Health Organization (WHO) and in France as a blood loss exceeding 500 mL in the first 24 hours postpartum. French maternity units are required to record and report the volume of each woman's blood loss. In practice, clinicians can rely on several methods of quantification - subjective (visual estimate) or objective (collector bag, or weighing compresses or sanitary pads, or laboratory analyses). Different studies have concluded that visual estimates are imprecise, tend to underestimate blood loss, and thus to delay diagnosis of PPH. When visual aids, such as "pocket-cards" or visual training were offered, the accuracy of these visual estimates improved significantly.

The principal objective of this study is to assess the accuracy of health professionals' visual estimates of blood loss, when a standard visual reference is provided at the same time.

A questionnaire available online at:
http://www.audipog.net/estim-perte-en.html)
asks respondents to estimate simulated PPH blood loss visually. Specifically, the questionnaire contains 16 photographs of 8 different quantities of simulated blood (100, 150, 200, 300, 500, 850, 1000, and 1500 mL). There are two copies of each photograph, placed randomly within the questionnaire (but never adjacent to one another). For each of the 16 photographs, participants are asked to choose only one response among the 7 choices. There are no time limits for completion. A photograph of a reference standard that simulated 50 mL of absorbed blood accompanies each of the 16 study photographs. This volume of 50 mL was chosen because it corresponds to the median volume of total menstrual blood loss.

The questionnaire was completed by voluntary midwives students in their fifth and final year and midwives in France. A cross-sectional study was performed to evaluate the answers of midwives students. Despite the help of a visual aid, both the accuracy and reproducibility of the visual estimates were low among midwives students.

This study thus points out — and makes both students and teachers aware — that estimating blood loss is difficult, even though it is the first-line method for the initial identification of PPH. Because this early clinical identification of PPH is essential for preventing maternal complications, methods of improving it must be developed. This training module is available on the internet and can be used free of charge by all students and teachers. This exercise must be used, in our opinion, as a prerequisite to other practical training sessions (electronic mannequin, role-playing games).

CONTACTS

Françoise VENDITTELLI
fvendittelli@chu-clermontferrand.fr

FURTHER READING

Reliability of student midwives' visual estimate of blood loss in the immediate postpartum period: a cross-sectional study
I Parayre, O Rivière, A Debost-Legrand, D Lémery, F Vendittelli
International Journal of Nursing Studies, in press

Scientific achievement #100
Severe Secondary Postpartum Hemorrhage: incidence, causes and risk factors

Postpartum hemorrhage (PPH) remains one of the leading causes of maternal mortality and morbidity worldwide. Few publications have examined secondary PPH (bleeding that occurs between 24 hours and 42 days after birth). There are no guidelines for its management in France. Our objectives were to assess the incidence of severe secondary PPH and to describe the distribution of the different causes of severe secondary PPH. We also aimed to determine risk factors of severe secondary PPH. In our cohort study, severe secondary PPH is a rare complication. Our study confirms that immediate PPH is a risk factor for severe secondary PPH thus that immediate PPH may be an intermediate factor between its own known risk factors and secondary PPH.

Postpartum hemorrhage (PPH) remains one of the leading causes of maternal mortality and morbidity worldwide. In France, 25.8 percent of maternal deaths are because of hemorrhages. Few publications have examined secondary PPH (bleeding that occurs between 24 hours and 42 days after birth). The incidence of these secondary PPHs is low, ranging from 0.2 to 3 percent. This frequency is probably underestimated, however, because studies generally include only severe PPH requiring hospitalization. No published European cohort study has assessed the frequency or causes of secondary PPH, and no scientific evidence supports any of the current treatment options . It is thus understandable that there are no guidelines for its management in France. Moreover, the cause of the secondary hemorrhage often remains unknown, in the absence of routine uterine surgical evacuation, which is not always essential to the woman's medical care.

Although the risk factors for immediate PPH have been clearly identified, only two published studies have reported predictive factors for secondary PPH.

Our objectives were to assess the incidence of severe secondary PPH and to describe the distribution of the different causes of severe secondary PPH. We also aimed to determine if immediate PPH is a risk factor for severe secondary PPH and we searched for other factors associated with severe secondary PPH.

We included all women who gave birth at the Clermont-Ferrand University Hospital Center (level III) from January 1, 2004, to February 13, 2013 and who had severe secondary PPH. In this study, severe secondary PPH has been defined as any significant bleeding from the genital tract, by any route (vaginal or intraabdominal) from 24 hours after childbirth to the 42nd day postpartum, resulting in medical, interventional radiology, or a surgical procedure during the initial postpartum hospitalization or a subsequent hospitalization.

In a historical cohort study at our hospital, we estimated the incidence of severe secondary PPH at 0.23 percent. Placental retention was the cause to which these hemorrhages were most frequently attributed (30.0%). Subinvolution of the placental bed was noted in 13.3 percent of the patients, endometritis in 10.0 percent, pseudoaneurysm of the uterine artery in 3.3 percent, and excessively strong resumption of menses in 3.3 percent; no cause could be determined for 16.7 percent of the cases. Neither clinical signs nor causes differed by parity. In conclusion, secondary PPH is a rare complication but one that can result in severe maternal morbidity. Its management is not well codified in the absence of population-based studies including an adequate number of individuals; its clinical and ultrasound features most often suggest placental retention to clinicians. Ultrasound does not enable the specific cause of secondary PPH to be identified, unlike a pathology examination, which is the only means of identifying subinvolution of the placental bed.

Our study confirms that immediate PPH is a risk factor for severe secondary PPH and reports for the first time an association between secondary PPH and advanced maternal age. It is likely that risk factors for immediate PPH are also risk factors for severe secondary PPH and thus that immediate PPH may be an intermediate factor between its own known risk factors and secondary PPH.

CONTACTS

Françoise VENDITTELLI
fvendittelli@chu-clermontferrand.fr

FURTHER READING

Risk Factors for Severe Secondary Postpartum Hemorrhages: A Historical Cohort Study
Debost-Legrand A., Rivière O., Dossou M., Vendittelli F.
Birth. 2015 May 29

Severe secondary postpartum hemorrhage: a historical cohort
Dossou M., Debost-Legrand A., Déchelotte P., Lémery D., Vendittelli F.
Birth. 2015 Jun;42(2):149-55

Scientific achievement #101
Partnership in mother and child health in Ukraine

Since 2013, a partnership is developed in Ukraine with obstetrical and neonatal health care structures of the area of Kiev (Ivankiv Hospital, Boïarka regional pediatric hospital) and the medical university Shupik, to assess the impact of chronicle intakes of cesium 137, pesticides and other micro pollutants, to help to improve the quality of regular care and to extend the network policy in neonatal care. It is funded by both European Union and the regional council of Rhône-Alpes. Due to the political situation, the two main studies only begun in November 2014.

Since 2013, a partnership is developed in Ukraine with obstetrical and neonatal health care structures of the area of Kiev (Ivankiv Hospital, Boïarka regional pediatric hospital) and the medical university Shupik, and is locally coordinated by the STCU (Science Center for Technology in Ukraine). It is funded by both European Union (STCU #9805/ EUROPAID/133104/C/SER/UA) and the regional council of Rhône-Alpes (14000036003 SAN 233).

On the whole, the program has seven axes that can be summarized in four main objectives which are:

1- to assess the impact of chronicle intakes of cesium 137 (Cs-137, in relation with the Chernobyl accident), and also pesticides and other micro pollutants, on the health of pregnant women and child. This is the main part of the study and is based on two surveys:
   a. a mother and child follow-up (from the beginning of pregnancy to the one year of the children), out of the Ivankiv Hospital, with 300 to 400 mothers and child followed every year during three years. The follow-up bean in November 2014.
   b. A cross sectional study of 3.000 children (1 to 17 years old) from Ivankiv area and Polesia checking health parameters and measures of pollutants. The cross sectional study began in November 2014.

2- to help to improve the quality of regular obstetrical, neonatal and pediatric care, in the particular context of the two collapses of the public health care system in late 90's and in the recent years, by qualifying and quantifying needs, giving new equipment (according to the European budget and rules) and continuous training of professionals.

3- to extend the network policy in neonatal care, and to assess its impact on the mother and child outcomes.

4- To develop health education and health advises fir the general population in order to reduce the exposition to CS-137 as well as pesticides and other micro pollutants and to assess the efficacy of this educational policy on morbidity and mortality indicators at the local level.

The intervention sector of Ivankiv was chosen as it is one of the most contaminated area by Cs-137. The regional pediatric hospital of Boïarka is the referee hospital for Ivankiv and is involved in the study. After a first set of studies, and according to the level of funding, other area should enter the program (such as Polesia, the expected second one, also depending on Boïarka pediatrics).

In 2013 and 2014, audit missions were made to assess the equipment needed, to help to build study's methodology and to put in place a medical database for both studies, according to the Ukrainian rules and the good practices in epidemiology.

Due to the political situation, we have some delay, but the two main studies (children screening and mother and child follow-up) begun in November 2014, while new equipment was in place and working in the Ivankiv hospital since June 2014. Training programs were also defined with the help of the Shupik University and three short training period in France were made for Ukrainian physicians.

The next steps is the integration of this project in the European Union – Ukraine partnership, with the help of head of the regional health administration of Kiev (where belong the area of Ivankiv).

CONTACTS

Laurent GERBAUD
lgerbaud@chu-clermontferrand.fr
André LABBE
alabbe@chu-clermontferrand.fr
Françoise VENDITTELLI
fvendittelli@chu-clermontferrand.fr

FURTHER READING

Efficacy of pectin in reducing cesium-137 load in chronically infected children: a literature review
C. Marie, L. Gerbaud, Y. Bandajevsky, D. Vernay, Pediatrics Eastern Europe; 4, 08: 104-117 (2014)

CONTRACTS

Européen: Union européenne (via le STCU) : STCU #9805/ EUROPAID/133104/C/SER/UA – 2012/2017

Regional council of Rhône-Alpes: 14000036003 SAN 233 – 2013/2016

PhD

C. Marie

Scientific achievement #102

Health risk assessment for babies linked to disinfection by-products detected in the chlorinated water of swimming pool

For young children, the increase of childhood asthma in industrialized countries is related to the exposure to chlorinated disinfectants used in the treatment of swimming pool water (and especially to disinfectant bi-products formed in situ by the reaction of chlorinated products with organic matter brought by swimmers into the swimming pool water). Characterization of disinfection by-products and photochemical reactions linked to the plant treatment of water swimming pools will help to understand the medical features and the respiratory abnormalities, detected by biological parameters and/or medical imaging techniques, in relation with intense aquatic activities of babies, child, and even of pregnant women (i.e., in utero exposure).

For several years, a large increase in the extent of allergic conditions (eczema, allergic rhinitis, asthma) has been recorded in most industrialized countries. The exact cause or causes of this situation remain unknown, but researchers are unanimous in attributing it to modifications to our environment or way of life. Between 2000 and 2010, a new hypothesis called « pool chlorine hypothesis » appeared. It attributes the increase of childhood asthma in industrialized countries in part to increasing uncontrolled exposure of young children (up to the age of 6) to chlorinated disinfectants used in the treatment of swimming pool water (and especially disinfectant bi-products formed in situ by the reaction of chlorinated products with organic matter brought by swimmers into the swimming pool water).

In fact, repeated or chronic aggression of the epithelial barrier of the distal respiratory tract by the bi-products of chlorinated disinfection (such as chloramines, trihalomethanes, haloacetic acids…), could alter this epithelium. It can also facilitate the penetration of allergens into the lung and increase the risk of sensitization and allergic illnesses. This is concerning, because recreative swimming programs are increasingly available in industrialized countries for infants from 6 to 36 months. In France, 8% of babies practice "baby swimming" activities.

Even though the most recent work in pediatrics seems to be reassuring and tends to contradict previous work, the meta-analysis of Goodmann et al (2008) did not find a statistically significant association between asthma and swimming pool activity in childhood (OR = 0.63 - IC 95% = 0.38-1.06). However, improved knowledge of the sanitary situation linked to regular attendance in French public swimming pools is necessary.

In this context, a study aimed at characterizing regular swimming pool activity as a risk factor of bronchiolitis and asthma in infants has been carried out at the Pediatric A&E of Estaing Hospital (Clermont-Ferrand, France). This cross-over study has been performed at the Pediatric Emergencies of the Hospital of Clermont-Ferrand during the winter 2010-2011. It included 139 babies from 6 to 36 months old, for which bronchiolitis or asthma was diagnosed. Data on the babies' exposure in swimming pool waters and the exposure of their mothers during the pregnancy were collected, thanks to a standardized questionnaire. The classical described risk factors of bronchiolitis and/or asthma were observed in this population of French children. Moreover, 40 % of the studied baby's population had a regular aquatic activity and 8.6 % practiced baby swimming activity. The global indicators of babies health (i.e., number of hospitalization and age of the first episode of bronchiolitis) does not differ significantly between babies having regular aquatic activity and babies without exposure to swimming pool waters. Although a significant exposure to swimming pool waters is described in 40% of the studied population, this study does not show significant effect on the short-term pulmonary morbidity. In France, prospective studies are necessary to quantify the impact of exposure to chlorinated waters on the respiratory function of babies.

Health risk assessment must be perform with a complementary approach by studying biological and clinical parameters of pregnant women, and the quality of swimming pool water. A better detection and identification of disinfection by-products will be helpful to characterize the health risk for swimmers, including babies and child. These data are necessary to assess the health risk linked to swimming pool water. For several years, questions about this topic are initiated by the French sanitary agency (Anses) and two scientific workshops (2007-2010, and since 2014) have been created (president: MP Sauvant-Rochat).

In this context, a collaborative project can be initiated with the chemists of the Pascal Institute for the chemical aspects (i.e., characterization of disinfection by-products, photochemical reactions …). Knowledge about the contaminants of swimming water will help to understand the medical features and the respiratory abnormalities, detected by biological parameters and/or medical imaging techniques, in relation with intense aquatic activities of pregnant women.

CONTACTS

Marie-Pierre SAUVANT-ROCHAT
m-pierre.sauvant-rochat@udamail.fr

FURTHER READING

Early swimming activities and risk of bronchiolitis and/or asthma in French child
V. Sablayrolles et al. Proceeding of the 12th Congress of the International Federation of Environmental Health (IFEH), 22-27 mai 2012, Vilnius (Lituanie), Medimond Editor (2012)

Rapport d'Expertise Collective AFSSET - Evaluation des risques sanitaires liées aux eaux de piscines
M.P. Sauvant-Rochat (présidente du groupe de travail) et al., AFSSET (Agence Française de Sécurité Sanitaire de l'Environnement et du Travail) (2010) (244 pages)

PhD

E. Fougere, V. Sablayrolles

Scientific achievement #103
Risk assessment after in utero phthalates exposure and obstetrical outcomes

For Phthalates are commonly used as plasticizers in PVC, and this context induced a great level of exposure for the population. Furthermore, pregnant women and fetus are described as vulnerable subjects according to the reprotoxic effects and the effects of endocrine disrupter of phthalates, although the detailed mechanism of action of these substances is still unclear. In a proposed cohort study, based on biomarker determination and medical imaging techniques used in the follow-up of pregnant women exposed to phthalates, fetal abnormalities and the fetal critical period of exposure can be specified. This coupled approaches will also be usefull in the understanding of the mechanism effects of phthalates.

Phthalates are a family of chemical products made up of dialkyl esters or alkyl and aryl esters of orthophthalic acid (1,2-dicarboxylic acid). High molecular weight (HMW) phthalates, such as DiDP, DiNP and DEHP, are widely used in industry as plasticizers to soften polyvinyl chloride (PVC). There are multiple sources of exposure to high molecular weight (HMW) phthalates such as food packaging, bottled water, children's toys, medical devices, flooring, and building materials. Low molecular weight (LMW) phthalates, such as BBP, DnBP, DiBP, DEP and DMP, are used in paints, inks, adhesives, solvents, insecticides, body-care products (cosmetics, perfumes) and medications. Phthalates are also commonly found in the home environment owing to the direct release, migration, leaching, evaporation and abrasion of and from PVC products. Hence, phthalates are ubiquitous environmental contaminants and humans are susceptible to exposure by ingestion, inhalation and dermal absorption. Phthalates are non-persistent contaminants in the organism. Furthermore, phthalates are identified as reprotoxic and endocrine disrupters.

The ongoing work has identified the most relevant biomarkers to characterized the in utero exposure to phthalates and the main related outcomes on the pregnancy. Premature birth and decreased anogenital distance were the most commonly reported outcomes resulting from a moderate level of exposure to phthalates. The principal metabolites detected and involved were primary metabolites of di-2(ethylhexyl)-phthalate (DEHP) and di-*n*-butyl-phthalate (DnBP). No clear conclusion could be drawn with regard to gestational age at birth, body size at birth and congenital malformations.

In a future cohort study, the coupled biomarker determination and the medical imaging techniques used in the follow-up of pregnant women exposed to phthalates will allow to detect early the fetal abnormalities, and to detemine the fetal critical period of exposure. Moreover, this coupled approaches will also be usefull in the understanding of the mechanism effets of phthalates.

CONTACTS

Marie-Pierre SAUVANT-ROCHAT
m-pierre.sauvant-rochat@udamail.fr

FURTHER READING

Obstetrical outcomes and biomarkers to assess exposure to phthalates: a review
C. Marie et al.. Environnement International 83, 116-136 (2015)

L'exposition in utero au phtalate de diisononyle (DiNP) est-elle associée à des effets anti-androgéniques ?
C. Marie et al.. Bull Veille Sci Anses 17 (2015)

PhD

C. Marie, G. Paillot de Montabert

Scientific achievement #104
Contractualization with SUPERSONIC IMAGINE CORP.

Human As a materialization of rising projects in obstetrical ultrasound imaging a contract of collaboration has been signed up during the first half of 2015 between our team via the University of Auvergne, the University Hospital of Clermont-Ferrand and Supersonic Imagine as the company producing the Aixplorer ® Ultrasound scanner. This collaboration is important in the history of our young team since it credibilize the aim of the studies we have designed and planned to design to rise up breakthroughs in obstetrical imaging. We are offered to use new setups, softs and image constructions in a pre-clinical configuration.

Today, three main fields have been identified:

1/ An ending study (POWUS) has been designed to evaluate how to improve image quality in obese patients, knowing that the prevalence of obesity in pregnant population is rising up all over the world. We are working on the celerity of ultrasound through fat tissue (1450 m/s), wich is slower than in non-fat one (1540 m/s). Since 1977, all the algorithms involved in image construction by ultrasound devices all over the world consider a unique standardized ultrasound celerity of 1540 m/s for any patient (obese or not). Eighty triplets of ultrasound scans of 4 different fetal areas of interest were snapshot at 3 different ultrasound speeds in 32 obese pregnant women. An online questionnaire has been presented to members of the french college of fetal ultrasound (CFEF). One hundred and fourteen of them ranked the pictures of each triplet (27 360 picture evaluations). The main result of this study is a preference for low speed when fat thickness is important. This introduces the fact that setups of an ultrasound device should include « low ultrasound speed image construction » adjusted on patients fat thickness would be a revolution in medical ultrasound industry. Those results are to be submitted to a high audience journal.

Fig. 1: The Powus Study Online questionnaire dnd the Aixplorer Diagnostic Ultrasound device.

2/ The use of real time quantitative Shear Wave ® imaging in pregancy has never been evaluated. This is of importance since this technique is the only usable one in fetus and uterus knowing that all other techniques would require direct contact with the explored fetus. Wich is, of course, impossible in utero. As a prerequisite, the risks for the fetus in terms of energy and pressure induced by the shear wave have to be evaluated . Then a clinical evaluation will be done for the assessment of placenta, lungs and cervix as a priority for daily practice.

3/ The high sensitivity Ultrafast ® Doppler will also be evaluated for mapping blood velocity regarding the intravascular region of the umbilical vein (central vs peripheral) in relation with blood viscosity wich partly reflects the haematocrit.

CONTACTS

Didier LEMERY
dlemery@chu-clermontferrand.fr

FURTHER READING

Echographie chez la patiente obèse :
D. Lemery, Conférence CNGOF Paris,
Décembre 2014

CONTRACTS

Purpose of the present document since it represents an actual rising point in our research program

Master 2

B. Chauveau, M. Issaoui

Tableau 1 : *Répartition des cotations A, B, C et des scores des images en fonction des 3 vitesses d'acquisition testées*

	Vitesse (en m/s)	1420	1480	1540	p	p *		
						1420 vs. 1540	1480 vs. 1540	1420 vs. 1480
114 lecteurs	Cotation – no. (%)							
	A	2944 (32.3)	3449 (37.8)	2727 (29.9)	<0.0001	<0.0001	<0.0001	<0.0001
	B	3037 (33.3)	3350 (36.7)	2733 (30.0)				
	C	3139 (34.4)	2321 (25.5)	3660 (40.1)				
	Score (de 0 à 10)	**(N=9120)** 4.9±1.1	**(N=9120)** 5.6±1.0	**(N=9120)** 4.5±1.0	<0.0001	<0.0001	<0.0001	<0.0001
35 lecteurs concordants	Cotation – no. (%)							
	A	932 (33.3)	1061 (37.9)	807 (28.8)	<0.0001	<0.0001	<0.0001	<0.0001
	B	951 (34.0)	1026 (36.6)	823 (29.4)				
	C	917 (32.8)	713 (25.5)	1170 (41.8)				
	Score (de 0 à 10)	**(N=2800)** 5.0±1.2	**(N=2800)** 5.6±1.0	**(N=2800)** 4.4±1.0	<0.0001	<0.0001	<0.0001	<0.0001

Les valeurs de plus-moins sont des moyennes ±DS.
* Test significatif pour p ajusté pour comparaisons multiples (correction de Bonferroni) <0.017.

Table 1: Preference of ultrasound speed in obese pregnant women.

INSTITUT PASCAL Highlights (2010 – 2015)